# Investigations on the cytology and life-cycle of the parasitic dinoflagellate *Hematodinium* sp associated with mortality of *Nephrops norvegicus*

**Paul Lawrence Appleton**

**Division of Environmental and Evolutionary Biology,**
**Institute of Biomedical and Life Sciences,**
**University of Glasgow,**
**Glasgow,**
**G12 8QQ**

**This thesis is presented in submission for the degree of Doctor of Philosophy in the Faculty of Science.**

**February 1996**

## SUMMARY

Dinoflagellate parasites of the genus *Hematodinium* are associated with heavy mortality of the Norway lobster (*Nephrops norvegicus*) off the west coast of Scotland. The Syndinean dinoflagellate has been isolated from *N. norvegicus* and has been successfully cultured axenically *in vitro*. Twelve isolates have been serially cultivated in a medium of 10% fetal calf serum in a balanced *Nephrops* saline with added antibiotics at 8-10°C. In this medium the parasite undergoes developmental changes that are believed to represent stages in the life cycle of the parasite *in vivo*. This is the first complete life cycle *in vitro* to be described for a Syndinean dinoflagellate.

Flagellate dinospores arise *in vitro* from circulating sporogenic parasite forms - sporoblasts removed in the haemolymph from infected lobsters. Sporogenic parasites are recognised by the presence in the cytoplasm of structures not found in the trophont. These are (1) trichocysts and (2) flagellar hairs within swollen endoplasmic reticulum cisternae. Dinospores are of two types - a larger macrospore and a smaller, more active microspore. Individual isolates produce one or the other, not both. Condensation of chromosomes in the nucleus is more pronounced in the microspore than in the macrospore. Both spore types germinate after 18-62 days in the culture medium to produce the main multiplicative stage of the parasite *in vitro* - the multinucleate filamentous trophont. No fusion of flagellates has been observed and each type of spore can germinate independently of the presence of the other, indicating that the spores are not gametes. The filamentous trophonts correspond to the only form of the type species of the genus, *Hematodinium perezi*, found circulating in the blood of infected crabs by Chatton and Poisson (1931). Subcultured at two to four week intervals, the parasites maintain the filamentous form. The filaments show characteristic bending and squirming motility and often form radiating 'gorgonlock' colonies. Gorgonlock

colonies can develop into interdigitated syncytia referred to as 'clump' colonies. Under certain conditions, as yet undefined, the filamentous trophonts adhere to the substratum and form syncytial networks which constitute the 'arachnoid' sporont stage of the life cycle. Sporogenic syncytia are formed from the centre of the arachnoid which becomes raised from the substratum to give a volcanic crater-like appearance. Sporogenic cells are released from the crater rim and eventually divide into flagellated dinospores that are believed to represent the transmissive stage of the parasite to a new host as they can initiate a new cycle of development *in vitro*.

The addition of a mixture of amino acids to the standard culture medium resulted in an increase in the length and in the number of nuclei within the filamentous trophonts without change to the ultrastructure.

Structures resembling apicomplexan micropores have been found in *in vitro*-cultured trophonts and in sporoblasts found in the host. The uptake of colloidal gold and ferritin indicates a cytostomal function for the micropores.

Histological investigation of infected *Nephrops* has revealed a number of developmental stages of the parasite. Early infections are characterised by the presence of circulating non-filamentous trophonts. Heavily infected lobsters contain large numbers of circulating uni- bi- and multinucleate sporoblasts. Attached syncytia may represent primary or secondary sporonts.

A polyclonal antibody against the parasite was successfully raised in rabbits using culture-derived material as antigen. An indirect fluorescence antibody technique (IFAT) was developed to detect *Hematodinium* in the haemolymph and tissues of *Nephrops*. The IFAT was found to be more sensitive and reliable than previously used field and laboratory diagnostic techniques. Low level haemolymph and tissue infections have been found in apparently uninfected lobsters at all times of the year,

including late summer and autumn, when the parasite was previously thought to be absent from lobsters. Lobsters with a subpatent infection detected in the autumn developed a patent infection the following winter and spring. Host response to the infection was largely through the activity of the fixed phagocytes associated with the hepatopancreas but this response appeared to be overwhelmed by the large parasite load.

Sporogenesis was observed in heavily infected lobsters. Dinospores left the host by discharge into the gill chambers and then dispersed in dense white clouds by the exhalent respiratory current. Spore release usually lasted between 18-24 hours at the end of which the lobster was dead. It is not clear how the parasite is transmitted between hosts. Since no resting stage (cyst) has been identified it is presumed that the dinospore is the infective stage. Entry into the host could either be through the gut or through the cuticle, presumably after ecdysis when the cuticle is soft.

The species taxonomy of the genus *Hematodinium* cannot be fully resolved until further information is gained on the type species *Hematodinium perezi* Chatton and Poisson (1931).

Mortality caused by infection of *Nephrops* by *Hematodinium* may have serious consequences for the state of some *Nephrops* populations and subsequent implications for fisheries management.

## LIST OF CONTENTS

# LIST OF FIGURES

# LIST OF TABLES

## DECLARATION

The results presented in this thesis are my own work except where there is an explicit statement to the contrary. Dr R. Field carried out the Leishmans staining described in Chapter 5 and some of the immunostaining.

Results from Chapters 5 and 8 have been published and are included in Appendix 1.

# ACKNOWLEDGEMENTS

I wish to thank Professor K. Vickerman for all the help, encouragement and advice he has given me over the last three and a half years. I am especially grateful for all the time he put into reading the several drafts of this thesis. Thanks to Rob Field who has passed on much of the practical aspects of working with diseased lobsters. I shall never forget returning from Loch Ewe in the snow with the Millport Landrover!

I am grateful to Professor Coombs for allowing me to work in the Laboratory for Biochemical Parasitology throughout the turmoil of the formation of IBLS. Thanks to Mike Turner for help and advice with antibody production and John Laurie for technical help.

I have spent many hours working in the EM centre, and am grateful to Dr Tetley for technical advice and help. Margaret and Eoin have been eager to help and offer advice throughout my time in the EM centre. Thanks to Maureen and Margaret who spent many hours printing the EM micrographs presented in this thesis.

This work was funded by the Ministry of Agriculture, Fisheries and Food.

# CHAPTER 1.

# Introduction

## 1.1. An introduction to the Dinoflagellata Bütschli, 1885

This thesis is concerned with the biology of a parasite associated with the mortality of an important fisheries crustacean, the Norway lobster. The parasite belongs to a poorly known class of dinoflagellates the Syndinea. The dinoflagellates are a distinctive group of protists with two heterodynamic flagella and a characteristic nuclear structure different from that of other eukaryotes.

Although dinoflagellates are often regarded by biologists as free-living autotrophic protistans, most are heterotrophic, and among the latter are important symbiotic (mutualistic) and parasitic forms.

They are predominantly biflagellated organisms with characteristic transverse and longitudinal flagella, with cortical alveoli and tubular mitochondrial cristae. In its organisation the dinoflagellate nucleus is strikingly different in several respects from that of other eukaryotes. The mitotic spindle is extranuclear, the chromosomes are attached to the persistent nuclear envelope during division (Kubai and Ris 1969, Soyer 1969, Oakley and Dodge 1974), and they do not decondense during interphase. In many dinoflagellates the chromosomes have a screw-carpet fibrillar structure when seen in transmission electron micrographs of sections, and lack the typical nucleosomal structure of eukaryotes as histone proteins are absent. The dinoflagellates are composed of both pigmented (possessing xanthophylls, chlorophylls and carotene) and non-pigmented forms, phototrophic and phagotrophic species, motile and non motile stages, solitary and colonial species, and thecate (armoured) and non-thecate (naked) forms.

Unlike many protists, dinoflagellates have an extensive fossil record dating from the late Precambrian (Fensome *et al.* 1993).

The taxonomy of the dinoflagellates (reviewed by Fensome *et al.* 1993) is confusing because they have been considered as plants or animals depending upon the discipline of the investigator, and hence classified under both Botanical and Zoological codes of nomenclature. Thus botanists traditionally refer to them as the Pyrrhophyta Pascher 1914 or Dinophyta while, in a recent zoological backlash, Cavalier-Smith (1981) has coined another alternative, the Dinozoa. The great importance of the photosynthetic dinoflagellates as primary producers in aquatic ecosystems and their lengthy fossil record in the past resulted in a classification of the dinoflagellates that largely followed the Botanical code of Nomenclature. It is now obvious, however, that dinoflagellates are basically heterotrophic protists some of which have secondarily acquired plastids and as this thesis is wholly concerned with parasitic heterotrophic dinoflagellates, the Zoological code will be followed here.

The term 'dinoflagellate' derived from the Order Dinoflagellata Bütschli, 1885 has remained a popular and convenient way of referring to this diverse group of protists. The content of this taxon has changed over time, and several workers have published different taxonomic hierarchies of the protists with different classifications and subdivisions of the dinoflagellates.

Recently gene sequencing techniques have given taxonomists new insights into the classification of the protists. One of the most interesting discoveries is that the apicomplexans, dinoflagellates and ciliates form a single clade (Gajadhar *et al.*, 1991). Morphological resemblance between the three groups is slight and their nuclear organisation could not be more different. All that the three groups have in common is

Unlike many protists, dinoflagellates have an extensive fossil record dating from the late Precambrian (Fensome *et al.* 1993).

The taxonomy of the dinoflagellates (reviewed by Fensome *et al.* 1993) is confusing because they have been considered as plants or animals depending upon the discipline of the investigator, and hence classified under both Botanical and Zoological codes of nomenclature. Thus botanists traditionally refer to them as the Pyrrhophyta Pascher 1914 or Dinophyta while, in a recent zoological backlash, Cavalier-Smith (1981) has coined another alternative, the Dinozoa. The great importance of the photosynthetic dinoflagellates as primary producers in aquatic ecosystems and their lengthy fossil record in the past resulted in a classification of the dinoflagellates that largely followed the Botanical code of Nomenclature. It is now obvious, however, that dinoflagellates are basically heterotrophic protists some of which have secondarily acquired plastids and as this thesis is wholly concerned with parasitic heterotrophic dinoflagellates, the Zoological code will be followed here.

The term 'dinoflagellate' derived from the Order Dinoflagellata Bütschli, 1885 has remained a popular and convenient way of referring to this diverse group of protists. The content of this taxon has changed over time, and several workers have published different taxonomic hierarchies of the protists with different classifications and subdivisions of the dinoflagellates.

Recently gene sequencing techniques have given taxonomists new insights into the classification of the protists. One of the most interesting discoveries is that the apicomplexans, dinoflagellates and ciliates form a single clade (Gajadhar *et al.*, 1991). Morphological resemblance between the three groups is slight and their nuclear organisation could not be more different. All that the three groups have in common is

the alveolate cortex hence the adoption of the name Alveolata (Cavalier-Smith 1993) for the clade.

The position of the dinoflagellates within Cavalier-Smith's (1993) recently produced classification of living protozoa is illustrated in Figures 1.1 and 1.2.

Cavalier-Smith's phyla Dinozoa and Apicomplexa are contained within the Superphylum Miozoa. Members of these two phyla have a single type of haploid nucleus, in contrast to the Ciliophora which have separate diploid micronuclei and polyploid macronuclei. The Dinozoa are distinguished from the Apicomplexa by possession of flagellated asexual stages and lack of an apical complex of organelles associated with host cell penetration.

Cavalier-Smith's phylum Dinozoa contains the subphylum Dinoflagellata, comprising the dinoflagellates and the subphyum Protalveolata containing all non-dinoflagellate alveolate zooflagellates that lack a sporozoan-type apical complex. The Protalveolata includes the classes Colponemea, Oxyrrhea and Ellobiopsea. Previously the poorly-known ellobiopsids have often been treated as dinoflagellates, although their nuclear organisation and flagellar disposition do not support this classification. The subphylum Dinoflagellata contains five classes: Syndinea Chatton, 1920; Noctilucea Haeckel, 1866; Haplozooidea Poche, 1911; Peridinea Ehrenberg, 1830; and Bilidinea Cavalier-Smith, 1993. Three different patterns of chromatin organization are used to separate these classes. Cavalier-Smith's superclass Syndina contains the Syndinea which have histone-rich chromatin throughout their life cycle. The Haplozooidea and Noctilucea have histones in their vegetative cells but not in their reproductive cells and are grouped in the in the superclass Hemidinia. The Peridinea and the Bilidinea have typical dinokaryotic nuclei that lack histones throughout their life cycle and are grouped in the superclass Dinokaryota.

Dinozoa cannot therefore be used as a synonym for dinoflagellates, but can be used to describe flagellates with ampulliform tubular mitochondrial cristae and cortical alveoli, but lacking an apical complex.

Empire EUKARYOTA
Superkingdom 1. ARCHEZOA (lacking mitochondria)
Kingdom ARCHEZOA
Superkingdom 2. METAKARYOTA (possessing mitochondria)
Kingdom 1. PROTOZOA Goldfuss, 1818 emend. Owen, 1858/9 emend. Cavalier-Smith, 1987
Subkingdoms: 1.Adictyozoa (lacking a Golgi apparatus)
2.Dictyozoa Cavalier-Smith, 1991 (possessing a Golgi apparatus)
Infrakingdom 1. Euglenozoa Cavalier-Smith, 1981
Infrakingdom 2. Neozoa Cavalier-Smith, 1983
Parvkingdom 1.Ciliomyxa Cavalier-Smith, 1993
Parvkingdom 2. Alveolata Cavalier-Smith, 1991

Kingdom 2. PLANTAE
Kingdom 3. ANIMALIA
Kingdom 4. FUNGI
Kingdom 5. CHROMISTA

**Figure 1.1.** The position of the Alveolata within the Kingdom Protozoa (from Cavalier-Smith 1993).

Assemblage Alveolata Cavalier-Smith, 1991

Phylum1. DINOZOA Cavalier-Smith, 1981 emend.
Subphylum 1. Protalveolata Cavalier-Smith,1991
Class 1. Colponemea Cavalier-Smith, 1993
Class 2. Oxyrrhea Cavalier-Smith, 1987
Class 3. Ellobiopsea Loeblich III, 1970*
Subphylum 2. Dinoflagellata Bütschli, 1885, Dinophyta auct., Dinophyceae Pascher, 1914)
Superclass 1. Syndina Cavalier-Smith, 1993*
Class 1. Syndinea Chatton, 1920
Superclass 2. Hemidinia Cavalier-Smith, 1993
Class 1. Noctilucea Haeckel, 1866
Class 2. Haplozooidea Poche, 1911 (includes order Blastodinida Chatton, 1906)*
Superclass 3. Dinokaryota Cavalier-Smith, 1993
Class 1. Peridinea Ehrenberg, 1830
Subclass 1. Gymnodinoidia Poche, 1913
Subclass 2. Peridinoidia Poche, 1913
Subclass 3. Prorocentroidia Lemmermann, 1899
Subclass 4. Desmocapsoidia Pascher, 1941
Subclass 5. Thoracosphaeroidia Cavalier-Smith, 1993
Class 2. Bilidinea Cavalier-Smith, 1993

Phylum 2. APICOMPLEXA Levine, 1970 emend.
Subphylum 1. Apicomonada Cavalier-Smith, 1993
Subphylum 2. Gamontozoa Cavalier-Smith, 1993
Infraphylum 1. Sporozoa Leuckart, 1879
Infraphylum 2. Hematozoa Vivier, 1982

Phylum 3. CILIOPHORA Doflein, 1901

**Figure 1.2.** The position of the Syndinea and Peridinea within the Phylum Dinozoa of the Alveolata (from Cavalier-Smith 1993). Asterisk indicates groups in the Dinozoa that contain parasites. The Peridinea represent the most studied class of Dinozoa. The Syndinea which form the subject of this thesis have been poorly studied in comparison.

## 1.2. Parasitic dinoflagellates of crustaceans

Parasitic dinoflagellates, although little studied, infect a wide range of marine organisms including algae, protozoans, annelids, molluscs, salps, tunicates, rotifers, fish and crustaceans. There are over 2000 recognised species of dinoflagellates, and of these about 140 are parasitic (Drebes 1984). Pouchet (1884) presented the first definite evidence for the existence of parasitic dinoflagellates when he described *Gymnodinium pulvisculus* (= *Oodinium pouchetti* (Lemm.) Chatton) parasitizing appendicularian tunicates. Unfortunately Pouchet's discovery was not accepted by Bütschli and it was not until the beginning of this century that a scientific interest in the parasitic dinoflagellates was aroused. The French protozoologist Edouard Chatton was the undoubted pioneer of studies on parasitic dinoflagellates and produced a substantial monograph on them in 1920. This is still regarded as a valuable reference piece of work today. Chatton's students Jean and Monique Cachon have continued his work and provided much ultrastructural and cytological information over the last 30 years (Cachon and Cachon 1987). The taxonomy of the parasitic forms is still unsatisfactory, this is probably due to the lack of adequate descriptions and published figures of many species.

There are two orders of dinoflagellates which contain parasites of crustaceans, the Blastodinida Chatton, 1906, and the Syndinida Loeblich, 1976. The Blastodinida are contained within Cavalier-Smiths Superclass Hemidinia, and the Syndinida within his Superclass Syndina. The Blastodinida and Syndinida contain at least 25 recognised species of dinoflagellate that parasitize crustaceans. The Syndineans display a cellular organisation quite different from that of the better known Peridinian dinoflagellates.

A generalised life cycle of a parasitic dinoflagellate involves alternation between an aflagellate trophic or vegetative parasitic stage (the trophont) and a flagellated infective dinospore which has a characteristic morphology and resembles a free-living dinoflagellate in the arrangement of its flagella. After attachment to or entry into the host, the dinospore becomes a trophont and initiates the parasitic phase. The trophont increases in size or divides and increases in numbers and loses its flagella. The parasitic phase of development terminates in sporogenesis, the production of motile dinospores. Sporogenesis may be by three different mechanisms:

1. The simplest mechanism is found in the Syndinida. The multinucleate trophic plasmodia of the parasite divide to multiply in numbers until the final division when dinospores are produced.

2. In palintomic (Chatton 1938) sporogenesis feeding and the production of dinospores are not concurrent processes. Palintomy, which is commonly observed in *Chytriodinium* is characterised by the trophic stage of the parasite remaining uninucleate but growing in size. When the parasitic phase is ended and the trophont has reached its maximum size nuclear and cytoplasmic divisions take place without interruption and dinospores are formed.

3. In the third mechanism of sporogenesis feeding and the production of dinospores are concurrent processes. The trophont divides into a trophocyte and gonocyte. The gonocyte divides without interruption to form dinospores. The trophocyte continues to grow and only divides again later. A single trophont can therefore produce several generations of dinospores. Chatton (1906) termed this mechanism 'palisporogenesis' which is commonly observed in *Blastodinium*.

As so little has been published on the life cycles of the Syndinea, compared with the Blastodinida, some background on the latter is given for comparison with the development of the syndinean *Hematodinium* that is discussed in this thesis.

**Class Haplozooidea Poche, 1911**

**Order Blastodinida Chatton, 1906**

Of the seven families forming the Blastodinida (Cachon and Cachon 1987) the two containing parasites of crustaceans will be described below.

Family Blastodinidae

Members of this family are extracellular marine parasites, possess plastids and occur in the gut of copepods. The nucleus is a dinokaryon for only part of the life-cycle (Cachon and Cachon 1987). The parasitic stage is unique amongst the Blastodinida in that it is not attached to the host. Palisporogenesis is the usual method of sporogenesis, involving division of the initial parasitic cell into a trophocyte and gonocyte. The dinospores are oval with a well marked transverse girdle (cingulum), and may have a longitudinal groove (sulcus) and possess plastids.

As in the case of other parasitic dinoflagellates, the life cycle of *Blastodinium* has not been fully elucidated. Chatton (1920) suggested that dinospores were ingested by the early stages of the copepod. A trophont develops from the dinospore, and divides into a trophocyte and a gonocyte. The gonocyte undergoes sporogony to form a series of sporocysts. Each generation of sporocysts is enclosed in a cuticle that dehisces during sporulation The trophocyte continues to grow and only divides much later to form sporocysts. At sporulation immature spores lacking flagella are expelled with the faeces and develop into mature dinospores. The dinospores encyst after 1-2 days, but

later stages of the life cycle are unknown. The trophocytes of *Blastodinium* spp possess well developed chloroplasts with photosynthetic activity. Pasternak *et al.* (1984) calculated that the energy produced by photosynthesis was about 50% of the energy budget of the parasite. The pusule is generally well developed in members of the Blastodinida.

Host castration is a common result of infection by *Blastodinium* spp. This could be due to the drain on host resources by the parasite or the mechanical pressure of the parasite on internal organs.

Family Chytriodinidae

There is a lack of ultrastructural data on this family to allow full comparison with the Blastodinidae or Syndinidae. Four genera in the Chytriodinidae parasitize crustaceans : *Chytriodinium*, *Schizochytriodinium*, *Dissodinium* and *Syltodinium*. Members of the Chytriodinidae live as ectoparasites on the eggs of copepods, euphausiids and penaeid shrimps. *Chytriodinium* spp. and *Syltodinium listii* undergo palintomy and *Schizochytriodinium calani* undergoes palisporogenesis.

In the general life cycle of the Chytriodinidae the dinospore attacks the host egg, eventually penetrating the thick chorion with a hypocone (stalk). On reaching the embryo the hypocone develops a holdfast-like anchor which contains a small band of hooks and the feeding apparatus or ampulla. After penetration by the hypocone the egg is consumed by the parasite within 1-2 hours. After the egg is consumed sporulation occurs. The dinospores are produced in long chains that dissociate before they develop 2 flagella. They lack plastids (except dinospores of *Dissodinium pseudolunula*).

Resting cysts have been found for *D. pseudolunula* (Stosch 1973, Drebes 1981, John and Reid 1983).

It has been suggested that the impact of egg parasites on the reproductive output of their hosts may hinder the population growth of that species (Wickham 1986).

## 1.3. Class Syndinea Chatton 1920

The class Syndinea contains a single order, Syndinida. Four families are found within the Syndinida, with the Syndinidae containing parasites of other protists such as radiolarians or algae, fish eggs and crustaceans. Members of the Syndinea are nonphotosynthetic marine osmotrophic parasites that are extracellular in the body cavities, or intracellular in the cytoplasm or nucleus of their hosts. Throughout most of their complex developmental cycles they are syncytial and bear no resemblance to classic Peridinian dinoflagellates in their appearance. They are regarded as dinoflagellates largely because of the dinoflagellate appearance of the dinospore which possesses two heterodynamic flagella. There are no fossil records for the Syndinea.

The mechanism of sporogenesis in the Syndinea is probably the simplest among the parasitic dinoflagellates. The parasite increases the size and numbers plasmodia until sporogenesis when biflagellated dinospores are formed. Some species produce spores of two different sizes (macro and microspores) which arise from different parent individuals (Chatton 1920, Jepps 1937, Meyers *et al.* 1987).

The chromosomes of the Syndinea never display the arched fibrillar structure characteristic of the free living dinoflagellates. Table 1.1 summarizes the differences between the parasitic Syndineans and the free-living Peridineans. Ris and Kubai (1974) studied the nuclear structure and division of *Syndinium*-like parasites found in the

colonial radiolarians. At this time Ris and Kubai found several dissimilarities between the nuclear division of *Syndinium* (4-6 chromosomes) and the free living dinoflagellates (20-300 chromosomes) : (a) an extranuclear spindle developed between typical centrioles during nuclear division, (b) the sites of chromosome-nuclear membrane attachment were highly differentiated dense disks (kinetochores) which were connected to the centrioles by a bundle of microtubules, and, (c) the chromosome-membrane attachments and the microtubules joining them to the centrioles persisted throughout the entire cell cycle.

Four genera of the Syndinidae parasitize crustaceans : *Actinodinium*, *Trypanodinium*, *Hematodinium* and *Syndinium*. There have been no significant investigations on *Actinodinium* or *Trypanodinium* since their original descriptions (Chatton and Hovasse 1938, Chatton 1952).

*Actinodinium apsteini* is found in the stomach wall of its copepod host *Acarti clausi*. A large trophocyte (75-125µm) projects numerous cytoplasmic rays into the haemal sinuses and lumen of the stomach (Chatton and Hovasse 1938).

*Trypanodinium ovicola* parasitizes several species of copepod eggs (Chatton 1920). It is thought that a host egg becomes infected when a swimming dinospore enters it. A plasmodium develops internally in the embryo and sporulation occurs when the contents of the egg are depleted. Little more is known about other members of these two genera.

*Syndinium*

Members of the genus *Syndinium* are primarily intracytoplasmic or intranuclear parasites of radiolarians and other protists. *Syndinium globiforme* and *Solenodinium fallax* both parasites of radiolarians have been most intensely studied (Chatton 1920, 1923, Hollande and Enjumet 1953, 1955).

Three species of *Syndinium* parasitize crustaceans and are found in the haemal sinuses and soft tissues of their hosts.

During the trophic phase they lose the dinoflagellate morphology of the dinospores : the flagella disappear, although the basal bodies remain. The amphiesma remains unchanged; there are polysaccharide and lipid inclusions, mitochondria with poorly developed cristae and trichocysts in the cytoplasm.

The type species *S. turbo* (Chatton 1920) was originally found in the haemal sinuses of copepods. More recently another species *S. gammari* was described from the haemal sinuses of the amphipod *Gammarus locusta* (Manier *et al.* 1971). It is presumed that copepods acquire an infection by ingesting dinospores. A parasite penetrates the gut wall and a plasmodium develops between the intestinal epithelial cells and the basal lamina (Chatton 1920, Jepps 1937). A host capsule forms around the plasmodium, but the plasmodium protrudes through it and eventually ramifies throughout the cavity of the host, filling all the haemal sinuses before sporulation. As the plasmodium grows it insinuates itself in the muscles, dorsal nerve ganglion and the gonad which is destroyed. The plasmodium appears to exert a considerable pressure on the internal organs (Jepps 1937) and in the advanced stages the muscle and other organs degenerate and lyse.

Sporulation takes less than two hours with the formation of macrospores and microspores. The spores have a cingulum and sulcus, have two flagella and trichocysts.

The dinospores escape from the host through a slit in the cuticle near the antennae but their fate after that is unknown.

Epizootics of *Syndinium* spp have been reported from Loch Striven, Scotland, the Gulf of Naples, south east Australia and the Mediterranean sea (Chatton 1920, Marshall *et al.* 1934, Ianora *et al.* 1987, 1990, Kimmerer and McKinnon 1990). Prevalences of up to 30% have been found, and the mortality rates of infected copepods were higher than uninfected copepods (Kimmerer and McKinnon 1990).

| | Class **Peridinea** | Class **Syndinea** |
|---|---|---|
| Nutrition | Photosynthetic species containing chlorophylls a and $c_2$ , non-photosynthetic phagotrophs. Both auto and heterotrophic forms found living as symbionts/parasites on or in other organisms | Totally non-photosynthetic, Osmotrophic nutrition; all known forms parasitic |
| Form | Displays typical dinoflagellate features of paired flagella which beat in characteristic surface furrows | Typical dinoflagellate features only revealed in the uninucleate zoospore (dinospore), the parasitic multinucleate phase does not display all these features |
| Amphiesmal morphology | Amphiesmal alveoli may contain thecal plates (armoured) formed from cellulose | Amphiesmal alveoli do not contain thecal plates (naked), and are absent in intracellular parasites |
| Chromosomes | Many chromosomes (14-400), condensed, contain arched whorls of chromatin fibres, poor in histones, attached to nuclear envelope | Low chromosome numbers (4-10), condensed, no whorls, histones easily detected, chromosomes V-shaped apex attached to nuclear envelope |
| Mitosis | Spindle extranuclear, no centrioles present, many membrane-lined microtubule-containing cytoplasmic tunnels pierce the dividing nucleus | Spindle extranuclear permanent centrioles associated with mitotic division, only one microtubule-containing membrane-lined tunnel piercing the dividing nucleus |
| Sexuality | Sexuality is known, with flagellated isogametes, zygotic meiosis, so that vegetative stage haploid | Sexuality questionable, vegetative stage haploid, dinospores do not appear to be gametes, |
| Cyst formation | Cysts formed by many | None described |

**Table 1.1.** A table outlining the major differences between members of the class Peridinea and the class Syndinea.

## 1.4. *Hematodinium*-like parasites of crustaceans

The members of the genus *Hematodinium* are primarily parasites of the brachyuran decapod crustaceans. There are at present two described species of *Hematodinium*.

The type species *Hematodinium perezi* was originally described by Chatton and Poisson (1931) from the haemolymph of the portunid crabs *Carcinus maenas* and *Liocarcinus depurator* from France. It was found in only 3 of 3500 crabs examined and detailed microscopic studies of this type species do not exist. They observed both multinucleate vermiform plasmodia and uninucleate vegetative forms circulating in the haemolymph. Their identification of the parasite as a Syndinean was based on the similarities between *Hematodinium* and *Syndinium*. These were as follows:

1. The plasmodial nature of the organism.
2. The presence of trichocysts in the cytoplasm.
3. The dinokaryon type of nucleus containing five chromosomes arranged in V-shapes, and an apparent absence of a nuclear membrane.
4. The identical appearance of the chromosomes of the two genera.
5. The continual state of mitotic activity of the nucleus.
6. The type of mitosis exhibited.

Although the macro and microspores of *Syndinium* had been described previously (Chatton 1920) Chatton and Poisson (1931) did not observe the dinospores of *Hematodinium*.

The second species, *Hematodinium australis*, has recently been described by Hudson and Shields (1994) from the portunid crab *Portunus pelagicus* in Australia. Dinospores have not been observed in this species either.

Since Chatton and Poisson created the genus, *Hematodinium*-like dinoflagellates have been identified in a wide range of host species from several geographic regions. More recently *Hematodinium* sp has been found in up to 30% of adult blue crab, *Callinectes sapidus* from coastal areas of North Carolina, Georgia and Florida, USA (Newman and Johnson 1975). Rare infections have been found in *Cancer irroratus*, *C.borealis* and *Ovalipes ocellatus* from the New York Bight area of the north-eastern United States (MacLean and Ruddell 1978). From the west coast of France *Hematodinium*-like organisms have been reported in 21% of *Cancer pagurus* (Latrouite *et al.* 1988) and 87% of *Necora* (=*Liocarcinus*) *puber* (Wilhelm and Boulo 1988).

On the eastern seaboard of Australia *Hematodinium* sp infects the sand crab *Portunus pelagicus* (Shields 1992), the mud crab *Scylla serrata* (Hudson and Lester 1994) and the coral crab *Trapezia aerolata* (Hudson *et al.* 1993).

The most informative study of a *Hematodinium*-like dinoflagellate has come from the commercially fished populations of Tanner crabs (*Chionoecetes bairdi* and *C. opilio*) in the Bering Sea and south-east Alaskan waters (Meyers *et al.* 1987, Meyers 1990, Meyers *et al.* 1990, Eaton *et al.* 1991). The processed meat from infected crabs had a bitter taste and was subsequently unmarketable. Prevalences of up to 95% were found in *C.bairdi*. The ultrastructure of both macro and microspores was reported by Meyers *et al.* (1987).

Outside the decapod crustacea a syndinid dinoflagellate similar to *H. perezi* in the appearance of the plasmodia, chromosomes and mitosis has been found in 13 benthic amphipods (Johnson 1986). In addition Bower and colleagues (Bower *et al.*

1993) have reported a *Hematodinium*-like protozoan in the spot prawn *Pandalus platyceros* from British Columbia. Meyers *et al.* (1994) also reported a dinoflagellate-like parasite in *P. platyceros* and in *P. borealis*.

The taxonomy of the genus *Hematodinium* needs further investigation. The dinospore, which may have taxonomic value has not been observed in the type species *H. perezi* or in *H. australis*, and has only been observed in the *Hematodinium* infecting *C. bairdi*. The lack of morphological differences between stages of parasites that have been described also complicates any further classification. The reasons given for assigning *Hematodinium australis* from the sand crab in Australia species status were the differences based upon (a) the size of the vegetative stage, (b) morphology of the plasmodium, (c) appearance of the chromosomes, (d) various life-history parameters, (e) the geographic location, and (f) a different host, *Portunus pelagicus*. No cross-infection studies were undertaken with *Carcinus maenas* or *Liocarcinus depurator*.

Further investigation will be required to establish the relationships between the *Hematodinium* spp so far described.

## 1.5. The discovery of *Hematodinium* infections in *Nephrops norvegicus* off the west coast of Scotland

The Norway lobster *Nephrops norvegicus* (L.) forms a commercially important fishery off the west coast of Scotland. First sale prices of the large trawl fishery are valued at £20 million per annum. These Astacidean decapod crustaceans live in burrows on mud bottoms at 10-800m and emerge at dawn and dusk to feed. They are caught either by trawling or by entrapment in creels on the sea floor. During the early 1980s, routine investigations into the biology of *N. norvegicus* in the Firth of Clyde

produced observations of a low incidence of lobsters which had an abnormal opaque appearance instead of the more healthy translucent look. The abnormal individuals were in a moribund state, had low haemolymph pressure and milky white haemolymph. From counts of total cell numbers in the haemolymph it was concluded that the abnormal white colour of the haemolymph in severely affected lobsters was due to an increase in cell numbers.

Field *et al.* (1992) reported that examination of haemolymph from abnormal lobsters led to the discovery of non-motile protistan parasites. The parasites were identified as dinoflagellates of the Order Syndinida, and resembled *Hematodinium perezi* Chatton and Poisson (1931), which is known to infect only brachyuran decapod crustaceans. The majority of the dinoflagellates were uninucleate. Also present were multinucleate plasmodial cells and multinucleate 'vermiform' cells closely associated with host tissue. Mitotic figures revealed the distinctive 'v'- shaped chromosomes typical of the dinokaryon nucleus of dinoflagellates (Cachon and Cachon 1987). The irregularly shaped parasite cells from infected haemolymph were between 6 and 10μm in diameter. The amphiesmal alveoli did not contain thecal plates, nor were there microtubules reinforcing the innermost membrane. Nuclei were bounded by a double membrane nuclear envelope and the chromosomes did not display a fibrillar organization of the DNA. The mitochondria showed the tubular cristae characteristic of the dinoflagellates, and chloroplasts were absent. Large numbers of parasites caused severe distention of the haemocoel and haemal spaces. Flagellated dinospores were not observed.

The poor quality and watery appearance of the tail muscle had by 1987 evoked comment from the fishermen and food processors. At least one catch of *N. norvegicus* in the Clyde has been refused at market due to poor meat quality. Following this, a

sampling programme to define more precisely the seasonality of occurrence and geographical extent of this condition around the west coast of Scotland was instigated by the Scottish Office Agriculture and Fisheries Department (SOAFD).

The prevalence of abnormal of *N. norvegicus* showed a marked seasonal pattern, being confined to the period between February and July (encompassing the annual moult), with peak numbers occurring between March and May. Females were found to exhibit a higher prevalence than males, and individuals of 25-35mm carapace length were most likely to be affected. Survey results suggested that there was a background level of abnormality (10-15%) over much of the west coast of Scotland, but in the North Clyde Sea area the proportion of affected lobsters was much higher and has been observed to reach 84.6% (Field *et al.* 1992). Survival experiments showed a higher mortality in affected *N. norvegicus* compared with healthy individuals (Field *et al.* 1992). In the summer of 1992 Professor K. Vickerman established a protocol for the *in vitro* culture of *Hematodinium*.

In order to further investigate the biology of this Syndinean dinoflagellate and its impact on the fishery a contract was awarded by the Ministry of Agriculture Fisheries and Food (MAFF) to continue investigations into this potentially serious pathogen.

## 1.6. Aims of project

The aim of this project was to produce as far as possible a structural and functional account of the parasite's developmental cycle. Much of the work presented here was in part fulfilment of a MAFF contract to investigate the infection of *N. norvegicus* by *Hematodinium*.

The questions that I wish to address are as follows:

1. What is the systematic position of the organism associated with *Nephrops* mortality? Why is it described as a Syndinean and how does the parasite conform to the definition of its Class? How does it differ from other described *Hematodinium* spp? Do the Syndinea show relationships with other groups? (e.g. Apicomplexa)

These questions will be answered by comparing morphological and descriptive data with existing published work.

2. What is the developmental cycle in the crustacean host? Do particular stages occur at particular times of the year? What are the characteristics of each stage? What is the rate of development of the infection *in vivo*?

A preliminary histological examination of the major organs of infected *Nephrops* has already been carried out (Field *et al.* 1992). A more detailed investigation at the light and electron microscopical level was intended to elaborate on this in order to identify and characterize parasite forms found in the host. It was also intended to try and follow the time course and progression of the disease to gain an insight into the life cycle of the parasite.

3. Does *in vitro* development reflect that *in vivo*?

In order to observe and characterize the developmental forms of *Hematodinium in vitro* I was to obtain new isolates for axenic culture.

4. What is the evidence associating the parasite with disease? Is the host able to control infections? How is the parasite transmitted from host to host?

Initial estimates of host mortality (Field *et al.* 1992) suggested that infection of *N.norvegicus* by *Hematodinium* sp caused significant mortality. My intention was to closely observe infected lobsters to determine how far the infection progressed in individual lobsters. I also intended to see if lobsters made any attempt at controlling the infection and if any were able to overcome it. Koch (1891) first presented a procedure for demonstrating the ability of an organism to cause disease. I intended to try and fulfil Koch's postulates by showing that the parasites serially cultivated *in vitro* could, on inoculation into healthy hosts, reproduce the characteristic disease symptoms.

# CHAPTER 2

# ISOLATION, SERIAL *IN VITRO* CULTIVATION AND DEVELOPMENTAL CYCLE *IN VITRO* OF *HEMATODINIUM*

## 2.1. INTRODUCTION

### 2.1.1. Previous work on the cultivation of parasitic dinoflagellates.

The culturing of free-living dinoflagellates has become routine practice, but the culturing of parasitic forms has proved difficult. The first free-living colourless dinoflagellate to be maintained axenically was *Crypthecodinium cohnii*. It was cultured in a medium consisting of peptone, yeast autolysate and acetate (Pringsheim 1956); a defined medium for this species was reported in 1962 (Provasoli and Gold).

*Chytriodinium parasiticum* has been maintained in culture for short periods (Cachon and Cachon 1968). Parts of the life cycle of *Dissodinium* have been observed in culture (Drebes 1978, 1984). No parasitic dinoflagellates have been maintained in culture for extended periods however.

There is only one account of the *in vitro* culture of a *Hematodinium*-like dinoflagellate, and this is that of Meyers *et al.* (1987) from the Tanner crab *Chionoecetes bairdi* in Alaska. The Tanner crab *C. bairdi* is a commercially important species in south-eastern Alaska. During 1985 a number of catches of Tanner crabs contained many individuals which on consumption had a bitter aftertaste. The affected crabs were found to contain a dinoflagellate parasite resembling *Hematodinium perezi*. Meyers *et al.* (1987) used haemolymph from

healthy crabs as the culture medium. Uninfected haemolymph was allowed to clot, centrifuged and finally passed through a 0·45μm filter. The parasite was found to be resistant to a mixture of the antibiotics- penicillin (100 IU $ml^{-1}$), streptomycin 100μg $ml^{-1}$) and amphotericin B (0·25μg $ml^{-1}$). Subculture of the parasite was carried out using unfiltered aseptically collected haemolymph containing the antibiotics. The cultures were incubated at 4 to 6 °C.

The initial inocula were circulating parasites from crab haemolymph. The parasites consisted of a range of round to oval single cells, multinucleate aggregates and binucleate forms. Host haemocytes were usually present in considerable minority to the parasite. The parasites had an uneven surface, were non motile and their cytoplasm contained several distinct round inclusion bodies. Within a few days of seeding the culture the circulating stages attached to the culture vessel, and in 12 to 15 days formed incomplete monolayers. Soon after this the cells detached from the vessel base and remained suspended in the culture fluid. After 19 days the parasite was centrifuged from the medium and subsequently resuspended in fresh Tanner crab haemolymph. It was possible to generate second, third and fourth generation dinoflagellate cultures in this way, with the monolayers becoming confluent in 15 to 18 days. It was found that if left undisturbed the cultures were able to survive for months.

Occasionally monolayers were not formed, but the parasites clumped together, these aggregates would periodically attach to the culture vessel by 'pseudopodia'. As the cells aged some became hypertrophied, suggesting degeneration of that cell.

One isolate started to produce microspores after 35 days in culture; sporulation was not simultaneous or complete, and those cells which did not

sporulate later died. Microspores eventually developed a bent corkscrew shape and possessed a refractile inclusion at the posterior end

Oval-shaped macrospores also developed after 25 days in one haemolymph culture. They were reported to change morphology by developing a keel-like structure and a beak-like protrusion at one end; many eventually settled onto the vessel surface attaching by extended pseudopodia to form large clumps of non-motile cells. These attached clumps were accompanied by chains of non-motile parasites loosely attached to the flask in a circular pattern.

The detail of the *in vitro* culture of *Hematodinium* reported by Meyers *et al.* (1987) was limited. The nature of the parasites isolated and the developmental stages obtained in culture were not characterised other than the macrospores and microspores.

### 2.1.2. Present work

The use of host haemolymph for the culture of *Hematodinium* as described by Meyers *et al.* (1987) was considered, but discounted for several reasons in the present project. First, the supply of healthy *Nephrops* was not always reliable throughout the year, and the aquarium available had very limited holding space. Second, the amount of haemolymph that can be extracted from each *Nephrops* is usually only 1-3ml depending on the size of the lobster, moreover filtration of the haemolymph, even through a 0·45µm filter proved extremely difficult and time consuming. Lastly, the appearance of healthy haemolymph varied widely between individual lobsters; this variation was

probably dependent on the stage in the moulting cycle and nutritional status of the lobster.

Concluding that a constant and consistent supply of sterile haemolymph could not be easily produced, Professor K. Vickerman experimented with several artificial media during the summer of 1992 and decided upon a medium consisting of 10% foetal calf serum in a *Nephrops* saline.

In this chapter I present an account of the *in vitro* culture of *Hematodinium sp.* from *Nephrops norvegicus.* I include a description of the different developmental stages of the parasite that were observed. I present evidence that the foetal calf serum medium allows indefinite serial cultivation of *Hematodinium* from *Nephrops* and that a sequence of developmental stages are obtained *in vitro*. This *in vitro* development may help towards the understanding of the development of the parasite in nature.

## 2.2. MATERIALS AND METHODS

### 2.2.1. Experimental lobsters

Lobsters were caught by trawling on grounds around the Isle of Cumbrae, Clyde Sea Area, Scotland, and transported to the Zoology Department, University of Glasgow, where they were maintained in well-aerated seawater. Three isolates were derived from infected lobsters caught in the Irish Sea. The aquarium water temperature ranged between 10 and 13°C and the salinity between 33 and 34‰. Lobsters were fed *ad libitum* on squid and mussel flesh. The chelipeds of the lobsters were immobilised with elastic bands to prevent fighting and cannibalism.

During the course of this investigation it was found that infected lobsters were very sensitive to the conditions under which they were kept. Before February 1995 I had great difficulty in maintaining infected lobsters for more than 24 hours in the Zoology Department aquaria. I believe that this was due to the poor water quality and a higher-than-optimum water temperature. From February 1995 infected lobsters were kept in a new separate closed seawater system. The seawater temperature was kept at a constant 10°C and water quality was closely monitored. An ultra-violet sterilising unit was built into the system to reduce the problems of secondary bacterial and protozoan infections which had previously claimed large numbers of lobsters.

### 2.2.2. Diagnosis of infection

The diagnosis of infected animals for use in the *in vitro* culture of the parasite was by external appearance of the host animal and by pleopod examination. They are described here in order of sensitivity.

#### 2.2.2.1. Diagnosis by external appearance of the lobster

Only advanced stages of infection could be diagnosed from the external appearance of the lobster. Heavily infected lobsters were recognised by the dull opaque orange colouration of the body and appendages in contrast to the translucent appearance of healthy animals. In severely-infected animals the outline of the heart was clearly visible beneath the dorsal thoracic cuticle and the arthrodial membranes gave the appearance of being yellow or white, due to the

underlying change of haemolymph colour caused by parasite cell proliferation (Field *et al.* 1992, Field and Appleton 1995). The yellowing or whitening of the arthrodial membranes was best observed at the claw joints or on the ventral side of the abdomen. Mild infections were difficult to diagnose by this method alone. Infected individuals were also in a moribund state (little activity, slow moving) compared with healthy lobsters.

#### 2.2.2.2. Diagnosis by pleopod examination

Diagnosis of infection was made more accurately by the microscopic examination of the pleopods under transmitted light, when aggregations of the parasite were visible as darkened areas. In this examination a degree of severity could be assigned to the infection from the extent of parasite aggregation beneath the cuticle of the pleopod. Severity was measured on a scale from I to IV (0 for uninfected animals) (Field *et al.* 1992, Field and Appleton 1995). If the lobsters were to be sacrificed, a whole pleopod could be removed for examination. If the animals were to be returned to the aquarium, however, it was possible to examine a pleopod *in situ*. Moult staging was carried out as defined by the moult staging technique of Aiken (1980).

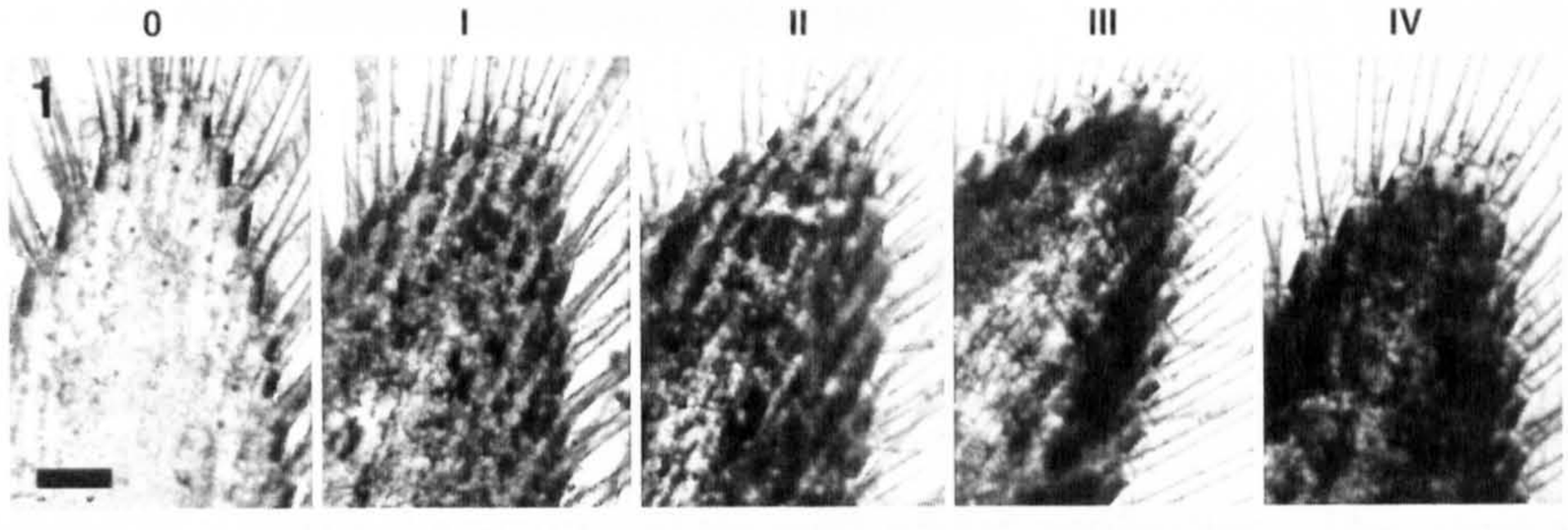


Light micrographs showing the appearance of pleopods of healthy and *Hematodinium*-infected lobsters. 0 = uninfected, I = slight infection, IV = heavy infection. Scale bar = 0.5mm. From Field and Appleton 1995.

### 2.2.3. Isolation of the parasite from *N. norvegicus*

Infected lobsters were removed from the aquarium and narcotised on ice for approximately 30 minutes. The ventral surface of the lobster was then swabbed with 70% ethanol while placed in a laminar flow hood. Haemolymph samples were collected from the base of a fifth pereiopod using 1ml sterile disposable syringes fitted with 25 gauge needles. The infected haemolymph was then transferred directly into the appropriate medium.

During the course of this investigation it was found possible to remove infected haemolymph from recently dead lobsters. For cultivation experiments the use of infected haemolymph from dead lobsters was necessitated by the fact that early in the investigation infected lobsters did not survive long in the aquarium and that during 1993 and 1994 both total catches of lobsters and catches of infected lobsters were low (Field *et al.* 1995).

### 2.2.4. *In vitro* culture medium and conditions

The culture medium consisted of 10% foetal calf serum (Labtech International Ltd., Uckfield, East Sussex, UK) heat inactivated at 56°C for 30 minutes in a sterile *Nephrops* saline with added antibiotics. The composition of the saline was as follows:

| | $g\ l^{-1}$ |
|---|---|
| NaCl | 27.99 |
| KCl | 0.95 |
| $CaCl_2$ | 2.014 |
| $MgSO_4$ | 2.465 |
| $Na_2SO_4$ | 0.554 |
| HEPES | 1.192 |

The saline was made up in double distilled water, the pH was adjusted to 7.8, and then autoclaved in 500ml glass bottles. The antibiotic Gentamycin (Sigma) was routinely added to the culture medium at a concentration of 25µg $ml^{-1}$. Initial isolates were incubated in medium containing benzylpenecillin (Britannia) at a concentration of 200µg $ml^{-1}$ in addition to the gentamycin.

Cultures were grown in either 3.5cm diameter well plates (Corning or Greiner), each well containing 5ml of medium, or in small 25ml triangular culture flasks (Corning) containing 10ml medium. Cultures were incubated in the dark at 8-10ºC.

The cultured dinoflagellates were usually subcultured into fresh medium every 2-4 weeks, however longer periods sometimes elapsed between transfers.

### 2.2.5 Microscopical methods for the examination of *in vitro* cultures

#### 2.2.5.1. Examination of living cultures

Cultures in well plates and flasks were routinely examined and photographed on inverted microscopes (Leitz and Zeiss) employing phase contrast optics. Care had to be taken not to allow the culture vessel to warm up to room temperature (20ºC); this limited the time during which each culture could be observed.

Dinospores were vitally stained with the fluorescent dye acridine orange (0.01% in *Nephrops* saline) and examined with a Zeiss Axioskop compound microscope employing ultra-violet epifluorescence through a fluorescein filter set.

#### 2.2.5.2. Examination of fixed dinoflagellates

Cultured parasites were centrifuged at 150g. for 5 minutes, washed in *Nephrops* saline and centrifuged again. The parasites were resuspended in a glutaraldehyde/paraformaldehyde mixture (see Chapter 3) and fixed for 30 minutes at 4°C. Fixed parasites were centrifuged and washed before mounting in DAPI (4',-6-diamidino-2-phenylindole, 10µg $ml^{-1}$ in phosphate buffered saline) and subsequently examined with a Zeiss Axioskop compound microscope employing ultra-violet epifluorescence through a DAPI filter set.

## 2.3. RESULTS

### 2.3.1. Initial isolation of *Hematodinium* from lobster haemolymph

The parasitic forms used to initiate cultures were usually those found in the haemolymph. Infected haemolymph had a milky white opaque appearance in contrast with the translucent blue colour of uninfected haemolymph. Parasites from the haemolymph were uninucleate or multinucleate 12-33μm in diameter, with a refractile appearance and an irregular contour when viewed with phase contrast microscopy (Figure 2.1). It was found that to initiate a viable culture only one or two drops (50-100μl) of infected haemolymph were sufficient in each well. After several minutes in the culture well, the host haemocytes were easily distinguished because they had spread on the bottom of the well, but the dinoflagellates had not (Figure 2.1). If there were very few host haemocytes present they spread randomly over the bottom of the well, however if there was a larger number of haemocytes they aggregated together but did not appear to multiply. The number of haemocytes that was present in the infected haemolymph was dependent on the infection status of the lobster. In infection stage I and II lobsters, 30-80% of the total cells were haemocytes, and in infection stage III and IV lobsters only 3-25% of cells were haemocytes (Field and Appleton 1995).

### 2.3.2. Contamination problems during isolation

Haemolymph removed from dead lobsters contained cellular elements, almost entirely composed of dinoflagellates, however bacterial growth was common in lobsters that were not recently dead. It was possible to culture the parasite from dead lobsters though a large number of these cultures were eventually discarded due to

contamination. The use of two antibiotics usually prevented bacterial growth in the initial isolates; unfortunately on several occasions it was not sufficient and cultures had to be discarded. Contamination of initial isolates by fungi and yeasts occurred occasionally and if identified in the early stages could be removed by serially diluting the culture. Contamination of infected haemolymph with protists other than *Hematodinium* was the most serious problem. Initial isolates often became contaminated with a *Paranophrys*-like ciliate which thrived in the culture medium. The ciliates appeared to attack and eventually devour the *Hematodinium* until only ciliates remained. Attempts to dilute out the ciliate were rarely successful and eventually cultures had to be discarded. More careful washing of the external cuticle with 70% ethanol did help, however but did not totally cure the problem. This suggested that in many cases the ciliates were present on the cuticle of lobsters and also in the haemolymph. The problem of contaminating ciliates was almost exclusively confined to lobsters that had been held in the Zoology aquaria; on only one occasion were ciliates observed in the haemolymph of a lobster that was examined immediately post-capture. Other cultures contained contaminants such as *Protaspis* (Thaumatomonadida) and *Rhynchopus* (Euglenozoa). These were presumed to be part of the rich epifauna of the crustacean cuticle.

### 2.3.3. Parasite forms present in early *in vitro* cultures

Refer to Figure 9.1 for a schematic developmental cycle of *Hematodinium in vitro*.

The parasite cells when placed into culture medium usually developed in one of two ways. In the first, the parasites clumped together to form large aggregations which persisted until eventually dispersing as sporogenic cells which gave rise to motile flagellated dinospores (Figures 2.2, 2.3). In the second, the parasites formed small

clumps of multinucleate cells which extended thin cytoplasmic threads from their base after 24 hours. I observed that the dinoflagellate cells did not produce these syncytia if large numbers of haemocytes had aggregated on the bottom of the well, but remained as large aggregations. If a syncytial network did develop, the cytoplasmic threads did not grow near the spread host haemocytes but formed a network avoiding them (Figure 2.4). The cytoplasmic threads grew out radially from the aggregations of cells and by repeated branching formed a spider's web-like or 'arachnoid' stage.

The arachnoid syncytia displayed varying degrees of complexity. In some instances the cytoplasmic threads were very thin and not attached to the substrate (Figure 2.5), in other forms the cytoplasmic threads were flattened and attached (Figure 2.6). Aggregated nuclei were often present in condensed masses of cytoplasm but were also visible along the cytoplasmic threads of the network (Figure 2.7). If the parasite aggregations were evenly dispersed in the well, each aggregation produced a discrete arachnoid syncytium. This was usually circular, with a large aggregation of cytoplasm and nuclei at the centre and the cytoplasmic threads radiating outwards in a branched manner (Figure 2.8). Sometimes the cytoplasmic threads from neighbouring arachnoid syncytia would meet and fuse, forming a large syncytial network which was often several millimetres in diameter.

### 2.3.4. *In vitro* sporogenesis of *Hematodinium*

Isolates from heavily infected animals (stages III-IV) often produced dinospores within 24 hours, but isolates from less severely infected lobsters often took several weeks to complete sporogenesis (the production of dinospores). Two types of dinospore were produced, a larger macrospore (16-20μm long) and a smaller

microspore (11-14μm long). In each isolate only one type of dinospore was generated. The identification of the dinospores to type was not always easy because some isolates produced spores that were not obviously one type or the other. The following data and descriptions refer to isolates that produced spores of a clearly recognisable type. Of the 40 isolates that were satisfactorily cultured, 8 survived to produce macrospores and 7 to produce microspores.

Isolates from stage IV infected lobsters that produced macrospores began sporogenesis within 4 days of isolation. Isolates from stages I-III infected lobsters began macro-sporogenesis between 16-155 days after isolation (Table 2.1). Sporogenesis of isolates from heavily infected lobsters was often completed in 24 hours but sometimes took up to seven days. Replicate isolates did not always begin sporogenesis at the same time, some wells began sporogenesis up to 23 days after other wells. Macrospores were produced directly from both aggregates of parasites (Figure 2.3) and arachnoid syncytia (Figure 2.9 a, b), however, they were more likely to be produced from arachnoid syncytia the longer the period between isolation and the start of sporogenesis.

Isolates from stages III and IV infected animals that produced microspores started sporogenesis 22 days after isolation and isolates from stage I and II infections produced microspores 24-32 days after isolation (Table 2.1).

During late sporogenesis aggregates of parasites began to disperse, and tri- and quadrinucleate sporogenic cells in the final stages of division and possessing flagella appeared (Figure 2.10). These sporogenic cells could be observed spinning on the bottom of the well before finally dividing to produce uninucleate dinospores (Figure 2.11).

Before sporogenesis, arachnoid syncytia changed appearance over a period of several days. The network of cytoplasmic threads contracted and the number of branches decreased, with each thread becoming more flattened. Nuclei became numerous and prominent among the network of cytoplasmic threads; the central mass of nucleated cytoplasm gave the appearance of being composed of an aggregate of parasites. Multinucleate sporogenic cells (sporoblasts) were formed from the central mass of the arachnoid colony and these gave rise to dinospores in the manner described above (Figure 2.9 a, b).

Early macrospores were oval in shape, and some developed a small lateral protrusion (Figure 2.11). The macrospores had usually developed a characteristic bullet shape after several days in culture. They moved sluggishly along the bottom of the well, and occasionally a burst of acceleration would lift them free of it; they would however sink back again a few seconds latter. When moving in suspension the macrospores travelled with a spiral motion without any sudden change in direction (Figure 2.12).

Early microspores were oval in shape (Figure 2.13), but, as they aged, the anterior end became blunted and the rest of the cell body developed a twisted corkscrew shape (Figure 2.14 a, b). The microspores moved more vigorously than the macrospores when active and with an erratic spiral motion. Again, these dinospores could occasionally free themselves of the substratum after a sudden acceleration. After several days in culture the microspores developed a distinctive rod-shaped refractile inclusion at the posterior end (Figures 2.14 a, b, 2.15). Refractile inclusions were situated in the anterior end of the early microspores (Figure 2.13). Fewer refractile inclusions were present at the anterior end of the mature microspores, as the large posterior refractile inclusion developed (Figure 2.15).

### 2.3.5. Germination of dinospores

After a period of several weeks in the culture medium both spore types became less motile and changed shape yet again, eventually becoming spherical and losing their flagella. The spherical post-spore cells then elongated to form multinucleate filaments (Figures 2.16, 2.17). The process of transformation of the dinospore into a filament will be referred to as germination.

The time between sporogenesis and germination varied from one isolate to another, but was on the whole longer for the macrospores. Germination was dated from the time the first short filament was observed in a particular culture. Macrospores germinated between 27 and 62 days post sporogenesis (the majority by 39 days) and microspores between 18 and 38 days (the majority by 36 days) (Table 2.1). Germination was not simultaneous. A mixture of cell forms was present in each isolate for a number of weeks following the onset of germination. Motile macrospores were still to be observed up to 135 days post-sporogenesis and motile microspores up to 95 days post-sporogenesis.

Not all dinospores survived the germination process to produce filaments. Many lost their flagella and their refractile appearance and eventually died. By observation the percentage of macrospores germinating into filaments was greater than for the microspores. The cultures producing microspores in addition to germinating faster than those producing macrospores also progressed more rapidly to produce arachnoid syncytia - see section 2.3.7.

The majority of the short multinucleate filaments produced at germination lengthened and multiplied by branching and severance of the branches. Only a few filaments transformed almost immediately into arachnoid syncytia.

### 2.3.6. Growth of filamentous trophonts in culture

Filaments multiplied in the culture medium free of the substratum; they constituted the principal growth phase of the parasite in *in vitro* culture and will therefore be referred to as the trophont stage in the developmental cycle. Vegetative growth was by branching and fragmentation. Filaments displayed marked lateral bending and longitudinal extension and contraction movements. They appeared to be able to migrate slowly along the substratum when observed in contact preparations. In some filaments these movements were quite vigorous and under phase contrast it was possible to see the cytoplasm and nuclei being rapidly 'shunted' up and down the filament. Trophont motility served as a guide to the state of health of the culture. Figure 2.18 shows the relationship between the length of the filamentous trophont and the number of nuclei it contained.

The filamentous trophonts preferred to grow in shoals at the centre of the wells. The social growth of the filaments, their apparent resentment of disturbance and their multinucleate nature made it impossible to obtain meaningful growth curves for the parasite in this culture system. In some wells trails of filamentous trophonts would radiate from the central shoal of filaments and grow densely but evenly dispersed around the circumference of the well. Well established cultures of filaments were optimally transferred into fresh medium every fortnight. The filaments would often swell and vacuolate if left in well plates for longer than four weeks before being transferred into fresh medium. Flask cultures that contained dispersed filamentous trophonts could be left undisturbed for several months and remain viable.

As the cultures aged the filamentous trophonts continued to branch without dividing and tended to produce a writhing mass of filaments with their tips pointing outwards radially (Figures 2.19, 2.20). Professor K. Vickerman remarked on their resemblance to the head of the mythical gorgon and such colonies will be referred to as 'gorgonlocks'.

### 2.3.7. Growth of arachnoid syncytia in culture

When filamentous or gorgonlock trophonts were placed into fresh medium they often elongated and flattened as they became attached and grew into small arachnoid syncytia. In some instances this transformation could be prevented by diluting the new medium with more of the used medium.

The trophont filaments in gorgonlock colonies can condense and interdigitate to form spherical masses of nucleated cytoplasm that will be referred to as clump colonies. Subculture of clump colonies can result in their redispersion into filamentous trophonts again. Under certain conditions clump colonies can attach by radial cytoplasmic extensions from their bases to form arachnoid syncytia (Figure 2.21 a,b).

Arachnoid syncytia could be serially subcultured by fragmenting them with the suction from a pasteur pipette before transferring them into fresh medium. Arachnoid syncytia could also be maintained by the careful removal of the old medium with a pipette and addition of fresh medium without dislodging the syncytium from the base of the well.

Although arachnoid syncytia were observed in well established cultures they were also sometimes present soon after the germination of dinospores. Small arachnoid syncytia appeared within 1-18 days of microspores germinating into filamentous

trophonts. The filaments derived from macrospores did not start to form arachnoid colonies until at least 14 days after the filaments had first appeared (Figure 2.22 a,b& c).

Filamentous trophonts (including gorgonlocks), arachnoid syncytia and clump colonies were the principal forms of *Hematodinium* that were obtained in culture. Several developmental stages could be present in an individual culture, or the culture could be populated by a single developmental form; development was usually asynchronous. Very often the act of subculturing an isolate would stimulate the production of a different form.

One culture, initially isolated by Professor K.Vickerman in the summer of 1992 has been successfully cultivated for 3 years and has produced a further generation of dinospores. The second generation dinospores were released from aggregations of sporogenic cells at the centre of arachnoid syncytia. Because dinospores are generated from the arachnoid syncytium it will be referred to as the sporont stage of the developmental cycle; the sporogenic cells released from the sporont will be referred to as sporoblasts.

## 2.4. Discussion

The above developmental cycle of *Hematodinium* in an *in vitro* culture system is the first to be fully described for a parasitic dinoflagellate. The culture system allows the growth and multiplication of the parasite, apparently indefinitely *in vitro*, and the production of different forms of the parasite. It therefore opens up the possibility of investigating the morphological and metabolic changes underlying a complex parasite life cycle.

Meyers and colleagues (1987) described some developmental stages that they observed in culture. Several of these stages appear to be similar to those that I have described. The *Hematodinium* sp. from the Tanner crab generated what appeared to be a form similar to the arachnoid syncytium that I have described soon after initial isolation. The 'monolayers' that Meyers *et al.* described seem to be the main developmental form in their cultures; they did not describe a form resembling a filamentous trophont. This is perhaps not surprising because although *in vitro* microsporogenesis was observed for the Tanner crab *Hematodinium* sp. subsequent germination was not reported. Macrospores were reported to germinate directly into "attached forms"on the flask surface eventually forming a "rosette-like pattern", but again no mention was made of a filamentous trophont.

Chatton (1952) emphasised the morphology of the dinospore as a primary taxonomic character of the parasitic dinoflagellates. Cachon and Cachon (1987) suggested that spore morphology is too variable to be useful to the taxonomy.

The dinospores that I have described would appear to be very similar to those described by Meyers *et al.* (1987) from the Tanner crab parasite. Two types of spore were produced and behaved in a similar manner. The macrospores produced in both

their isolates and mine were similar in shape and size, although the lateral and beak-like protrusions that Meyers *et al.* describe were often not as pronounced in the *Hematodinium* sp. from *N. norvegicus*. The microspores also resembled those described by Meyers *et al.*, although the refractile body in the *Nephrops* parasite was more rod-shaped than that found in the microspores from the tanner crab. The microspores and macrospores are much larger than the dinospores of *Syndinium gammari* which are only 7-8μm long with a hardly noticeable sulcus and girdle (Manier *et al.* 1971). It is interesting to note that the microspores bear a striking resemblance to the microspores (form β) of *Syndinium* sp. described by Chatton in 1920, although the macrospores do not resemble the macrospores of *Syndinium* . Chatton describes the rarely seen form β microspores as containing at the posterior end 'one or more shining bacilliform crystalloid bodies'.

From my observations it is clear that only one spore type is produced by each isolate (in agreement with the findings of Meyers *et al.* 1987). The stimulation for sporogenesis appears for the large part to be lacking in these culture conditions. It is possible that a necessary nutrient is lacking or not present in high enough concentrations in the culture medium. A subtle change in pH, temperature or dissolved gases present in the culture medium may be the trigger for sporogenesis.

The functional significance of two spore types is not clear. Chatton (1920) postulated that the different spore types of *Syndinium* sp. may be anisogametes. Eaton *et al.* (1991) have shown that the macrospores, microspores and trophonts of *Hematodinium* sp. from the Tanner crab contain approximately the same amount of DNA per nucleus (measured by potassium acetate precipitation and ethidium bromide spectrofluorometry) which suggests that the dinospores are not gametes. Microspores of the *Nephrops* parasite begin germinating earlier than the macrospores (Table 2.1) and

develop into arachnoid syncytia at a faster rate. Germination of dinospores is further discussed in chapter 4. It appears that the requirements of the *Nephrops* parasite for the development of a series of stages are relatively non-specific if the FCSG medium can substitute for *Nephrops* plasma and living host cells. The absence of a dominant trophont phase in Meyer's cultures suggests he had only part of the developmental cycle *in vitro*.

The possibility cannot be discounted that the distinctly different dinospore types belong to two different species that can only be distinguished during the free-living dinospore stage and not during the parasitic stage. This seems unlikely, however, as two types of dinospore have been repeatedly encountered in syndiniid infections of particular hosts (Chatton 1920, Jepps 1937, Meyers *et al.* 1987, Eaton *et al.* 1991).

I have shown that dinospores regardless of type can germinate to produce trophonts. This observation rules out Chatton's suggestion that macro and micro -spores are isogametes. It also suggests (but does not prove) that an interpolated resting stage (hypnospore) - such as occurs at the zygote stage in free-living peridinians is not a necessary part of the cycle.

| Isolate number | Date of isolation | Location | Infection status of lobster | Tissue origin of isolate | Time from isolation to sporogenesis (days) | Dinospore type | Time from sporogenesis to germination (days) |
|---|---|---|---|---|---|---|---|
| 1 | 5/2/93 | Clyde Sea Area | III | Haemolymph | 46 | macro | 37 |
| 2 | 5/2/93 | Clyde Sea Area | IV | Haemolymph | 4 | macro | 36 |
| 3 | 11/3/94 | Clyde Sea Area | III/IV | Ovary | 20 | macro | 36 |
| 4 | 11/3/94 | Clyde Sea Area | III/IV | Midgut | 20 | macro | 39 |
| 5 | 16/2/95 | Clyde Sea Area | Uncertain | Haemolymph | 155 | macro | 53 |
| 6 | 16/2/95 | Clyde Sea Area | II (Dead) | Haemolymph | 16 | macro | 27 |
| 7 | 13/4/95 | Irish Sea | I | Haemolymph | 32 | macro | 62 |
| 8 | 5/2/93 | Clyde Sea Area | II (Dead) | Haemolymph | 32 | micro | 38 |
| 9 | 11/3/94 | Clyde Sea Area | I/II (Dead) | Haemolymph | 31 | micro | 36 |
| 10 | 11/4/95 | Irish Sea | II | Haemolymph | 24 | micro | 18 |
| 11 | 13/4/95 | Irish Sea | III | Haemolymph | 22 | micro | 19 |
| 12 | 13/4/95 | Irish Sea | III/IV | Haemolymph | 22 | micro | 19 |

**Table 2.1.** Origin of the isolates maintained in *in vitro* culture. Isolates were examined every day; time from isolation to sporogenesis, the spore type produced and the time from sporogenesis to germination into trophonts were recorded.

**Figure 2.1.** Living dinoflagellates in a fresh haemolymph contact preparation. The host haemocytes (HC) have settled onto the glass slide and spread. One obviously binucleate parasite is clearly visible (arrow). Isolate no. 7. Phase contrast. Scale bar = 100μm.

**Figure 2.2.(left)** An aggregate of sporogenic dinoflagellates (s) from a recently isolated culture giving rise to macrospores (arrows). Isolate no. 7. Phase contrast. Scale bar = 100μm.

**Figure 2.3.(right)** A aggregate of sporogenic dinoflagellates (s) from a recently isolated culture giving rise to microspores. Several of the microspores are already beginning to show a slightly bent profile (arrows). Isolate no. 10. Phase contrast. Scale bar = 100μm.

**Figure 2.1.** Living dinoflagellates in a fresh haemolymph contact preparation. The host haemocytes (HC) have settled onto the glass slide and spread. One obviously binucleate parasite is clearly visible (arrow). Isolate no. 7. Phase contrast. Scale bar = 100μm.

**Figure 2.2.(left)** An aggregate of sporogenic dinoflagellates (s) from a recently isolated culture giving rise to macrospores (arrows). Isolate no. 7. Phase contrast. Scale bar = 100μm.

**Figure 2.3.(right)** A aggregate of sporogenic dinoflagellates (s) from a recently isolated culture giving rise to microspores. Several of the microspores are already beginning to show a slightly bent profile (arrows). Isolate no. 10. Phase contrast. Scale bar = 100μm.

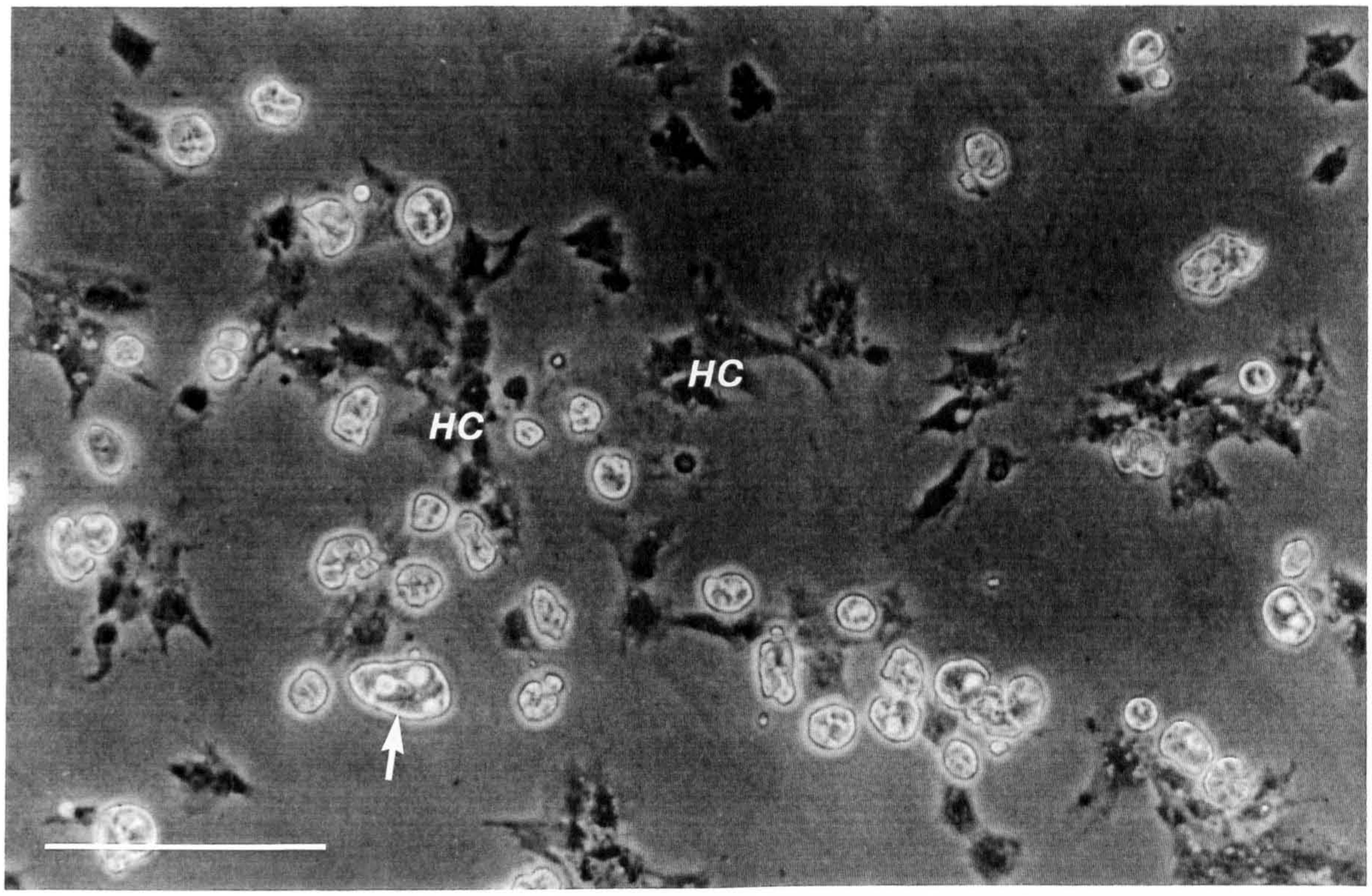
HC
HC

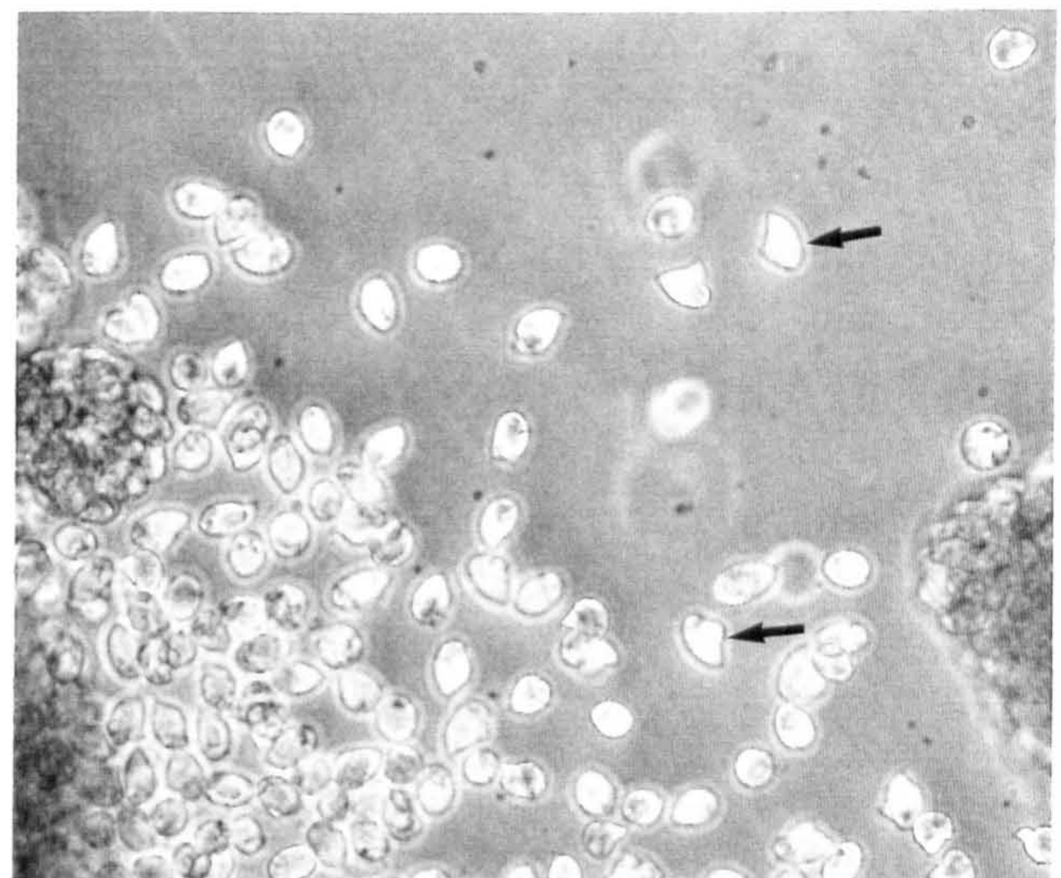
S

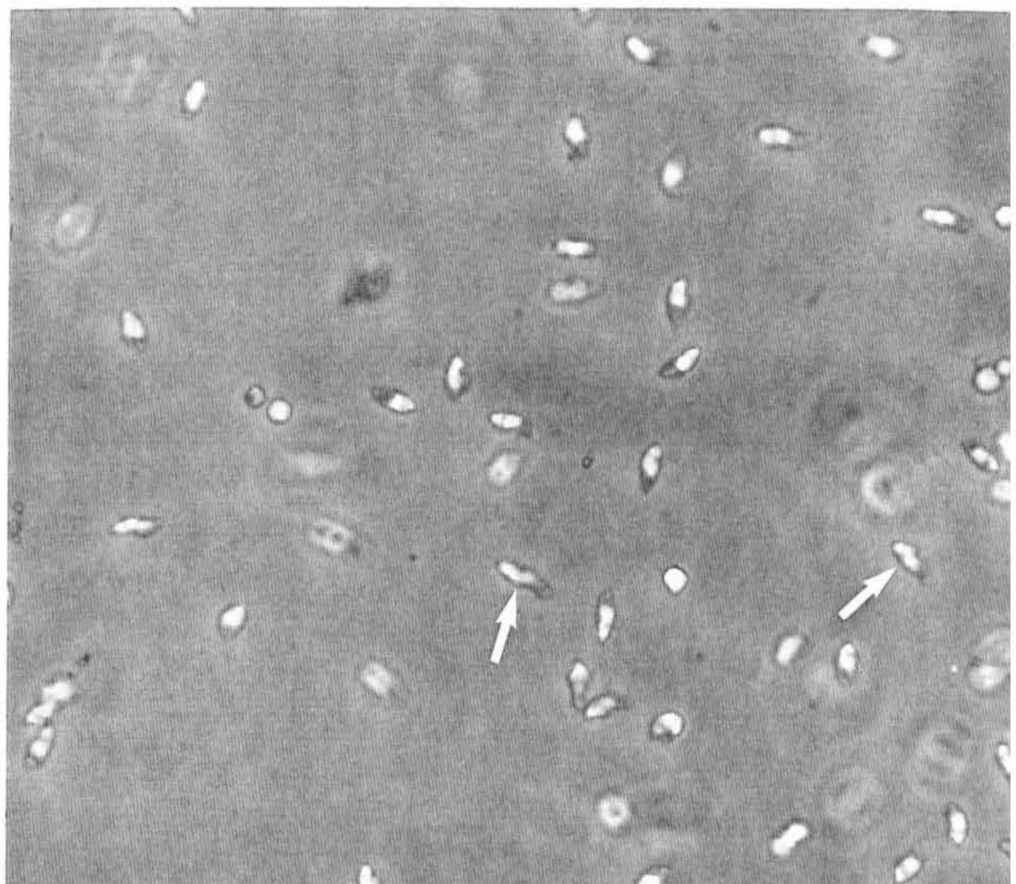
S

**Figure 2.4.** Five days after isolation the aggregates of dinoflagellates have produced thin cytoplasmic threads which have formed an arachnoid syncytium. The cytoplasmic threads have not developed near the few spread host haemocytes (HC). Isolate no. 7. Phase contrast. Scale bar = 100μm.

**Figure 2.5.** A large parasite network formed by fusion of many arachnoid syncytia. Thin cytoplasmic threads have extended from central sporoblast masses (c). Many of the cytoplasmic threads are not attached to the substratum and sway in the medium. Isolate no. 8. Phase contrast. Scale bar = 100μm.

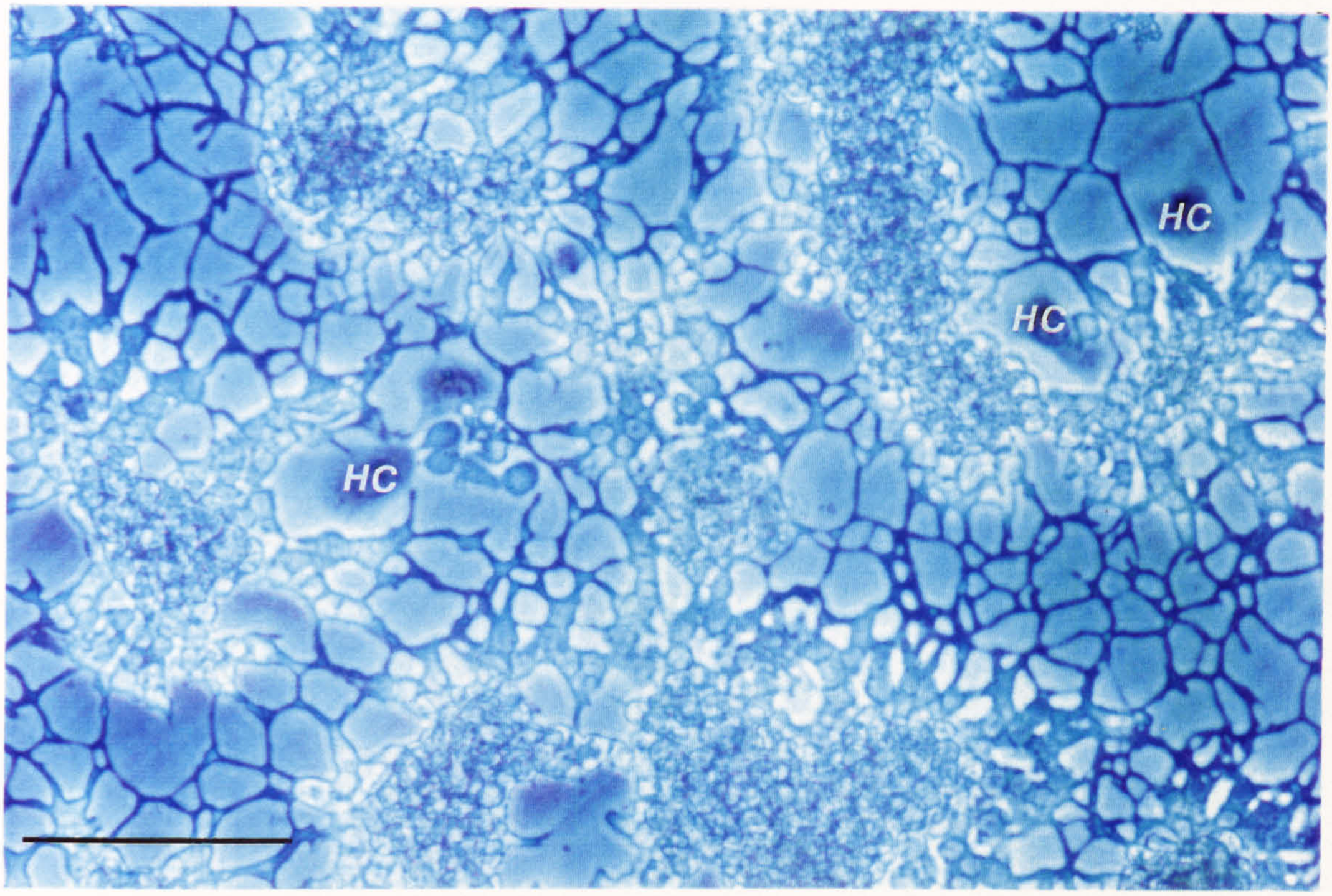
HC
HC
HC

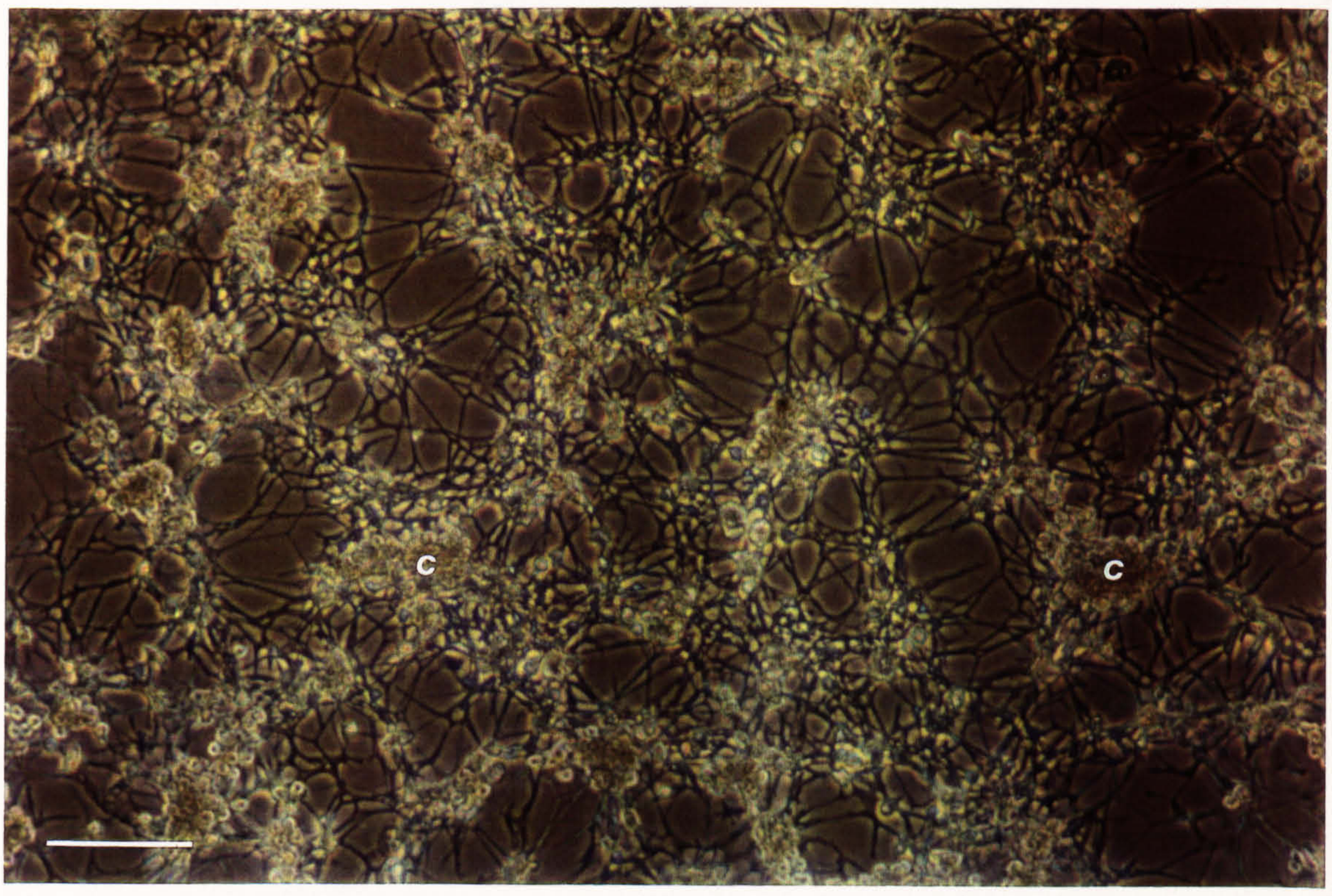
C
C

**Figure 2.6.** Part of a loose arachnoid syncytium that is characterised by the presence of numerous flat cytoplasmic threads (arrows). Isolate no. 1. Phase contrast. Scale bar = 100μm.

**Figure 2.7.** A sporogenic arachnoid syncytium (sporont) that has been fixed with osmium vapour and postfixed with 2% aqueous uranyl acetate. A small central mass (c) of parasite has produced some sporogenic cells (sporoblasts) (s). Nuclei (arrows) are located at the junctions of the cytoplasmic threads and are well stained to show the prominent condensed chromosomes. Numerous small darkly staining inclusions (lipid) are dispersed throughout the syncytium. Isolate no. 2. Differential interference contrast. Scale bar = 20μm.

**Figure 2.8.** The central area of a discrete arachnoid syncytium, the aggregation of cytoplasm and nuclei (c) at the centre surrounded by flattened cytoplasmic threads containing a few dispersed nuclei (arrows) may represent a prelude to sporogenesis. Isolate no. 2. Phase contrast. Scale bar = 100μm.

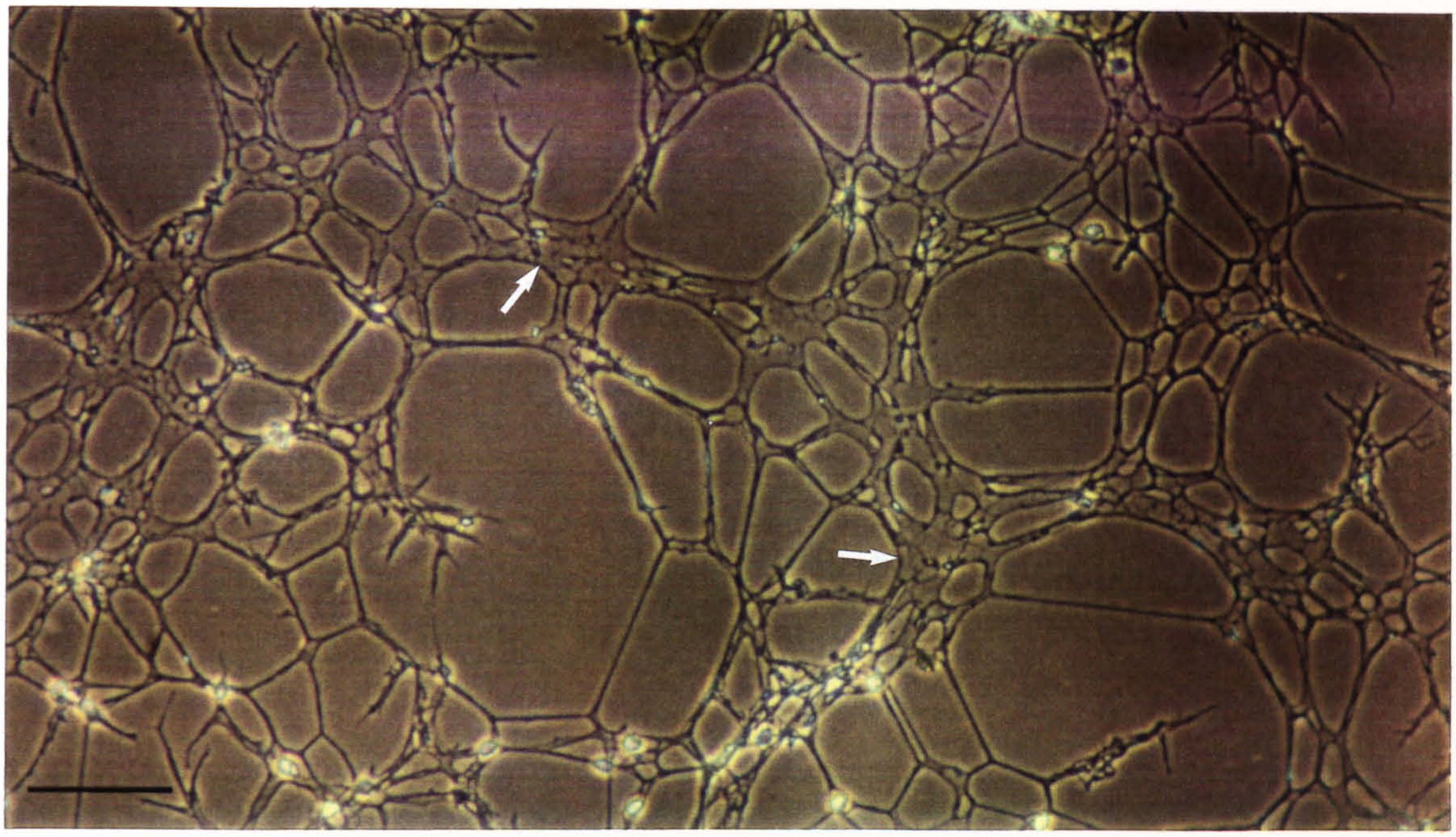

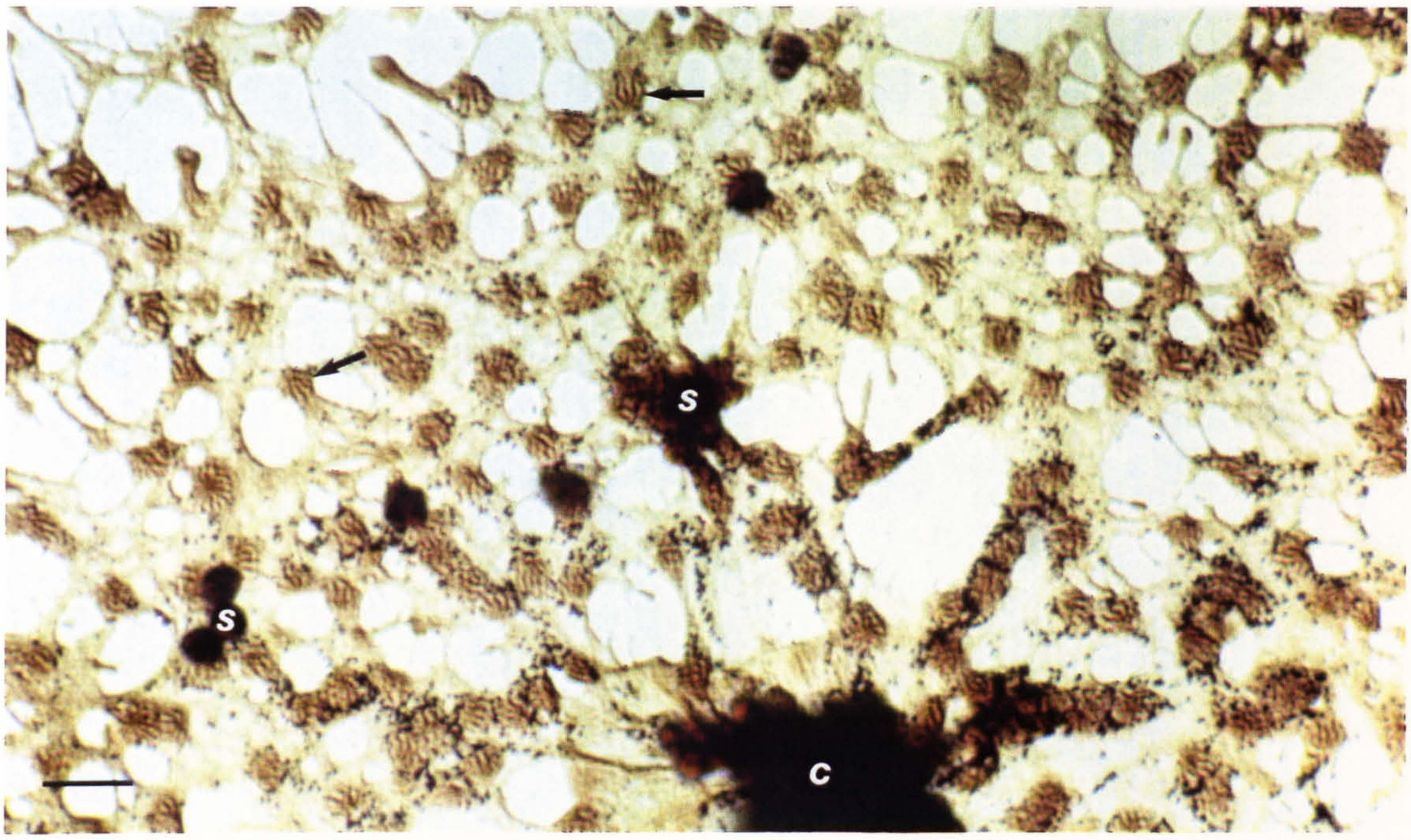
S
S
C

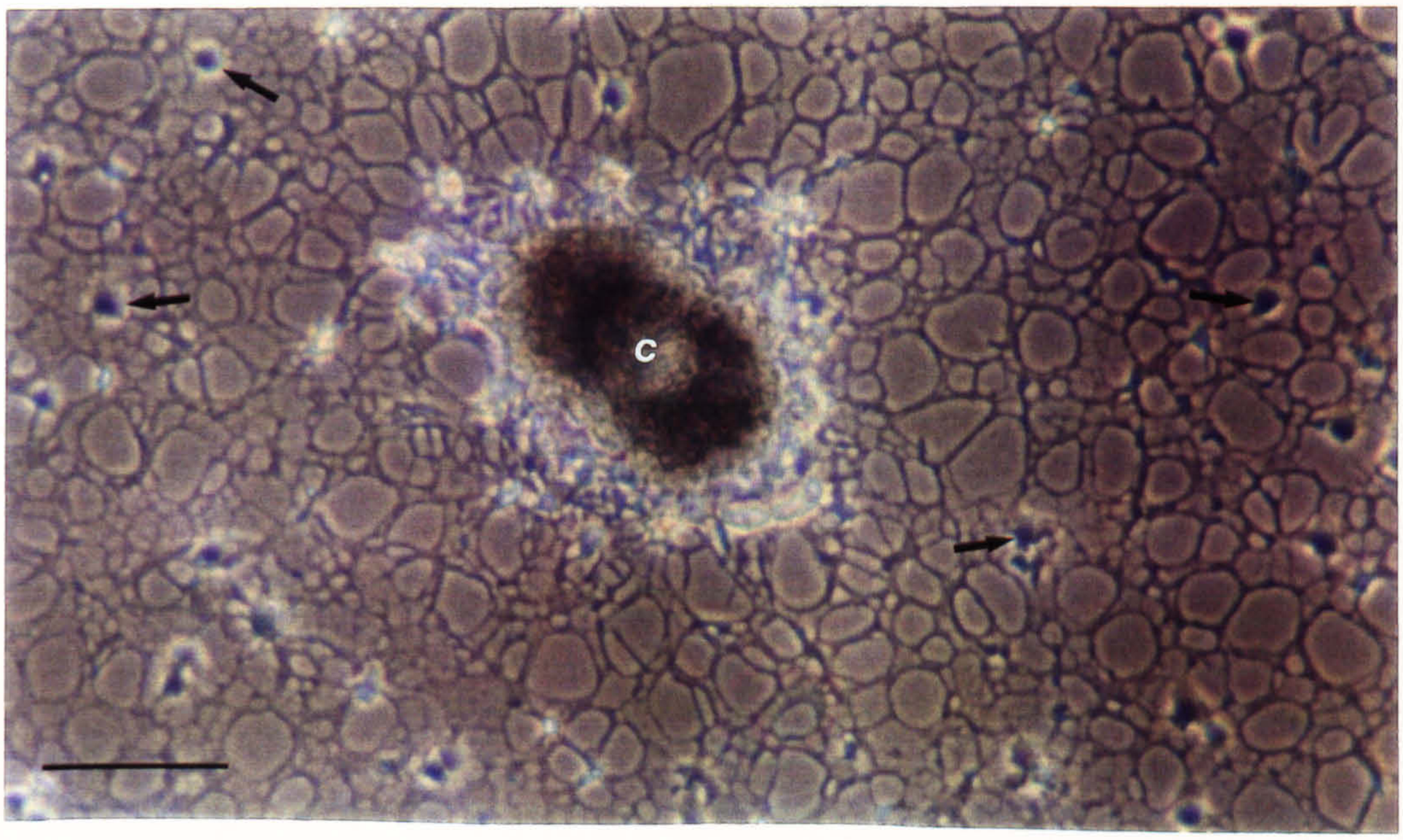
C

**Figure 2.9 a, b.** These complex arachnoid syncytia (sporonts) are producing macrospores (d) from the sporogenic cell (sporoblast) masses (s) four weeks after isolation. Note the pile-up of sporoblasts close to lacunae where the cytoplasmic threads of the syncytium have been withdrawn.

**a)** Nuclei of the syncytium are plainly visible, bottom left.

**b)** The phase dense peripheral dentritic processes of the arachnoid are clearly shown in this micrograph.

Isolate no. 7. Phase contrast. Scale bars = 100μm.

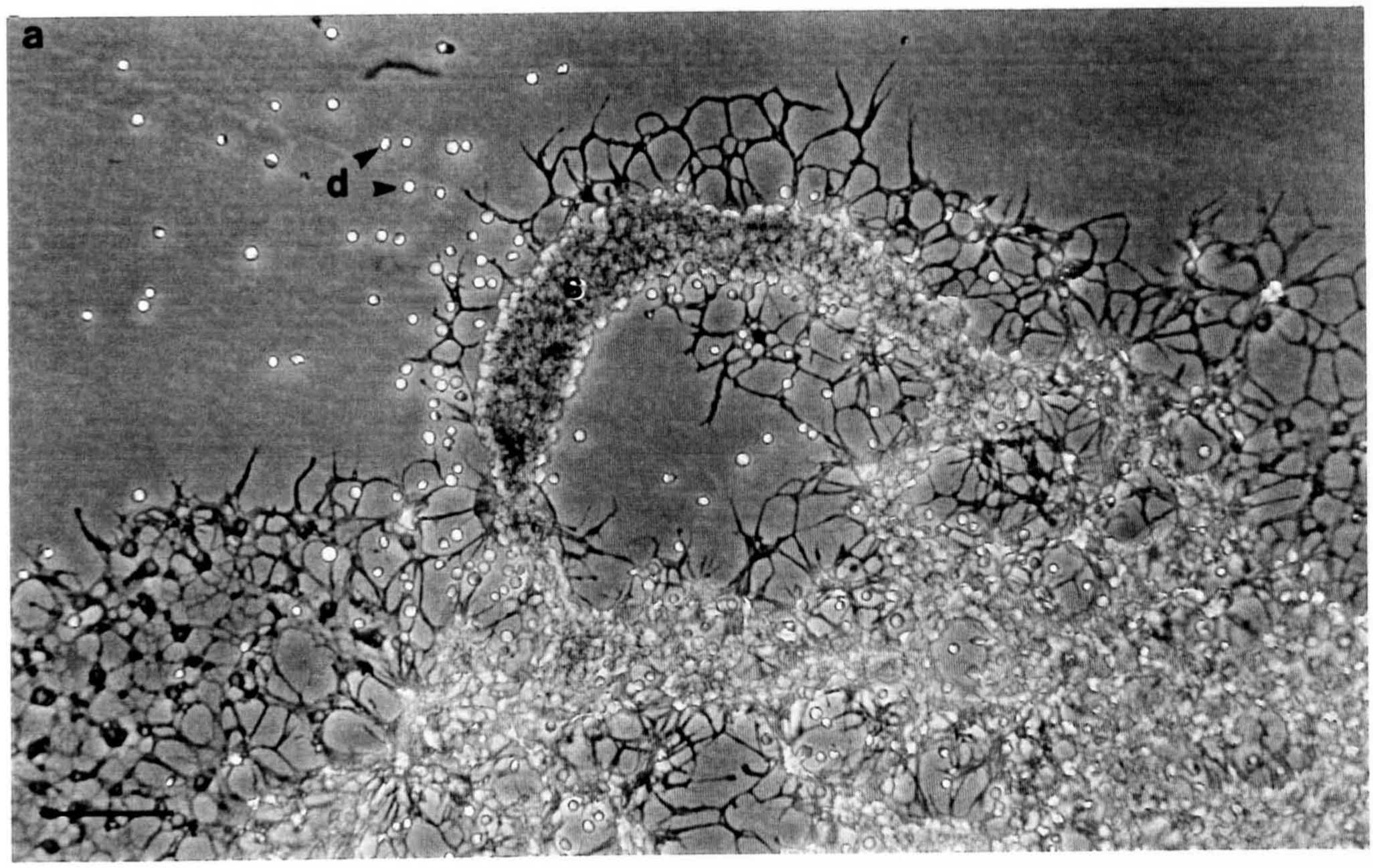
a
d
s

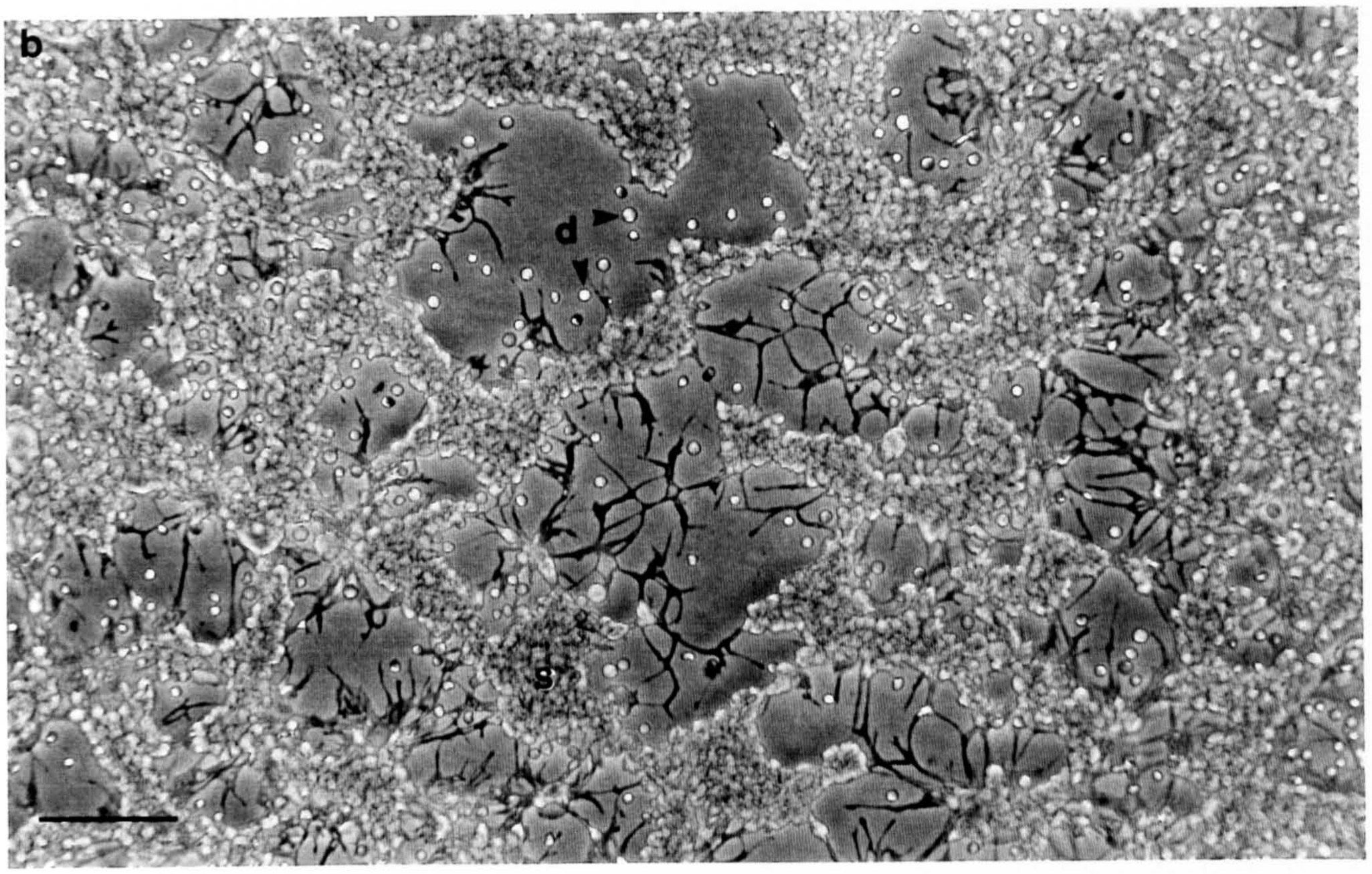
b
d
s

**Figure 2.10.** Final stages of division (arrows) in the formation of macrospores. The fission furrow passes from anterior to posterior end of the sporoblast, and up to four individual dinospores may be formed simultaneously. Flagella are present but not visible in the micrograph. Isolate no. 2. Glutaraldehyde fixed dinoflagellates. Differential interference contrast. Scale bar = 20μm.

**Figure 2.11.** Early macrospores with distinct lateral protrusion (arrows), however, these protrusions are not present in macrospores older than 2 weeks. Isolate no. 1. Glutaraldehyde fixed dinoflagellates. Differential interference contrast. Scale bar = 20μm.

**Figure 2.12.** An ovoid macrospore (d) and the typical spiral track of this flagellate as it moved in front of the camera during the exposure. Isolate no. 2. Live macrospores stained with acridine orange. Epifluoresence. Scale bar = 20μm.

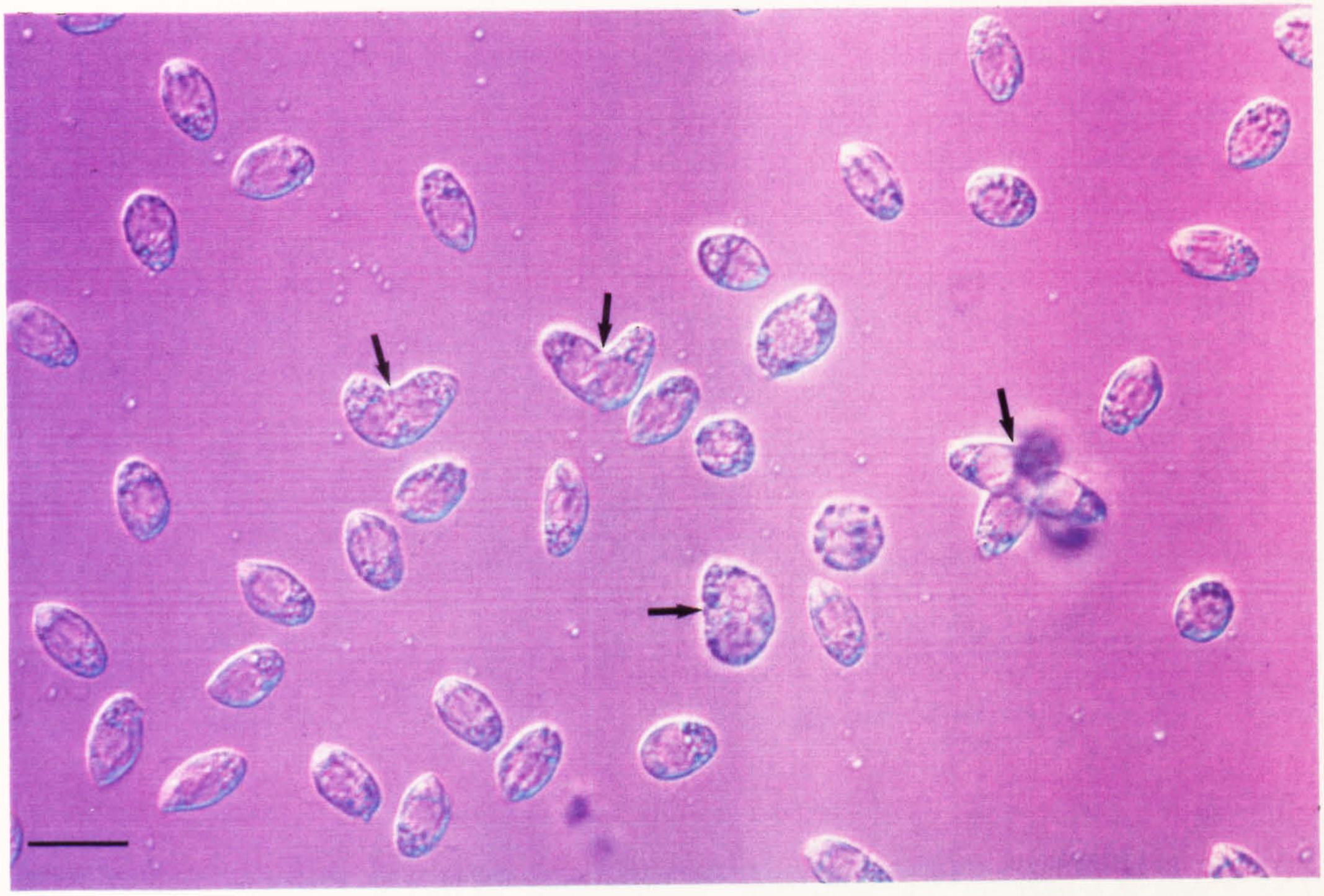

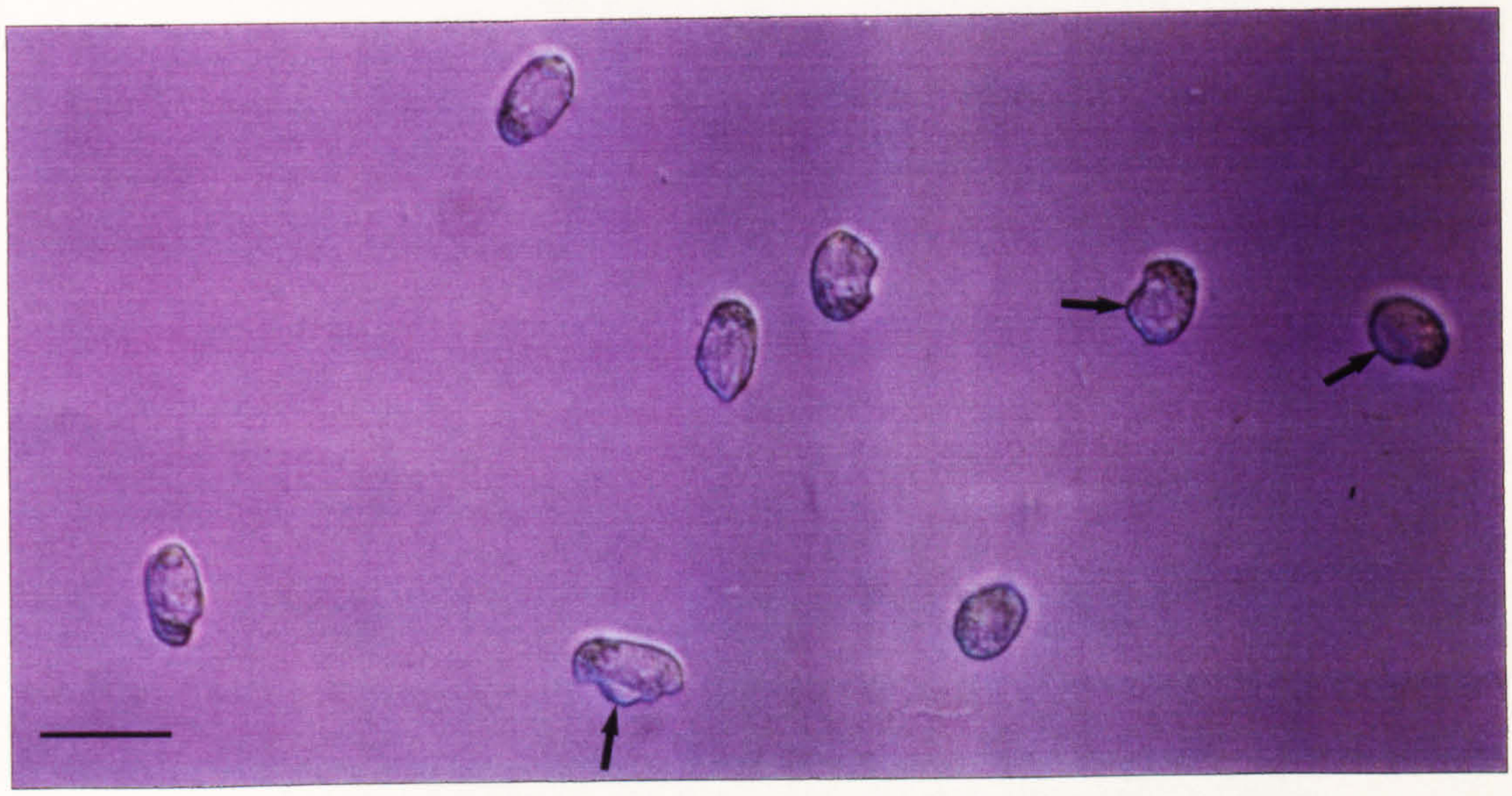



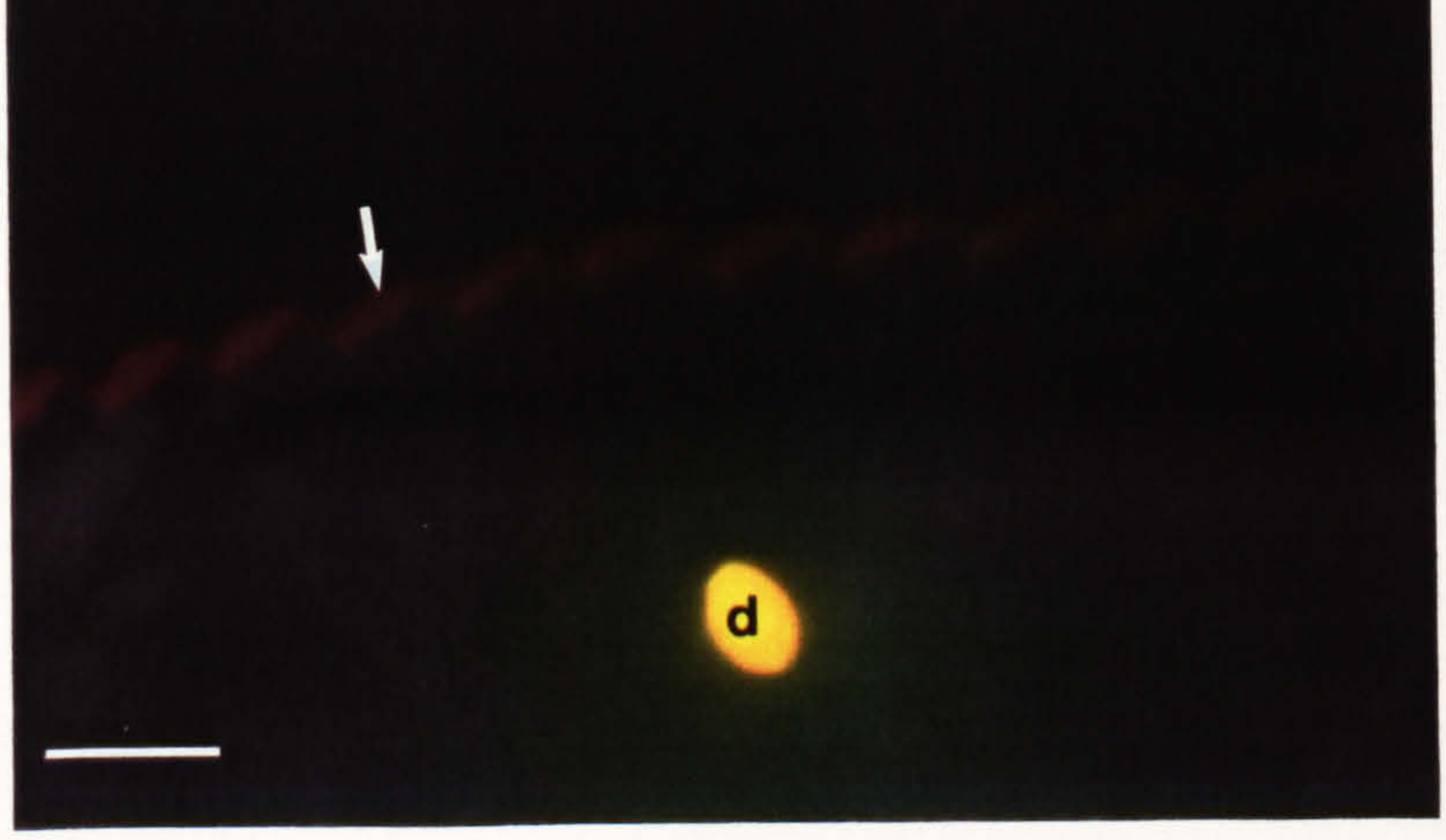
d

**Figure 2.13.** Microspores after the final divisions of sporogenesis. They have a rounded anterior end containing refractile inclusions (arrows). Isolate no. 9. Glutaraldehyde fixed dinoflagellates. Differential interference contrast. Scale bar = 10μm.

**Figure 2.14 a, b.** Microspores eventually develop a pronounced corkscrew shape. After several weeks in culture the microspores develop a distinctive rod-shaped refractile body at the posterior end of the dinospore (arrows). Isolate no. 9. Glutaraldehyde fixed dinoflagellates. Differential interference contrast. Scale bars = 10μm.

**Figure 2.15.** Although the refractile body (rb) is present in the posterior end of the microspore there are also smaller refractile inclusions (arrows) present in the anterior end of the microspore. Isolate no. 9. Glutaraldehyde fixed dinoflagellates. Differential interference contrast. Scale bar = 10μm.

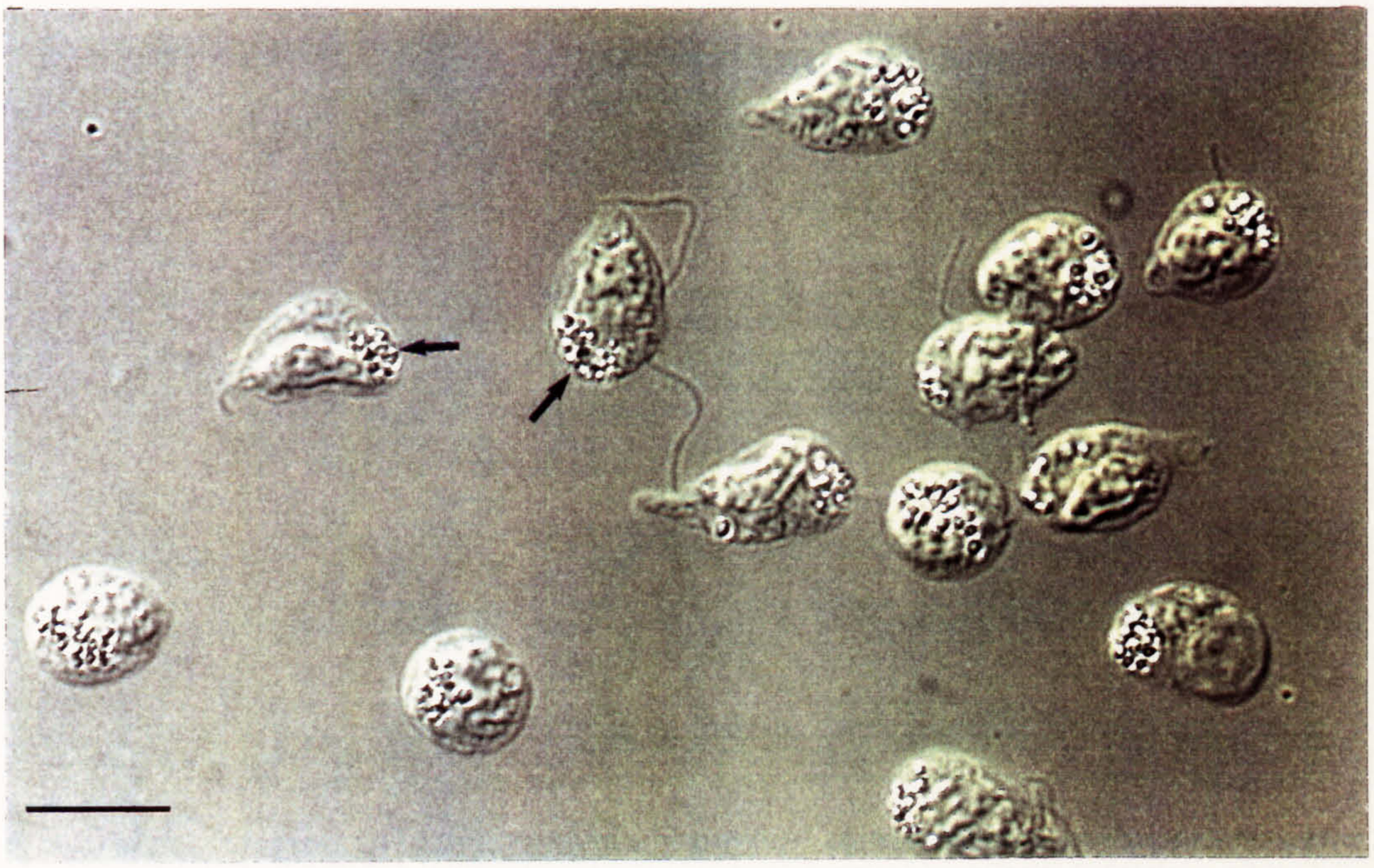

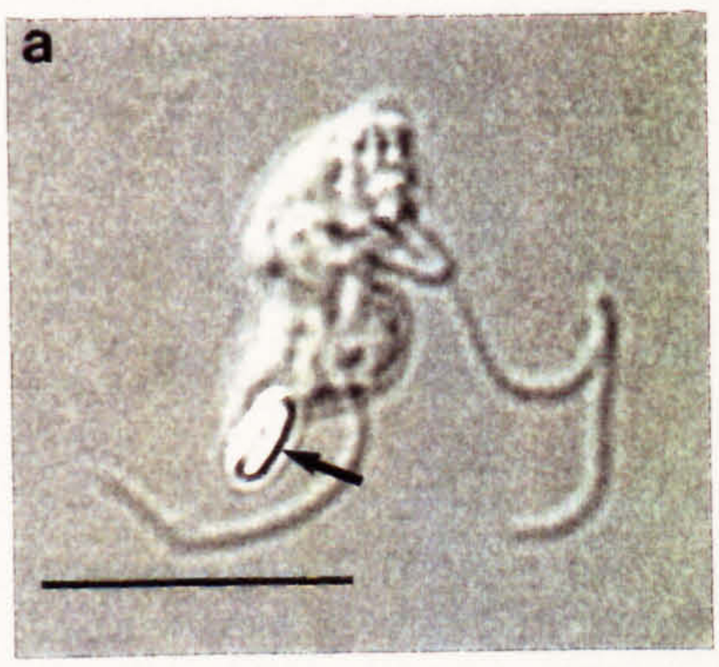
a

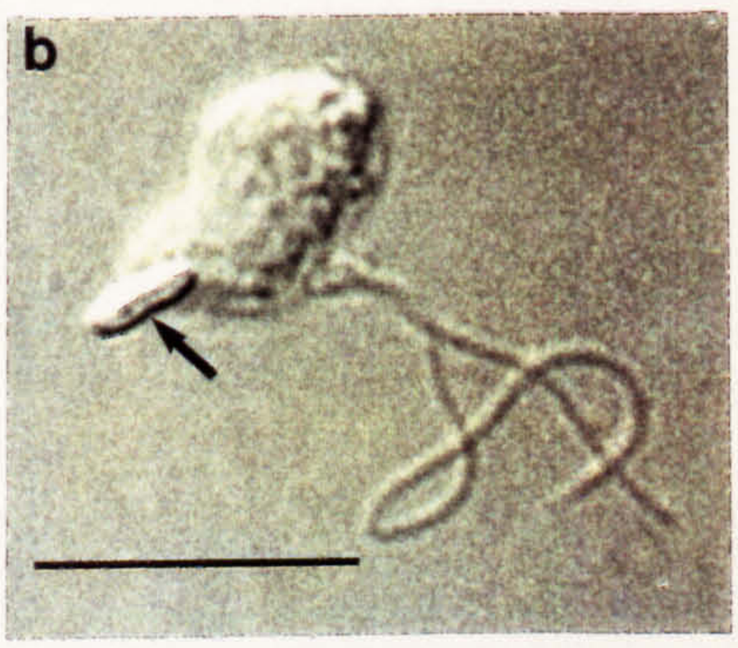
b

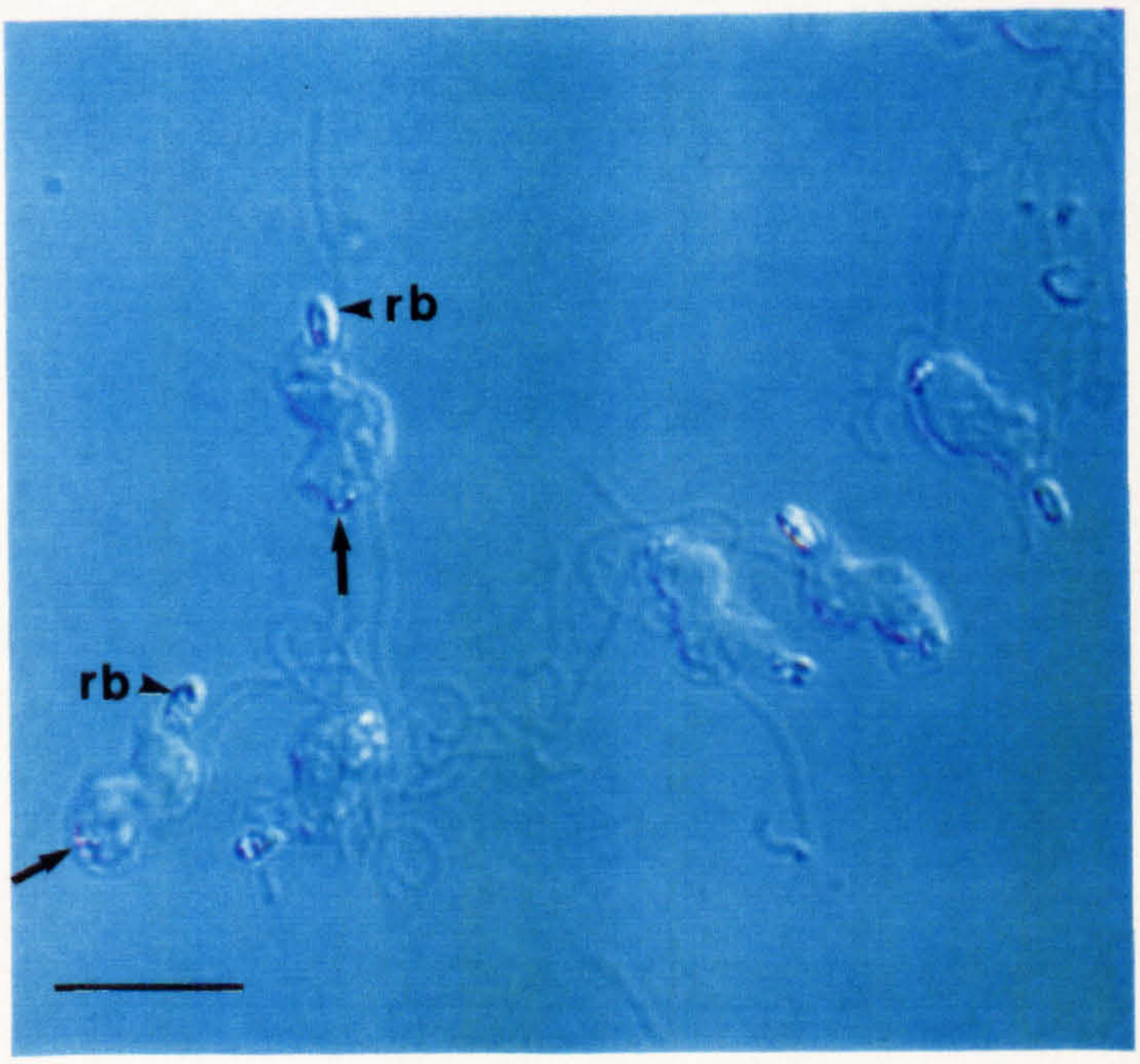
rb
rb

**Figure 2.16.** Germination of macrospores. During the process of germination the macrospores become spherical and lose their flagella (r). They then elongate into multinucleate filamentous trophonts (tp). Many of the macrospores do not survive to germinate, and eventually die, losing their refractile appearance (dd). A thin thread (arrow) has emerged from one filamentous trophont and is attached to the substratum. Isolate no. 7. Phase contrast. Scale bar = 100μm.

**Figure 2.17.** A microspore culture in the early stages of germination consists of motile uninucleate dinospores (d) which become spherical and lose their flagella (r), and eventually elongate into filamentous trophonts (tp). Isolate no. 11. Phase contrast. Scale bar = 100μm.

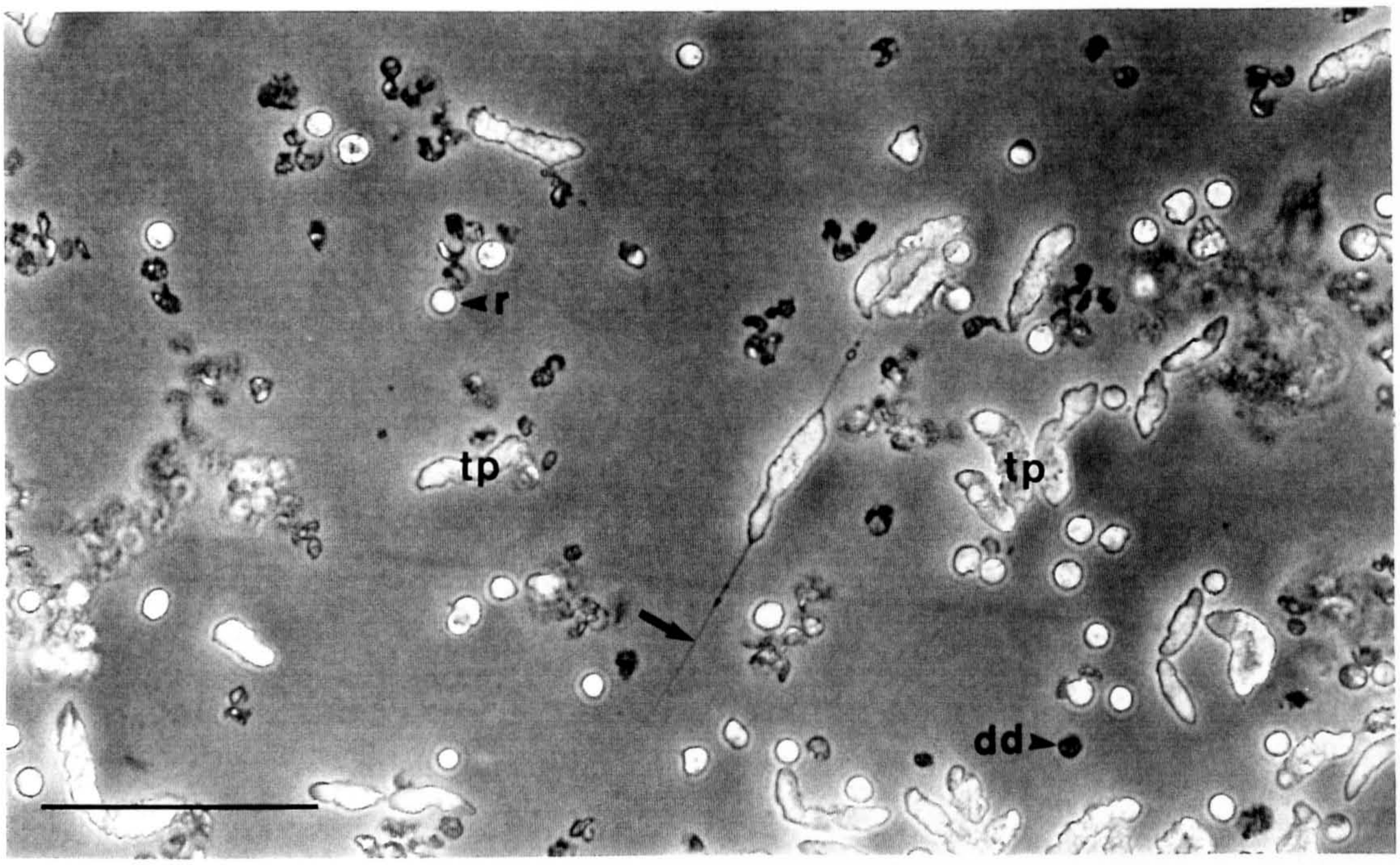
tp
tp
dd

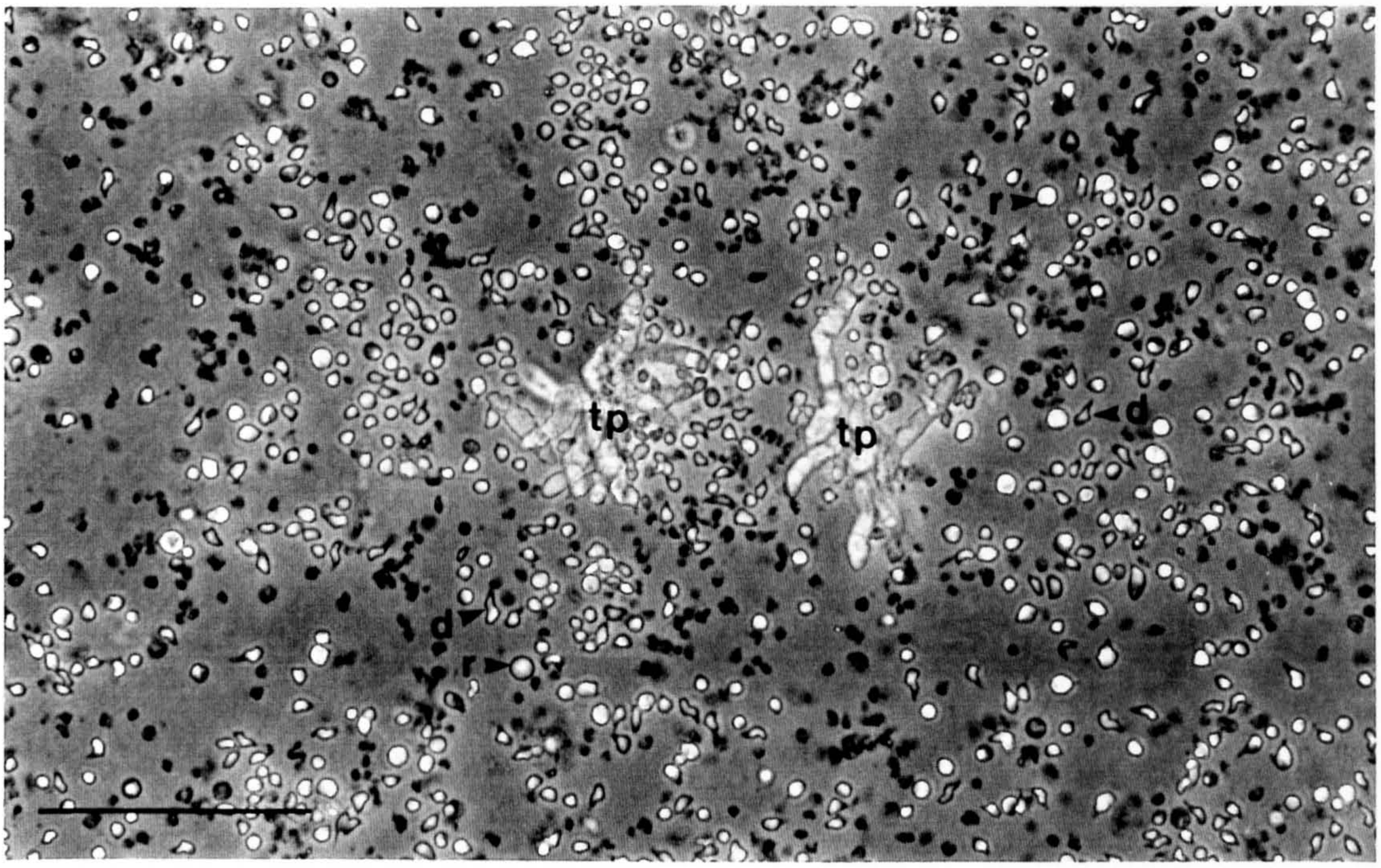
tp
tp
r
d
d
r

**Figure 2.18.** A series of 3 histograms showing the relationship between length of filamentous trophonts and the number of nuclei that they contain. A sample of filaments was taken from isolate number 2 (27 months after isolation, 26 months post-germination), fixed and stained with DAPI. A total of 83 filaments were measured and the number of nuclei they contained was recorded. Histogram A shows the 50.6% of filaments that contained 1 nucleus; histogram B the 43.4% of filaments that contained 2 nuclei and histogram C the 6% of filaments that contained 3 nuclei.

**A.**

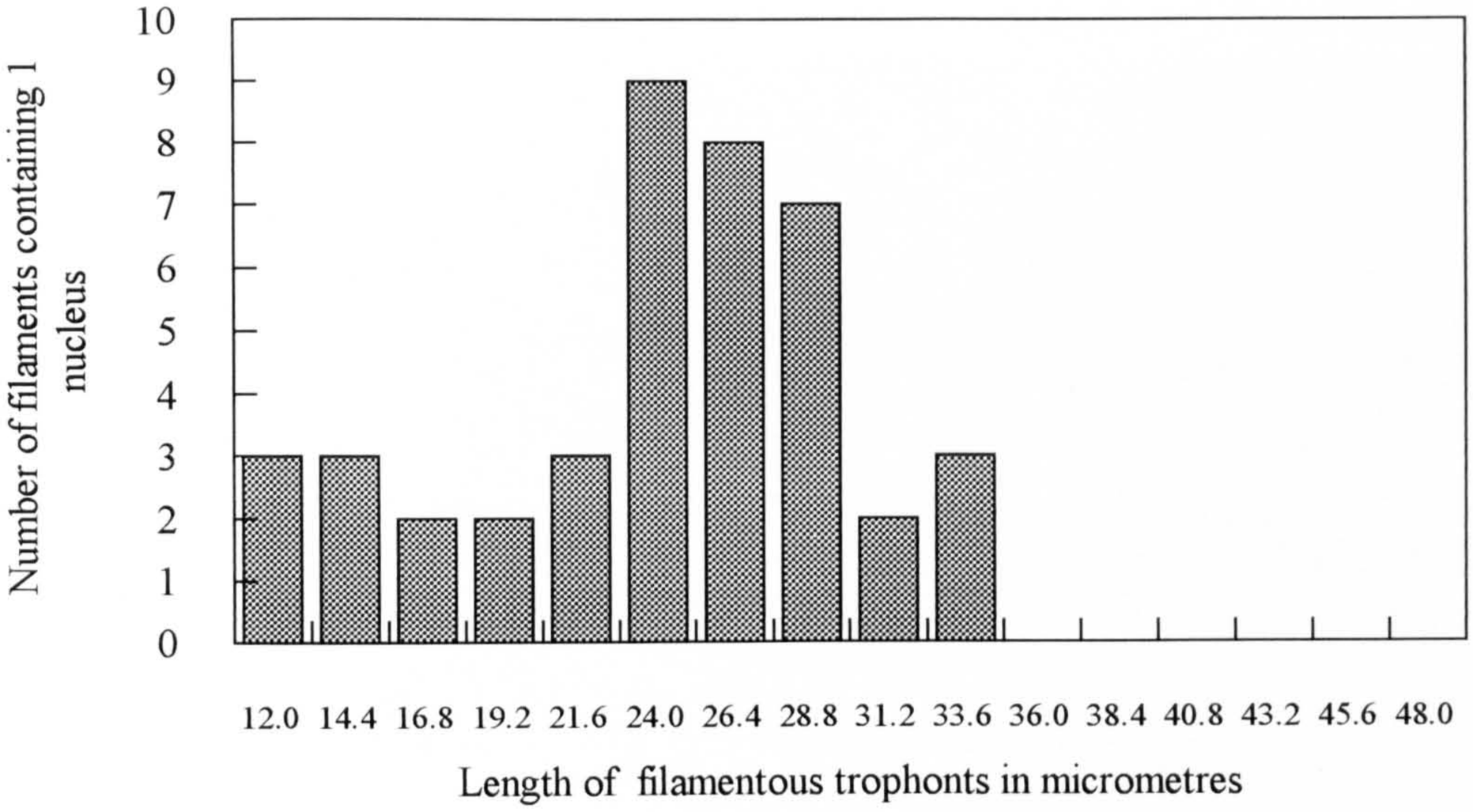
Number of filaments containing 1 nucleus
0
1
2
3
4
5
6
7
8
9
10
12.0 14.4 16.8 19.2 21.6 24.0 26.4 28.8 31.2 33.6 36.0 38.4 40.8 43.2 45.6 48.0
Length of filamentous trophonts in micrometres

**B.**

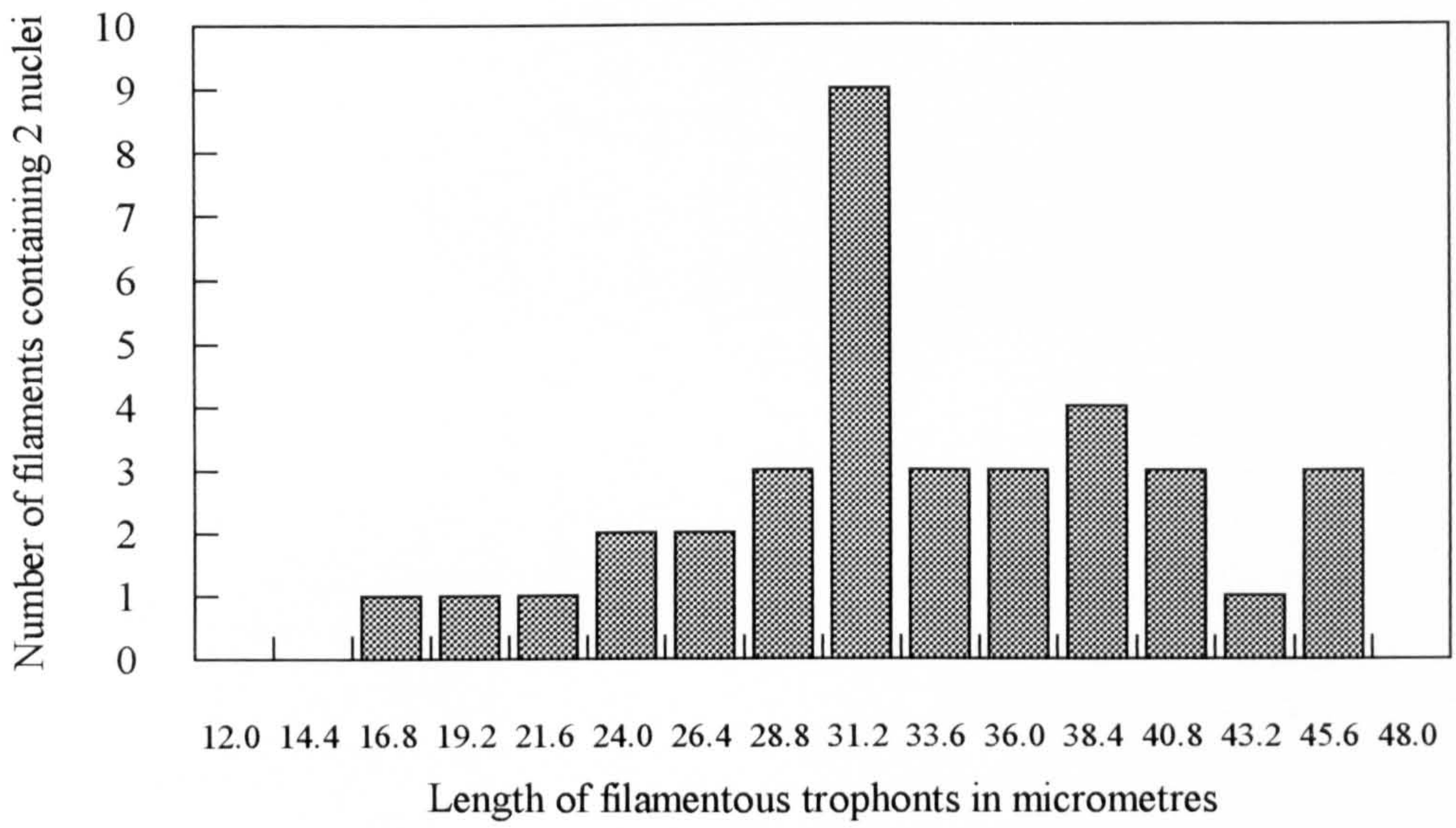
Number of filaments containing 2 nuclei
0
1
2
3
4
5
6
7
8
9
10
12.0 14.4 16.8 19.2 21.6 24.0 26.4 28.8 31.2 33.6 36.0 38.4 40.8 43.2 45.6 48.0
Length of filamentous trophonts in micrometres

**C.**

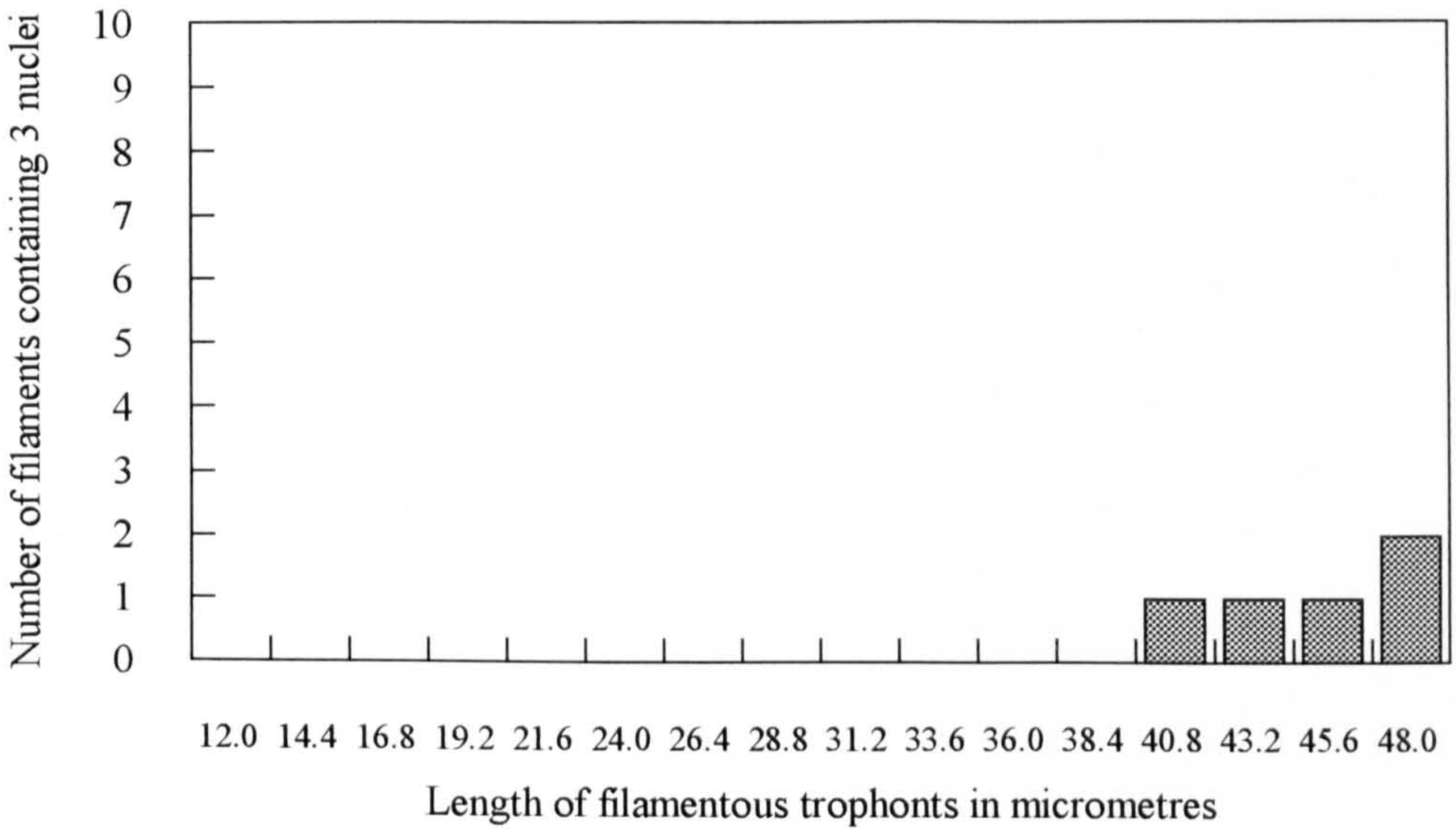
Number of filaments containing 3 nuclei
0
1
2
3
4
5
6
7
8
9
10
12.0 14.4 16.8 19.2 21.6 24.0 26.4 28.8 31.2 33.6 36.0 38.4 40.8 43.2 45.6 48.0
Length of filamentous trophonts in micrometres

**Figure 2.19.** A culture two months after germination containing different developmental forms, most prominent are filamentous gorgonlock colonies (gc) which form from the growth of filamentous trophonts (tp). Arachnoid syncytia (arrows) are growing on the substratum beneath the filamentous and gorgonlock trophonts. Isolate no. 2. Phase contrast. Scale bar = 100μm.

**Figure 2.20.** A writhing filamentous gorgonlock colony. The filaments have a very wrinkled appearance produced by the irregular alveolar structure. Isolate no. 2. Differential interference contrast. Scale bar = 100μm.

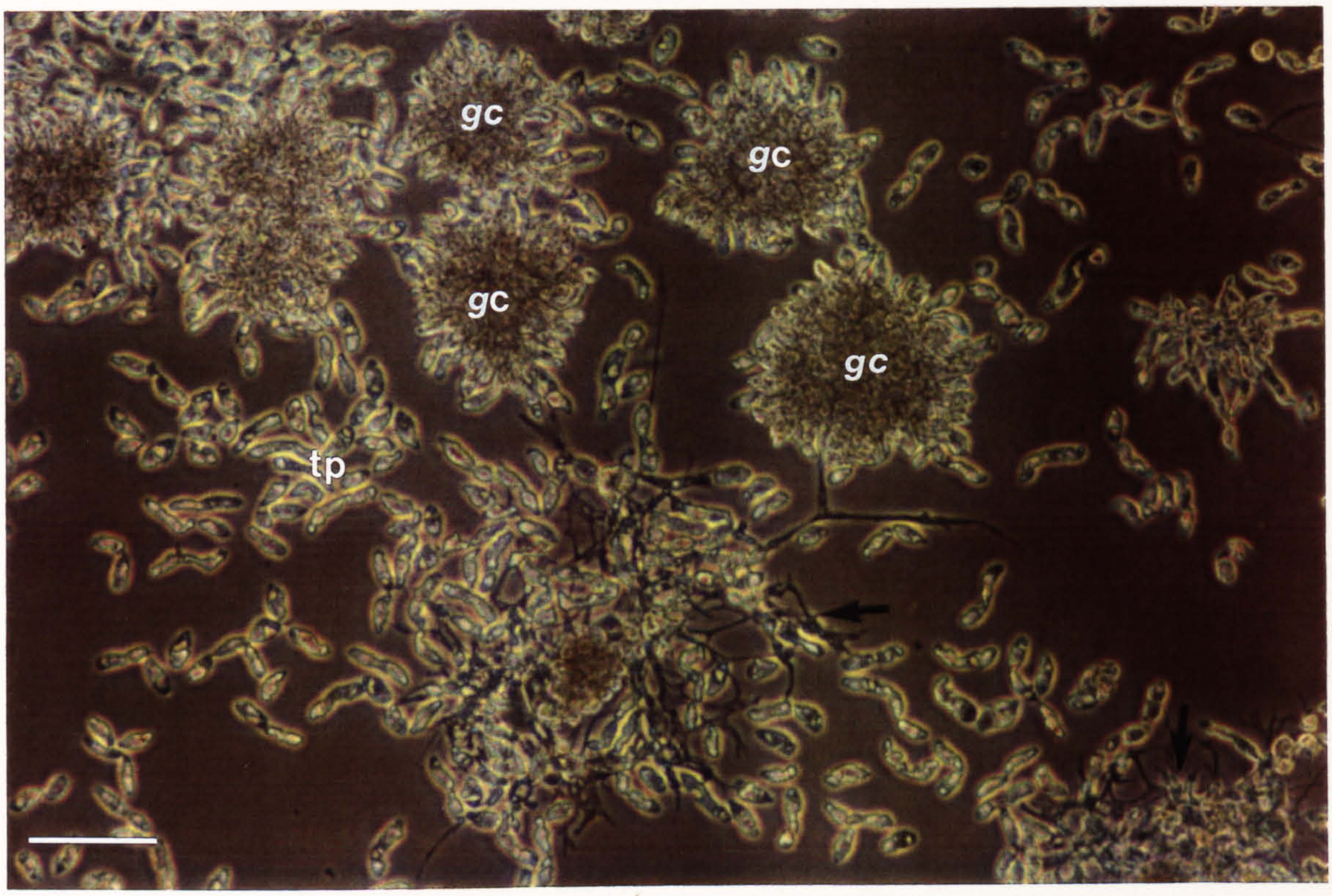
gc
gc
gc
gc
tp

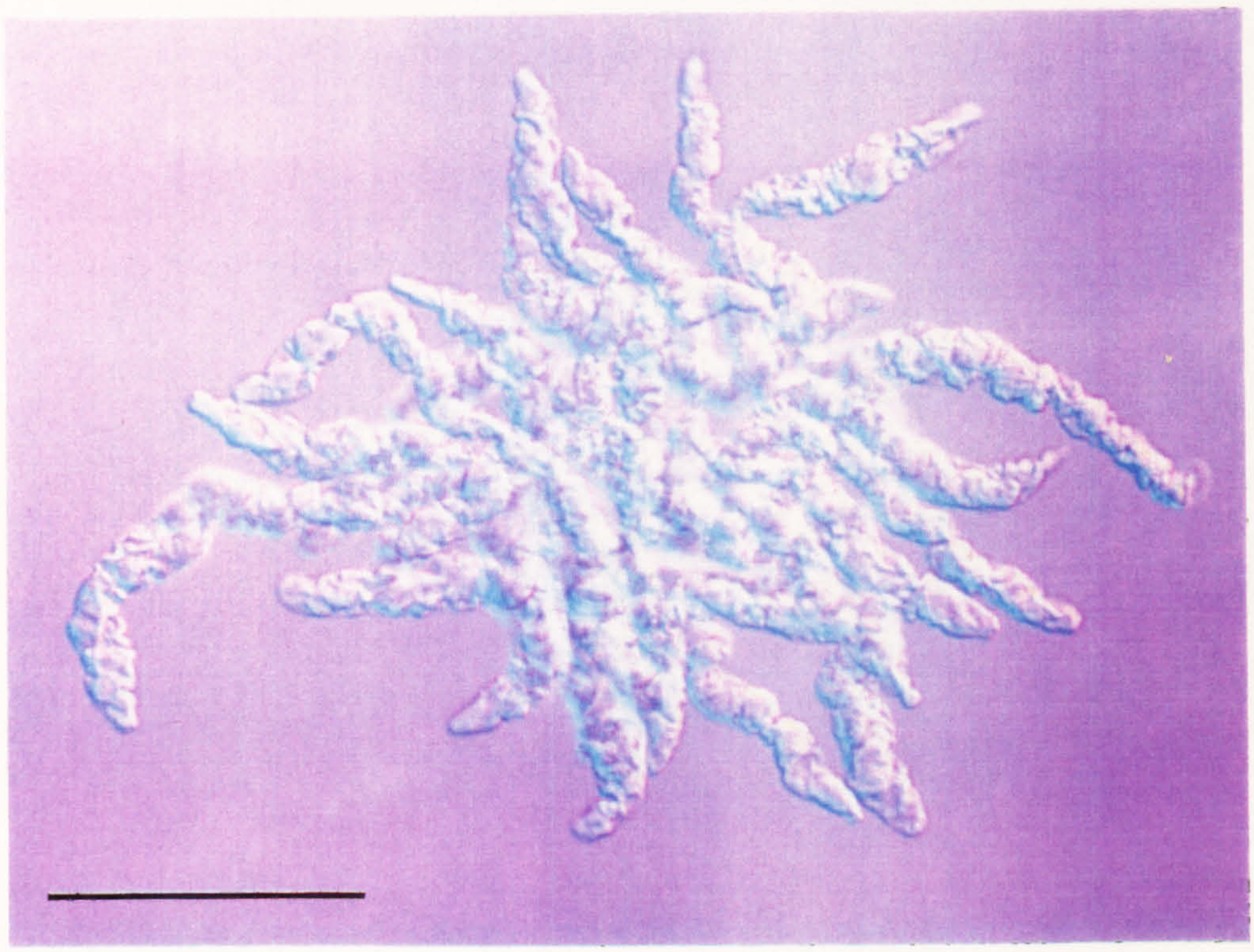

**Figure 2.21 a, b.** Two specimens from 4 month old parasite isolate that had previously produced microspores.

**a)** An arachnoid syncytium has developed from a clump colony. The clump colony attaches by extending cytoplasmic threads (ct) from the base. The central mass of the arachnoid syncytium (c) forms from the interdigitated trophonts of the clump colony.

**b)** As the arachnoid syncytium ages the central mass of nucleated cytoplasm (c) grows and the cytoplasmic threads form a dense network, with the tips enlarged into a droplet shape (arrows).

Isolate no. 11. Phase contrast. Scale bars = 100μm.

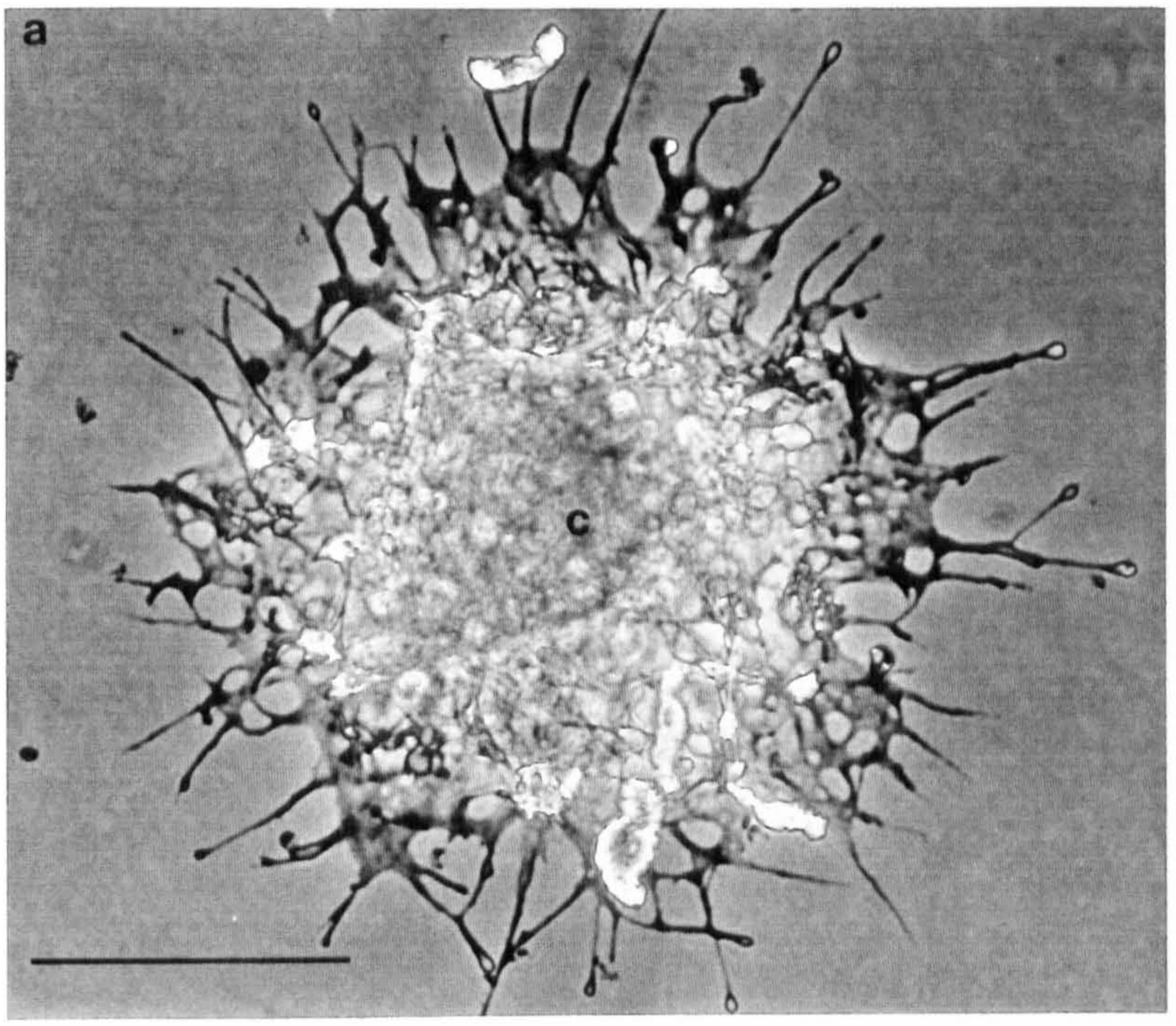
a
c

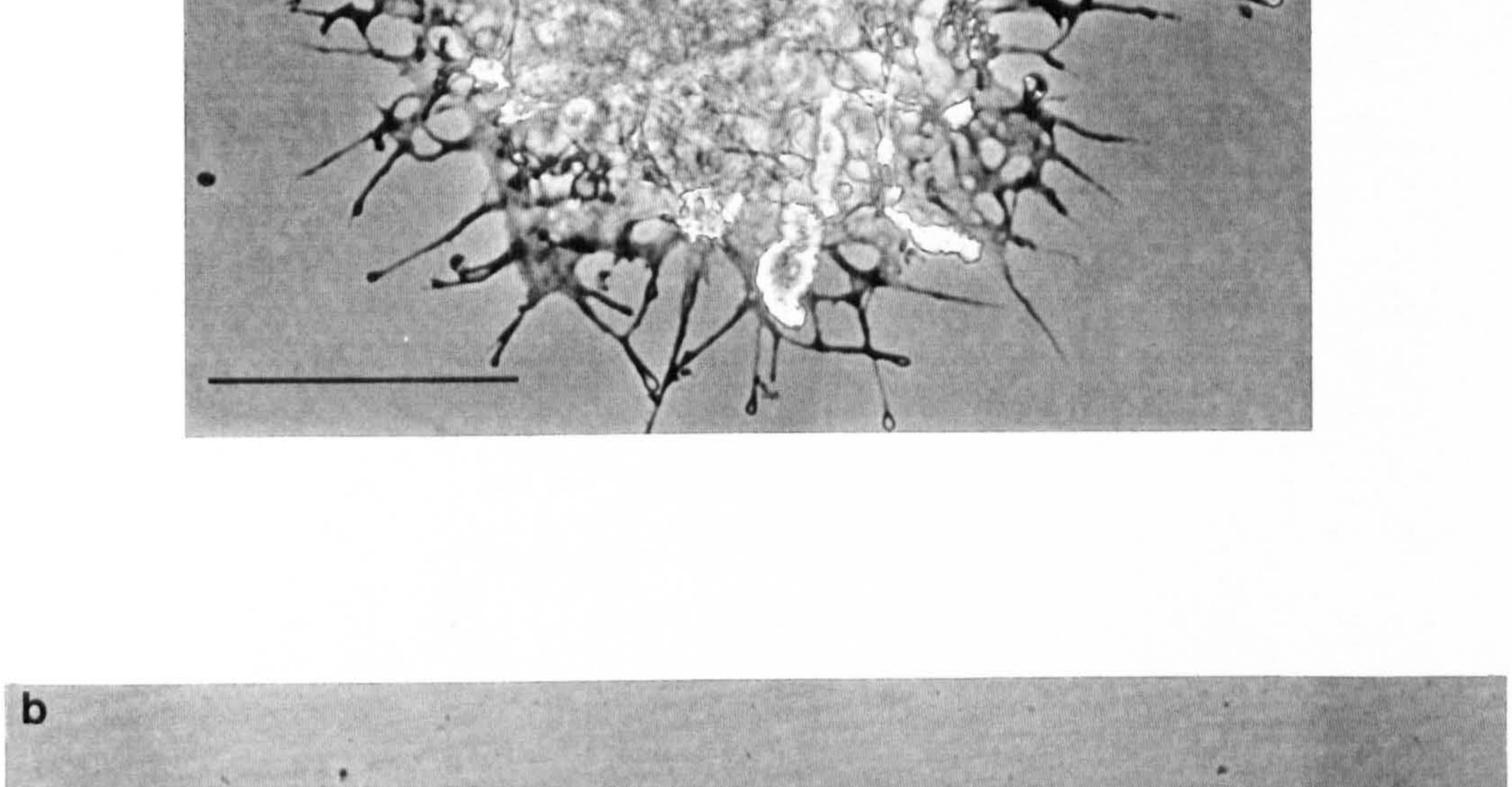
b
ct
c

**Figure 2.22.** Micrographs showing the developing arachnoid syncytia that occur simultaneously in a germinating culture of macrospores (isolate no. 7).

**a.** Many macrospores have died before reaching germination (dd), although some have become spherical post-spores (r) and eventually elongate into filamentous trophonts (tp). One of the filaments (arrow) is beginning to elongate.

**b.** As a filament elongates (arrow) it produces several unbranched cytoplasmic extensions. As a small arachnoid syncytium develops the cytoplasmic threads (ct) begin to branch and join.

**c.** The arachnoid syncytium continues to grow and produce longer cytoplasmic threads, and a mass of nucleated cytoplasm begins to develop at its centre (c).

Phase contrast. Scale bars = 100μm.

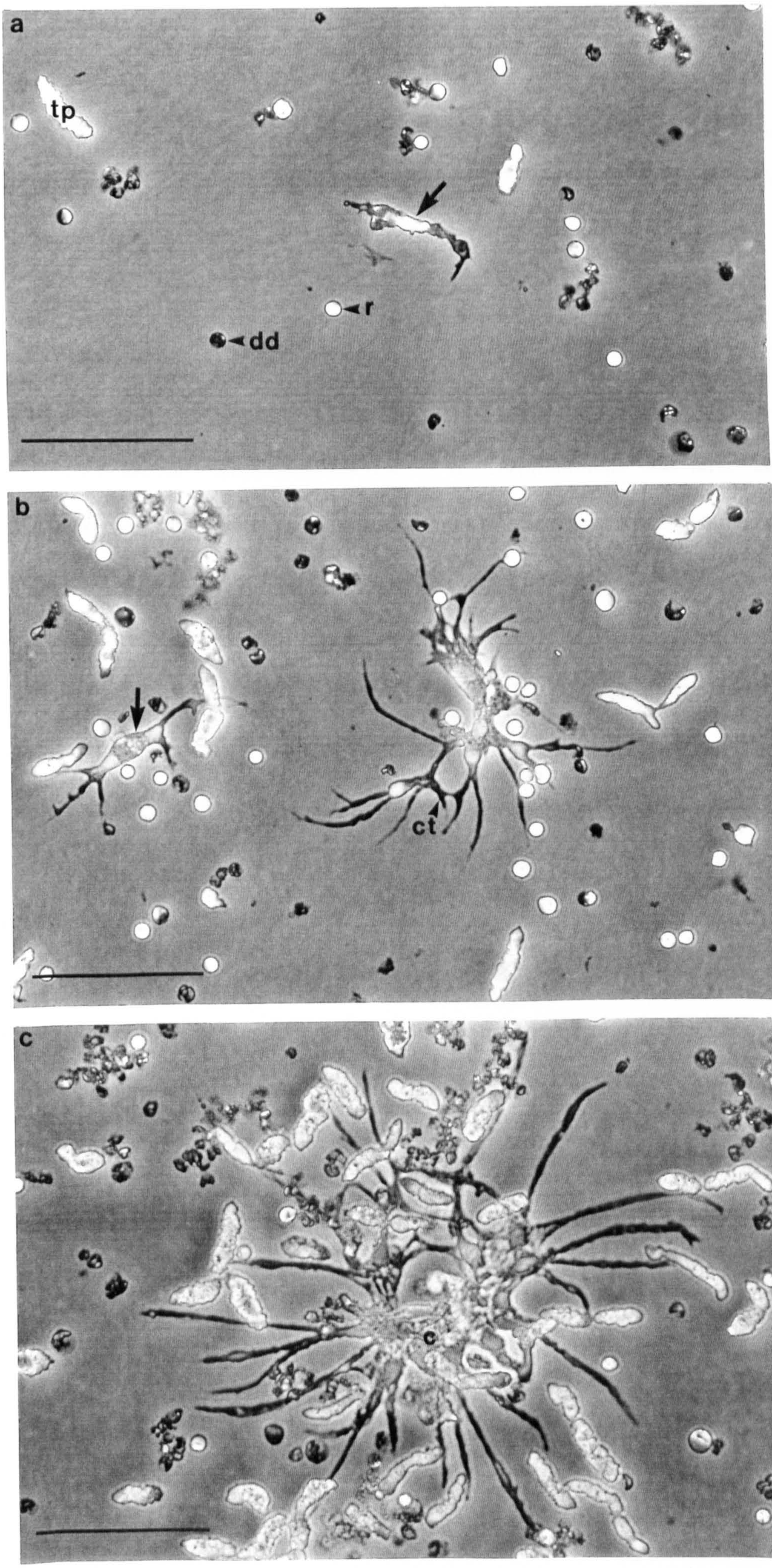
a
tp
r
dd
b
ct
c

# CHAPTER 3

# THE ULTRASTRUCTURE OF THE DEVELOPMENTAL FORMS OF *HEMATODINIUM* OBSERVED IN *IN VITRO* CULTURE

## 3.1. Introduction

The only *in vitro* developmental forms of *Hematodinium* that have been previously described with reference to ultrastructure are the dinospores, by Meyers *et al.* (1987). A comparison with the dinospores of *Syndinium* spp. is possible using Chatton's (1920) descriptions and illustrations and a limited amount of ultrastructural detail given by Manier *et al.* (1971) and Soyer (1974). More detailed ultrastructural work on the *Syndinium* sp. infecting radiolarians has been carried out by Ris and Kubai (1974) mainly describing the mechanism of nuclear division; Hollande (1974) described the ultrastructure of *Syndinium globiforme* and *Solenodinium fallax* also infecting radiolarians.

In this chapter I will present a description of the ultrastructure of the various developmental forms of *Hematodinium* that have been observed in *in vitro* culture. I will also compare the ultrastructure with those developmental forms of *Hematodinium* and *Syndinium* previously described by other workers.

## 3.2. Materials and Methods

### 3.2.1. Fixation of cultures for transmission electron microscopy (TEM)

Dinoflagellate forms that were not attached to the culture vessel were removed by pipette and concentrated by centrifugation at 150-600*g*. for 10 minutes depending on the parasite form. Filamentous trophonts were centrifuged at about 150*g*. and dinospores at 600*g*. The culture medium was removed and the pellet resuspended in chilled (10ºC) *Nephrops* saline to remove the foetal calf serum. The cells were centrifuged again and then suspended in the fixative which consisted of 2% paraformaldehyde and 1% glutaraldehyde in 0.1M phosphate buffer (pH 7.4) with 2% sucrose and 1.5% sodium chloride. Samples were fixed for one hour at 4ºC and then rinsed twice in 0.1M phosphate buffer containing 6.5% sucrose. Postfixation was carried out with 1% osmium tetroxide in 0.1M phosphate buffer containing 6.5% sucrose for one hour at room temperature. After rinsing in distilled water the suspended parasite material was pelleted by centrifugation and embedded in 1.5% agarose before further processing. Block staining was carried out with 0.5% aqueous uranyl acetate for one hour before dehydration through an ethanol series. Specimens were embedded in Spurr's resin (Spurr 1969).

Attached forms of the parasite were grown on glass coverslips and fixed and dehydrated as detailed above. When the specimens had been infiltrated with resin the coverslips were placed specimen down onto a polymerised disc of resin, and care taken to remove any excess resin encroaching the top of the coverslip. After polymerisation it was possible to remove the coverslip, leaving the embedded specimen attached to the top of the disc.

Thick resin sections (0.35-1μm) were cut with a glass knife, mounted on glass slides and stained with 1% aqueous toluidine blue for examination preparatory to selecting an area for ultrathin sectioning.

Gold or silver interference colour sections were cut using a diamond knife and mounted on uncoated palladium-gilded copper grids (300 mesh) or on Formvar coated copper grids (75-200 mesh). The thin sections were stained with 2% methanolic uranyl acetate for five minutes and then with Reynold's lead citrate for five minutes before examination. Thin sections were examined in a Zeiss 902 transmission electron microscope operating at 80kV.

Dinospores were negatively stained using uranyl acetate. Dinospores were fixed in the aldehyde mixture described above and washed in buffer. After resuspending in distilled water the microspores were allowed to settle on a carbon-coated Formvar covered grid. After 1 minute, excess water was removed with filter paper. A drop of 5% uranyl acetate (aqueous) was then placed on the grid. After 1 minute the uranyl acetate was completely removed using filter paper and the grid then allowed to dry. Grids were then viewed in the Zeiss 902 TEM.

### 3.2.2. Fixation for scanning electron microscopy (SEM)

Specimens for examination by scanning electron microscopy were fixed as described above and then dehydrated through an acetone series. Samples in suspension were retained on polycarbonate membrane filters with a 0.2µm pore size (Poretics Corporation, USA) for critical point drying. Specimens in 100% acetone were placed in the critical point drier and the vessel filled with liquid $CO_2$. The vessel was flushed through with liquid $CO_2$ three times over a period of 45 minutes. After 45 minutes the $CO_2$ supply was closed and the vessel slowly heated until the $CO_2$ reached it's critical point and became gaseous. The pressure in the vessel was slowly released over 15 minutes whilst keeping the temperature of the vessel above room temperature to prevent water condensation on the specimen. The dried filters were mounted on stubs and the specimens sputter coated with gold/palladium before viewing in a Philips 500 SEM operating at 12kV.

## 3.3. Results

### 3.3.1. Ultrastructure of sporogenic arachnoid syncytia (sporonts)

When sporoblasts were initially placed into *in vitro* culture they often formed sporogenic arachnoid syncytia which represent secondary sporonts. Secondary sporonts are syncytia first formed as large networks of cytoplasmic threads connecting nucleated regions (Figure 3.1). When examined by scanning electron microscopy the secondary sporonts were covered with a large number of small particles which could be discharged trichocysts. As the secondary sporonts approached sporogenesis the cytoplasmic threads became smaller with less branching. Scanning electron microscopy confirmed

the light microscopical observation that the central mass of the sporont formed a crater-like structure which gave rise to spherical bodies believed to be sporoblasts (see below and Figure 3.2). Light microscopical observations revealed that the sporoblasts produced by the secondary sporont transformed into dinospores.

When examined by transmission electron microscopy the attached secondary sporont contained numerous nuclei, trichocysts, membrane bounded organelles distributed throughout the cytoplasm (Figure 3.3a, b, 3.4 a, b & c, 3.5). The highly osmophilic spherical inclusions were thought to be lipid because of the lack of an obvious surrounding membrane. Irregularly shaped 'speckled-matrix organelles' (smo) were 1-4μm in their greatest dimension and bounded by a 10nm membrane. The speckled-matrix organelles contained an osmophilic substance of varying density that formed a network throughout the organelle (Figure 3.4 b). The anchoring cytoplasmic threads around the periphery of the sporont did not contain any recognisable organelles but did possess amphiesmal alveoli. Some circular membrane bound organelles 0.5-0.7μm in diameter contained a crystalline core 0.14-0.22μm square (Figure 3.4 a). The crystalline core was surrounded by an amorphous substance and was similar in appearance and size to trichocysts, suggesting that these organelles may be trichocyst precursors. Also present in the sporont were organelles surrounded by a 10nm membrane that were filled with an amorphous sometimes granular substance but did not contain a crystalline core (Figure 3.4 b, 3.5). The circular organelles were 0.25-0.5μm in diameter and will be referred to as 'granular matrix organelles' (gmo). Lipid droplets, trichocyst precursors, trichocysts and speckled matrix organelles were present throughout the cytoplasm of the developing sporoblasts in the inner raised mass of the secondary sporont (Figure 3.3 c). Small flagellar hair vesicles were found closely associated with the nuclei of the secondary sporont (Figure 3.5). One organelle found

in secondary sporonts resembled the appearance of Swiss cheese and was termed the 'caseiform organelle' (co). The caseiform organelle was an irregularly-shaped membrane bound (10nm) organelle 1-4μm in the greatest dimension that was partially filled with a homogenous osmophilic inclusion (Figure 3.5).

Some fixed attached sporonts possessed well preserved nuclear and mitotic features. Condensed V-shaped chromosomes were sometimes seen in ultrathin sections (Figure 3.6 a). The chromosomes in *Hematodinium* nuclei attach at their apices to a kinetochore-like structure inserted in the persistent nuclear envelope. Microtubules permanently connect the kinetochore to the bases of the two centrioles located in a pocket of the nucleus. The presence of a cytoplasmic tunnel and microtubule bundle illustrated that mitosis was occurring in the sporont (Figure 3.6 b).

### 3.3.2. Ultrastructure of macrospores

Macrospores that developed *in vitro* were 16-20μm in length and 8.5-11.5μm (n=25) in width. The anterior end of the macrospore was rounded and bulges of the amphiesma caused by underlying lipid droplets (see below) were prominent when viewed by scanning electron microscopy (Figure 3.7 a, b). The posterior end of the macrospores narrowed to a rounded point. Both flagella arose towards the anterior end of the macrospore (Figure 3.7 a, b). The longer transverse flagellum originated within a shallow groove close to the anterior end and partially encircling the macrospore, but a circumscribing girdle was not present. Flagella of the macrospore were rendered particularly brittle by the fixation process and usually detached from the spore body and subsequently fragmented. Limited measurements of the macrospore flagella were made using scanning electron microscopy because flagella viewed after negative staining

were inadequately preserved. The transverse flagellum was longer than the spore body, up to 30μm long (n=5). The shorter longitudinal flagellum (~13μm, n=5)) was attached behind the transverse flagellum but they were separated by a ridge (Figures 3.7 a, b). The longitudinal flagellum was initially located in a straight sulcus which ran half the length of the macrospore. The distal part of the longitudinal flagellum emerged from the sulcus but did not extend beyond the length of the spore body. The macrospores were covered with numerous hair-like projections, and these were presumed to be discharged trichocysts. Discharge of the trichocysts may have been triggered by the addition of the primary fixative.

Transmission electron microscopy of macrospores showed that the bulging spherical inclusions located at the anterior end of the dinospore were highly osmophilic without an obvious surrounding membrane; suggesting that they are lipid droplets (Figures 3.8 a, b, 3.9 a). The nucleus was located towards the centre of the dinospore; the chromosomes were condensed. Numerous clear vacuoles were located from the middle to the posterior end of the macrospore (Figures 3.8 a, b). Flagellar hair vesicles were found usually at the anterior end of the macrospore. Trichocysts were distributed throughout the cytoplasm. Some trichocysts were located at the periphery of the macrospores in a position ready for discharging (Figure 3.9 a). Clusters of granular matrix organelles were found from the middle to the posterior end of the macrospores (Figures 3.8 a, b, 3.9 b). Some of the granular matrix organelles were flattened and up to1.5μm long. Caseiform organelles were present; in some the homogeneous inclusion was limited to the periphery of the organelle (Figure 3.9b). In some macrospores bands of microtubules were visible in places beneath the alveoli (Figures 3.9 b, c). Microtubules were not found consistently in every isolate processed for electron microscopy, however in those where they were observed they were present at the

anterior end of the macrospore. The flagella axonemes had a conventional 9+2 structure and were 320-392nm (n=5) in diameter.

### 3.3.3. Ultrastructure of microspores

The microspores produced in *in vitro* culture were 11-14μm (n=25) in length and 4.5-6.5μm (n=25) in width. Early microspores observed soon after sporogenesis were oval in shape with pointed anterior and posterior ends with a smooth surface when examined by scanning electron microscopy (Figure 3.10). As the microspores matured the anterior end became blunted and the posterior end became pointed. Both flagella originated towards the centre of the microspore, whereas the flagella of the macrospore arose from the anterior end. As in the macrospore, the longer transverse flagellum (~50μm, n=5, negatively stained) was located anterior to the longitudinal flagellum (~15μm, n=5, negatively stained) in a shallow groove. The longitudinal flagellum was located behind the transverse flagellum but separated from it by a ridge. A circumscribing girdle formed a deep grooved channel which spiralled around the body, giving it a characteristic 'corkscrew' shape (Figure 3.11 a). The longitudinal flagellum extended beyond the posterior end of the spore body. The boundaries of amphiesmal alveoli were very visible in many microspores, forming a corrugated surface over the middle and anterior part of the spore (Figure 3.11 c). The posterior end of the microspore was much smoother than the rest of the spore surface and it was in this region that the refractile body was located (Figure 3.11 b). Discharged trichocysts were also evident (Figure 3.11 b); they were much longer than those seen by SEM on the macrospores.

Negative staining showed the length of both flagella in comparison with the microspore body (Figure 3.12 a). Negative staining also revealed the presence of hair-like structures protruding from the transverse flagellum of microspores (Figure 3.12 c, d). The hairs were 1-2μm long and arose every 50-160nm along the entire length of the transverse flagellum. The hairs were found mainly along one side of the flagellum. Similar hairs were not observed on the longitudinal flagellum or on the fragmented macrospore flagella that were negatively stained. Discharged trichocysts were observed in the negatively stained preparations. These trichocysts were 50nm wide and up to 20μm in length (Figure 3.13 a); they had a characteristic repeating banding pattern of 78nm total length, the periodicity of which is shown in Figure 3.13 b.

Multinucleate sporoblasts through a series of uneven divisions gave rise to uninucleate dinospores. Eventually all sporoblasts divided into uninucleate dinospores. Transmission electron microscopy was carried out on sporoblasts fixed during late microsporogenesis (Figure 3.14 a, b). At this stage the cytoplasm had begun to invaginate around the individual nuclei. Dividing sporoblasts contained flagellar hair vesicles , lipid droplets, trichocysts and granular matrix organelles. Numerous clear vacuoles were present in the region of division (Figure 3.14 a, b); the clear vacuoles may be involved in the synthesis of the new amphiesma.

Mature microspores showed a characteristic bent profile when viewed in longitudinal section (Figures 3.15 a, b). The nucleus was virtually entirely filled with condensed chromosomes. When viewed using phase contrast the refractile body was found be 3.4-3.9μm (n=10) long. In the transmission electron micrographs this size corresponded to that of the posteriormost vacuole (Figure 3.15 a, b). The refractile body contained a small amount of weakly stained material. Microspores contained flagellar hair vesicles, trichocysts, lipid droplets and granular matrix organelles (Figures

3.15 a, b, 3.16. In one sectioned microspore two micropores were present in a flagella pocket (Figure 3.17). The basal bodies of the flagella were closely associated and clearly show the flagella emerging from two separate pockets (Figure 3.25). The flagellar shaft had a conventional axoneme structure and was 290-370nm in diameter (Figure 3.20). In some glancing sections through microspores bands of microtubules were observed beneath the alveoli (Figure 3.21), however, it was not clear whether these were microtubular ribbons of the basal bodies. Cortical microtubules were not observed in longitudinal or transverse sections.

### 3.3.4. Ultrastructure of filamentous trophonts

In transmission electron micrographs the filamentous trophonts which form the main growth stage *in vitro* were readily distinguished from the sporogenic developmental forms of the parasite in that they did not possess trichocysts or flagellar hair vesicles. As did other developmental forms of the parasite, the filamentous trophonts possessed nuclei that contained condensed chromosomes interspersed with a darkly staining granular material (Figure 3.22 b, 5.4). Nucleoli of a granular appearance were not visible in all nuclei. The trophonts contained numerous mitochondria, endoplasmic reticulum and lipid droplets (Figure 3.22 a, b). Empty vacuoles were distributed throughout the cytoplasm and clusters of granular matrix organelles were also present (see Figure 5.3). The amphiesmal alveoli were compressed in the filamentous trophonts and in some places micropores were found (see Figures 8.1, 8.2, 8.3 a, b). Although the filaments displayed quite vigorous writhing movements I did not identify any cytoskeletal components which might underlie these movements. The apparent absence of cytoskeletal components maybe artifactual due to method of fixation which may not adequately preserve these structures.

### 3.3.5. Ultrastructure of arachnoid syncytia

Filamentous trophonts are capable of attaching to the substratum and developing into arachnoid syncytia (primary sporonts). By scanning electron microscopy two main forms of arachnoid syncytia were observed. First, discrete syncytia comprised a central mass of nucleated cytoplasm connected by thick cytoplasmic threads with finer-branched threads radiating outwards (Figure 3.23 a); nuclei were located where

cytoplasmic threads branched. As seen by SEM such syncytia were not covered in small particles as were the secondary sporonts (Figure 3.1) and when examined by TEM did not contain trichocysts (see below). Secondly, large arachnoid syncytia were produced when smaller syncytia fused were composed of a delicate network of fine cytoplasmic threads with nuclei located where the threads branched (Figure 3.30), they did not possess a raised mass of nucleated cytoplasm.

Examination of ultrathin sections by transmission electron microscopy showed that the arachnoid syncytia did not contain trichocysts or flagellar hair vesicles. Numerous lipid droplets were found throughout the cytoplasm (Figure 3.24a, c). Arachnoid syncytia also contained numerous membrane bound (10nm) organelles (1-5μm diameter) which contained a dense osmiophilic material around their periphery (Figure 3.24 c); these organelles will be referred to as peripheral inclusion organelles (pio). Granular matrix organelles 0.5-0.75μm diameter were found individually or in clusters of 3-4 throughout the cytoplasm. The cytoplasmic threads that formed the syncytial network contained mitochondria and granular matrix organelles (Figure 3.24). Alveoli appeared to missing from the fine extensions of the cytoplasmic threads (Figure 3.24 b). Neither microtubules or microfilaments were observed in the cytoplasmic threads or in any other part of the arachnoid syncytium. Amphiesmal alveoli were swollen in places and were present over the entire surface of the arachnoid syncytium; except for the fine extensions of the cytoplasmic threads as mentioned above.

### 3.3.6. Ultrastructure of clump colonies

The clump colonies that developed in *in vitro* culture possessed an ultrastructure quite distinct from the other developmental forms. The evidence from transmission electron microscopy of sectioned clumped colonies suggests that they are formed from a large mass of interdigitated trophonts. Numerous interlocked alveoli-covered regions of cytoplasm 1-4μm diameter were observed in TEM sections: these structures may form cytoplasmic protrusions which intertwine and hold the colony together (Figure 3.25 a). In some places the plasma membrane and alveolar sacs were sharply folded and intruded into the cytoplasm of a body (Figure 3.25 b). The clumps contained numerous lipid droplets but did not contain any trichocysts or flagellar hair vesicles. Large vacuoles were present in some parasites suggesting degeneration.

## 3.4. Discussion

The ultrastructure of all the developmental stages of *Hematodinium* from *in vitro* culture have been investigated. The dinospores that I observed *in vitro* are similar to those observed by Meyers *et al.* (1987). The macro and microspores were the only developmental form that Meyers and colleagues describe from *in vitro* culture. Tables 3.1 and 3.2 show a comparison between the dinospores derived from *N. norvegicus* and *C. bairdi*. Inadequate descriptions of the dinospores from *C. bairdi* by Meyers *et al.* limits the conclusions that can be drawn from comparison with the dinospores that I have described. Comparison with the data that are available shows that there is some similarity between the dinospores that develop in the two hosts.

| | Host | |
|---|---|---|
| | *Nephrops norvegicus* | *Chionoecetes bairdi* |
| Dimensions | 11-12 x 4.5-6.5µm (n=25)<br>DIC | 12 x 4.4µm (n=5) |
| Length of transverse flagellum | ~50µm (n=5)<br>-ve staining | ~18µm<br>SEM |
| Length of longitudinal flagellum | ~15µm (n=5)<br>-ve staining | ~5µm<br>SEM |
| Flagellar insertion | Midbody of spore | Midbody of spore |
| Flagellar hair vesicles | Present | Present |
| Refractile body | Bacilliform | Spherical |
| Trichocysts | Present | Present |
| Inclusions | Granular matrix organelles, lipid droplets | Uncharacterised |
| Nucleus | Highly condensed chromosomes take up most of nuclear space | Highly condensed chromosomes take up most of the nuclear space |

**Table 3.1.** A comparison of the microspores described in this Chapter with those described by Meyers *et al.* (1987) from the Tanner crab *Chionoecetes bairdi*.

| | Host | |
|---|---|---|
| | *Nephrops norvegicus* | *Chionoecetes bairdi* |
| Dimensions | 16-20 x 8.5-11.5µm (n=25) DIC | 15.2 x 11.4µm (n=8) |
| Length of transverse flagellum | ~30µm (n=5) SEM | ~15µm SEM |
| Length of longitudinal flagellum | ~13µm (n=5) SEM | ~5µm SEM |
| Flagellar insertion | Anterior end of spore | Anterior end of spore |
| Flagellar hair vesicles | Present | Present |
| Trichocysts | Present | Present |
| Inclusions | Lipid droplets, granular matrix organelles, caseiform organelles | Uncharacterised |
| Nucleus | Chromosomes condensed, but less condensed than in microspores, surrounded by much nucleoplasm | Chromosomes condensed, but less condensed than in microspores, surrounded by much nucleoplasm |

**Table 3.2.** A comparison of the macrospores described in this Chapter with those described by Meyers *et al.* (1987) from the Tanner crab *Chionoecetes bairdi*.

I have described different types of inclusion in the dinospores, but Meyers *et al.* (1987) did not characterise the 'electron dense bodies' in the dinospores of *C. bairdi*. The dinospores (7-8 x 3-3.5μm) of *Syndinium gammari* contain some unidentifiable dense inclusions, trichocysts and flagellar hair vesicles (Manier *et al.* 1971). The highly condensed chromosomes which entirely fill the nuclei of *S. gammari* dinospores resemble the appearance of the nuclei in the microspores that I have described.

The nuclei of the dinospores of the *Syndinium* sp. described by Soyer (1974) were similar to those I have described in macrospores. The stages of mitosis that I have observed in sections of *Hematodinium* viewed in the TEM match the descriptions of mitosis that Ris and Kubai (1974) provided for *Syndinium*. The *Syndinium* dinospores Soyer describes contain many trichocysts and dilated perinuclear spaces (possibly flagellar hair vesicles) and organelles containing a homogenous granular material similar to the granular matrix organelles I have described in *Hematodinium* sp.

The nature of the inclusion organelles in the developmental stages of *Hematodinium* is unclear. Hollande (1974) has shown that *Syndinium* spp. of radiolarians contain both lipid droplets and spherical polysaccharide inclusions. It is possible that the caseiform organelles that I have described consist of polysaccharide, although this has not yet been demonstrated. The large number of inclusions may represent energy reserves that are vital for the survival of dinospores during their free-living stage.

The fibril-containing swollen perinuclear spaces and vesicles present in the sporont, sporoblasts and dinospores are thought to contain flagellar hairs (Leadbeater 1971) - hence the term 'flagellar hair vesicle'. Flagellar hairs have previously been found on the transverse flagellum of *Aureodinium pigmentosum* (Dodge 1967) and *Amphidinium carteri* (Dodge and Crawford 1968). Movement of fibrils from the

vesicles to the cell surface and incorporation into the flagellum has yet to be demonstrated. The presence of hairs solely on the transverse flagellum of *Hematodinium* microspores suggests that their function may be related to propulsion of the dinospore. The presence of hairs on the flagella of macrospores was not confirmed due to the adverse effects of fixation, however, I would expect them to be present because flagellar hair vesicles were found.

A refractile body similar to that which I have described in the microspore has been observed in the microspores from the *Hematodinium* sp. infecting *C. bairdi* (Meyers *et al.* 1987) and in the *Syndinium* microspores described by Chatton (1920). The composition and function of the refractile body is not known.

Is the absence of trichocysts and flagellar hair vesicles in culture trophonts real or artifactual? The absence of these structures in culture trophonts could be due to loss through prolonged culture, or the ability to produce them. The absence of selection to produce a particular stage in the life cycle is common in artificially cultured protozoa (e.g. loss of ability to form cysts in *in vitro* cultured *Entamoeba*). A lack of selection can allow fast overgrowing mutants to replace the form found in nature. Alternatively the parasite may be deprived of the appropriate precursors/nutrients to enable it to synthesise the missing structures. The evidence that trophonts are able to attach to the substratum and develop into sporonts and in a few isolates produce further generations of dinospores suggests that the trophonts remain fully functional and the absence of trichocysts and flagellar hair vesicles is not artifactual. The presence of trichocysts and flagellar hair vesicles therefore indicates a sporogenic developmental form of the parasite.

One conflict with the hypothesis that flagellar hair vesicles and trichocysts are markers for sporogenesis occurs with the arachnoid syncytia (sporonts) which have

grown in long term cultures and lack these structures. This anomaly may be interpreted in two ways. Firstly, the absence of sporogenic markers may be due to inadequacies of the culture system or absence of selection for spore formation *in vitro*. Secondly, the lack of sporogenic markers may indicate that commitment to sporogenesis (differentiation) occurs later, enabling early arachnoid syncytia to revert to unattached trophonts if favourable conditions for sporogenesis are not present. The fact that *in vitro* produced arachnoid syncytia from a few isolates have produced dinospores suggests that the first interpretation is unlikely. The problem of observing directional transformation in cultures containing a range of developmental forms has made it difficult to produce hard evidence that arachnoid syncytia can revert to trophonts. Limited evidence comes from cultures which appear to consist entirely of attached sporonts that are able to revert back to trophonts over a period of weeks.

I propose that the attached sporont is the developmental stage where the commitment to sporogenesis occurs. The nature of the trigger for the differentiation into a sporogenic form containing the appropriate markers is unclear, and it is possibly this trigger which is lacking from the culture system. The lack of a trigger for differentiation into a sporogenic form in my culture system may explain why most of the isolates derived from circulating sporoblasts were able to produce one generation of dinospores but rarely able to produce more though capable of indefinite survival as the trophont stage.

The use of the term 'vegetative stages' by previous workers is highly misleading as it has been used to cover all developmental stages other than the dinospore. I have shown that the trophont does not contain trichocysts or flagellar hair vesicles but the sporont, sporoblasts and dinospores do. The use by other workers, particularly Hudson

and Shields (1994) of the presence or absence of trichocysts in 'vegetative' stages as a comparative ultrastructural feature for differentiating species is therefore misleading.

The ultrastructural information I have presented in this chapter provides further characterisation of the developmental forms of *Hematodinium* maintained *in vitro*. I have identified structures such as the trichocyst, flagellar hair vesicle, refractile body and numerous inclusion organelles whose composition and function remain to be investigated.

**Figure 3.1. and 3.2.** Scanning electron micrographs of sporogenic arachnoid syncytia (secondary sporonts) from *in vitro* culture.

**Figure 3.1.** Sporont showing the network of cytoplasmic threads (ct) of differing thickness which connect islands of nucleated cytoplasm. The surface of the secondary sporont is covered with small particles (arrows) which could represent discharged trichocysts. Scale bar = 10μm.

**Figure 3.2.** A a crater-like secondary sporont during sporogenesis. Unnucleated filopodium-like extensions radiate from the periphery and are still attached to the substratum. The raised inner part of the structure gives rise to sporoblasts (s) which divide into dinospores after release. Scale bar = 100μm.

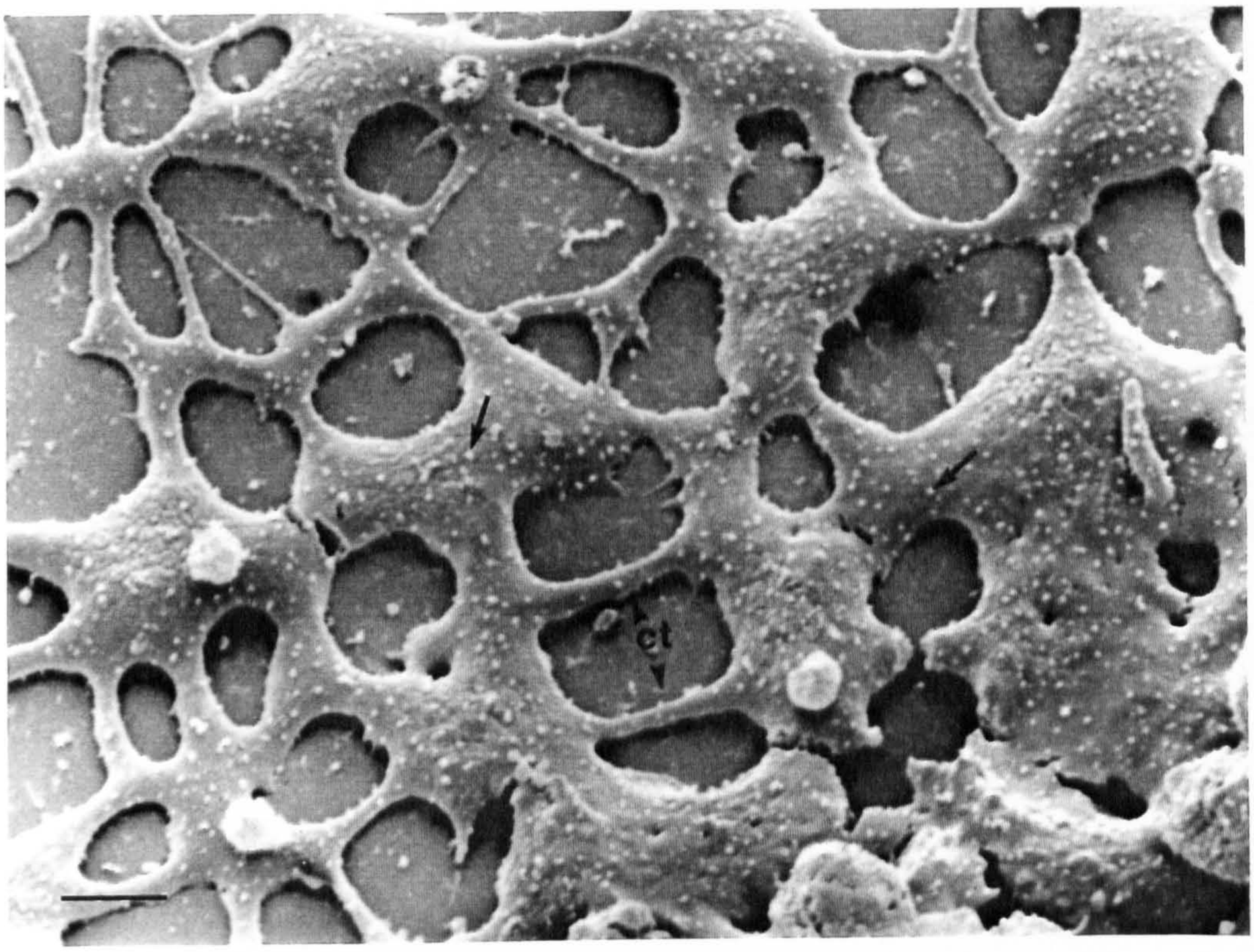
ct

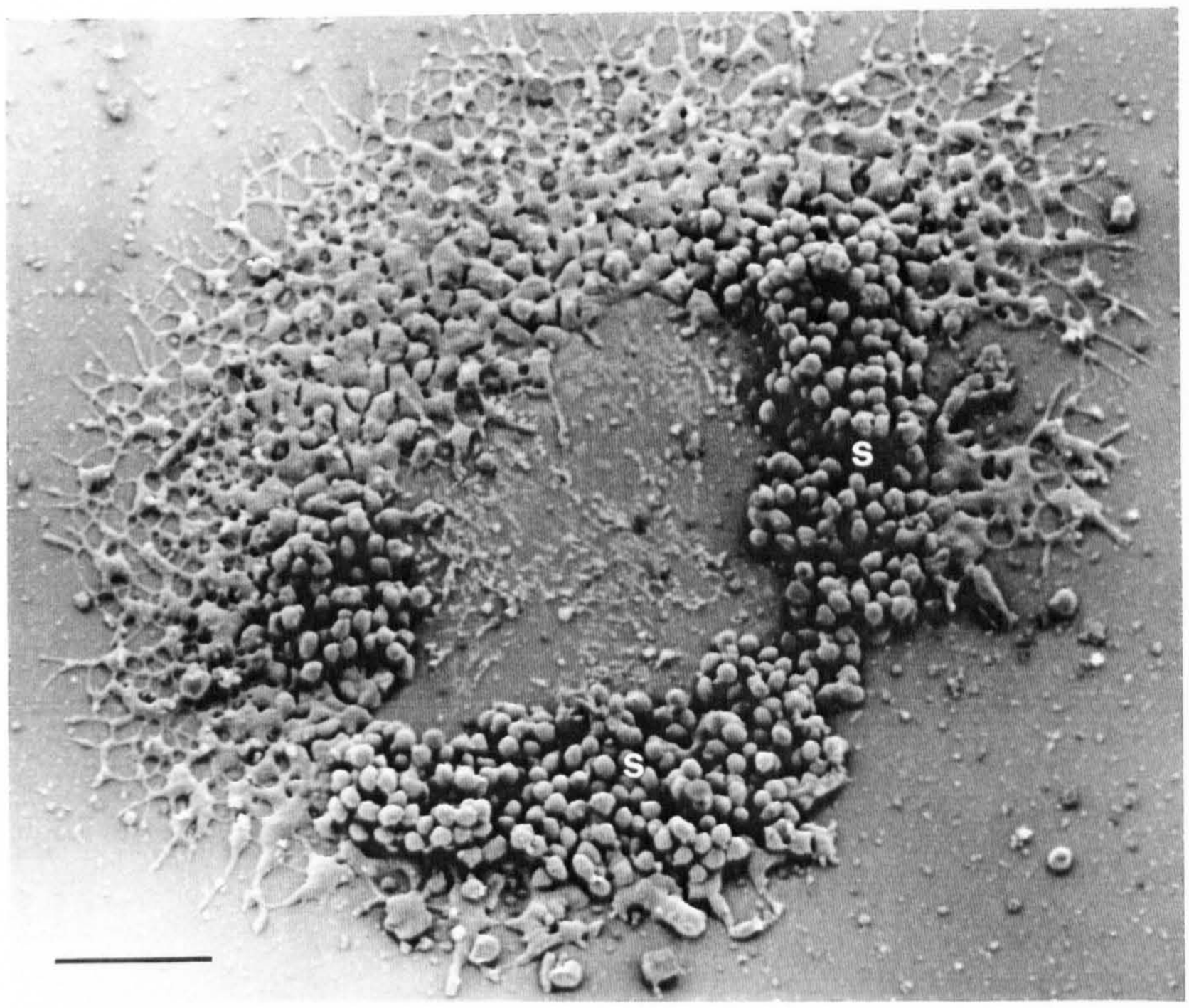
S
S

**Figures 3.3.** Transmission electron micrographs of sections of nucleated areas of secondary sporonts.

**a, b)** Vertical sections through the attached base of the sporont; the substratum is at the bottom of the sections. Numerous lipid droplets (l), trichocysts (tr) and mitochondria (m) are present throughout the sporont. Irregular membrane-bound organelles with a speckled matrix (smo) are a striking feature of this stage of the life-cycle. g = Golgi apparatus, n = nucleus, arrow = point of attachment of sporont to well.

**a.** Scale bar = 2μm.

**b.** Scale bar = 5μm.

**c)** A horizontal section through the raised inner mass of nucleated cytoplasm of an attached secondary sporont reveals a developing sporoblast. smo = speckled matrix organelle, l = lipid droplet, n = nucleus. Scale bar = 5μm.

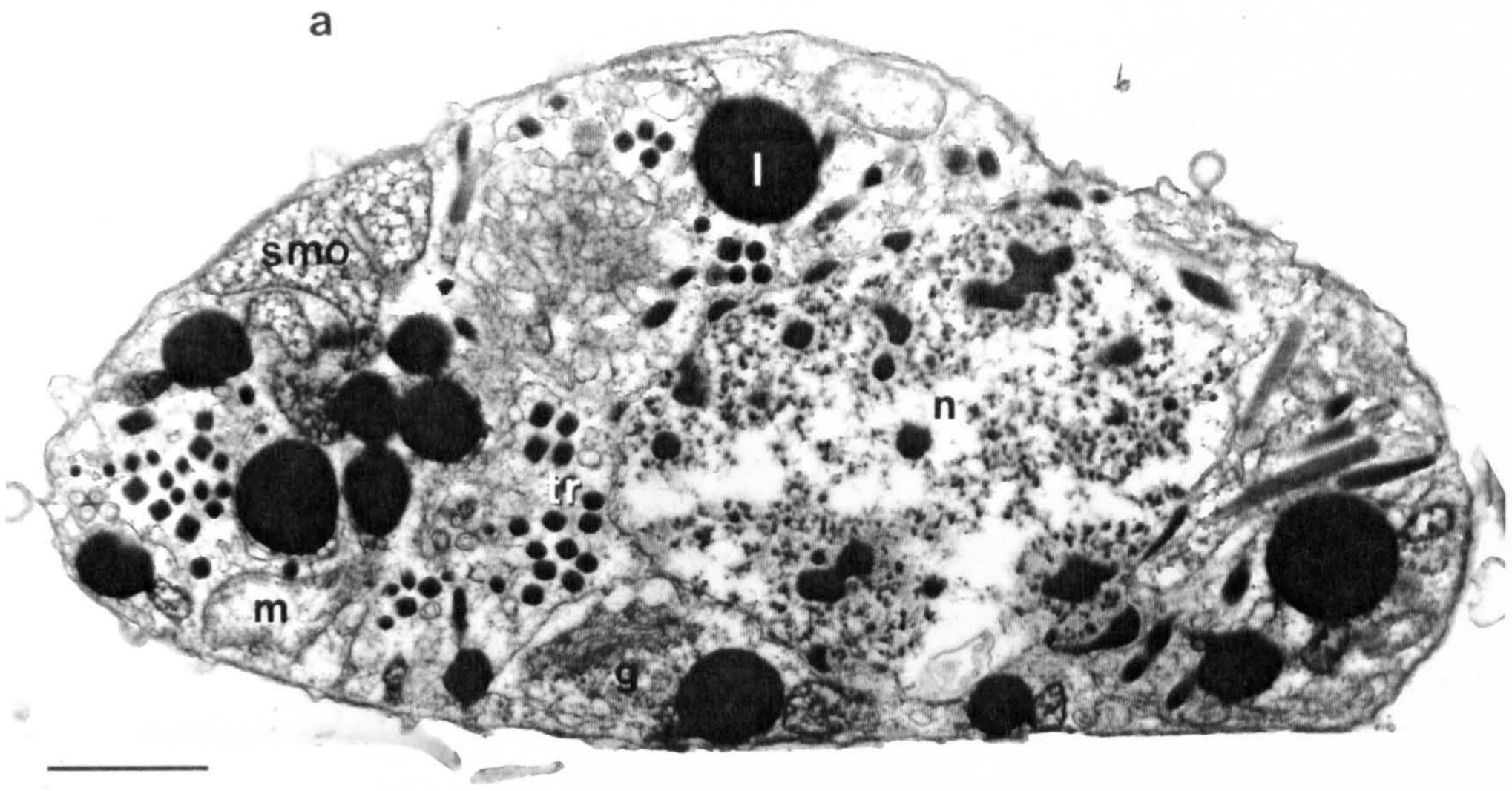
a
l
smo
n
tr
m
g

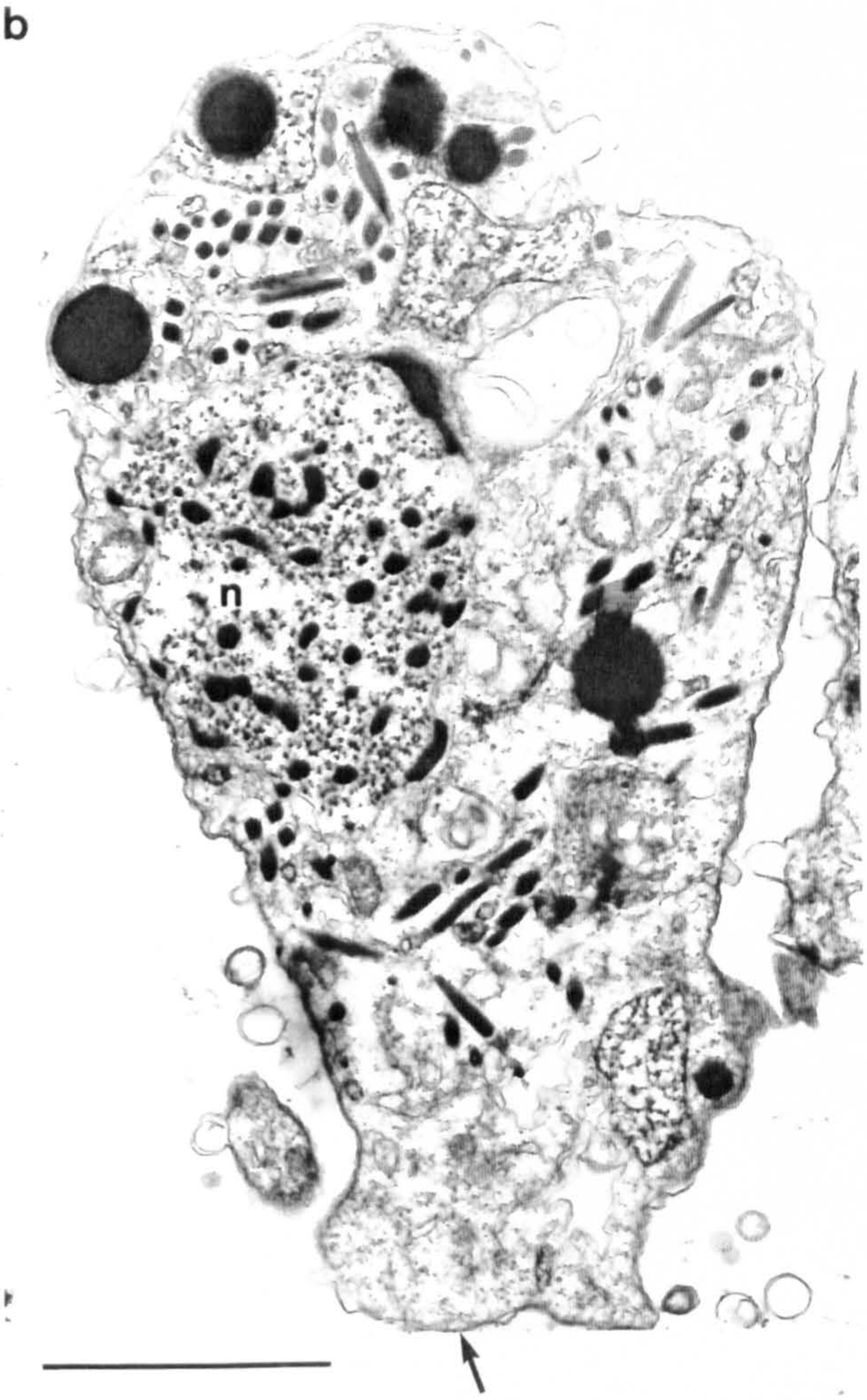
b
n

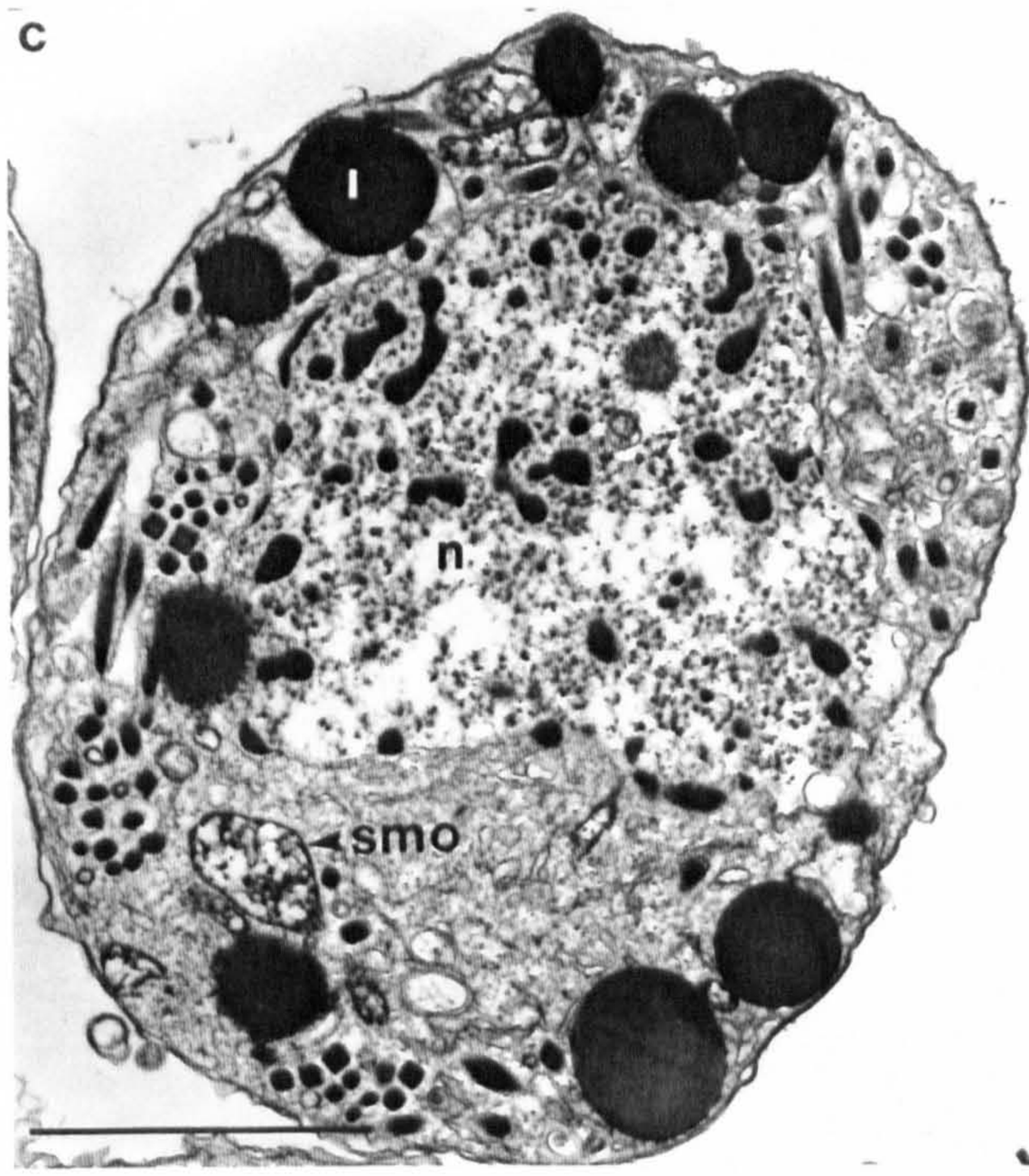
c
l
n
smo

**Figure 3.4.** Transmission electron micrographs of sections through secondary sporonts. **a)** Membrane bound organelles (arrows) with a crystalline core are observed in this stage. The similarity of the crystalline core to the trichocysts suggests that these organelles are trichocyst precursors. Inset shows the crystalline core (arrow) surrounded by an amorphous material. Scale bars = 0.5μm.

**b)** The speckled matrix organelle (smo) contains a heterogenous material that forms a network across the membrane bound organelle. The granular matrix organelle (gmo) differs from the trichocyst precursors shown above in it does not contain a crystalline core. l = lipid droplet. Scale bar = 0.5μm.

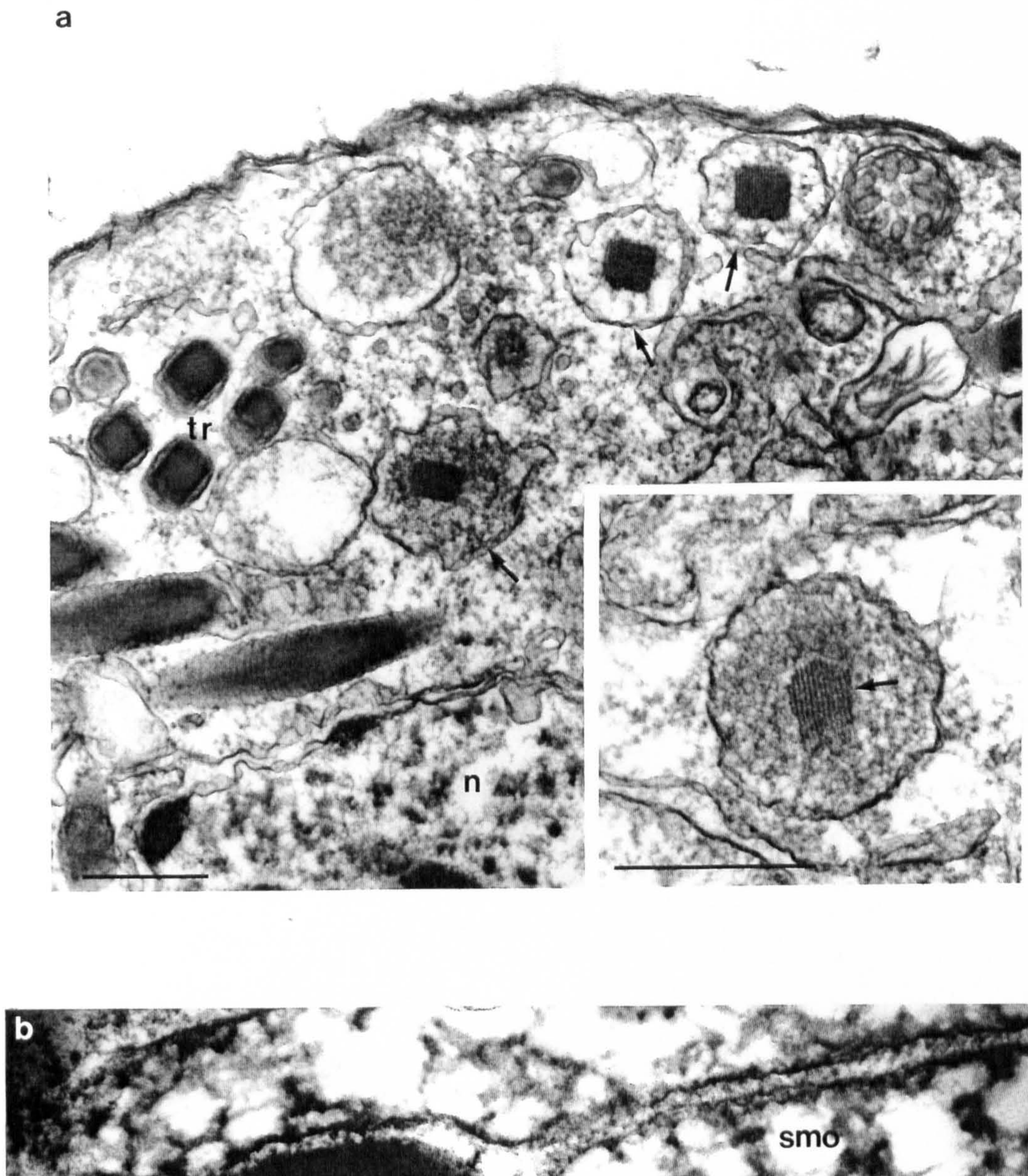
a
tr
n
b
l
smo
gmo

**Figure 3.5.** A horizontal section through an attached secondary sporont. Flagellar hair vesicles (fv) are found closely associated with the sporont nuclei (n). The chromosomes (ch) are highly condensed, indicating that the sporont will give rise to microspores. Amphiesmal-lined extracellular spaces are evident (as) as well as large clear intracellular vacuoles (va). The cytoplasm contains membrane bound caseiform organelles (co), granular matrix organelles (gmo) and lipid droplets (l). A membranous whirl (arrow) may represent a myelin figure, an artifact associated with chemical fixation. Transmission electron micrograph. Scale bar = 2μm.

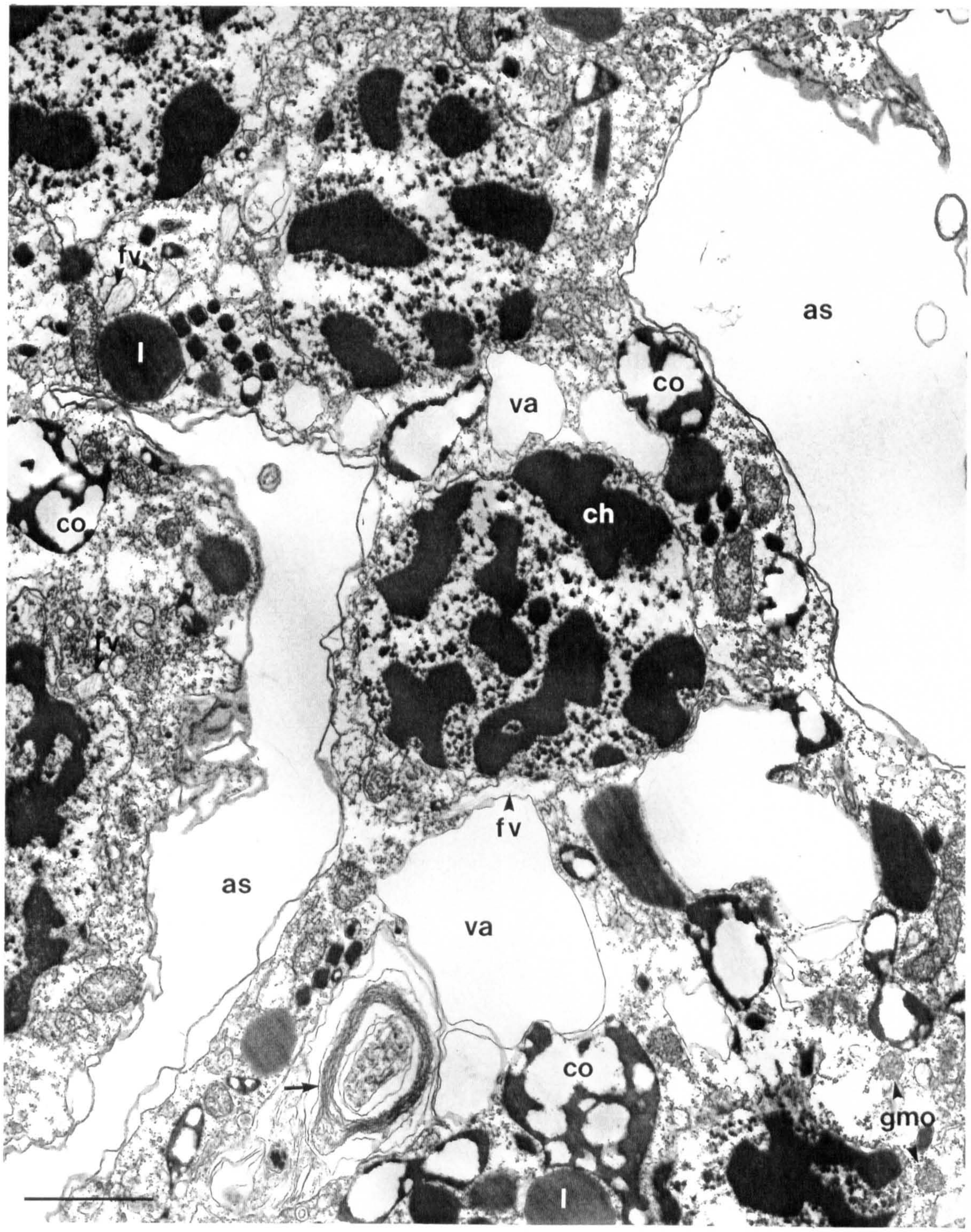
fv
I
co
va
ch
as
co
fv
as
va
fv
co
gmo
I

**Figure 3.6.** Transmission electron micrographs of horizontal sections of the nuclei from a secondary sporont.

**a)** A centriole (cn) is attached via microtubules (arrows) to 4 V-shaped chromosomes (1-4) in the nucleus. The chromosomes and microtubules are attached via kinetochores located in the nuclear envelope. Scale bar = 0.5μm.

**b)** Part of the cytoplasmic tunnel that passes through the nucleus at mitosis is visible. The cytoplasmic tunnel contains the microtubule bundle (arrow) that pushes the centrioles apart. The nuclear envelope remains intact during this process. cn = centriole, m = mitochondrion. Scale bar = 1μm.

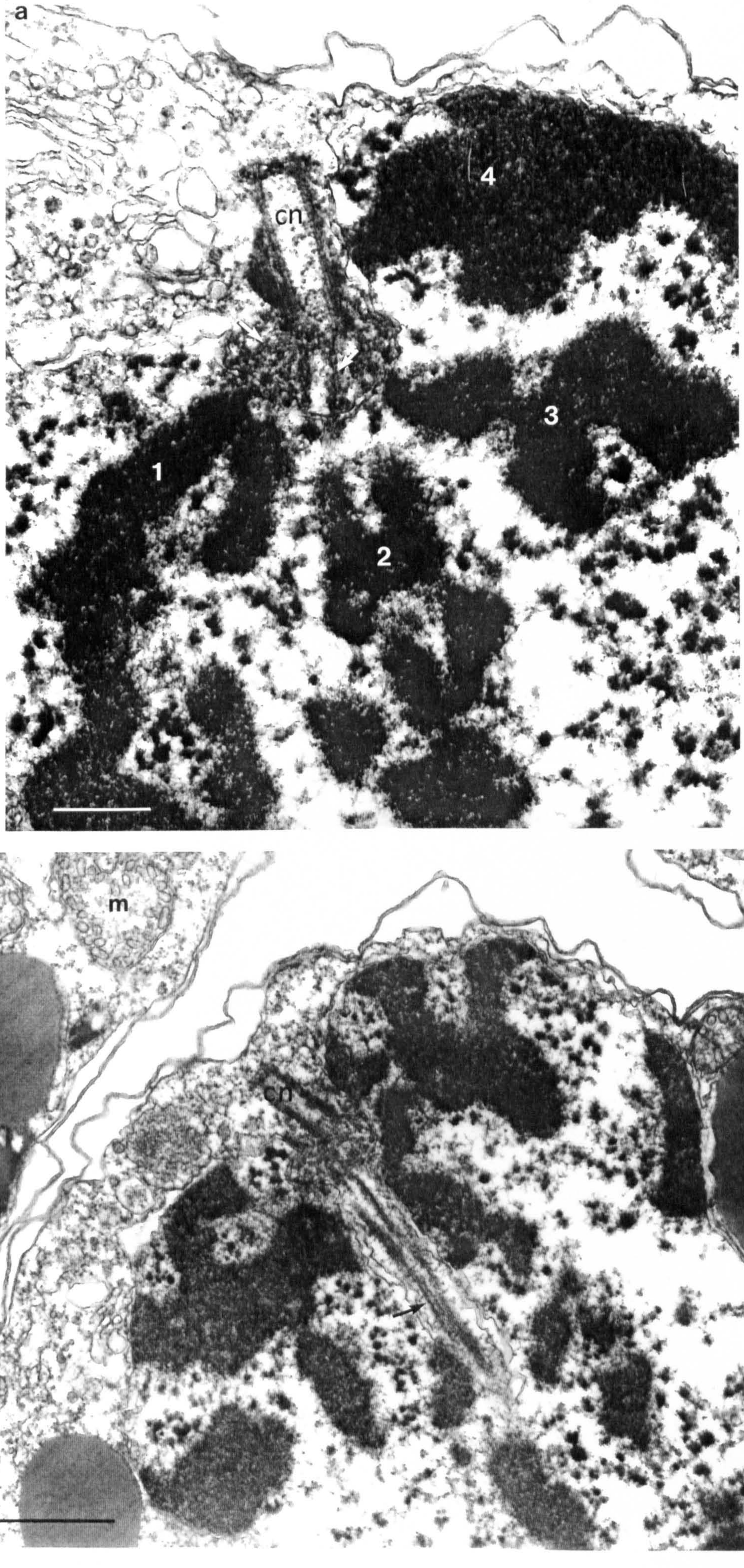
a
cn
4
3
1
2
b
m
cn

**Figure 3.7.** Scanning electron micrographs of mature macrospores from *in vitro* culture.

**a)** The anterior end (an) of the macrospore is rounded and contains lipid droplets (l) seen as bulges beneath the amphiesma; and the posterior end (po) narrows to a rounded point. Both flagella arise toward the anterior end of the macrospore. The longer transverse flagellum (tf) arises in a groove (arrrow) close to the anterior end. The shorter longitudinal flagellum (lf) arises behind the transverse flagellum and is initially located in a straight sulcus (su) which runs half the length of the macrospore. Scale bar = 5μm.

**b)** Numerous hair-like projections (tr) cover the macrospores, these are likely to be discharged trichocysts. Scale bar = 5μm.

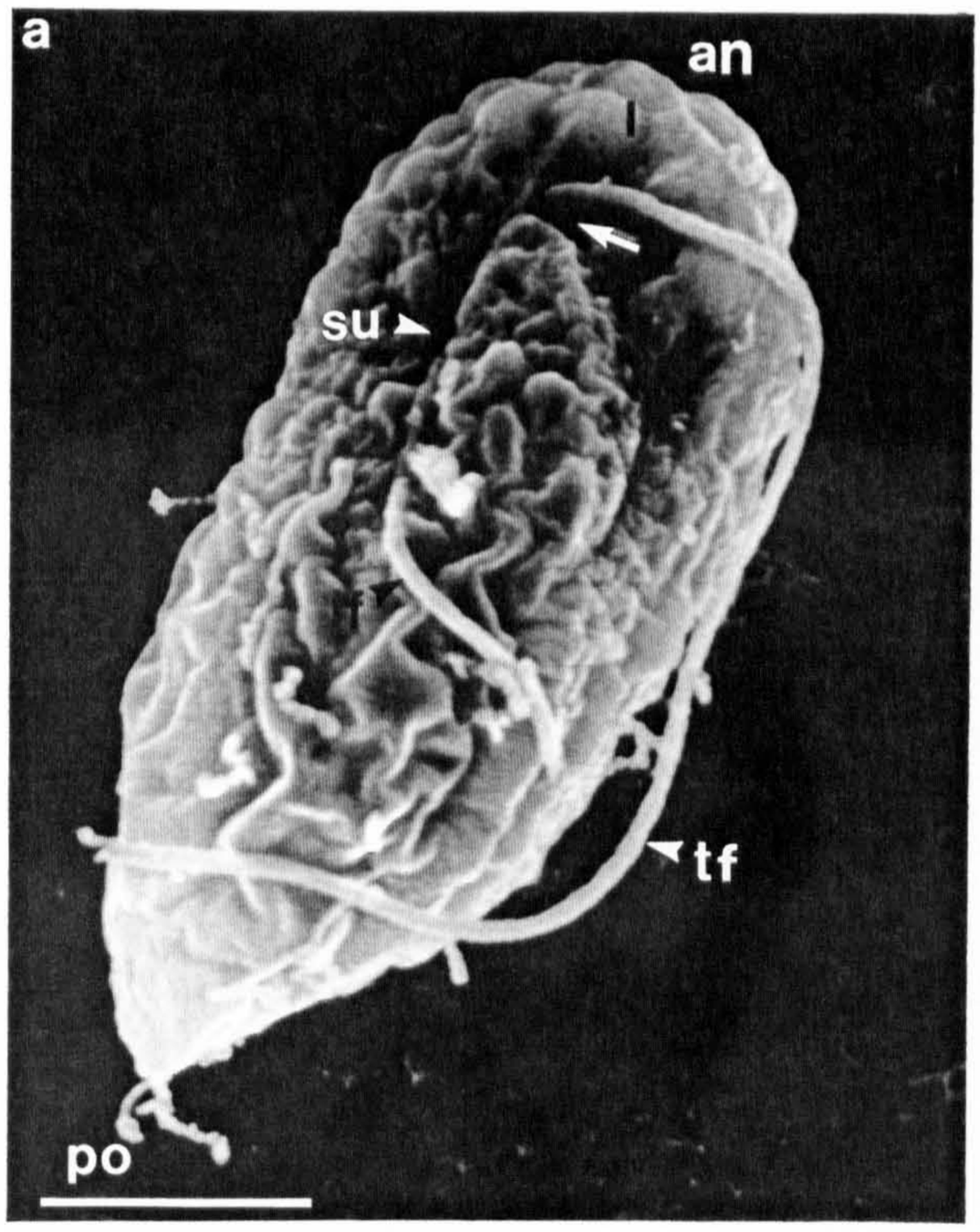
a
an
su
tf
po


b
tf
an
tr
lf
tr
po

**Figures 3.8.** Transmission electron micrographs of longitudinal sections through mature macrospores from *in vitro* culture.

**a)** Shows the centrally located nucleus (n), an aggregation of lipid droplets (l) at the anterior end and the large vacuoles (va) situated from the middle to the posterior end. A cluster of granular matrix organelles (gmo) are situated at the posterior end m = mitochondria, tr = trichocysts. Scale bar = 5μm.

**b)** Flagellar hair vesicles (fv) are found in the anterior end of the macrospore in close proximity to the Golgi apparatus (g). n = nucleus, l = lipid droplet, va = vacuole, gmo = granular matrix organelles, f = flagellum. Scale bar = 2μm.

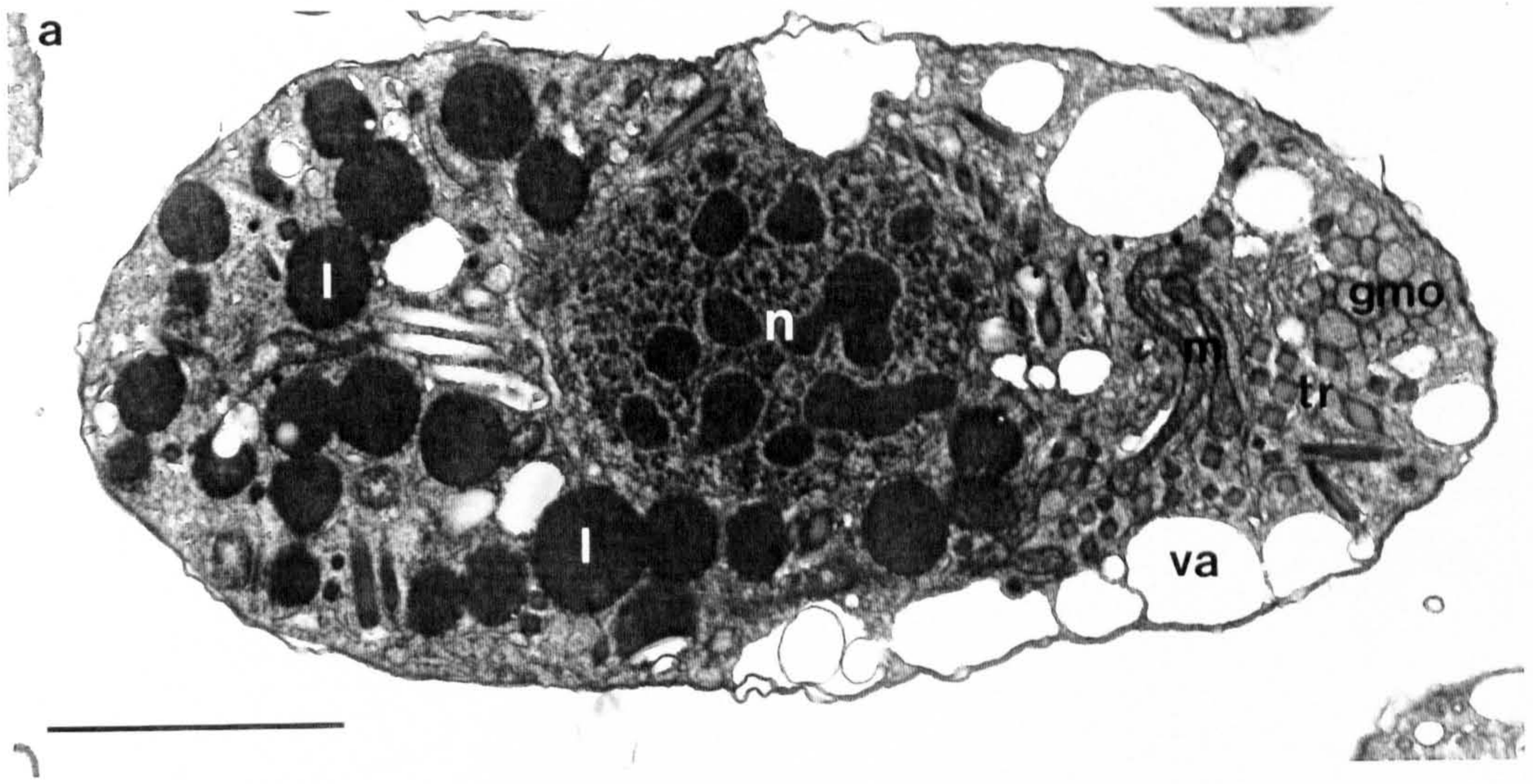
a
l
n
gmo
m
tr
l
va

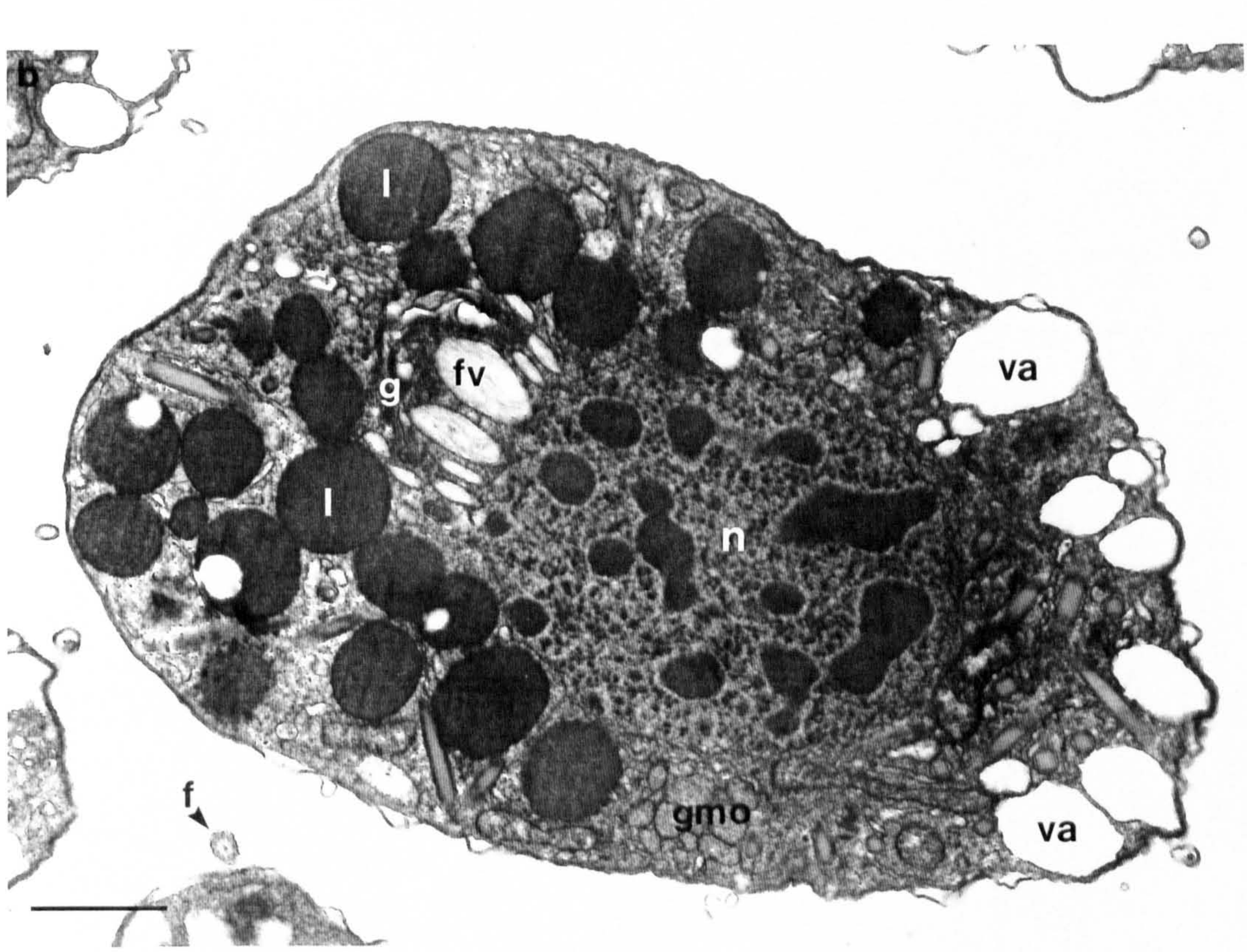
b
l
g
fv
va
l
n
f
gmo
va

**Figure 3.9.** Transmission electron micrographs of sections of macrospores from *in vitro* culture.

**a)** A longitudinal section through the anterior end of a macrospore. A trichocyst (arrow) is seen at the periphery of the macrospore in preparation for discharging. fv = flagellar hair vesicle, l = lipid droplet, er = endoplasmic reticulum. Scale bar = 1μm.

**b)** A transverse section through the middle of a macrospore. The extent of a large alveolar profile (a) is shown. Microtubules (arrows) are visible below the alveolus. A large aggregation of granular matrix organelles (gmo) are present. Part of a caseiform organelle (co) is also shown. l = lipid droplet. Scale bar = 1μm.

**c)** A band of microtubules (mt) is present beneath an alveolar sac (a). m = mitochondrion. Scale bar = 0.5μm.

a

n

fv

l

er

b

l

m

gmo

a

co

c

a

mt

m

**Figures 3.10-3.11.** Scanning electron micrographs of microspores from *in vitro* culture.

**Figure 3.10. (Top left)** An early microspore that was fixed on the same day that sporogenesis occurred. The microspore is oval in shape with pointed anterior and posterior ends. Both flagella bases are located toward the centre of the microspore. The longer transverse flagellum (tf) is located anterior to the to the shorter longitudinal flagellum (lf). Scale bar = 5μm.

**Figure 3.11.** After 3-4 days microspores the mature, the anterior end is blunted and the posterior end pointed.

**a)** The girdle (gi) forms a deeply grooved channel around the microspore giving it a characteristic 'corkscrew'-shape.

**b)** The projection at the posterior end of the microspore is smoother than the rest of the spore body and houses the refractile body (rb). Discharged trichocysts (tr) are visible atached to the surface of some microspores; they are much longer than those seen on the macrospores. tf = transverse flagellum, lf = longitudinal flagellum. Scale bars = 5μm.

**c)** Over most of the spore body the swollen edges of the collapsed amphiesmal alveoli (a) are visible.

Scale bars = 5μm.

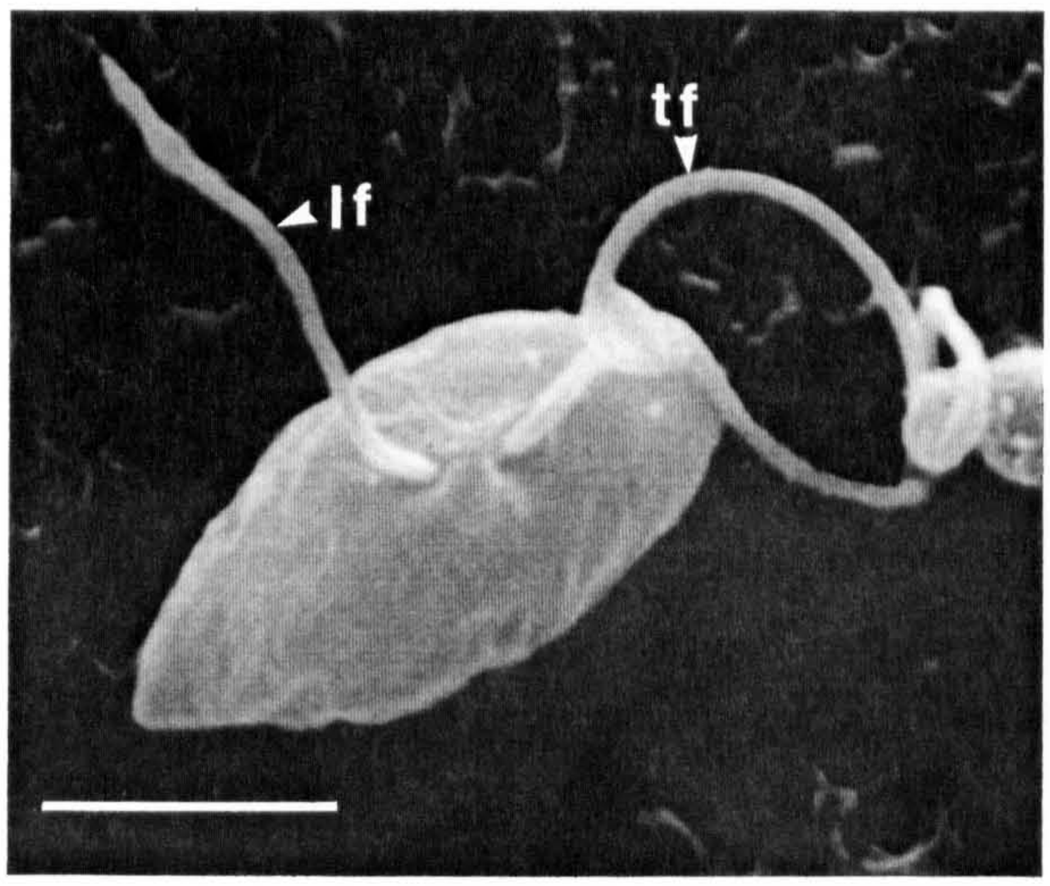
tf
lf

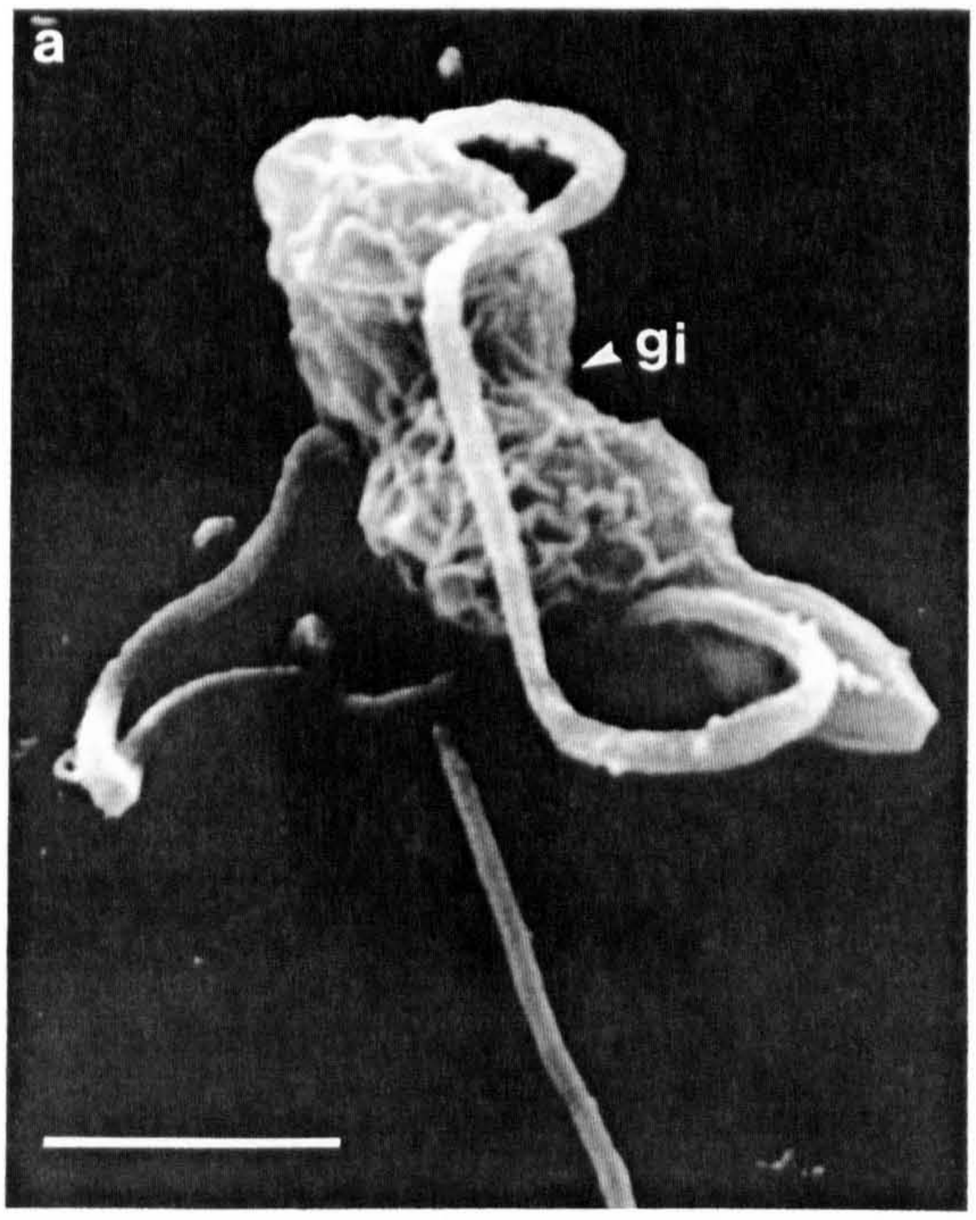
a
gi


b
lf
rb
tf
tr


c
tf
a
lf

**Figures 3.12-3.13 a.** Transmission electron micrographs of negatively stained early microspores from *in vitro* culture.

**Figure 3.12. a) (Top left)** Shows the length of the two flagella in comparison with the microspore body. The transverse flagellum (tf) is up to 50μm long, the longitudinal flagellum (lf) up to 15μm long. Scale bar = 10μm.

**b) (Middle left)** Discharged trichocysts (tr) are up to 20μm long. Scale bar = 5μm.

**c) (Top right)** Hair-like structures (arrows) protrude from the transverse flagellum (tf) of microspores, but not from the longitudinal flagellum (lf). Scale bar = 2μm.

**d) (Bottom left)** A negatively stained transverse flagellum (tf) showing the hair-like structures (arrows) up to 2μm long that protrude from it. Scale bar = 0.2μm.

**Figure 3.13. a) (Middle right)** A discharged trichocyst 50nm wide that shows a repeating banding pattern along its length. Scale bar = 100nm.

**b) (Bottom right)** A diagram showing a repeating unit of banding found along a discharged trichocyst.

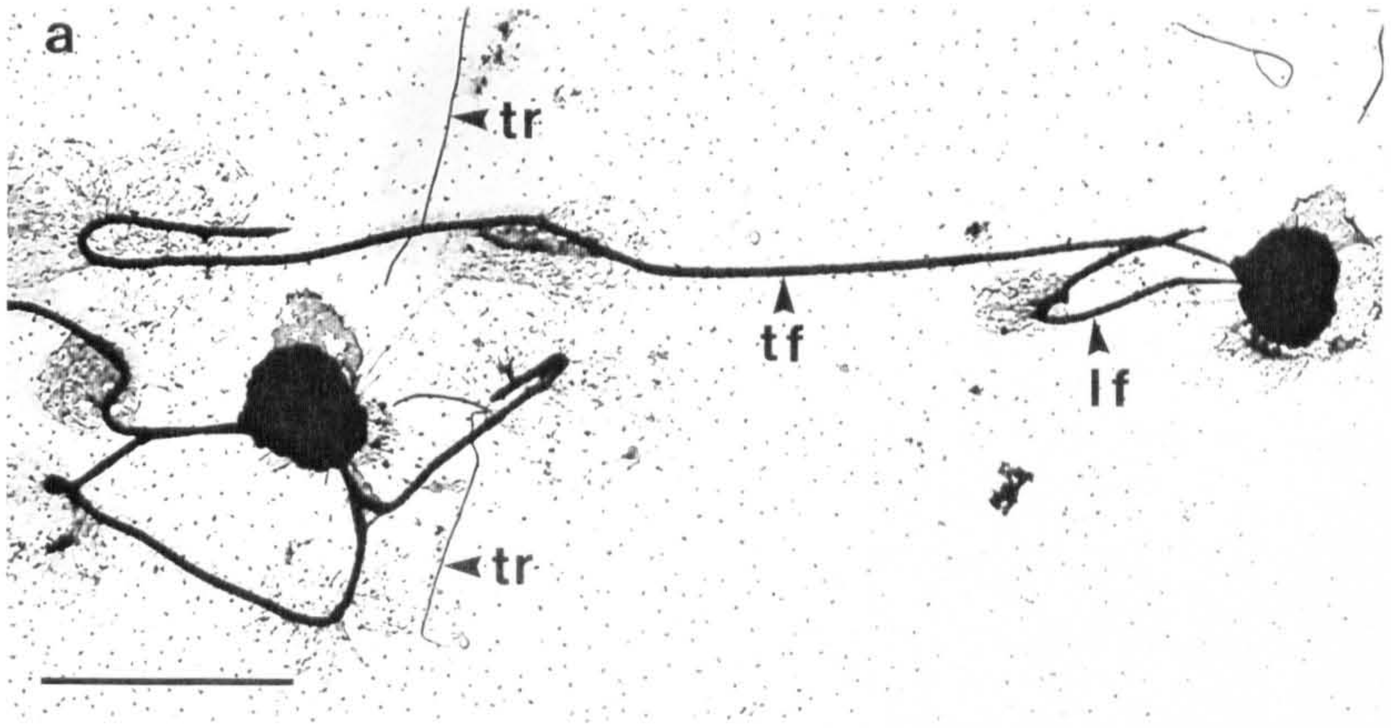
a
tr
tf
lf
tr

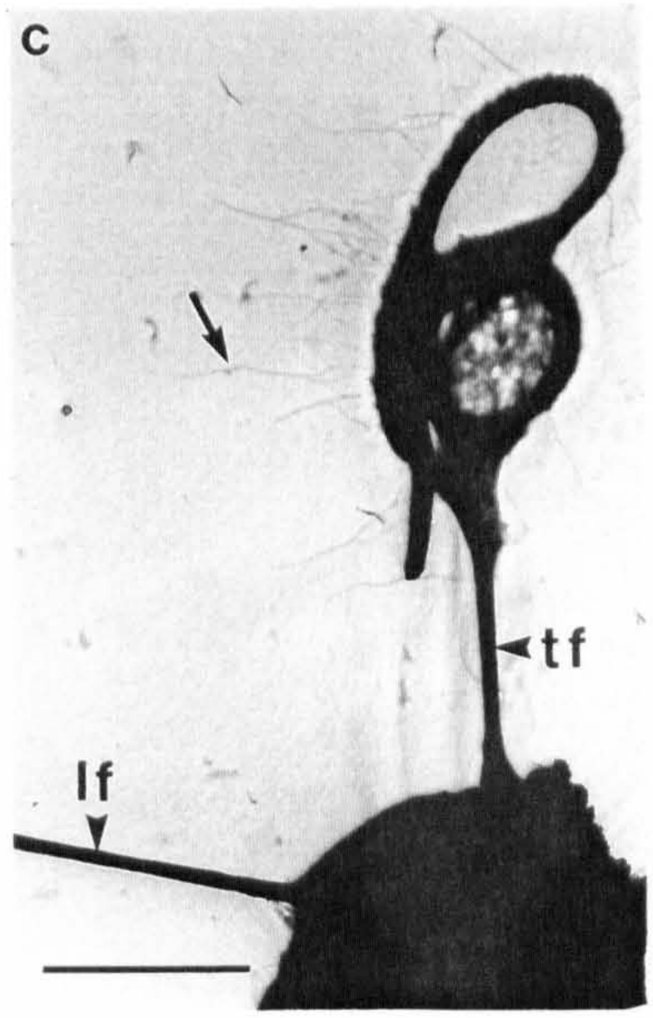
c
tf
lf

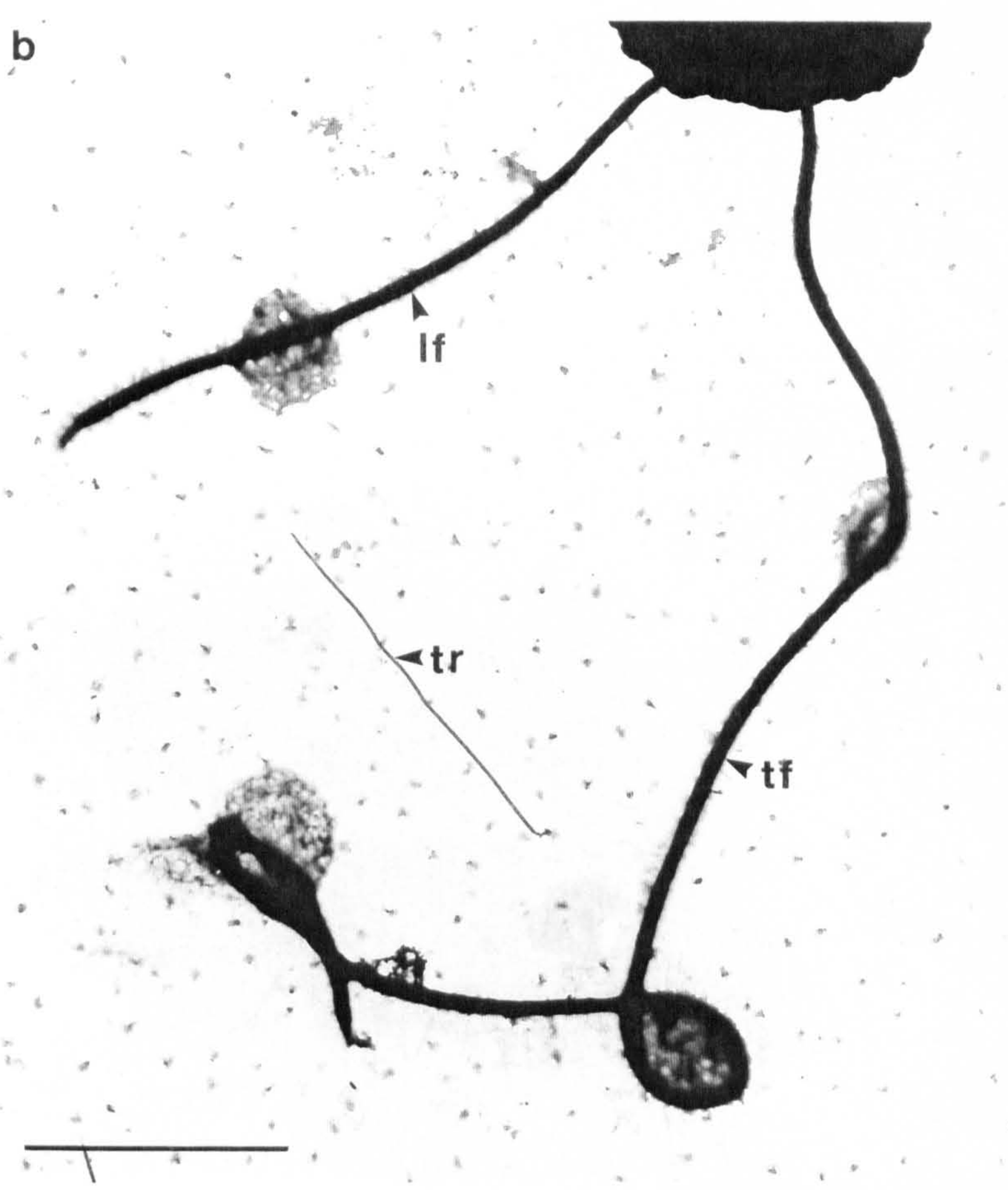
b
lf
tr
tf


a

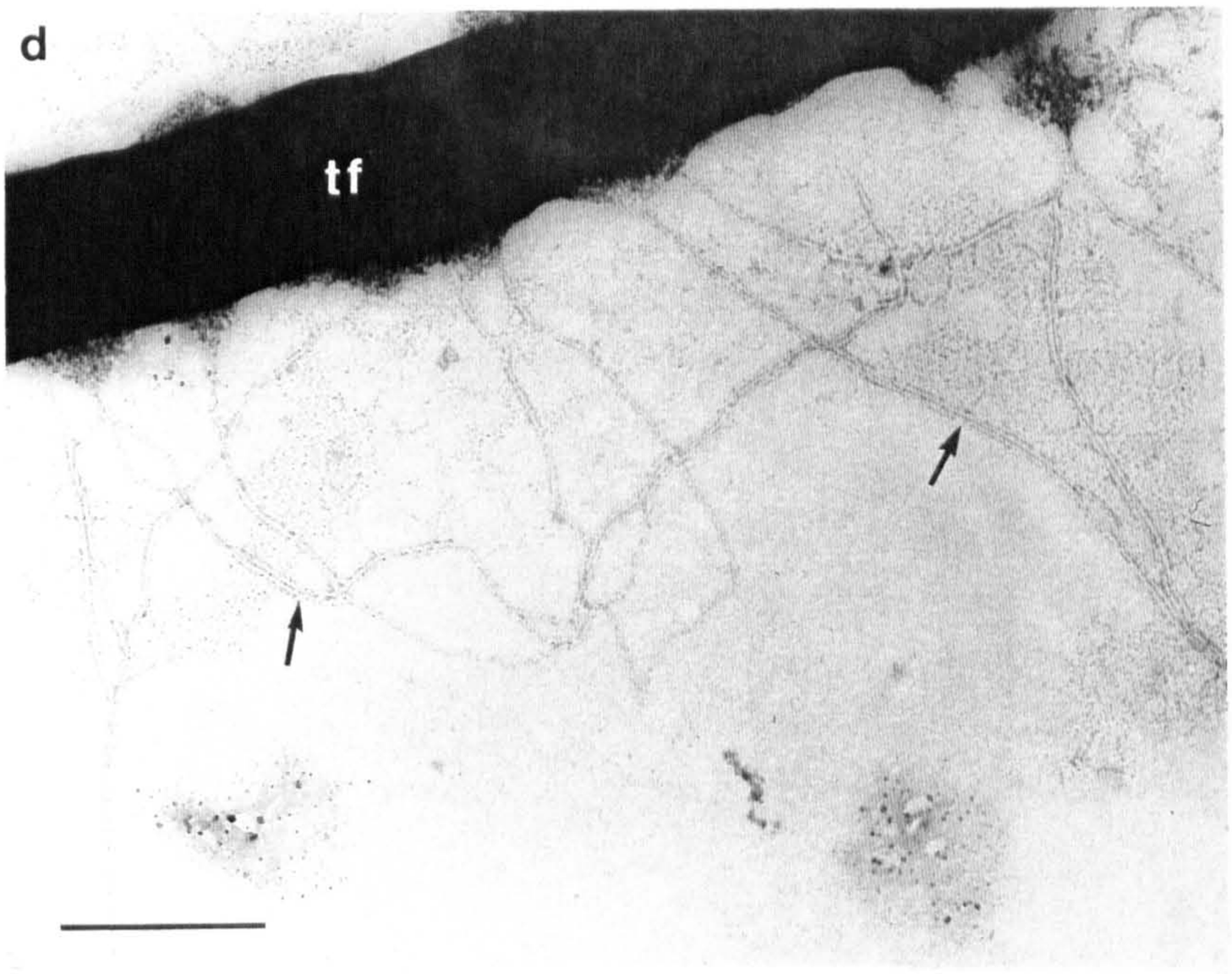
d
tf

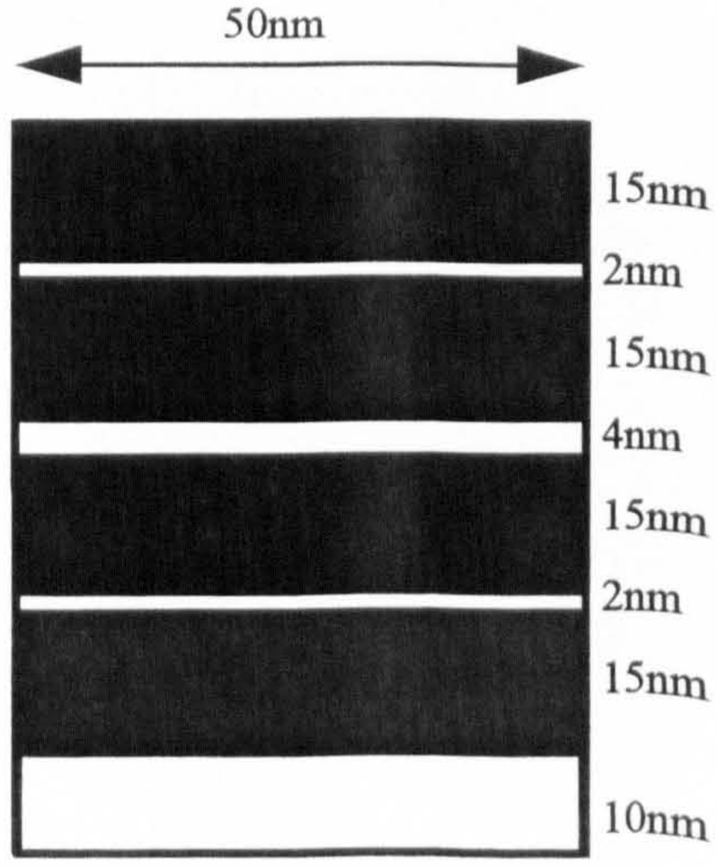
b
50nm
15nm
2nm
15nm
4nm
15nm
2nm
15nm
10nm

**Figure 3.14.** Transmission electron micrographs of sections of sporoblasts in the final stages of microsporogenesis.

**a)** The nuclei (n) of the dividing sporoblasts contain highly condensed chromosomes characteristic of microspores. The dividing sporoblast also contains numerous empty vacuoles (va) and trichocysts (tr),

**b)** A binucleate (n) dividing sporoblast contains lipid droplets (l), granular matrix organelles (gmo), trichocysts (tr) and numerous empty vacuoles (va). A dilation of the perinuclear space contains flagellar hairs (fv). Scale bar = 2μm.

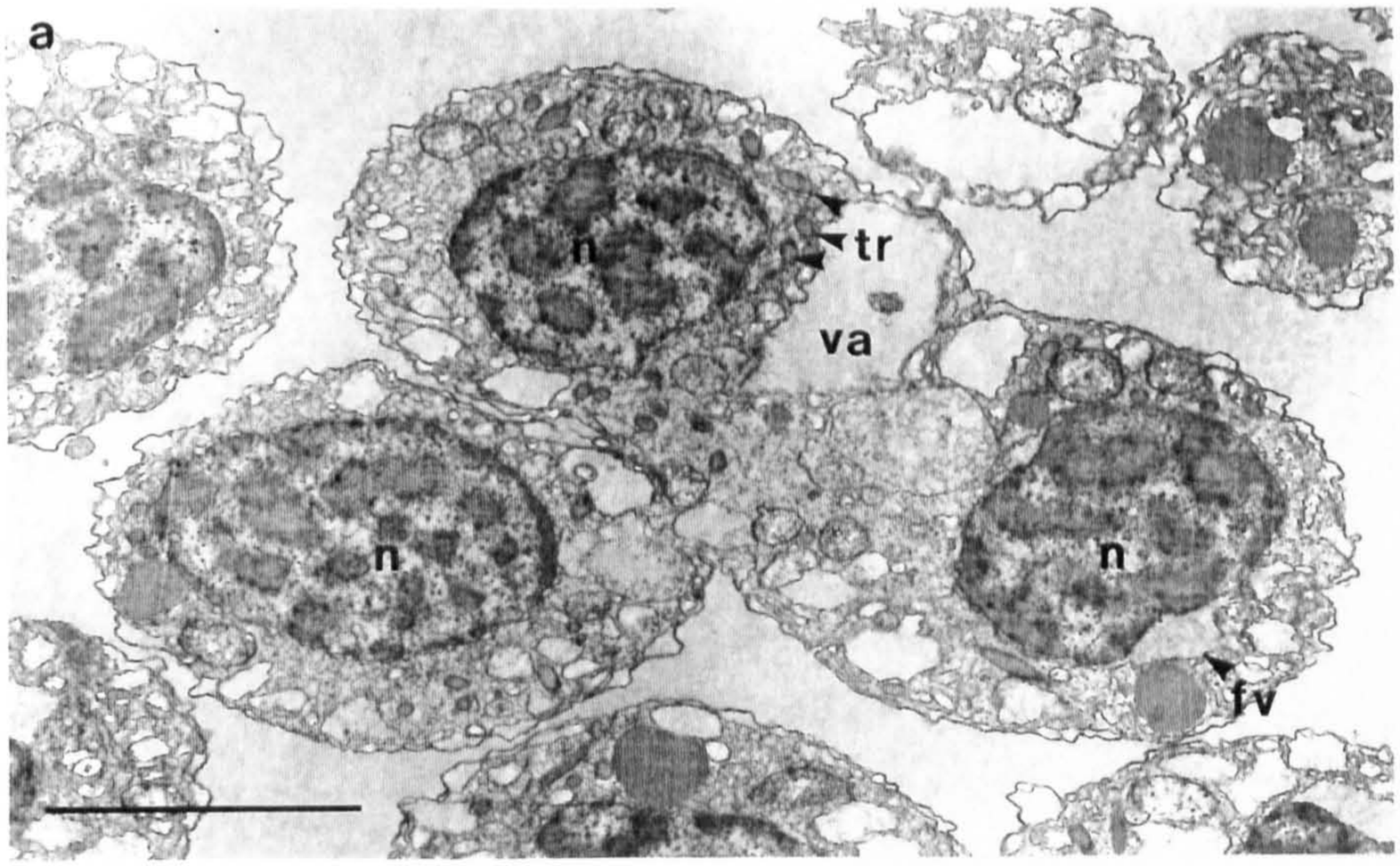
a
n
tr
va
n
n
fv

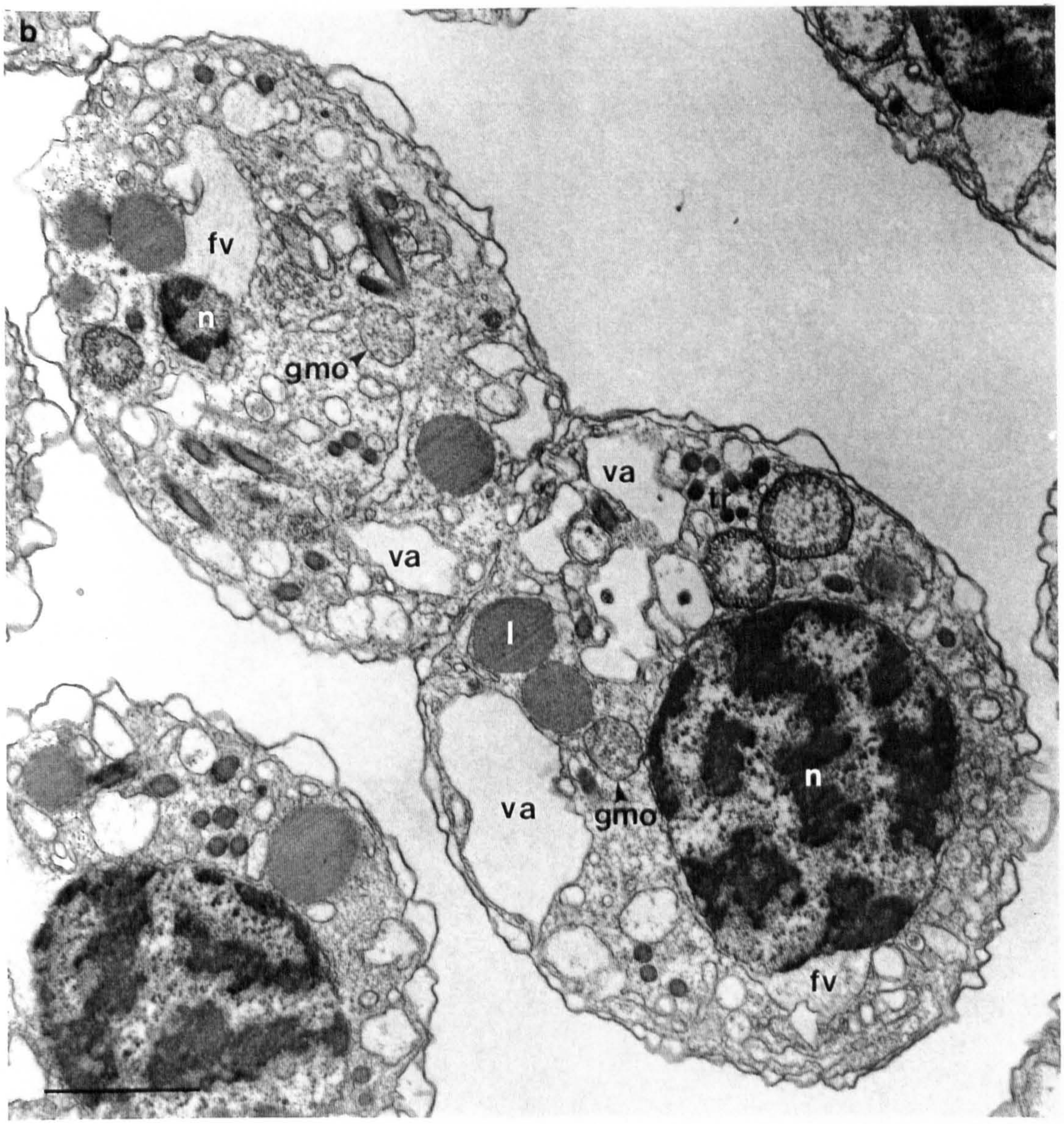
b
fv
n
gmo
va
va
l
va
gmo
n
fv

**Figures 3.15, 3.16.** Transmission electron micrographs of sections of mature microspores from *in vitro* culture.

**Figure 3.15 a, b.** Longitudinal sections through 'corkscrew'-shaped microspores. The condensed chromosomes (ch) entirely fill the nucleus. The swollen alveoli (a) give a corrugated appearance to the microspore surface. The refractile body (rb) situated at the posterior end contains a small amount of weakly staining material. m = mitochondrion, f = flagellum, gmo = granular matrix organelles. Scale bars = 2μm.

**Figure 3.16. (Bottom)** A transverse section through a microspore. Many flagellar hair vesicles (fv) are present. The Golgi apparatus (g) is situated close to a dilation of the perinuclear space containing flagellar hairs. tr = trichocysts, l = lipid droplet. Scale bar = 1μm.

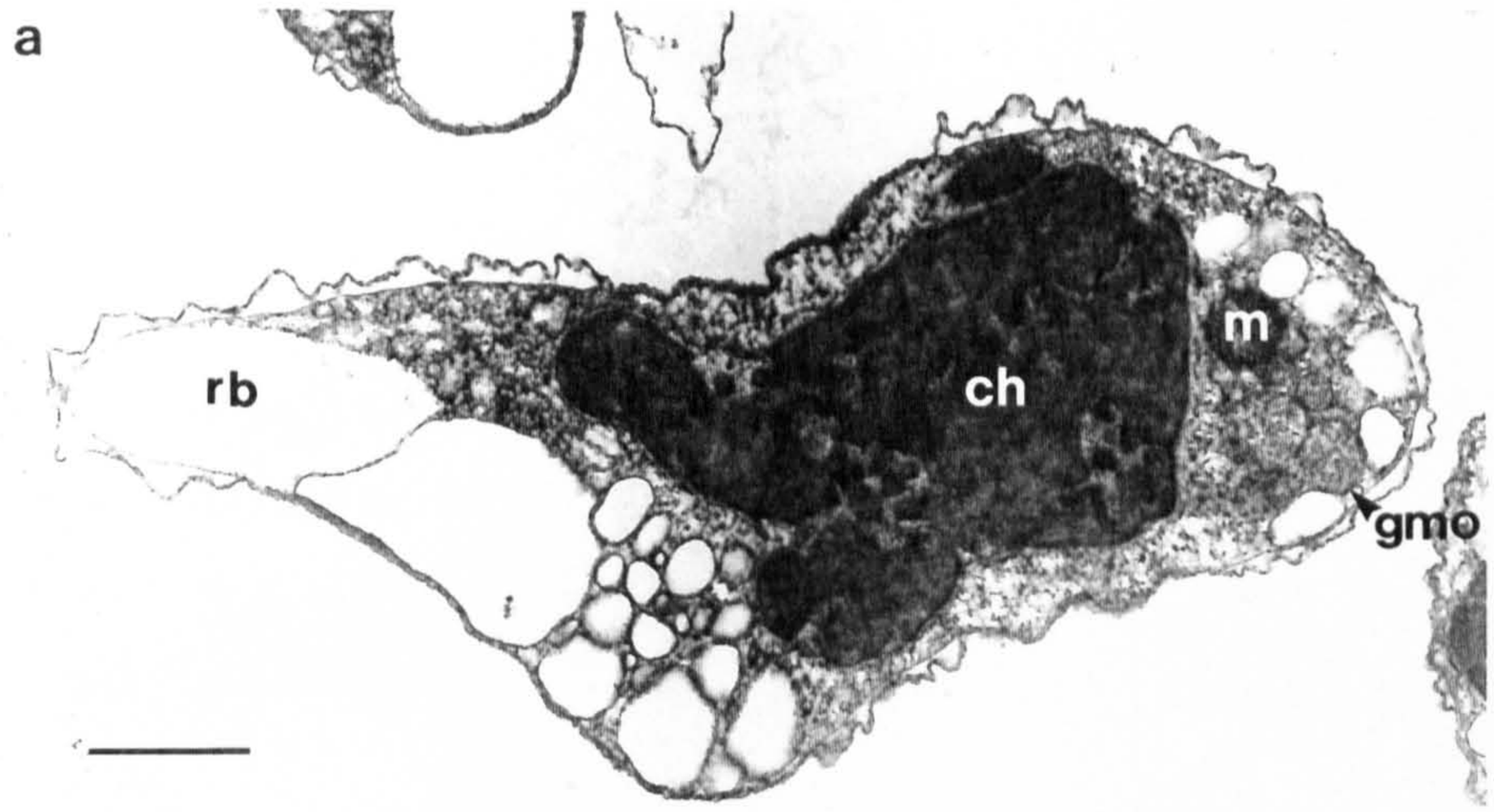
a
rb
ch
m
gmo

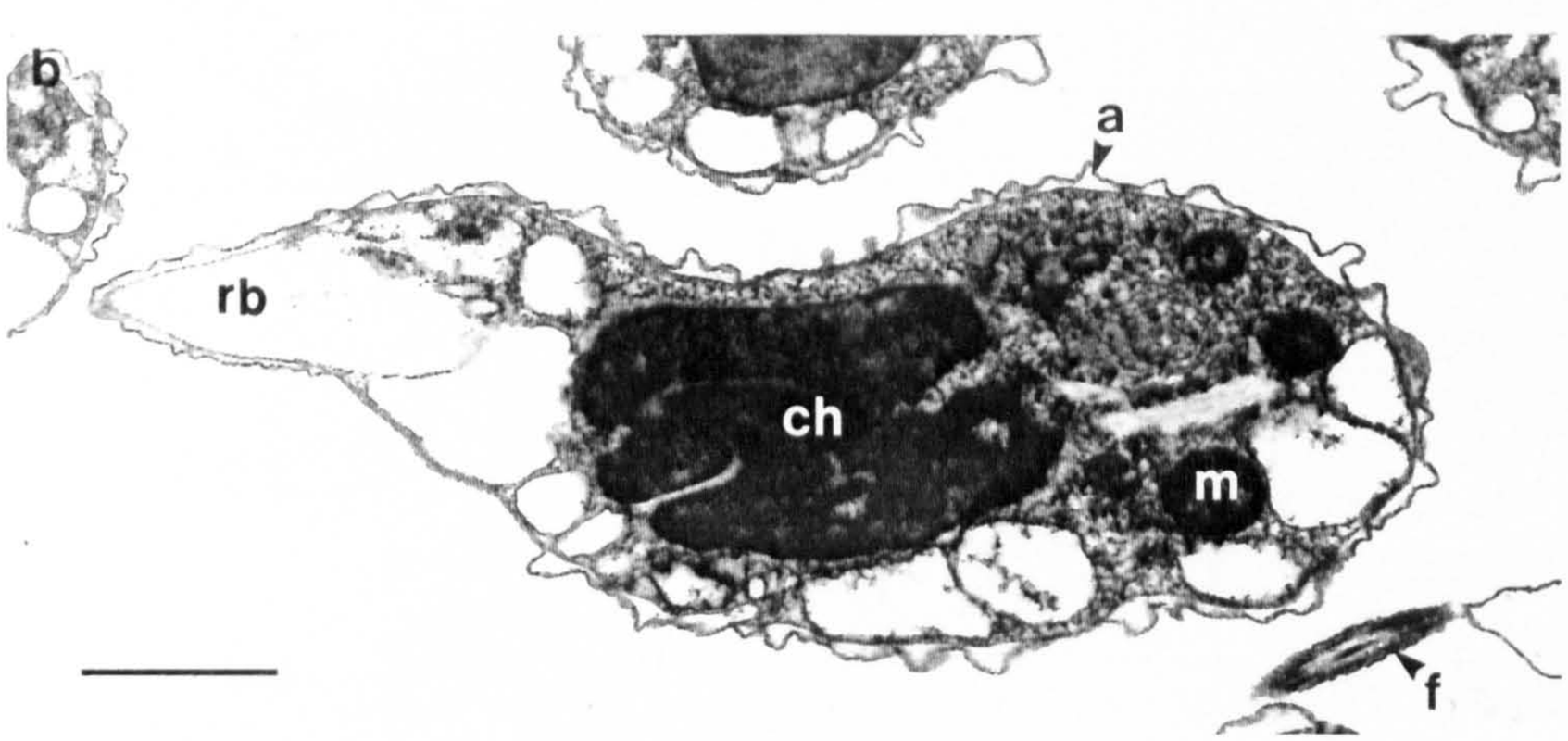
b
a
rb
ch
m
f


tr
l
g
fv
fv

**Figure 3.17.** A longitudinal section through a microspore showing two micropores (arrows) located within a flagellar groove. f = base of a flagellum, mt = microtubule, fv = flagellar hair vesicle located within the perinuclear space. Transmission electron micrograph. Scale bar = 0.5μm.

**Figure 3.18.** A transverse section through a microspore showing a flagellum located within a groove. A microtubular rootlet (mt) is visible on one side of the groove. fv = flagellar hair vesicles. Scale bar = 1μm.


f
mt
fv

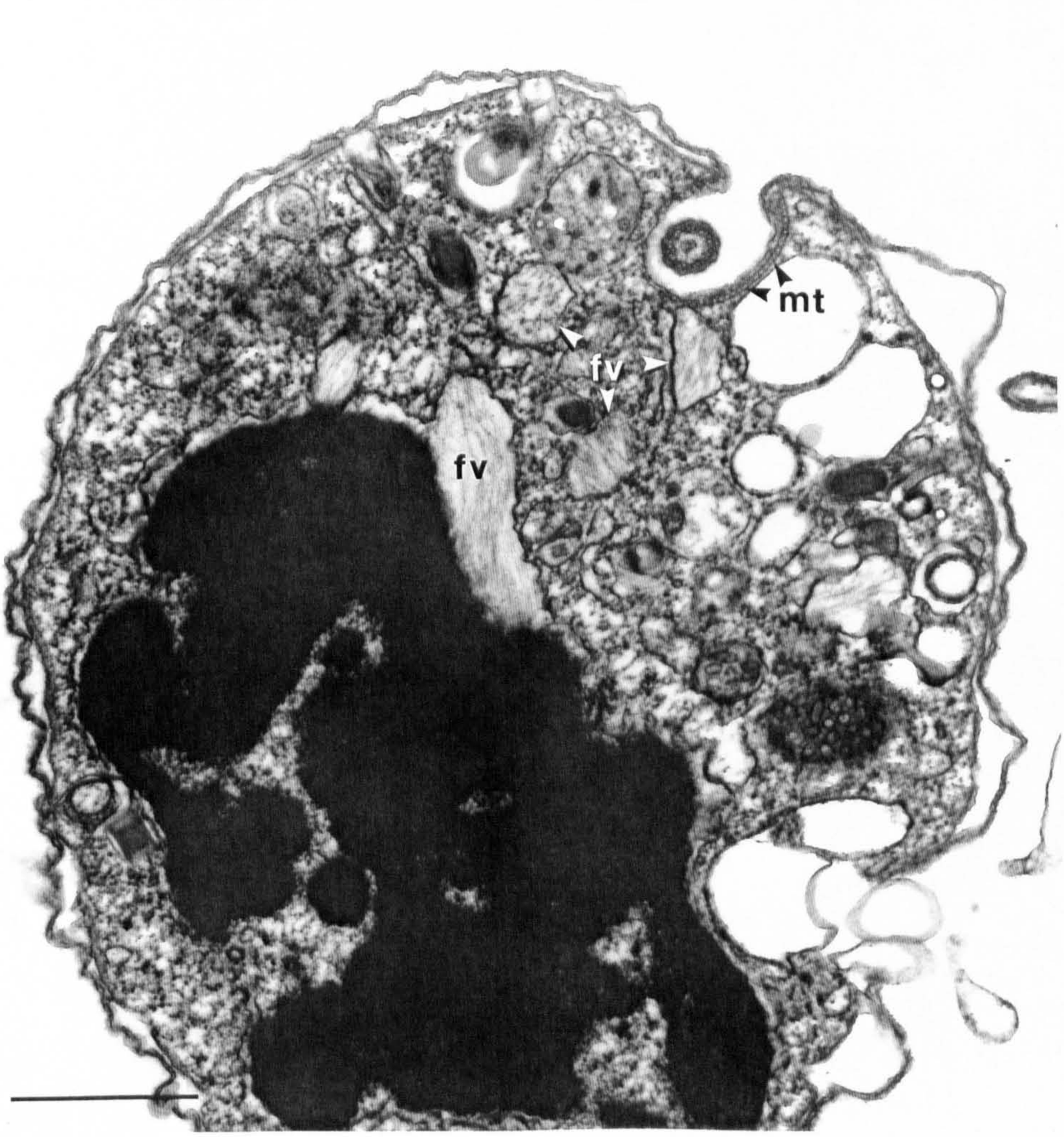
mt
fv
fv

**Figures 3.19-3.21.** Transmission electron micrographs of sections of mature microspores.

**Figure 3.19. (Top left)** An oblique section showing two closely associated basal bodies (b) of the flagella. The microtubular rootlet (arrows) passes along the periphery of the microspore. A large empty vacuole (va) is also present. Scale bar = 1μm.

**Figure 3.20. (Top right)** A micrograph showing flagella in transverse and longitudinal section. The flagellar axoneme shows the conventional nine outer doublets and two central singlet microtubule arrangement, electron dense connectives (arrows) between the doublet microtubule and the flagellar membrane are evident. Scale bar = 0.2μm.

**Figure 3.21. (Bottom)** A glancing section through the microspore surface showing a band of microtubules (mt) located beneath the alveoli. Scale bar = 0.5μm.

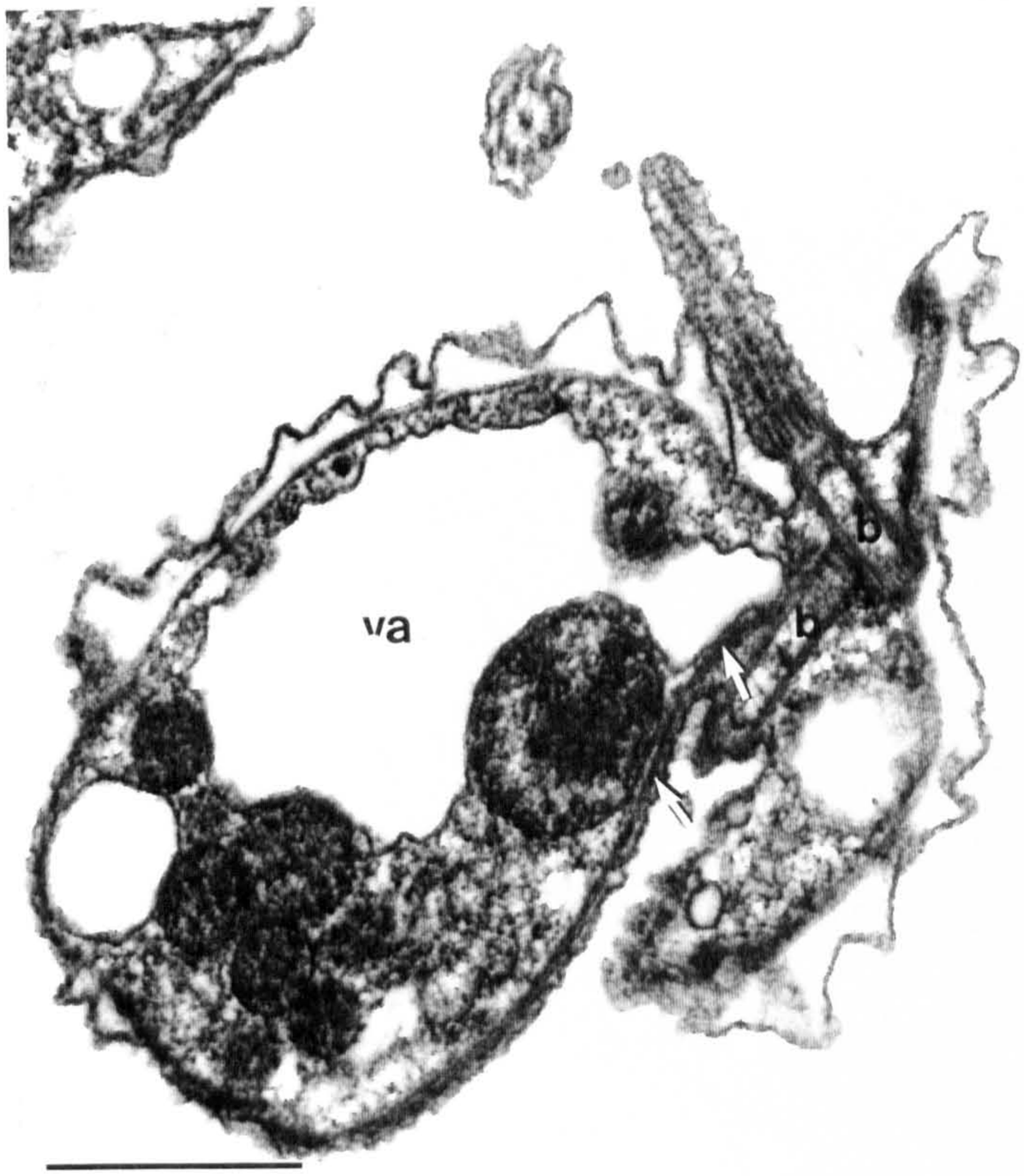
va
b

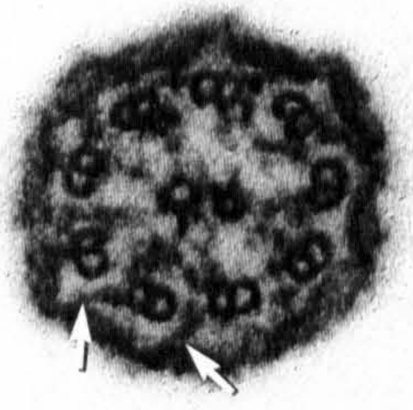

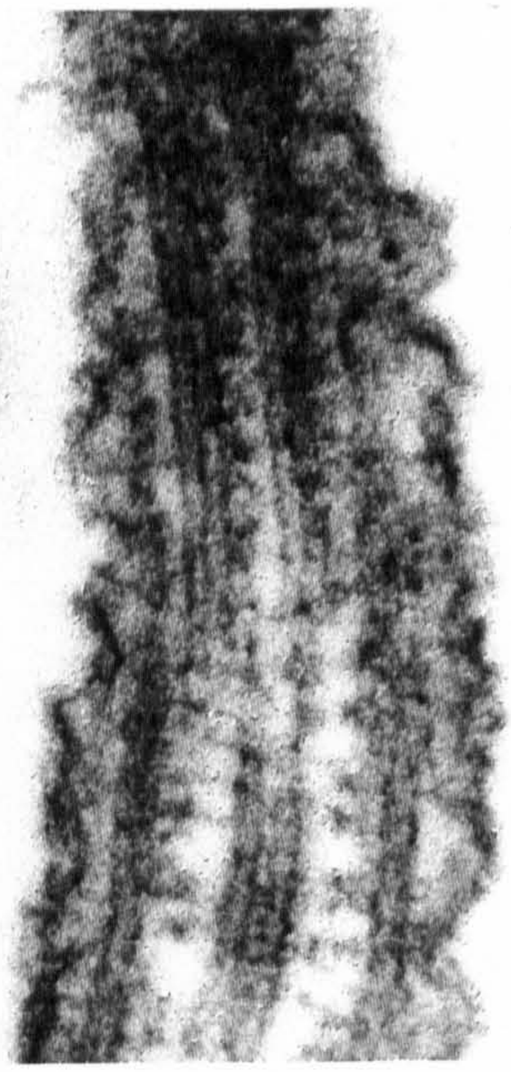

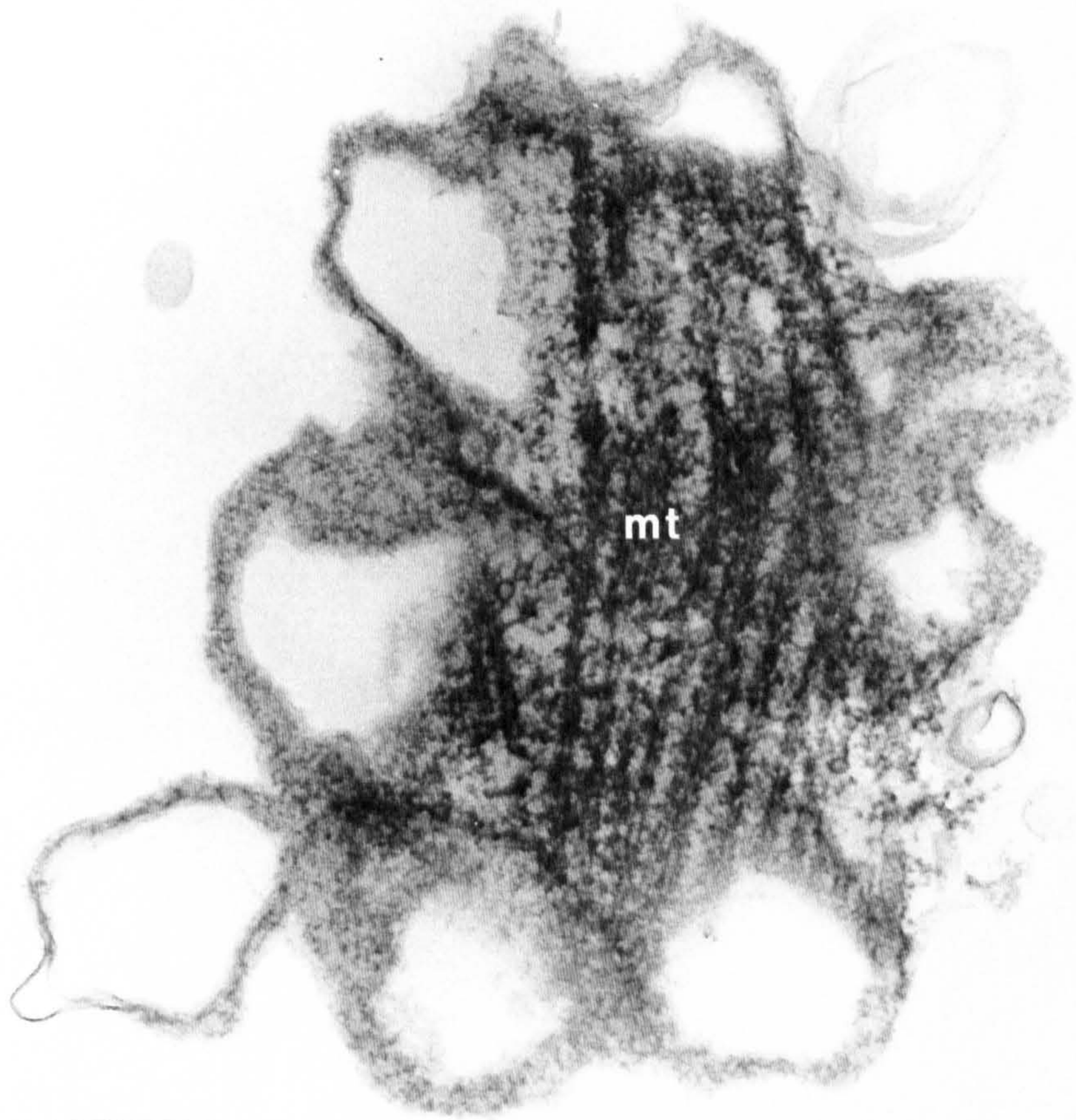
mt

**Figure 3.22.** Transmission electron micrographs of longitudinal sections through filamentous trophonts from *in vitro* culture.

**a)** The alveolar sacs (a) are compressed. The vesicular cytoplasm contains lipid droplets (l), , mitochondria (m) and numerous vesicles. Trophonts lack trichocysts and flagellar hair vesicles. Scale bars = 1μm.

**b)** The condensed chromosomes in the nucleus (n) are surrounded by a darkly staining granular material. The alveolar sacs (a) have few swollen regions. One mitochondrion (m) is swollen and contains a dense granular inclusion (mgr). g = Golgi apparatus.

a

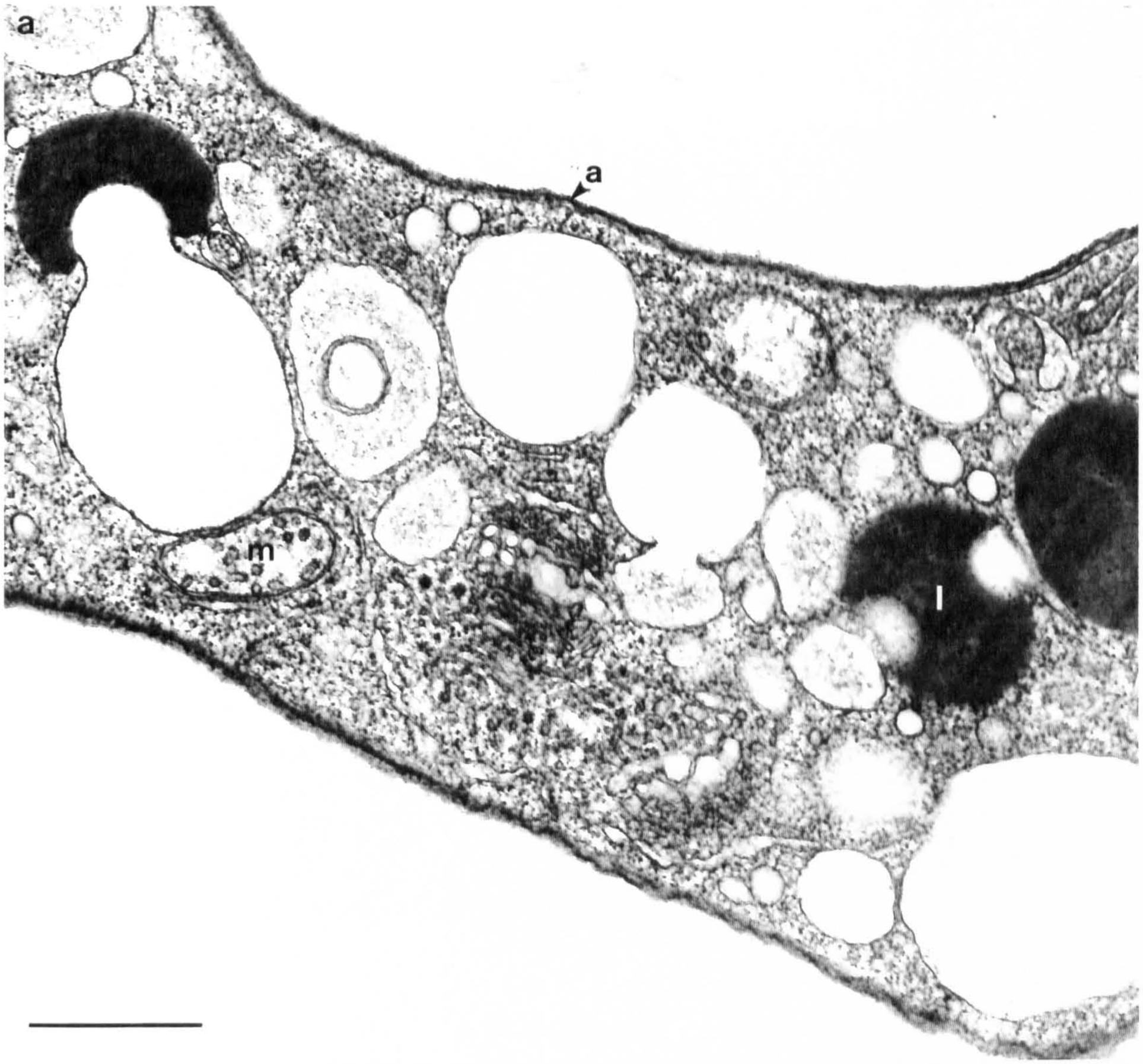


b

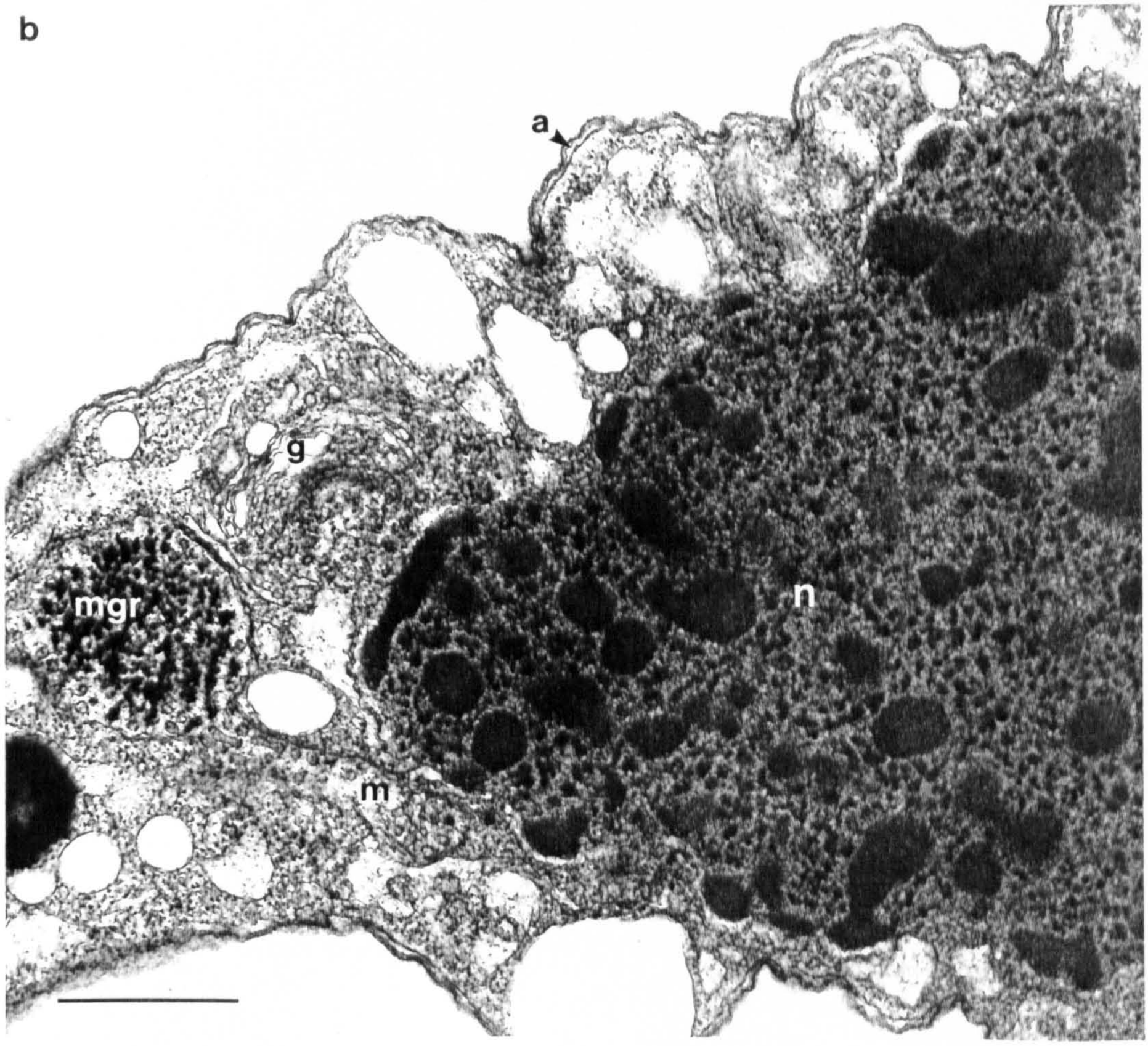

**Figures 3.23.** Scanning electron micrographs of the arachnoid syncytia (primary sporonts) that develop in *in vitro* culture.

**a)** An arachnoid syncytium comprising a central mass of nucleated cytoplasm (c) from which radiates out a network of cytoplasmic threads (ct). Scale bar = 100μm.

**b)** Part of a large arachnoid syncytium that occurs when smaller syncytia meet and fuse. Nuclei (n) are located where cytoplasmic threads (ct) branch. Scale bar = 50μm.

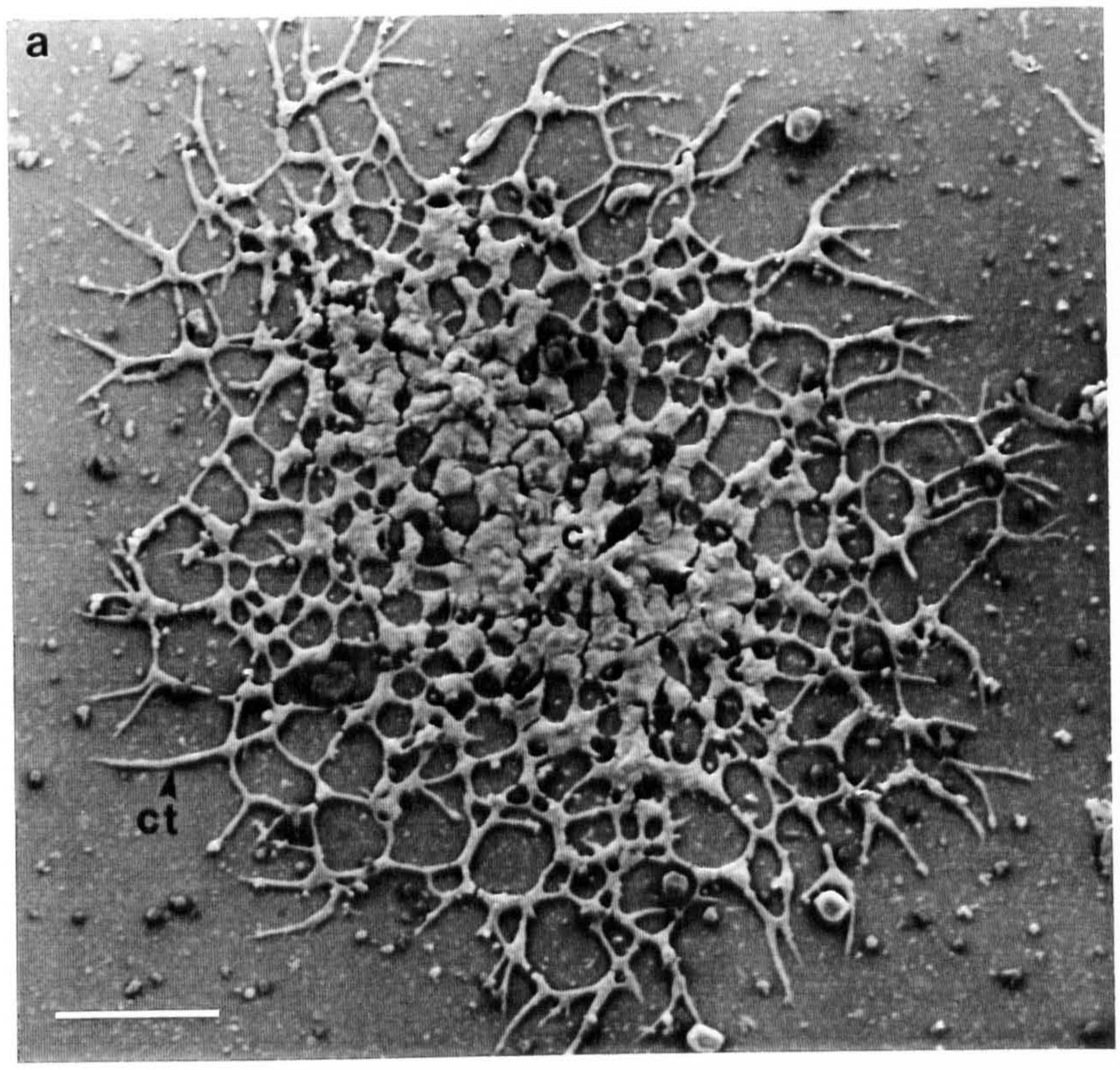
a
c
ct

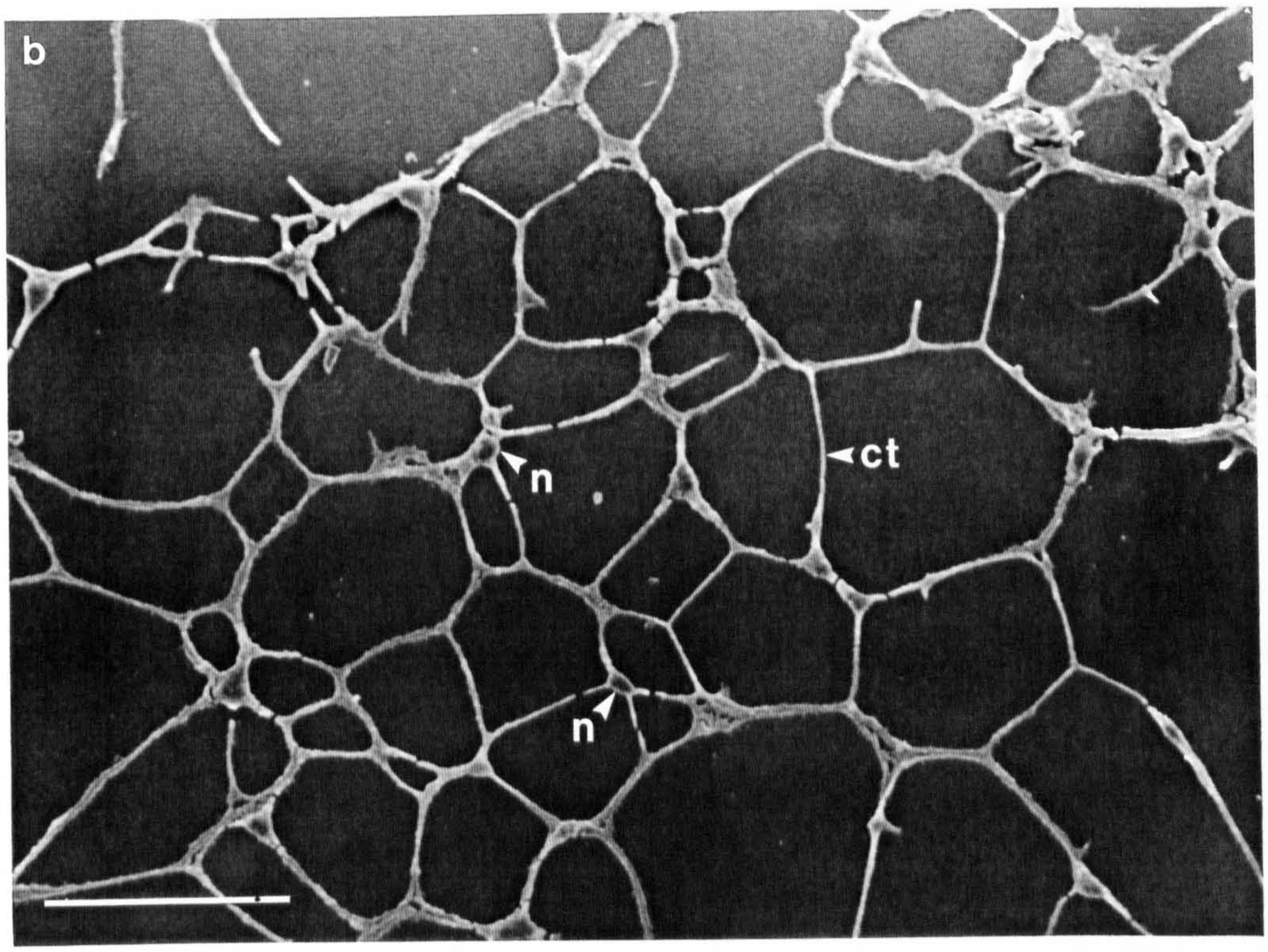
b
n
ct
n

**Figure 3.24.** Transmission electron micrographs of horizontal sections through the arachnoid syncytia (primary sporonts) that develop in *in vitro* culture.

**a)** Nucleated portion of syncytium containing numerous lipid droplets (l) throughout the cytoplasm. The condensed chromosomes are small and the nucleolus (nu) is visible. The amphiesmal alveoli are swollen in places. Scale bar = 5μm.

**b)** A section through a cytoplasmic thread at the periphery of an arachnoid syncytium. The cytoplasmic thread (ct) contains alveoli (a) and mitochondria (m). The fine extensions (arrows) of the cytoplasmic thread do not appear to contain an alveolar structure, however the extensions could be artifactual hernias resulting from chemical fixation. Scale bar = 2μm.

**c)** Inclusion organelles are present in some arachnoid syncytia. The membrane bound peripheral inclusion organelles (pio) have a dark deposit around their periphery. Granular matrix organelles (gmo) are found in the cytoplasm, often in small clusters. No trichocysts or flagellar hair vesicles are present. Scale bar = 5μm.

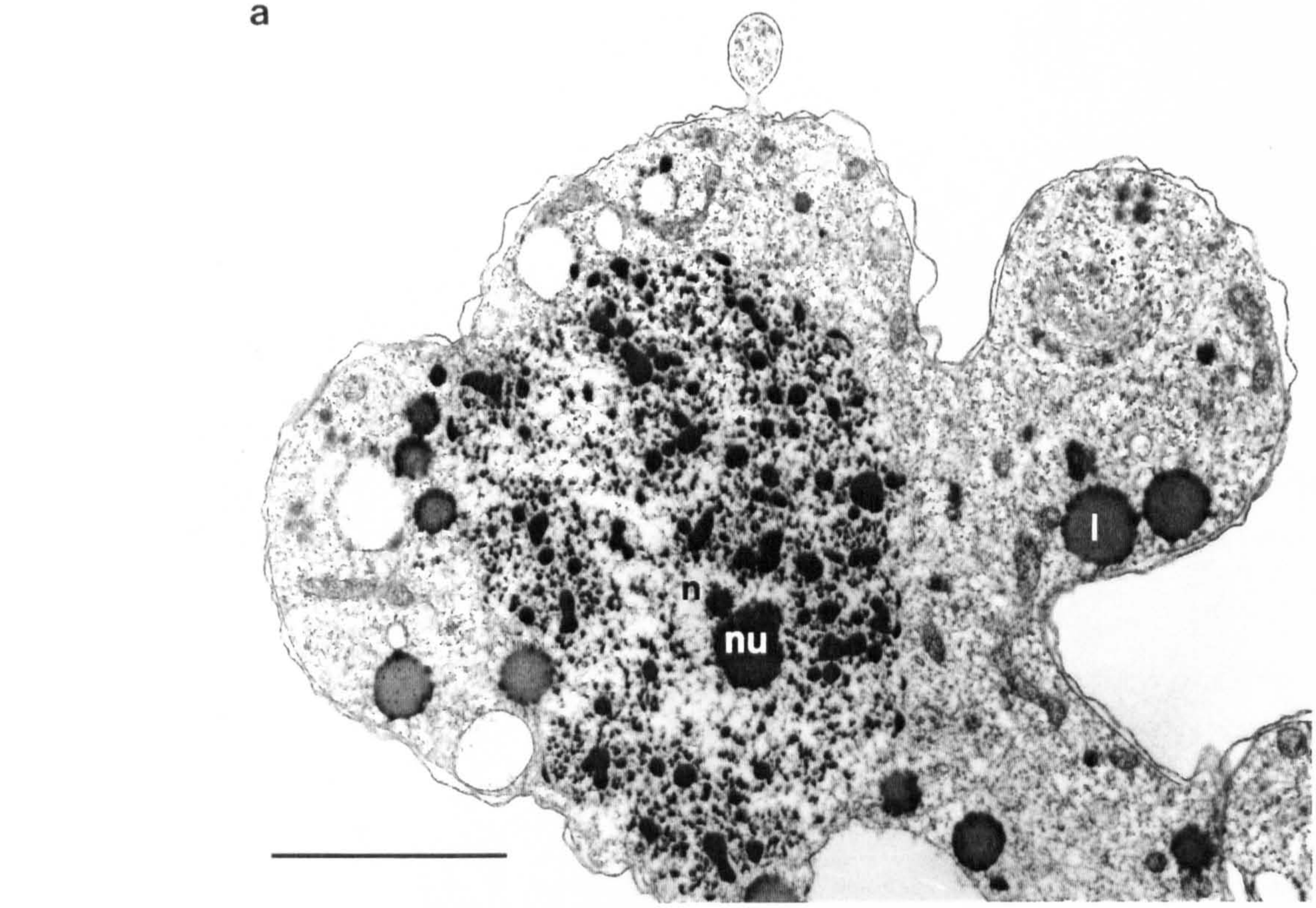
a
l
n
nu

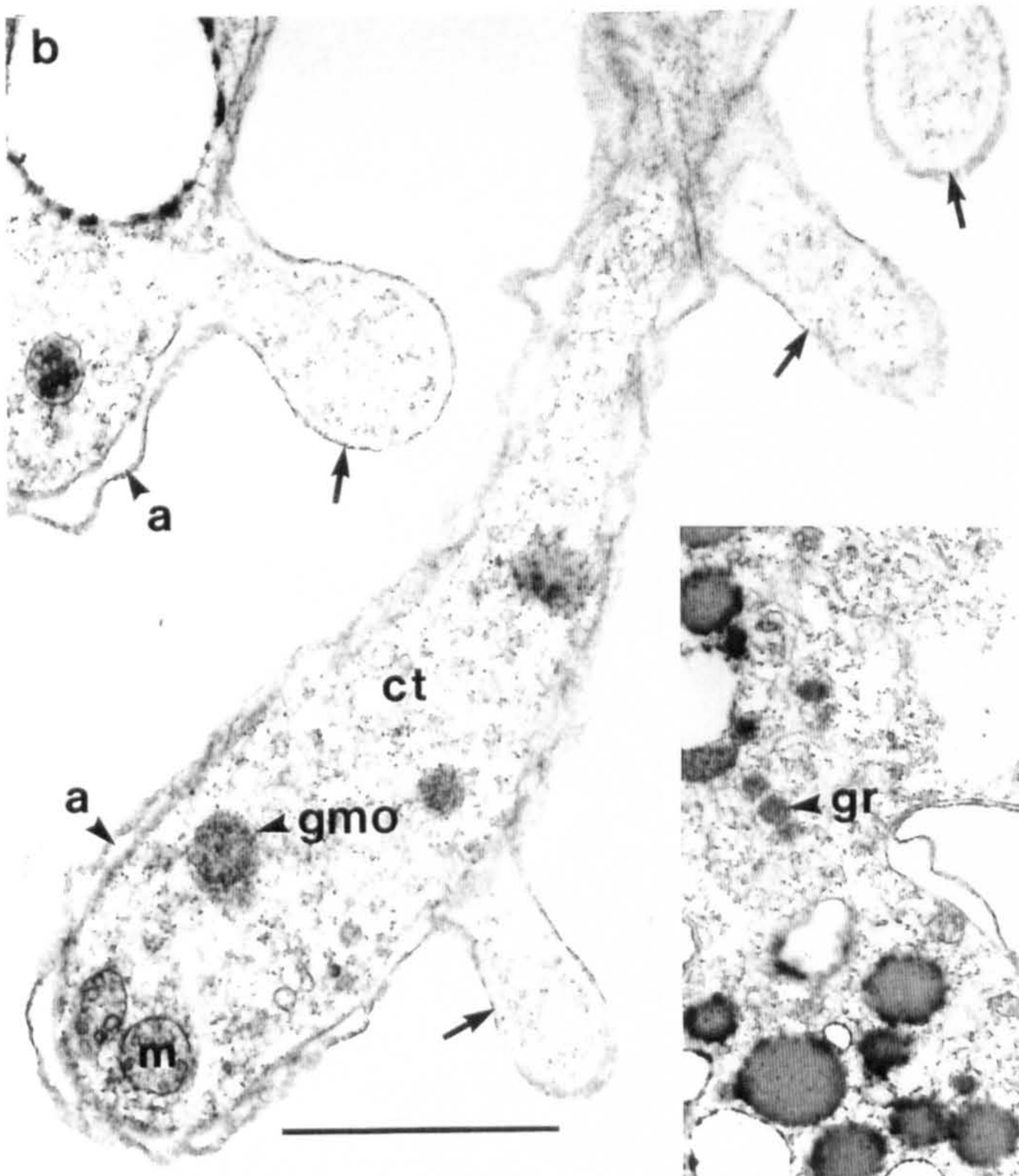
b
a
ct
a
gmo
m

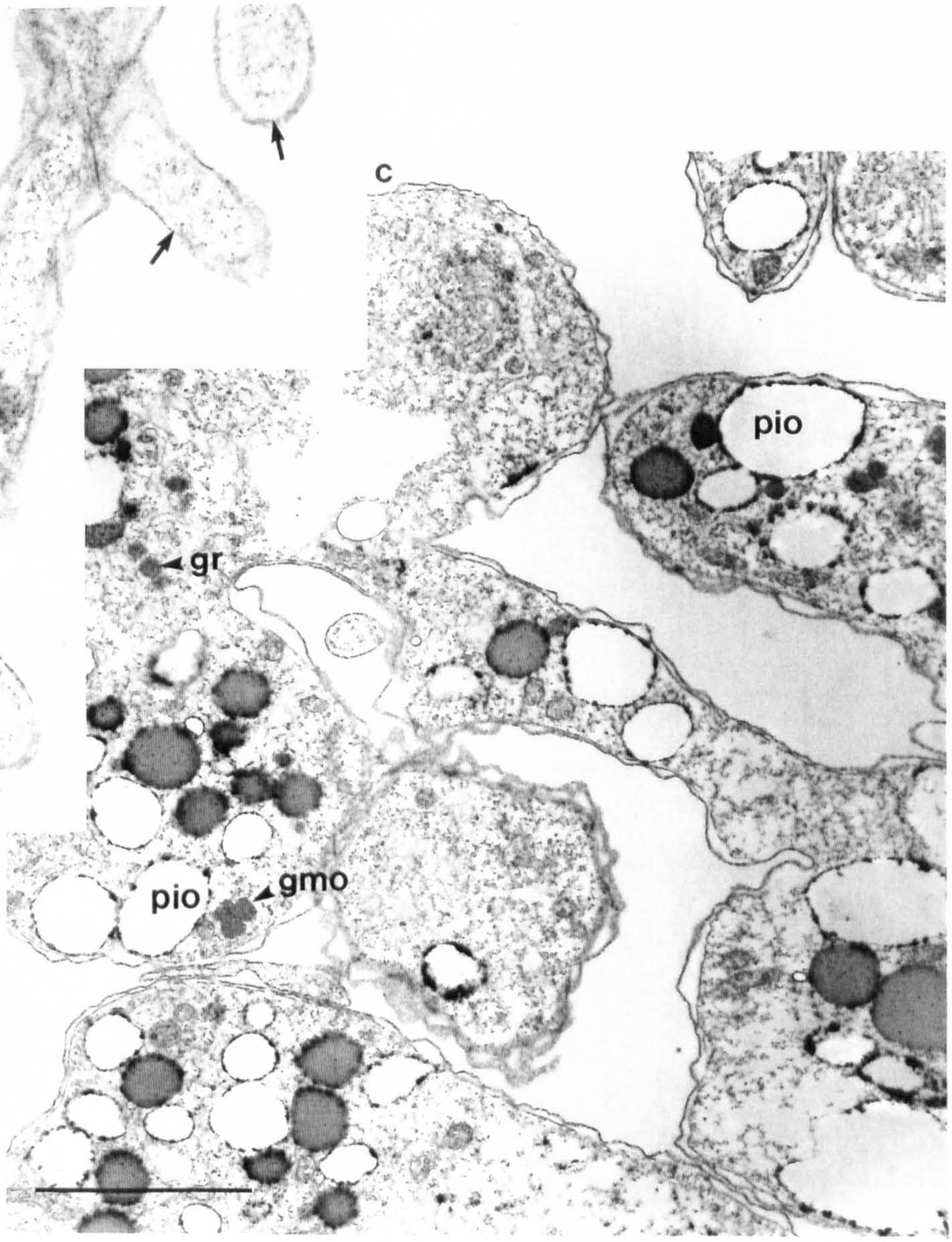
c
pio
gr
pio
gmo

**Figure 3.25.** Transmission electron micrographs of sections of parts of clump colonies that develop in *in vitro* culture.

**a)** The clumped colonies are formed from a large mass of interdigitated parasites. Interdigitations (in) are numerous and are bounded by alveoli. The cytoplasm of the clumped colonies is highly vesicular and contained many lipid droplets (l). Many of the parasites within the clumped colony contained large vacuoles (va). n = nucleus, nu = nucleolus. Scale bar = 5μm.

**b)** A feature found only in this developmental stage was the presence in some places of the plasma membrane and alveolar sacs being sharply folded and protruding towards the centre of the parasite (arrows). Scale bar = 2μm.

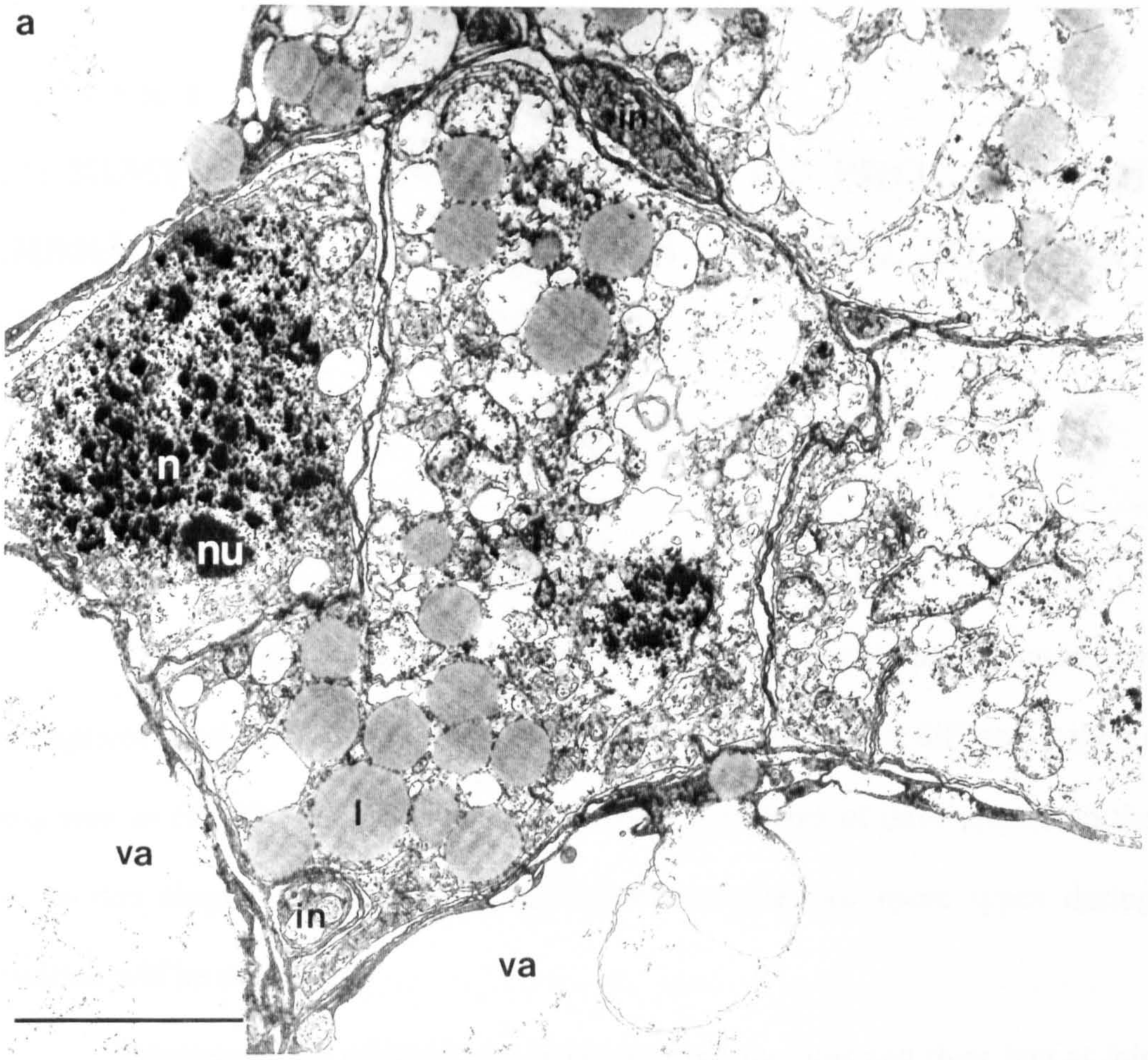
a
n
nu
l
va
in
va
b
l
m
nu
in
in
l
va

# CHAPTER 4

# EXPERIMENTS TO INVESTIGATE THE PROGRESS OF GERMINATION OF DINOSPORES AND THE SURVIVAL OF DINOSPORES IN SEAWATER

## 4.1. INTRODUCTION

One possible answer to the question of the significance of the production of two types of dinospore is that the macrospore and microspore have different patterns of behaviour in effecting transmission and/or different patterns of development in the host. In this chapter the pattern of development of the two spore types during germination will be described.

Dinospores are released into seawater from the host and their fate at this stage is of interest. Meyers *et al.* (1987) were able to maintain macrospores in seawater for 73 days and microspores for 52 days. Some bacterial contamination did occur and this may have affected their results.

In this chapter I will describe experiments to investigate the rate of germination for each type of dinospore and the survival of dinospores in seawater.

## 4.2. MATERIALS AND METHODS

### 4.2.1. Progress of germination of dinospores

*Macrospores*. Infected haemolymph was aseptically removed from a male stage IV infected animal (CL 32mm) and ~100µl placed into each of two small culture flasks containing 10ml culture medium containing both gentamycin and penicillin. This lobster was releasing dinoflagellates naturally into the seawater in its exhalant gill current at the time. Dinoflagellates from the haemolymph were examined under the microscope and were found to be in the late stages of sporogenesis. Multinucleate sporoblasts were present, as well as macrospores. Two samples of culture medium (~ 50µl each) were removed from each of the two flasks every week, and numbers $ml^{-1}$ of the different forms of the parasite were immediately counted using an Improved Neubauer haemocytometer. Dinoflagellate forms that were counted were:

- motile macrospores
- non motile spherical dinoflagellates
- filamentous trophonts.

The mean count (n=2) for each parasite form was calculated weekly over a period of eight weeks.

*Microspores*. To investigate the germination of microspores, haemolymph was removed from a dead female lobster (CL 42mm), infection stage III and transferred to five culture flasks. This isolate started to produce microspores 31 days after isolation, and by day 33 only microspores were present in the cultures. On day 38 observations of the progress of germination were started. Every 7-10 days a two samples of the culture (~50µl each) were removed from each of the five flasks and numbers of parasite forms counted. The following dinoflagellate forms were counted:

- 'corkscrew'-shaped motile microspores
- spherical, motile microspores
- spherical, non motile dinoflagellates
- filamentous trophonts

The experiments were terminated when the dinoflagellate cells appeared vacuolated indicating that they were in need of subculturing, or when a developmental form not included in the above list appeared.

### 4.2.2. Survival of dinospores in seawater

After washing twice in sterile seawater I maintained both macrospores and microspores in sterile seawater with added antibiotics. Three isolates of macrospores and microspores were transferred into seawater for observation. Survival of a dinospore was judged by its ability to remain motile or remain refractile without becoming bloated. Dinospores were judged to be dead if they were non motile, had an unrefractile appearance or were lysed.

## 4.3. RESULTS

### 4.3.1. Experiments to investigate the progress of germination of macrospores

Two days after isolation into culture medium all the dinoflagellates had become characteristically 'bullet'-shaped macrospores. After 68 days the macrospores began to lose their motility and began germinating, it was at this point that counting of the dinoflagellate forms present in the culture commenced.

Initially the majority of the dinoflagellates were spherical and non motile. A few motile macrospores were present up until day 124. As the numbers of non motile dinoflagellates and macrospores decreased the numbers of filamentous forms showed an increase. Germination was virtually completed by 125 days. It is clear that a large proportion of macrospores do not survive to germinate. The number of filamentous trophonts decreased towards the end of the observation, this was probably due to a deterioration of the culture, indicating that subculturing was necessary. The filamentous trophonts that derived from the macrospores did not transform into arachnoid syncytia during these observations although in other macrospore derived cultures such syncytia appeared as early as 14 days post germination.

### 4.3.2. Experiments to investigate the progress of germination of microspores

The microspore germination experiment did not produce results as consistent as those from the macrospore experiment. In one of the five flasks germination did not take place even though the microspores had become non-motile and produced the spherical precursors of filaments. In two flasks the numbers of filaments produced were so low that they were not always present in the sample of culture taken for counting, although they were always present in low numbers in the flask after they first appeared. In flasks c and d filaments appeared on day 72 and 64 respectively, the observations could not be followed for much longer than 90 days because the filamentous trophonts began to transform into small arachnoid syncytia at 92 days post sporogenesis.

The length of time between sporogenesis and germination of the microspores was not typical of the other microspore derived cultures in that germination took place far later (Table 2.1). These experiments show the dynamics of germination but highlight the variability that is found between duplicate isolates from the same host.

### 4.3.3. Survival of dinospores in sea water

Microspores that had been kept in seawater for up to 7 weeks were still capable of germinating when returned to the normal culture medium. Microspores maintained in seawater developed a more pronounced corkscrew shape than those kept in the normal culture medium and developed a more distinctive posterior refractile body.

The survival time of the macrospores in seawater appears to be much shorter than that of microspores (Table 4.1). They often did not survive for more than 2 weeks before degenerating.

The survival of both spore types in seawater was not consistent. Dinospores often became vacuolated and hypertrophied after 24 hours in seawater, lost their motility and lysed. Neither type of dinospore was observed to germinate in seawater.

## 4.4. Discussion

The results show that there are distinct differences in the progression of germination between the two types of dinospore. Microspores generally began germinating earlier than macrospores (Table 2.1). The isolates from the Irish sea giving rise to microspores consistently germinated 18-19 days after sporogenesis (Table 2.1). Observations suggested that there is a higher percentage of microspores than macrospores that do not germinate.

The observations of the survival times in seawater are difficult to draw conclusions from, but it is interesting to note that neither dinospore type appears capable of surviving for a prolonged period, and that neither produces a resting stage (cyst).

Meyers *et al.* (1987) reported that macrospores and microspores were able to survive in seawater for 73 and 52 days respectively. The maximum period for which I managed to maintain viable microspores in seawater, 49 days, would compare with this. The fact that macrospores are much larger and move less energetically than the microspores would suggest that their energy reserves (stored as lipid or carbohydrate) would allow them to survive longer in seawater. Meyers *et al.* (1987) also reported that macrospores were capable of germinating after 25 days in seawater into "chains of non-motile organisms loosely attached to the flask in a rosette-like pattern". Unfortunately no more information was given as to the development and survival of the attached forms. It is not made clear if crab haemolymph was washed from the dinospores before they were placed into the seawater. Any residual haemolymph could affect the development of that particular isolate.

One explanation for the inconsistent results that I achieved for dinospore survival in seawater could be that they have to undergo a maturation period of a few days in the host before they are able to become free-living in sea water. It is possible that some of the dinospores used in these experiments did not reach maturity before they were transferred into seawater and consequently did not survive for long.

In addition to microspores germinating earlier than macrospores they also produced arachnoid syncytia sooner than germinating macrospores (Chapter 2). The significance of spore dimorphism is not clear, although there are several possible explanations. Microspores may represent a rapidly developing transmission stage of the parasite that is capable of transmitting the infection to new hosts during a single season. The macrospore may give rise to a more slowly-developing infection that carries the infection from year to year. Producing different spore types may enable the parasite to increase the range of host species that it is able to infect, although I have not yet thoroughly investigated other crustacea in the Clyde sea area for *Hematodinium* infections. It is also possible that the different spore types have a different means of entry into a new host. One spore type may rely on the moult of a lobster as a means of entry, whereas the other may enter the host through the gut.

From these observations it is clear that a large proportion of both types of dinospore do not survive to germinate into filamentous trophonts, and that mortality of microspores was greater than that for macrospores. The small number of isolates used in these experiments limits the conclusions that are drawn from the data.

| | Survival time of 3 dinospore isolates in sea water (days) | | |
|---|---|---|---|
| Macrospores | 4 | 6 | 41 |
| Microspores | 32 | 58 | 63 |

**Table 4.1.** The survival time of 3 isolates of macro- and microspores in seawater culture.

# CHAPTER 5

# THE DEVELOPMENT AND PROGRESSION OF HEMATODINIUM INFECTION IN *NEPHROPS NORVEGICUS*

## 5.1. Introduction

Our knowledge of the developmental cycle of *Hematodinium* in its natural hosts is almost non-existent and confined to observations on: a) seasonality of appearance of parasites in the haemolymph and dinospore production, b) experimental infections of crab hosts resulting in data on the duration of infection.

Some of the *Hematodinium* spp. which have been previously described from a number of crustaceans have shown distinct seasonal peaks in prevalence. High haemolymph infection rates for *Hematodinium* spp. occur from June to August in the Tanner crab *Chionoecetes bairdi* in Alaska (Eaton *et al.* 1991, Love *et al.* 1993), from January to May in *Liocarcinus puber* in France (Latrouite *et al.* 1988, Wilhelm and Boulo 1988), and from January to May in the Norway lobster *N. norvegicus* (Field *et al.* 1992). In the crab *Callinectes sapidus* (Eastern USA), the parasite is absent from winter to early spring and peaks in prevalence during early autumn (Newman and Johnson 1975). Haemolymph infections in the Tanner crab are detected in fixed and stained smears all year round, but in the Norway lobster there is a distinct season where infections are found.

Transmission experiments with *Hematodinium* from crabs have shown that both the circulating stages and dinospores are capable of reproducing the infection in a healthy host when artificially introduced into the haemolymph. Meyers *et al.* (1987)

found from transmission experiments in Tanner crabs using circulating stages that did not contain trichocysts (deemed here to be trophonts) that the pre-patent period (the time from initial infection to the disease becoming patent) was between 55-69 days. Eaton and colleagues (1991) furthered this work by showing that crabs injected with a mixture of both dinospore types (from the haemolymph) developed an infection that resulted in the unusual production of a further generation of both dinospore types in the same host after 399 days. A crab that was injected with microspores developed an infection that resulted in macrosporogenesis after 419 days. The earliest circulating forms of the parasite were observed in the haemolymph between 23-63 days post-injection. These were small round forms with dense nuclei and little cytoplasm that occurred as unicells or in plasmodia composed of two to eight cells. Later stages observed between 100-370 days post-injection were larger with a less dense nucleus and extensive cytoplasm and were uninucleate or plasmodia with up to 30 nuclei. The prespores were present as plasmodia with diffuse nuclei and extensive cytoplasm which before sporulation developed into smaller plasmodia with little cytoplasm and dense nuclei. The results of this experiment suggested a year-long developmental cycle in the host for the parasite which infects *C. bairdi*.

Hudson and Shields (1994) showed that the pre-patent period of *H. australis* in *Portunus pelagicus* and *Scylla serrata* could be as short as 16 days in crabs injected with circulating stages containing trichocysts (sporoblasts). They did not follow an infection for longer than 16 days and did not observe the production of dinospores in experimentally- or naturally-infected crabs. It was not possible to transmit the infection by feeding infected animals to uninfected ones.

Although both Meyers *et al.* (1987) and Eaton *et al.* (1991) have observed both types of dinospore in the haemolymph they have not observed how the dinospores leave

the infected host. Meyers *et al.* (1990) suggested that dinospores are released from decaying crabs after death.

The major questions that I intend to answer in this chapter are as follows :

- How does the development of the parasite *in vivo* relate to the development *in vitro* as described in chapters 2 and 3?
- How does *in vivo* development relate to the seasonality of the disease?

In order to answer these I have conducted a histological examination of infected lobsters to determine the parasite forms present during the progression of the infection. Diagnosis of early infections to facilitate the observation of their progression from an early stage was accomplished by developing a polyclonal antibody against the parasite for use in immunofluorescence reactions. This antibody has enabled the identification of latent infections (present only in the tissues, not circulating in the haemolymph) and sub-patent infections (parasite present in both tissues and haemolymph, but not readily detectable in wet smears). An observational experiment involving infected lobsters was carried out in order to gain more information on their survival and to observe how dinospores were liberated from the host.

Work reported in this chapter has been published in two papers which are included in appendix 1 as additional material.

## 5.2. Materials and Methods

### 5.2.1. Diagnosis of infection

Diagnosis of patently infected lobsters was carried out according to the procedures detailed in section 2.2.

### 5.2.2. Preparation of infected tissues for light and electron microscopy

Before dissection, lobsters were narcotised on ice for about one hour. Major tissues and organs were dissected from a total of 29 lobsters. The stage of their *Hematodinium* infection was estimated by pleopod examination as described previously. Of these, nine were apparently uninfected, five showed stage I infection, five stage II, five stage III and five stage IV. The organs and tissues removed for examination were hepatopancreas, antennal gland, midgut, abdominal muscle, haemopoetic tissue, heart, gills, and in some cases brain and eye/eyestalk Tissue and haemolymph samples were prepared for electron microscopy using the 1% glutaraldehyde, 2% paraformaldehyde fixative described in section 3.2. Tissue samples for wax embedding were fixed in Helly's mercuric chloride fixative (Johnson 1980) and embedded in paraffin wax. Thick sections (6μm) were treated with Lugol's iodine solution to remove mercury, and stained with haematoxylin and eosin (H&E).

### 5.2.3. Development of a polyclonal antibody from culture-derived *Hematodinium*

A polyclonal antibody was raised in rabbits immunized with a mixture of trophonts of *Hematodinium* from *in vitro* culture (obtained as described in Chapter 2). The method used (after Harlow and Lane, 1988) was briefly as follows. Trophonts were washed five times in *Nephrops* saline and then lysed by three cycles of freeze-thawing. Insoluble material was removed by mild centrifugation. After samples of pre-immunisation control serum had been taken, primary inocula of between 30µg and 300µg soluble protein in buffered *N. norvegicus* saline were injected with an equal volume of Freund's complete adjuvant into six rabbits at six sub-cutaneous sites in each. After test bleeds at two weeks, the two rabbits showing the highest titre responses were selected for further inoculation. Secondary, tertiary and quaternary inocula were injected with Freund's incomplete adjuvant every four weeks, with further test bleeds taken two weeks after each inoculation. Rabbits were exsanguinated four weeks after the final inoculation (14 weeks in total), and serum separated from clotted blood and frozen at -70ºC until required.

### 5.2.4. An indirect fluorescent antibody technique (IFAT) for the detection of *Hematodinium* in haemolymph and tissue samples

The IFAT employed was similar to that described by Marks *et al.* (1992) for the diagnosis of *Aerococcus viridans* in lobster (*Homarus americanus*) haemolymph. The technique was applied initially to fixed smears of cultured *Hematodinium* originally isolated from infected *N. norvegicus*, and later to fixed smears of haemolymph from infected and control lobsters.

Haemolymph samples were withdrawn from the ventral haemal sinus of lobsters into a syringe containing 2% formol saline (33‰ NaCl) at a ratio of 2:1 and allowed to fix for approximately 15 min. The mixture was then smeared onto clean glass slides and air dried. Culture material was smeared directly onto slides, air dried and fixed in ice cold 70% ethanol for one hour. Tissue smears were made from organs of killed lobsters directly fixed in a mixture of 2% paraformaldehyde and 0.1% glutaraldehyde, 4% sucrose and 3% NaCl in 0.1M phosphate buffer, pH7.4. Tissue samples were rinsed in 0.1M phosphate buffer containing 6.5% sucrose and stored in the same buffer containing 0.02% sodium azide, at 4°C until required. Small pieces of tissue (~1mm$^3$) were then macerated with a razor blade and smeared onto clean glass slides. The smears were then air dried and incubated in phosphate buffered saline (PBS)(pH 7.2) with 0.2% Tween 20 and either 3% bovine serum albumen (BSA) or 10% foetal calf serum for 15 minutes. Slides were incubated with primary anti-*Hematodinium* sp. rabbit antibody, diluted to 1:100 with PBS/BSA, for 1 hour at room temperature. They were then washed with 3 changes of PBS/0.1% BSA for 10 min [each] and incubated with secondary donkey anti-rabbit fluorescein labelled antibody (Scottish Antibody Production Unit) at a dilution of 1:100 with PBS/BSA plus 10µg ml$^{-1}$ 4',-6-diamidino-2-phenylindole (DAPI) (Sigma) as counter stain, for one hour. Finally, smears were washed thoroughly with PBS/0.1% BSA. Control slides were exposed to PBS/BSA containing no rabbit immune serum during the first incubation, or were incubated in pre-immune rabbit serum. Control staining was also performed on smears of haemolymph containing another protist commonly found in moribund *N. norvegicus* in captivity, the *Paranophrys*-like ciliate. Specimens were mounted in 10% PBS in glycerol with 25mg ml$^{-1}$ 1'4-diazabicyclo-[2.2.2] octane (DABCO) antifadant and examined using a Zeiss Axioskop compound microscope with ultraviolet (UV)

epifluorescence through fluorescein and DAPI filter sets. Entire treated slides were examined for the presence of immunoreactive dinoflagellates under low power objective (x10), and for closer examination under a x40 objective.

Upon detection of parasite material, the relative proportions of haemocytes and parasites were calculated after a total of approximately 400 cells had been identified and counted. A characteristic of *Hematodinium* spp. is that some individual parasites are multinucleate, therefore counts were based on the number of nuclei of parasites or haemocytes present, as determined by DAPI nuclear counter stain. Quantitative counts of parasites from tissue smears were not possible, so the presence or absence of parasite material alone was recorded.

Although different fixation methods were used here for parasites in culture, haemolymph and tissue samples, there was found to be no difference in the reliability or sensitivity of immunostaining with these different fixatives . Differing fixation methods were chosen for practical reasons.

### 5.2.5. Experimental comparison of diagnostic methods

Haemolymph samples were obtained from a total of 165 lobsters in the spring and summer of 1994, and the status of both *Hematodinium* infection (Field and Appleton, 1995) and moult stage (after Aiken, 1980) were determined by pleopod examination. One haemolymph smear from each animal was immunostained as described, and one was stained with Leishman's stain. Smears for Leishman's staining were post-fixed in methanol for one hour and stored before staining with a 0.2% w/v solution of Leishman's stain (BDH Chemicals Ltd, Poole, England) for 30 minutes.

Haemolymph smears were examined microscopically to record the presence or absence of dinoflagellate parasites observed using each staining method.

### 5.2.6. Detection of latent *Hematodinium* infection using IFAT

Staining by IFAT was used to determine whether latent (not detectable in the haemolymph) *Hematodinium* infections were present in adult *N. norvegicus* at different times of year. Previous work had shown that detectable (patent) infections were present in *N. norvegicus* populations only during spring (Field, 1992; Field *et al.* 1992).

Between 11 and 30 individuals were collected in each of the months of January, February, March, August, October and November, 1994. Lobsters were selected at random from trawl samples, but were all diagnosed as uninfected by pleopod examination. Thereafter haemolymph smears were made from each individual. Tissue smears were prepared from samples of hepatopancreas, midgut, heart and abdominal muscle removed from lobsters killed by decapitation. Both haemolymph and tissue smears were immunostained and examined for the presence of fluorescing parasites.

### 5.2.7. Progression of the infection

In order to obtain some indication of the time course of the infection an experiment was set up to follow the parasitaemias of a number of lobsters from as early as possible in the infection. From trawled catches of lobsters during October and November 1994 a subsample was taken and placed in the aquarium. Each individual from this sample was tagged and a haemolymph sample taken for immunostaining. The 13 individuals found positive for the presence of *Hematodinium* were separated for

further study, while those individuals that were negative were maintained in the aquarium and subsequently tested again for the presence of *Hematodinium* in January 1995. One lobster was found to be positive and was moved into the study group.

The lobsters in the study group were maintained in the aquarium as previously described in Chapter two. At intervals varying from 1-3 weeks, a small haemolymph sample (50µl) was removed from each lobster with a sterile syringe. To 180µl of formol saline was added 20µl of haemolymph to give a concentration of 9:1 haemolymph to formol saline. The total number of cells (dinoflagellates and haemocytes) in a sample of the fixed haemolymph was counted using a haemocytometer and smears made with the remaining fixed haemolymph.

The fixed smears were immunostained as described above and the percentage of dinoflagellates and haemocytes recorded. From the total cell counts the actual numbers of dinoflagellates and haemocytes were calculated using the percentages of each cell type from the immunostaining. During February 1995 a further 14 lobsters were added to the study based on diagnosis by body colour alone.

### 5.2.8. Progression of infection in unstressed lobsters

From a trawled catch of lobsters a total of 30 infected individuals were transported successfully to the Departmental aquaria on 24 April 1995. The lobsters were tagged and infection staged before placing in tanks. The tanks were inspected every day and the deaths of lobsters recorded where possible. The lobsters were not stressed by subsequent handling or disturbed after placing them in tanks until they were removed after death. The water temperature was kept at a constant 10ºC and was well oxygenated.

## 5.3. Results

### 5.3.1.1. Developmental forms of *Hematodinium* present in *N. norvegicus* as revealed by conventional light and electron microscopy

*Haemolymph*: When infected haemolymph was observed unfixed on a slide by phase contrast microscopy the dinoflagellates were present as irregularly shaped refractile cells. Fixed sectioned material showed that the parasites were predominantly uni- and binucleate, however multinucleate forms were present (Figure 5.1).

Dinoflagellates circulating in the haemolymph of lobsters with early stage I infections showed a marked difference in ultrastructure to dinoflagellates from lobsters with heavier infections. Circulating dinoflagellates from lobsters with low level infections (stage I) often did not contain trichocysts or flagellar hair vesicles. Numerous membrane bound organelles were observed in the cytoplasm by electron microscopy some of which appeared empty, whilst others resembled the granular matrix organelles described in chapter 3; lipid droplets were also present (Figure 5.2). The amphiesmal alveoli were reduced to small vesicles in some areas of the cell periphery. These developmental forms from the early stages of infection closely resembled the trophonts from *in vitro* culture in their ultrastructural detail. The trophonts from *in vitro* culture did not possess trichocysts or flagella hair vesicles (Figure 5.3), but did contain numerous vesicles, lipid droplets and granular matrix organelles. The dinoflagellates circulating in the haemolymph during the early stages of infection that do not contain trichocysts or flagellar hair vesicles were therefore identified, and will be referred to, as trophonts. The trophonts observed both *in vivo* and *in vitro* had compressed

amphiesmal alveoli when compared with sporoblasts and dinospores (see Chapter 3).

Dinoflagellates from heavily infected lobsters (stage III-IV) contained a large number of membrane bound trichocysts which were often formed into 'batteries' when observed by electron microscopy (Figure 5.4). There was no evidence of trichocysts being discharged into the haemolymph even at the electron microscopical level. Numerous organelles resembling caseiform organelles were also present, as well as lipid droplets (Figures 5.4, 5.5). These later haemolymph stages contained more lipid droplets and inclusion organelles than the trophonts. Enlarged perinuclear spaces contained a fibrous material, thought to be flagellar hairs (Figures 5.5, 5.6). Close examination of the amphiesma revealed that the alveoli did not appear to be uniform in size and arrangement, but were in fact irregular in size and swollen in some places while compressed in others (Figures 5.5, 5.7). The circulating parasite developmental forms found in lobsters with heavy infections and characterised by the possession of trichocysts and flagellar hair vesicles will be referred to as sporoblasts as these forms give rise to dinospores *in vitro* and *in vivo* (Chapter 2).

*Hepatopancreas:* Enlarged spaces within the hepatopancreatic haemal sinus were found to contain large numbers of uninucleate (and occasionally binucleate) parasites, but haemocytes were rarely seen. Occasionally, parasite syncytia were seen in infected animals, attached to the outside of the hepatopancreatic tubules (Figures 5.8, 5.9). In some cases trichocysts were not visible in toluidine blue-stained sections viewed using brightfield microscopy (Figure 5.9). In other cases trichocysts were visible in toluidine blue stained resin sections of attached syncytia indicating that these were sporogenic (Figure 5.9).

During some routine immunostaining work arachnoid syncytia were observed on several occasions in hepatopancreas tissue smears from lobsters with latent infections (i.e. parasites present only in the tissues, not in the haemolymph) (Figure 5.10), although they were not readily observed in sectioned material.

The involvement of the fixed phagocytes which surround the hepatic arterioles in a defensive response against *Hematodinium* infection is described in Chapter 6.

*Antennal Gland:* The antennal gland is an excretory organ involved in the production of urine. As in the hepatopancreas, the majority of the parasites present within the haemal spaces and connective tissue were uninucleate, but multinucleate syncytia were also present, especially attached to the basal side of the labyrinthal epithelium (Figure 5.11). There was an increase in numbers of syncytia attached to the to the labyrinthal epithelium with increasing infection stage, though even light infections of stage I showed well established groups of attached parasite syncytia in the labyrinth.

*Midgut:* The midgut wall of lobsters from all pleopod infection stages showed large scale infiltration by the dinoflagellates. The connective tissue and muscles of the outer midgut wall had been almost completely replaced by parasites, even in stage I lobsters. The haemal spaces were enlarged and partially occluded by large numbers of attached upright filamentous parasite syncytia in which trichocysts were not observed (Figure 5.12). Few haemocytes were observed in these haemal spaces in infected animals, especially in stage III and IV individuals.

*Abdominal Muscle:* In wax embedded sections of stage I animals parasite invasion of muscle fibres was not apparent, even though free uninucleate parasites were frequently

encountered in interstices between muscle fibres. The interstitial connective tissues of skeletal muscle remained intact. In stage III and IV lobsters, however, arachnoid syncytia were present within skeletal muscle interstices (Figure 5.13), and connective tissue was reduced. Furthermore, peripheral areas of some fibres were lysed, and uninucleate parasites were also present in the haemal spaces surrounding the fibres. Multinucleate forms of the parasite, were often closely associated with the sarcolemma (Figure 5.14). Batteries of trichocysts were visible in ultrathin sections indicating that the parasite was a sporont.

*Haemopoietic Tissue:* The haemopoietic tissue of *N. norvegicus* forms a thin sheet on the dorsal and lateral surfaces of the cardiac stomach (gastric mill) and probably on the ventral floor of the cephalic cavity, adjoining the antennal glands. The haemopoietic tissue of dinoflagellate-infected *N. norvegicus* showed a dramatic increase in size from the healthy state, evident even to the naked eye during dissection of stage III and IV animals. This hypertrophy was due, in part, to a much increased level of haemopoietic activity, with many nodes containing differentiating cells, mitotic figures and stem cells. However, despite this vast increase in both the number and activity of stem cells, very few newly differentiated haemocytes were visible in the haemal spaces surrounding the haemopoietic nodes (Figure 5.15). Instead these spaces were filled with many uninucleate and multinucleate sporoblasts, even in lower level stage I and II infections. Attached parasite syncytia were not observed in the haemopoetic tissue.

*Heart:* In the heart there was again invasion of all haemal spaces by the parasite. In wax sections the lumen, haemal spaces and connective tissue of the myocardium were massively infiltrated mainly by attached dinoflagellate syncytia, already well

established in stage I animals. Arachnoid syncytia were also seen to ramify through the interstices of the myocardial muscle in all stages (Figure 5.16), similar to those in abdominal muscle interstices. Identifying the arachnoid syncytia in ultrathin sections proved very difficult. It was possible to locate dinoflagellate nuclei and sometimes to trace the cytoplasmic processes that infiltrated the host tissue using transmission electron microscopy (Figure 5.17). These parasites contained large vesicles, often enclosing unidentifiable debris; lipid droplets were usually present, although trichocysts were rarely seen, even in ultrathin sections.

*Gills:* The major effect of the parasite on the gills was the occlusion of haemal spaces by large numbers of circulating sporoblasts. This was more severe in infection stages III and IV, but still apparent in stage I and II lobsters. Attached parasite syncytia were not observed in this tissue, but evidence of host reaction to infection was seen and is described in Chapter 6.

*Brain and eyestalk:* In these tissues there were no overt signs of parasite infiltration or tissue change. Parasites were restricted to circulating forms in the haemal sinuses and vessels of these tissues.

It should be noted that in some organs (particularly heart and hepatopancreas) the numbers of unattached parasites observed in sections of haemal spaces and lumina may have been an under-representation of actual numbers, due to losses during processing for both light and electron microscopy.

### 5.3.1.2. The ultrastructure of dinospores circulating in the haemolymph

Early dinospores were identifiable in toluidine blue stained resin sections of infected tissues viewed using brightfield microscopy because sectioned flagella were visible (Figure 5.18). Closer examination using electron microscopy revealed that macrospores (Figures 5.19, 5.20) and microspores closely resembled their counterparts from *in vitro* culture with the same chromosome appearance and presence of trichocysts and flagellar hair vesicles.

## 5.3.2. Evaluation of the indirect fluorescent antibody technique for detection of *Hematodinium* infections and stages in development of the parasite

Staining of *Hematodinium* in haemolymph smears by IFAT showed good antibody specificity for the parasite (Figure 5.21). Host haemocytes were unreactive whilst background staining and autofluorescence were low in haemolymph smears. Although there was no binding of the antibody to host cells in tissue smears (Figure 5.22), there was a degree of autofluorescence, especially in hepatopancreas. This autofluorescence was minimised by ensuring thorough maceration of samples. All controls tested gave negative results. The rabbit antibody showed no affinity for host haemocytes or ciliates; there was no non-specific binding of the secondary donkey-anti-rabbit antibody to *Hematodinium*, haemocytes or ciliates..

The accuracy of pleopod diagnosis of *Hematodinium* infection compared with diagnosis from immunostained and Leishman-stained haemolymph smears is shown in Table 5.1. This assessment is based on the parallel examination of samples containing both sexes of lobsters by all three methods. Immunostaining detected 37 (22.4%) individuals within the sample that were infected, 12 more than by pleopod and three

more than by Leishman's stain. Three individuals were diagnosed as infected by immunostaining alone. No infected lobsters diagnosed by pleopod examination were classified as being uninfected by other methods. All mis-diagnoses by pleopod examination and Leishman's staining were made in lobsters initially staged as uninfected by pleopod examination but were subsequently found to be infected by immunostaining or by both smear examination methods. Those sub-patent infections detected by immunostaining, but undetected by Leishman's stain showed the lowest proportions of parasites to haemocytes, ranging from 0.3 to 1.7%. The lowest proportion detected by Leishman's stain was 2.4%.

### 5.3.3. Detection of latent *Hematodinium* infections using the indirect fluorescent antibody technique.

Throughout the year, some animals diagnosed as uninfected by pleopod examination were shown to be harbouring sub-patent (low parasite numbers in haemolymph but not yet a patent infection) or latent *Hematodinium* sp. infections, detectable by IFAT (Table 5.2). Using this technique animals at all times of the year were found that contained parasites only in the tissues (latent infection), with no detectable haemolymph infections. During most of the year some animals were infected with parasites in both the tissues and haemolymph.

In cases of tissue infection where no haemolymph infection occurred (i.e. latent infections) parasite abundance was often low, sometimes with only one parasite detected in a smear. In all cases of tissue infection where haemolymph infection also occurred (sub-patent), parasites in the tissues were more abundant. Due to the disruptive nature of the preparation of tissue smears for immunostaining it was difficult to identify the parasite forms that were present in every smear reliably. Uninucleate

(Figure 5.22) and multinucleate parasites were seen in smears as well as filamentous syncytia. Well-established arachnoid syncytia were observed in abdominal muscle and hepatopancreas smears (Figure 5.23). There was no obvious pattern to the parasite developmental stages observed and the time of year, or between the parasite form and the tissue type. In the majority of the cases of a latent infection, parasites were detected in only one tissue even though several were examined.

### 5.3.4. The progression of *Hematodinium* infection in *N. norvegicus* in captivity

Sub-patent levels of parasite were detected in haemolymph samples taken outside the normal disease season. Table 5.3 shows the progression of infection as assessed by pleopod examination and immunostaining in 14 lobsters that were caught during October and November 1994. Lobsters nos 1 and 5 had very low initial infections, but no parasite was detected in their haemolymph using immunostaining during the rest of the study, suggesting that the infection had either been overcome or was to remain latent in the lobster for a further length of time. All the other lobsters which showed an initial sub-patent infection subsequently developed patent infections (diagnosable by pleopod) during the winter and spring of 1995.

The haemolymph of lobster number eight was examined regularly for over 180 days and revealed some changes in its cellular composition (Figure 5.25).

Three infection stage I lobsters moulted during the course of the study (Table 5.3). Two lobsters (nos 9 and 14) survived only 1½ and 3½ weeks respectively. The new cuticle failed to harden but it was not clear what the final cause of death was. Lobster number eight survived for two months after moulting although its shell did not fully harden.

Table 5.4 shows infection progress for the lobsters caught in January 1995 that were initially diagnosed as infected by colour only. Of the 14 lobsters three were found to be uninfected by immunostaining and remained uninfected during the study. Unfortunately apart from no. 15 (survived 104 days) the lobsters did not survive much longer than 30 days. No. 15 was initially diagnosed as having a stage I infection and parasites represented 25% of the cells in the haemolymph.. The growth data for lobster 15 are shown in figure 5.26. In 104 days the numbers of dinoflagellates in the haemolymph had risen from $3 \times 10^6$ to $3 \times 10^8$ cells $ml^{-1}$, a hundred fold increase.

The uninfected lobsters that were observed during the study also showed slight fluctuations in the number of haemocytes circulating in the haemolymph (Figure 5.27). These fluctuations in the numbers of haemocytes in healthy lobsters must be considered when interpreting the data from infected animals.

In an attempt to discover if dinospores and sporoblasts were infective to healthy *Nephrops* by injection, in conjunction with Dr R. Field I started some transmission experiments in May 1993 and January 1994 at The University Marine Biological Station, Millport and the SOAFD field site Aultbea, Loch Ewe owing to the lack of an adequate aquarium facility in the Zoology Building. Unfortunately soon after both experiments were started the lobsters died relatively quickly and no infections were detected in the dead animals. As we could give little supervision to these experiments while they were running, on account of the travelling distance between Glasgow and Loch Ewe no further experiments were started within the period of study.

### 5.3.5. Survival time and progression of infection in unstressed lobsters in captivity

Table 5.5 shows the survival times of a group of 30 infected lobsters that were caught on the 24 April 1995 and infection staged by pleopod examination. The mean survival time for each infection stage is shown in Table 5.6. Stage I lobsters survived an average of 25 days and this decreased to 9 days for stage IV lobsters.

### 5.3.6. Observations on dinospore release from infected lobsters

Three of the 30 lobsters represented in Table 5.5 produced and released dinospores during this study. These lobsters were initially pleopod staged at I, II and III. The natural release of dinospores from an infected lobster has been observed not only in this survival experiment but also in seven other infected lobsters that were kept as stock. The following is an account of the natural release of *Hematodinium* dinospores from *N. norvegicus* which has been compiled from several observations of dinospore release.

The first signs that the *Hematodinium* infection in a lobster had reached sporogenesis and produced dinospores was usually that the surrounding seawater developed a cloudy appearance. When the lobster was closely examined under incident light the dinospores were seen to be released from the gill chambers and then dispersed in dense white clouds by the exhalant respiratory current (Figure 5.28). Although large numbers of dinospores were released, the lobsters were still able to walk, groom and to produce a tail flip escape response. The clouds of dinospores were much denser and larger if the lobster was moving or had just ceased moving. Streams of dinospores were also released from areas on the ventral side of the lobsters where previously damaged

cuticle had become melanized (Figure 5.29). The process of spore release never lasted more than 24 hours and usually after 18 hours the lobster had become moribund, stopped moving and become completely unresponsive. One such lobster which was subsequently dissected still had a beating heart but this appeared completely empty of haemolymph and parasite cells. Examination of a pleopod showed no sign that parasites were still present. The heart, hepatopancreas, midgut, antennal gland and abdominal muscle of a lobster that had released dinospores were fixed and resin embedded. Examination of toluidine blue-stained sections from two areas of each tissue did not reveal the presence of any parasites. I would expect immunostaining of these tissues to reveal some parasites remaining in the cadaver.

I have observed four macrospore and three microspore emissions. Infected lobsters of all infection stages have naturally released dinospores and those for which cell counts were made are shown in Table 5.7. Although lobsters emitting dinospores had different pleopod stagings the cell counts were similar and higher than infected animals that were not releasing dinospores.

## 5.4. Discussion

### 5.4.1. Seasonality of infection

The fact that there is a clear seasonal pattern in the expression of *Hematodinium* infections must reflect the life-cycle of the parasite. The presence of sub-patent and latent dinoflagellate infections at times of the year when overtly-diseased *Nephrops* are absent (Table 5.2) suggests a long latency and development period for infection and that infection acquisition in one year leads to disease patency in the next, or even later. The

experiments to follow the progress of infection have shown that subpatent infections detected in the late autumn of one year develop into patent infections during the spring and early summer of the following year (lobster no. 2-4,6-14 Table 5.3). Lobsters presumably become infected during the late winter and spring either by the dinospore or could be ingested in an as yet unknown secondary host. The infection remains latent until the late autumn when sub-patent infections are detected. The numbers of parasite increases in the tissues and haemolymph over the winter and patent infections first occur in the late winter of the following year. It is not yet clear whether infections remain latent for only six to nine months and develop into a patent infection the following year or are able to remain latent for longer and develop into a patent infection in subsequent years. Eaton *et al.* (1991) showed that the infection produced when Tanner crabs were injected with dinospores required between 399 and 419 days to produce another generation of dinospores. This evidence suggests that the life-cycle for *Hematodinium* sp. in the Tanner crab is an annual cycle.

It is interesting to note that in the Clyde Sea Area the seasonality of *Syndinium* infections of *Calanus finmarchicus* (Jepps 1937) follows the same pattern as *Hematodinium* infection of *N. norvegicus* (Field *et al.* 1992). Margaret Jepps found *Syndinium* infections of *C. finmarchicus* from January through until early May and not during the summer or autumn.

### 5.4.2. Parasite developmental stages

The developmental forms of the parasite found *in vivo* resembled many of the forms observed in *in vitro* cultures. The trophonts observed *in vivo* were comparable in ultrastructure to the filamentous and gorgonlock trophonts observed *in vitro*, but they

were not filamentous. Attached syncytia containing trichocysts, observed in the hepatopancreas were identified as sporogenic forms. Attached sporogenic syncytia may be derived from circulating sporoblasts that have settled and attached to host tissue and would then be regarded as secondary sporonts. The filamentous nature of attached secondary sporonts may be due to the restricted space in which they have to grow. Secondary sporonts may give rise to further circulating sporoblasts.

The filamentous and gorgonlock trophonts that developed in *in vitro* culture displayed marked writhing movements. It seems likely that the filamentous syncytia found *in vivo* (particularly in the midgut wall) would also perform these movements. The function of these movements could be to enable the parasite to manoeuvre its way into tissues. Attached filamentous syncytia could use the movements to maintain haemolymph flow around themselves in confined areas to ensure a steady supply of oxygen and nutrients and removal of waste products.

The arachnoid syncytia observed by phase contrast in the hepatopancreas possessed the same network of cytoplasmic threads as the arachnoid syncytia observed *in vitro*. Arachnoid syncytia were easily recognisable in tissue smears but were difficult to identify in ultrathin sections viewed in the electron microscope. This may be because the cytoplasmic threads were insinuated through the various tissues, making them difficult to detect. Attached filamentous and arachnoid syncytia have not been observed in previous cases of *Hematodinium* sp. infection.

Circulating filamentous syncytia have not been observed in *N. norvegicus*, although they have been observed in the blue crab *Callinectes sapidus* (Newman and Johnson 1975, Messick (1994), *Carcinus maenas* and *Liocarcinus depurator* (Chatton and Poisson 1931).

Comparison of the sizes of the circulating forms found in other decapods shows that there are some differences, though there is also overlap (Hudson and Shields 1994). The majority of the circulating so-called 'vegetative' parasite forms described to date by other workers are larger than those originally described by Chatton and Poisson (1931), moreover the comparison of 'vegetative' stages by Hudson and Shields (1994) as a taxonomic criterion is misleading because some of the forms described by other workers are clearly sporoblasts because they possess trichocysts.

In this study I have shown that, in the early stages of infection, the *Hematodinium* stage circulating in the haemolymph does not possess either trichocysts or flagellar hair vesicles and represents the trophont. In late stage infections the circulating parasites possess both trichocysts and flagellar hair vesicles and are identified as sporoblasts; both types of dinospore also possess these features. These observations suggest that the formation of trichocysts and flagellar hair vesicles is a precursor to sporogenesis. The fact that some other workers have not reported trichocysts in circulating *Hematodinium* sp. (Meyers *et al.* 1987) suggests that they may have observed trophonts present only in the early stages of an infection.

The trichocysts observed in *Hematodinium* resemble those possessed by numerous ciliates and dinoflagellates (Livolant 1982, Knoll *et al.* 1991), although their function is still not clear. The trichocyst is composed of a central core which is square in section and has a crystalline appearance. The core is surrounded, but not in contact with, a single unit membrane. This particular extrusome is called a trichocyst because the discharged forms are present as extremely elongated shafts (see Chapter 3). Trichocysts have been observed in a discharged state in fixed infected haemolymph samples (Field *et al.* 1992) and in dinospores (Chapter 3) fixed *in vitro* but there are no confirmed reports of trichocyst discharge in the host. It is possible that the process of

fixation stimulated the discharge of trichocysts. The streaming filamentous structure that Meyers *et al.* (1987) drew attention to in their Fig. 4, a wet smear of compressed circulating dinoflagellates, could be a discharged trichocyst. Trichocyst discharge can be induced by squashing dinoflagellates (Livolant 1982). It has been suggested that trichocysts may play a part in defence, conjugation, osmoregulation, swimming behaviour, geotactic behaviour, food uptake and scavenging toxic substances (Maupas 1883, Hausmann 1978, Wichterman 1986, Adoutte 1988, Haacke-Bell *et al.* 1990). Experimental evidence only exists to verify defence as a function. It has been shown that *Paramecium* uses the exocytosis of trichocysts as a means of rapid propulsion away from the attacking predatory ciliate *Dileptus* (Knoll *et al.* 1991). *Hematodinium* dinospores may use trichocysts as a means of defence or perhaps they are somehow involved in adhesion to and invasion of a new host.

In Chapter 3, I have shown that microspores possess very condensed chromosomes which fill virtually the whole nucleus, whereas the macrospores have less condensed chromosomes. Thus, when observing dinoflagellates from a lobster with a heavy infection it is possible to predict the type of spore to be produced by observing the appearance of the chromosomes. The dinoflagellate present in figure 5.4 has highly condensed chromosomes suggesting that during the final stages of sporogenesis microspores will be produced.

Although I made no specific study of nuclear division during sporogeny the observations that I have made suggest that it is similar to that described for *Syndinium* by Ris and Kubai (1974). The presence, in a trough in the nucleus of centrioles, which are attached to kinetochores by microtubules recalls the situation in *Syndinium*. A single microtubule-containing tunnel which pierces the dividing nucleus has been observed on a few occasions in material from infected *Nephrops*. The fact that there are

few obvious signs of active mitosis in parasites prepared for electron microscopy suggests that mitosis is intermittent and cell proliferation is a slow process.

The development of a reliable and specific IFAT for the detection of *Hematodinium* has enabled the detection of previously undiagnosed infections. Using this technique it has been shown that lobsters are harbouring an infection throughout the year. This observation would support a hypothesis that the invasion of tissues occurs soon after the acquisition of infection. The fact that early infections are present only in the tissues poses problems for investigating the time span of the latent period of infection, because lobsters have to be sacrificed for removal of tissue samples.

Lobsters of all infection stages have released spores, suggesting that pleopod diagnosis is not a reliable indicator of the maturity of the infection. The sudden increase in the number of dinoflagellates present in the haemolymph in the late stages of sporogenesis (Figure 5.26) suggests that the attached parasite forms in the tissue transform totally into dinospores and are released from the host. This suggestion is further supported by the observation that no dinoflagellate material was detected in lobster tissue after natural spore release. It would appear that the dinospores make full use of the haemolymph circulation of the lobster and the water currents through the gill chambers to ensure dispersal. It is not clear how the dinospores breach the cuticle of the lobster. Release could be through the production of a chitinase by dinospores, or perhaps through the mechanical pressure from increased cell numbers in the haemolymph rupturing the thin cuticle of the gills. Although dinoflagellates were found in the lumen of the hepatopancreas, there was no observed release of dinospores from either the mouth or anus. Dinoflagellates were found in the lumen of the antennal gland and dinospores have been released from the antennal gland opening (nephropore). The release of a syndinid dinospore from its host has previously been observed only by

Chatton (1920) who described the active *Syndinium* dinospores leaving the copepod host by a split in the exoskeleton, usually in the first antenna.

There is an accumulation of lipid droplets and inclusion organelles as circulating parasites increase in number and become sporoblasts. The lipid droplets and inclusions are probably energy reserves that the free-living dinospore will utilise. The accumulation of energy reserves may be a slow process that is dependent upon the physiological condition of the lobster, since the material that forms the energy reserves must derive from the host. Maturation of dinospores may be dependent upon a certain level of energy reserve accumulation and if this level is not met the parasite may perish with the host.

### 5.4.3. Survival of infected lobsters

A previous study by Field *et al.* (1992) showed that mortality of infected lobsters was greater than that of uninfected lobsters, though infected lobsters died before the infection reached maturity and dinospore release was not observed. The slightly longer survival times for all stages of infected lobsters that I achieved (Table 5.6) have probably been enabled by improvements in handling and care of lobsters and better aquarium facilities. The fact that 10% of lobsters from the group of 30 (Table 5.5) were able to release dinospores naturally supports the suggestion that maintenance of the lobsters had been improved. The percentage of lobsters that released dinospores may be lower than that reached at this stage in the natural habitat. Ecdysis was not inhibited by the infection, although lobsters died within a few weeks after moulting (Table 5.3). It is likely that some lobster deaths were compounded by the stress of capture, transport and handling. It would have been better to carry out survival

experiments with creel caught infected lobsters which are subject to less stress, but catches of these were very poor during this study.

There was a single occurrence of a lobster apparently overcoming infection during the early sub-patent period when parasites were detectable only in the haemolymph. A parasite was detected in the initial smear from Lobster no. 5 in the progress of infection experiment (Table 5.3), but no parasites were detected thereafter. It is possible that early haemolymph infections can be overcome but the tissue infection may remain to produce a further haemolymph infection at a later date. All the evidence I have gathered (Table 5.3, 5.4, 5.5) suggests that infections which reach patency are eventually fatal, although death often occurs before the release of dinospores.

### 5.4.4. Conclusions

The results presented in this chapter provide more information towards the establishment of the life-cycle of *Hematodinium* in *N. norvegicus*. It is suggested that the earliest forms of the parasite in the lobster are present only in the tissues and not in the haemolymph. These attached forms include both filamentous and arachnoid syncytia which are also the earliest parasite forms to occur after germination of dinospores *in vitro*. The tissue infection remains latent for an unknown period of time before the tissue forms divide and release trophonts into the haemolymph. The earliest developmental forms present in the haemolymph are trophonts. The circulating trophonts probably spread the infection throughout the lobster. Later in infections the circulating parasites are all sporoblasts. Both trophonts and sporoblasts are capable of forming arachnoid syncytia when transferred into *in vitro* culture. Both trophonts and sporoblasts therefore have the potential for spreading the infection throughout the

tissues of the lobster. In *in vitro* culture sporogenic arachnoid syncytia give rise to sporoblasts, the precursors of the dinospores. By analogy the attached arachnoid syncytia in tissues probably give rise to the sporoblasts circulating in *Nephrops*. Sporogenic filamentous syncytia have not been observed in *in vitro* culture but attached filamentous syncytia containing trichocysts have been observed in *Nephrops*. Eventually the sporoblasts and attached syncytia give rise to dinospores and leave the host. The observations presented above suggest that all developmental forms of the parasite present in *Nephrops* eventually become sporogenic. It is not clear what the triggers are for the changes from trophont to sporont, sporont to sporoblast and sporoblast to dinospore. Changing physiological conditions within *Nephrops* during the course of the infection may provide the stimuli for the transition between developmental forms.

**Figure 5.1.** A toluidine blue stained 1μm resin section of haemolymph from a heavily infected lobster. The sporoblasts are predominantly uni- and binucleate, although multinucleate plasmodia are sometimes found circulating in the haemolymph. The dinoflagellate nuclei (n) containing condensed chromosomes are very distinct from the diffuse chromatin observed in the nuclei of host haemocytes (HC). Lipid droplets (arrows) are present in most of the dinoflagellates. Brightfield. Scale bar = 10μm.

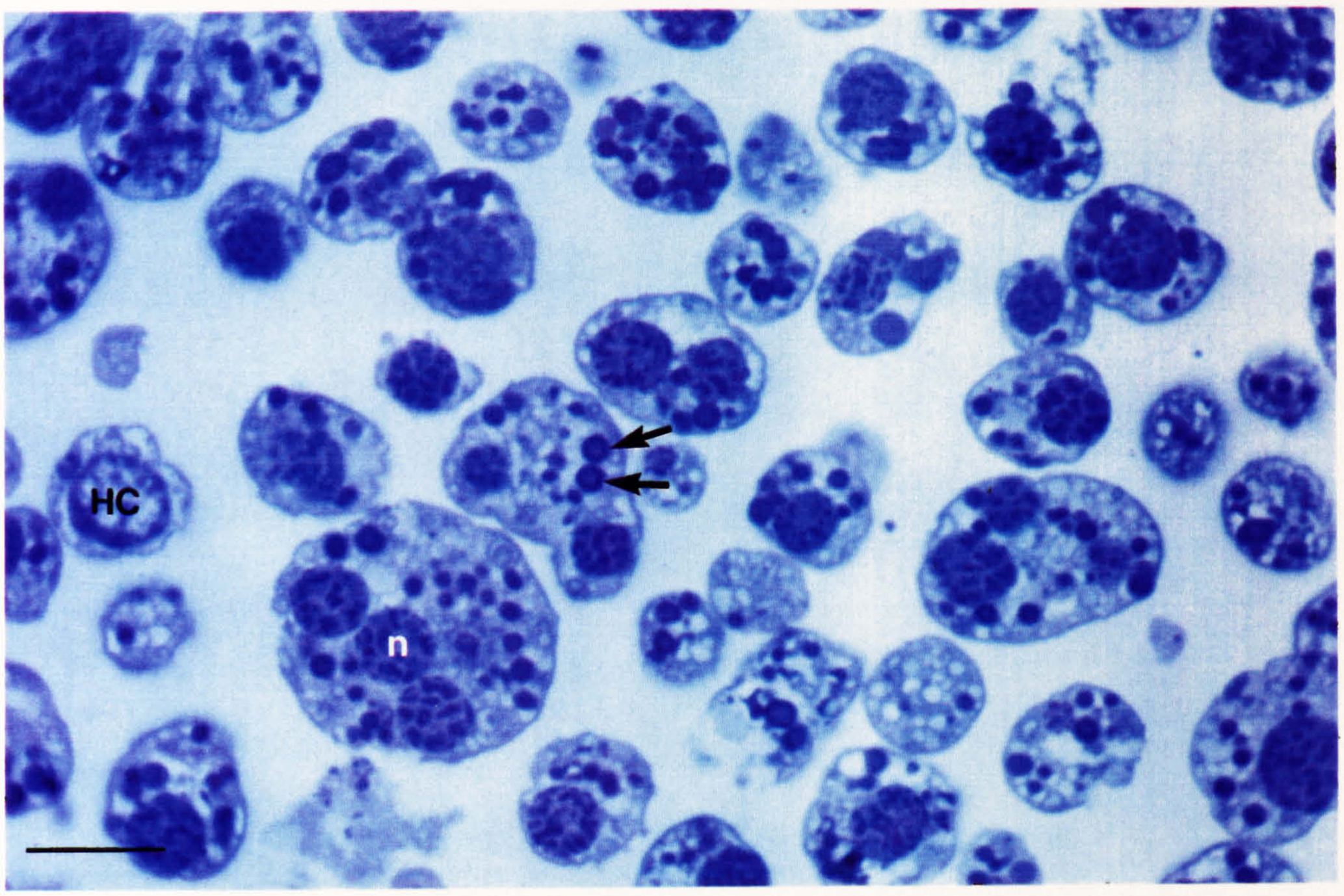
HC
n

**Figure 5.2.** A trophont from the haemolymph of a stage I infected lobster. The condensed chromosomes (ch) in the nuclei (n) are very distinct. Mitochondria (m) are abundant in the cytoplasm, as are lipid droplets (l) and granular matrix organelles (gmo). In some places the amphiesmal alveoli are reduced to small vesicles (arrows). Note the absence of trichocysts. TEM. Scale bar = 2μm.

**Figure 5.3.** A transmission electron micrograph of a cultured trophont for comparison with a trophont from *Nephrops* haemolymph above. Like the *in vivo* trophont the cultured trophont does not contain trichocysts or flagellar hair vesicles. The cluster of granular matrix organelles (gmo) is a feature of the trophont stage. co = caseiform organelle, n = nucleus, m = mitochondrion, g = Golgi apparatus, , v = large vesicle containing unidentifiable debris, arrow = micropore. Scale bar = 5μm.

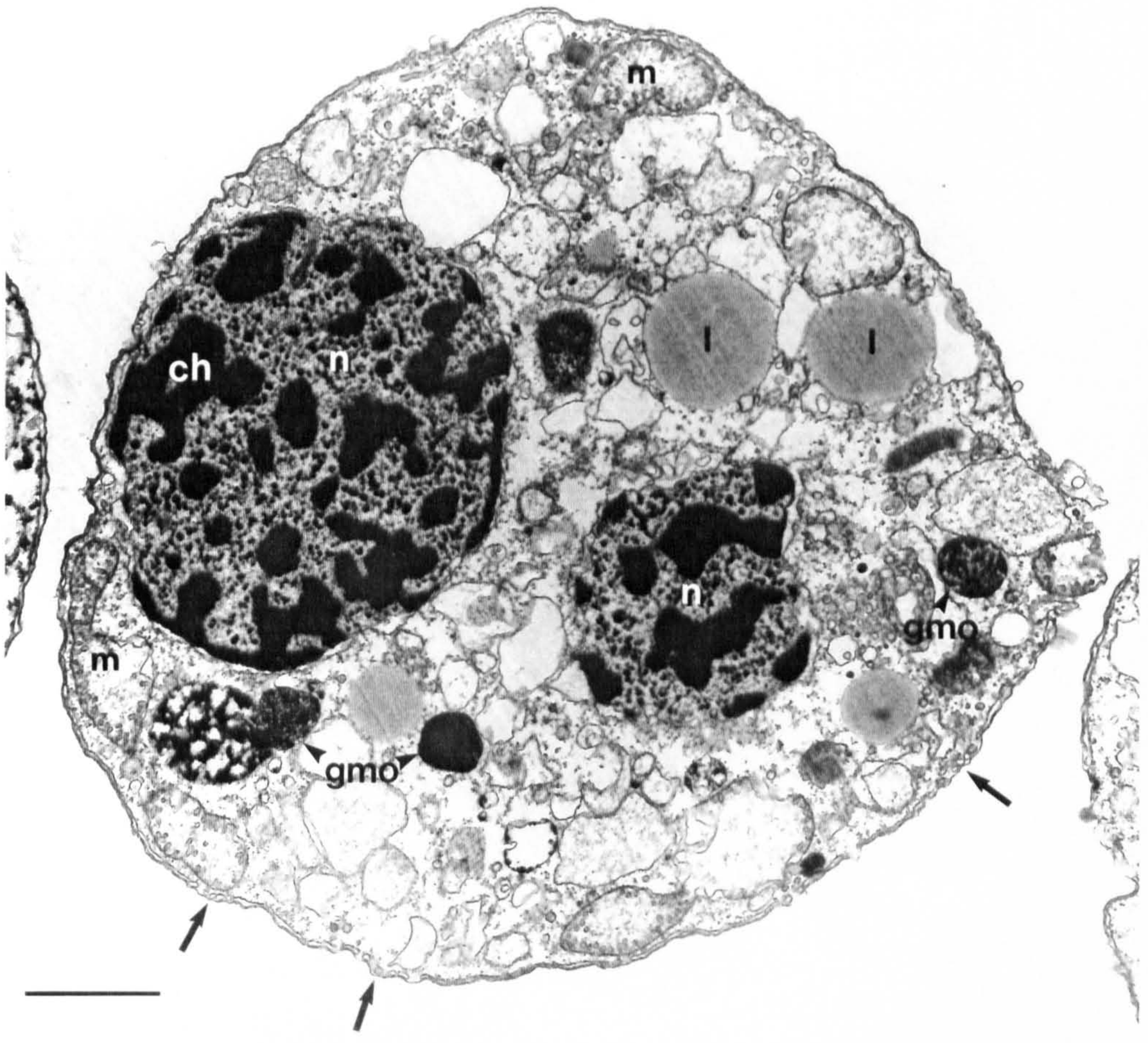
m
ch
n
l
l
n
gmo
m
gmo

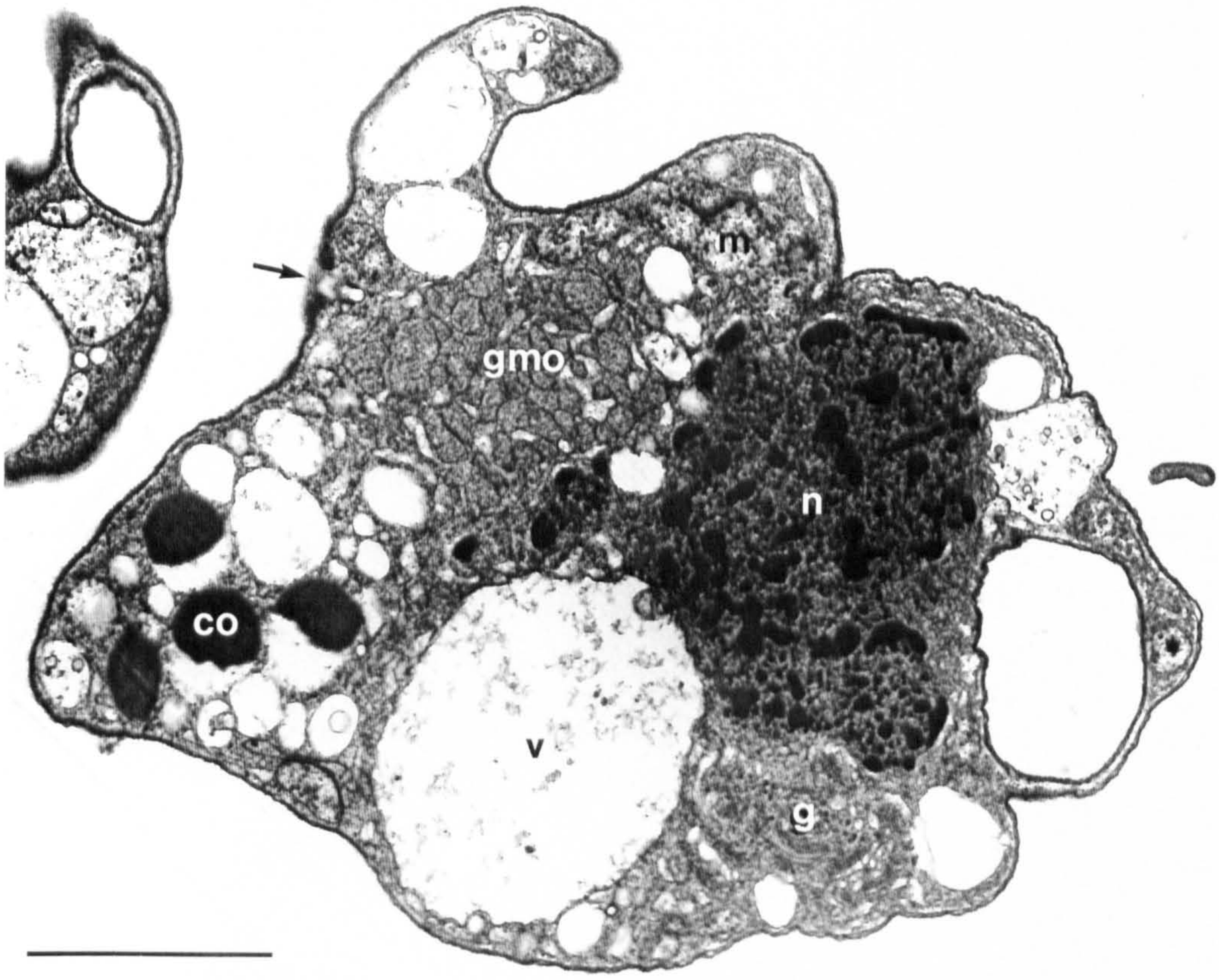
m
gmo
n
co
v
g

**Figures 5.4. to 5.7.** TEM micrographs of sporoblasts from the haemolymph of a stage III infected lobster.

**Figure 5.4.** The chromosomes (ch) are highly condensed in the nuclei of the dinoflagellates. A large number of membrane bound trichocysts (tr) are present, lipid droplets (l) are numerous and there many caseiform organelles (co). The amphiesmal alveoli (a) are swollen, and prominent around the periphery of the cell. Scale bar = 2μm.

**Figure 5.5.** The trichocysts (tr) are square when observed in transverse section and are clearly bounded by a membrane. Note the extent of a single amphiesmal alveolus (a). The perinuclear space is enlarged and forms a flagellar hair vesicle (fv) close to a condensed chromosome (ch) within the nucleus. On either side of a large lipid droplet (l) are caseiform organelles (co). Scale bar = 0.5μm.

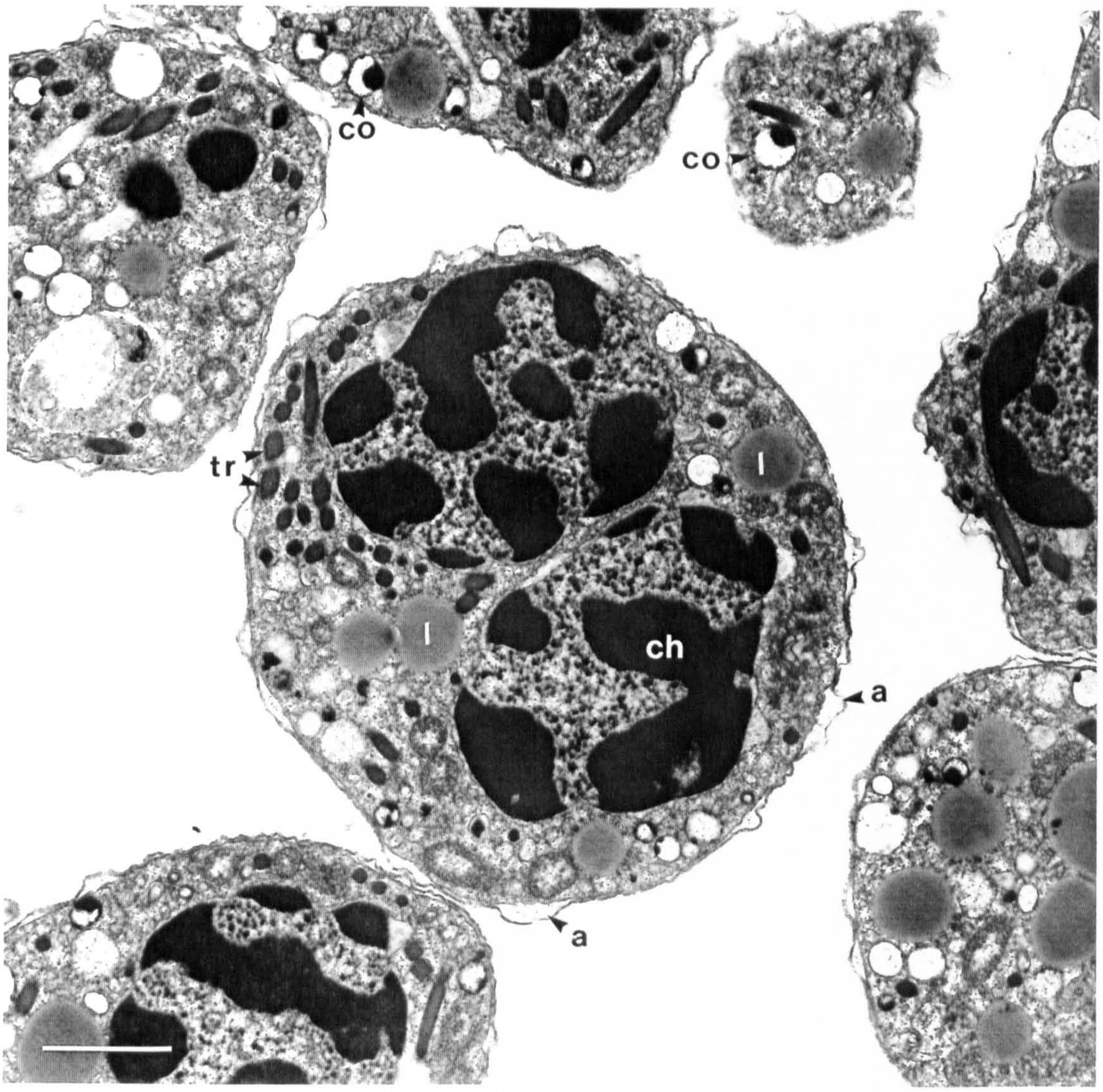
co
co
tr
l
l
ch
a
a

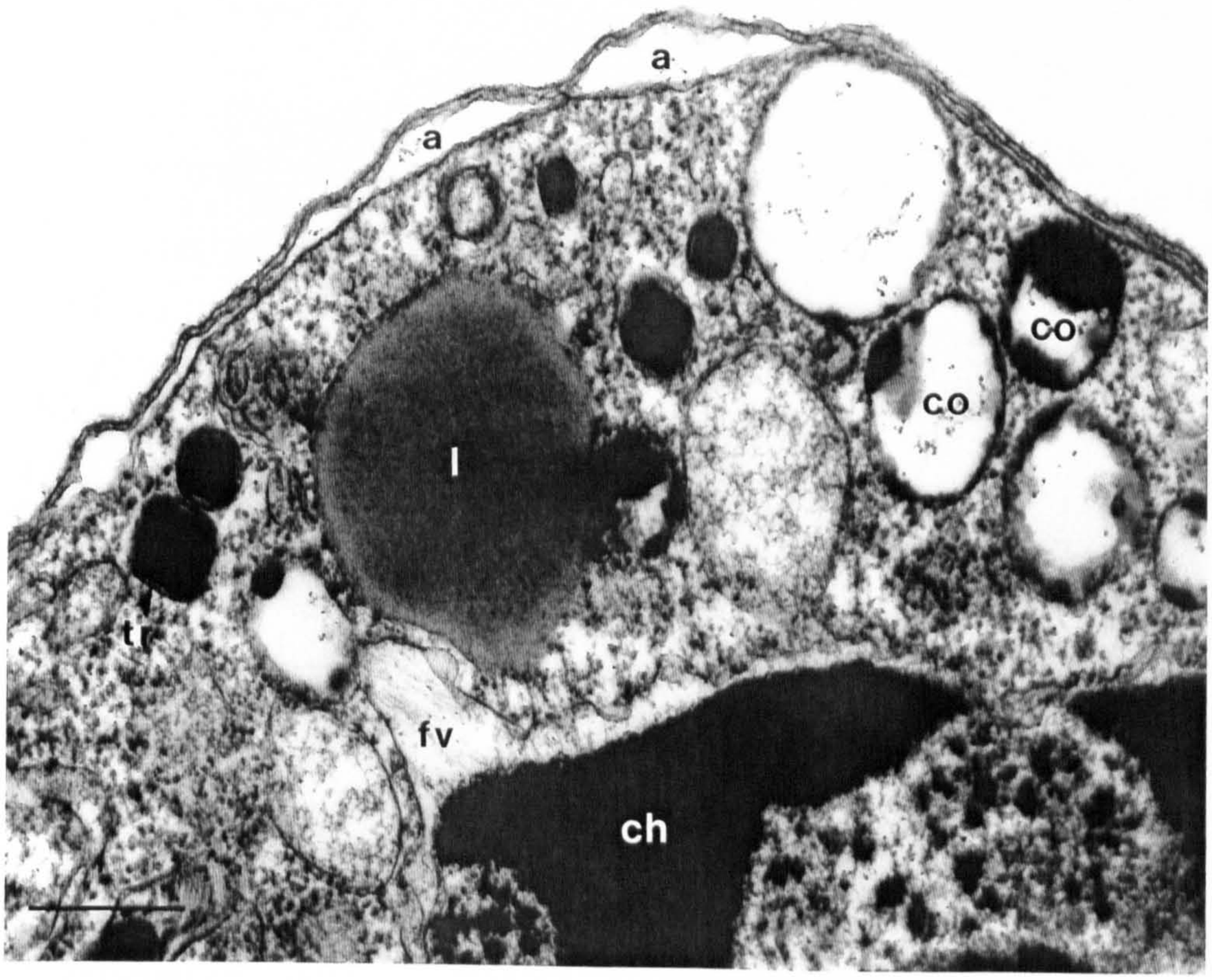
a
a
co
co
l
tr
fv
ch

**Figure 5.6.** Two flagellar hair vesicles (fv) have formed in the perinuclear space on either side of a furrow in the nucleus that contains a centriole (cn). ch = chromosome. Scale bar = 1μm.

**Figure 5.7.** Amphiesmal alveoli are large irregular shaped structures - not regularly arranged as in the ciliate cortex. Close examination of the amphiesma shows that a large alveolus is swollen in places (a) and that between these swollen pockets the alveolus is very much compressed. Arrows indicate two apposed membranes of the alveolus and the outer plasma membrane. ch = chromosome, tr = trichocyst, m = mitochondrion. Scale bar = 0.5μm.


fv
cn
fv
ch

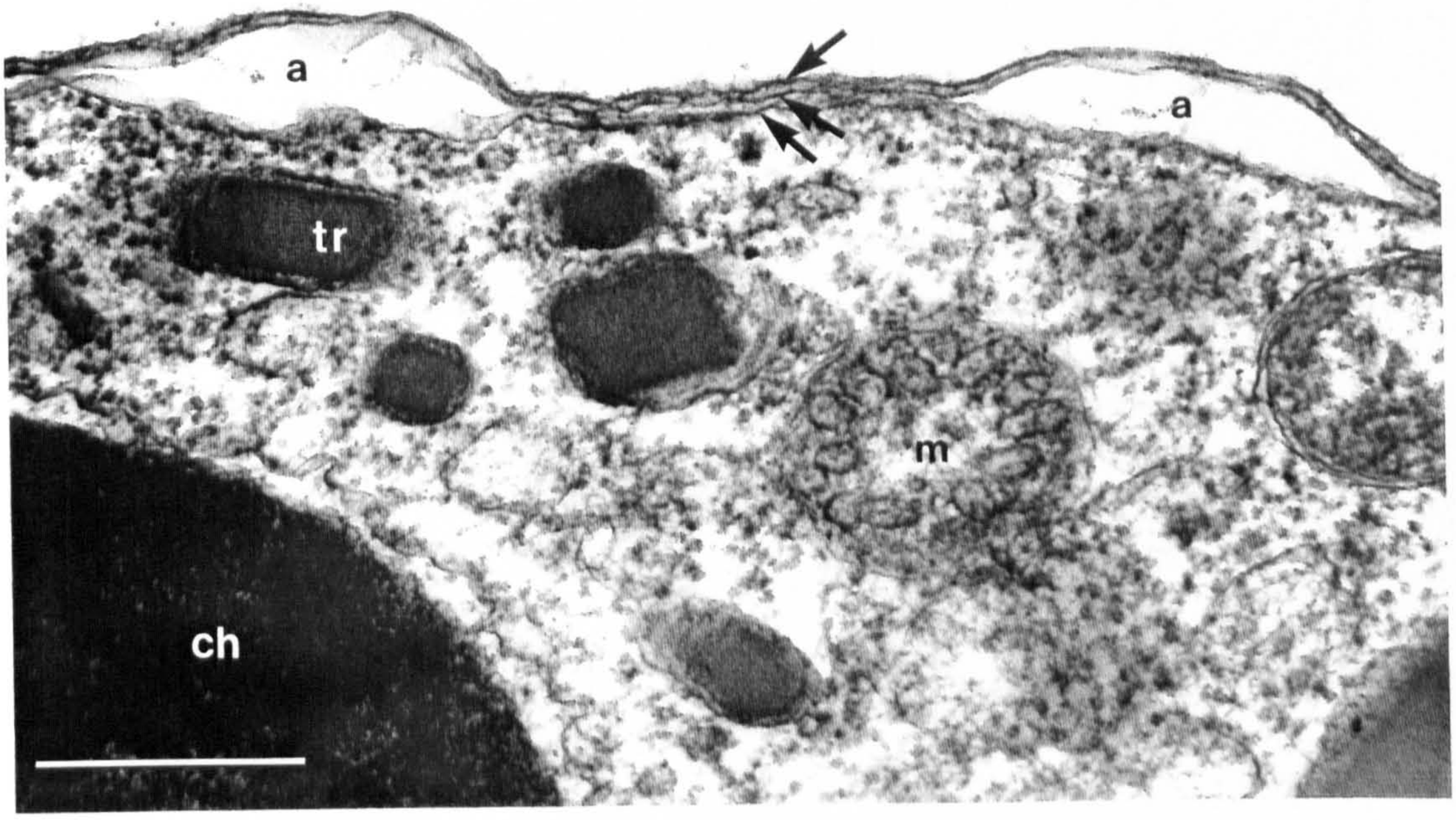
a
a
tr
m
ch

**Figure 5.8.** Light micrograph showing a branched syncytium attached to the outer wall of a hepatopancreatic tubule of a stage III infected lobster. No trichocysts are visible H = haemal sinus of hepatopancreas; p = parasite; T = epithelial cell of hepatopancreatic tubule. A 0.5µm thick resin section stained with toluidine blue. Scale bar = 15µm

**Figure 5.9.** Light micrograph showing many filamentous parasite syncytia (p) attached to the outside of a hepatopancreatic tubule (T). The attached syncytia contain numerous trichocysts (arrows) and caseiform organelles (co). The presence of trichocysts indicates that these attached syncytia although filamentous are sporogenic. H = haemal sinus, n = parasite nucleus. A 0.5µm thick resin section stained with toluidine blue. Scale bar =

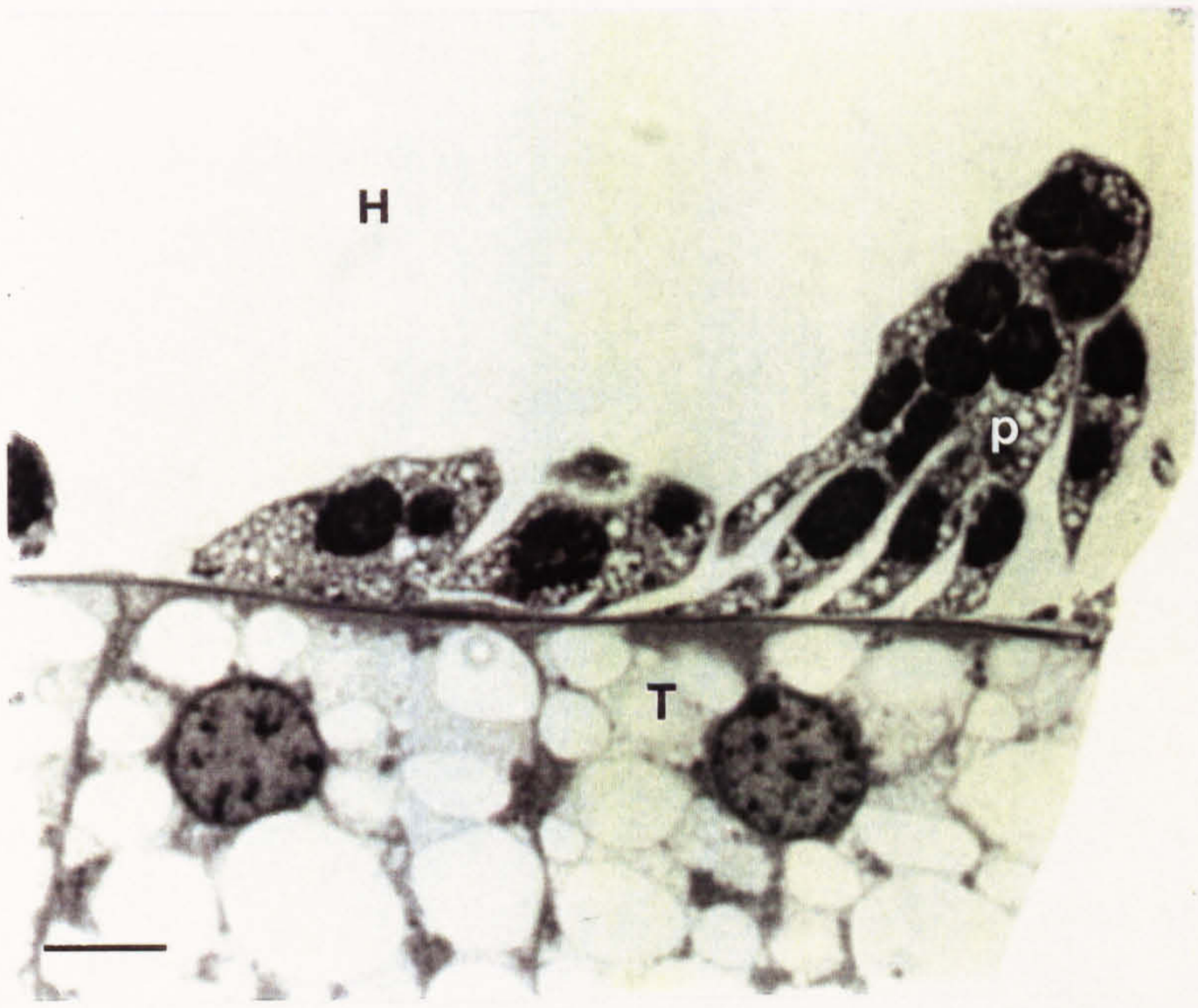
H
p
T

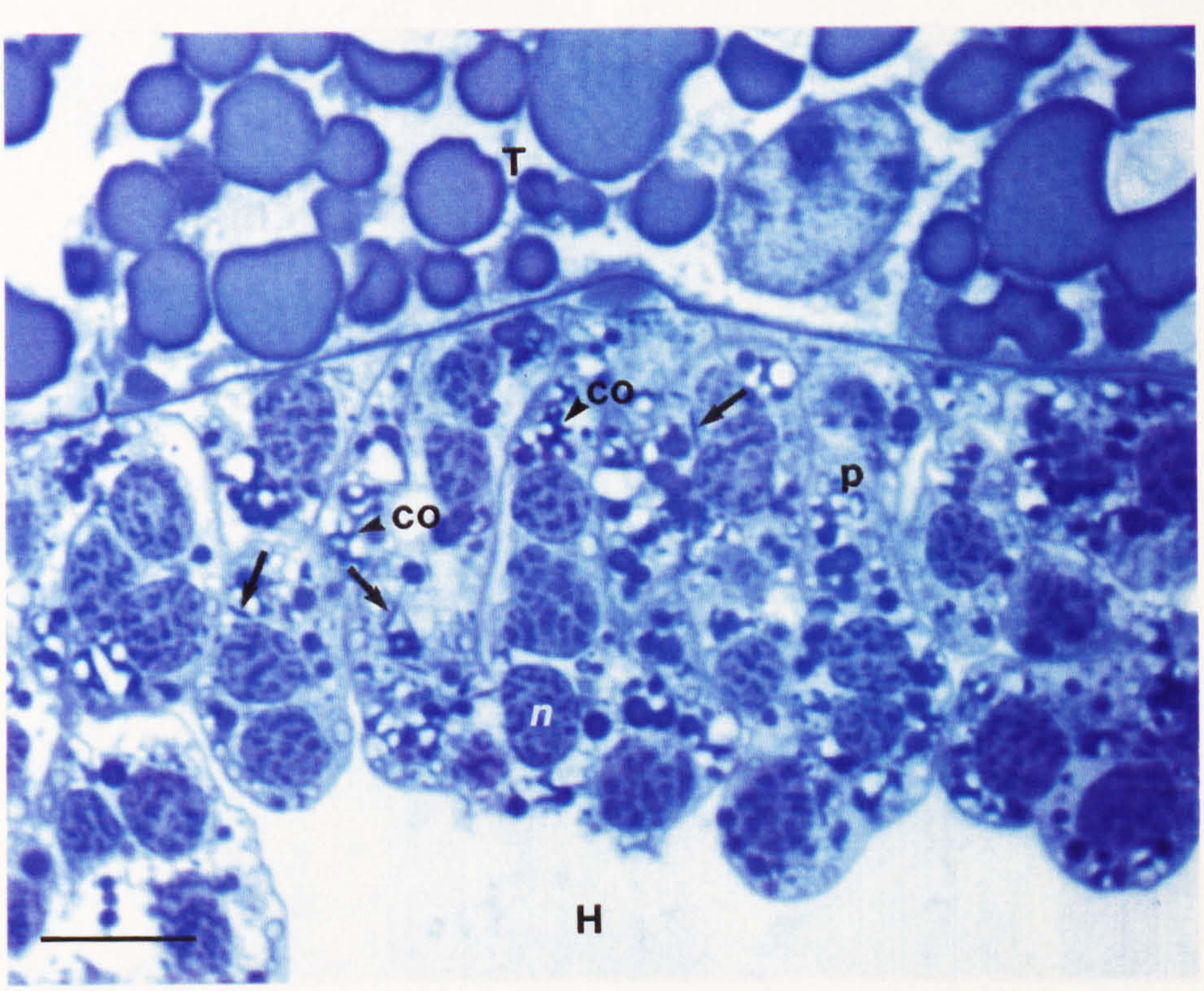
T
co
co
p
n
H

**Figure 5.10.** A light micrograph showing an arachnoid syncytium which was observed during the routine examination of a fixed tissue smear from the hepatopancreas of a lobster with a low level of infection. n = nuclei of parasite. Phase contrast. Scale bar = 50μm.

**Figure 5.11.** Light micrograph of the labyrinthal epithelium of the antennal gland of a stage III infected individual, showing attachment of filamentous parasite syncytia (p) within the haemal spaces and the presence of dinoflagellates within the lumen of the labyrinth (arrows). Unattached parasites are present within the narrower haemal spaces of the labyrinth. LE = labyrinthal epithelium; L = labyrinthal lumen. Wax section stained with haematoxylin and eosin. Scale bar = 50μm.

**Figure 5.12.** Light micrograph of the midgut wall of a stage II infected individual showing attached filamentous syncytia (p) located within the midgut sinus (MS). Trichocysts and inclusion organelles are not visible, suggesting that the syncytia are trophonts. M = circular muscle layer of midgut wall; BM = basement membrane; ME = midgut epithelium; HL = haemocoel, L = lumen, arrows = host haemocytes. A 0.5μm resin section stained with toluidine blue. Scale bar = 50μm.

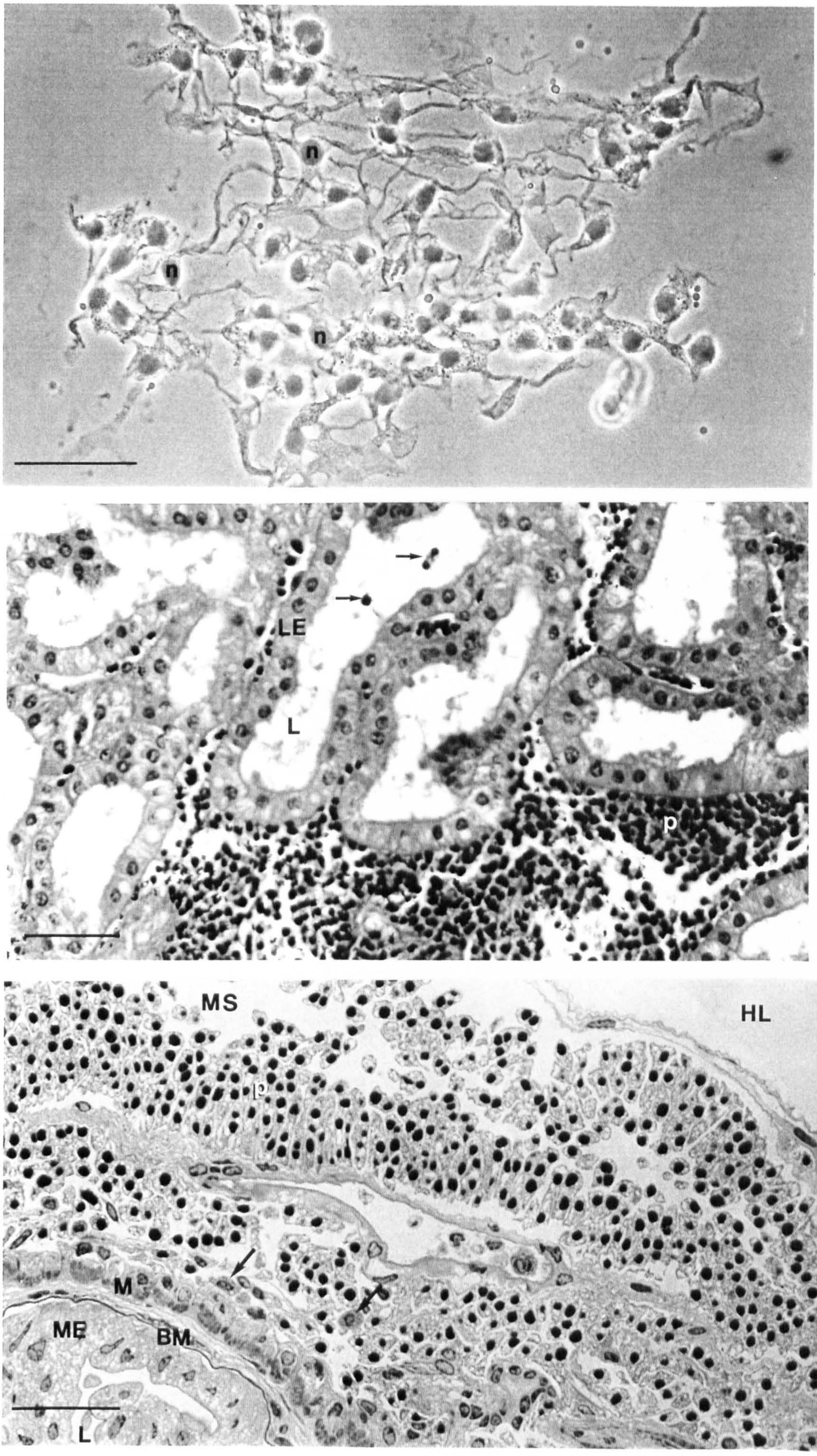
n
n
n
LE
L
p
MS
HL
p
M
ME
BM
L

**Figure 5.13.** Light micrograph of abdominal muscle of a stage II infected individual showing densely-staining arachnoid-like parasite syncytia within the muscle interstices. Parasite nuclei (n) are visible in the wider areas of the muscle interstices, and cytoplasmic threads of the syncytium (arrows) pass along the narrower regions. M = abdominal muscle fibres, N = muscle nuclei. Wax section stained with haematoxylin and eosin. Scale bar = 50μm.

**Figure 5.14.** Transmission electron micrograph showing part of a dinoflagellate syncytium attached to the sarcolemmal membrane of an abdominal muscle fibre from a stage IV infected lobster. This could be a section through a secondary sporont as trichocysts (tr) are present. m = mitochondrion of parasite, n = dinoflagellate nuclei, l = lipid droplet; SA = sarcolemma of abdominal muscle fibre, M = muscle fibre, co = caseiform organelle, arrow = amphiesmal alveolus of dinoflagellate. Scale bar = 2μm.

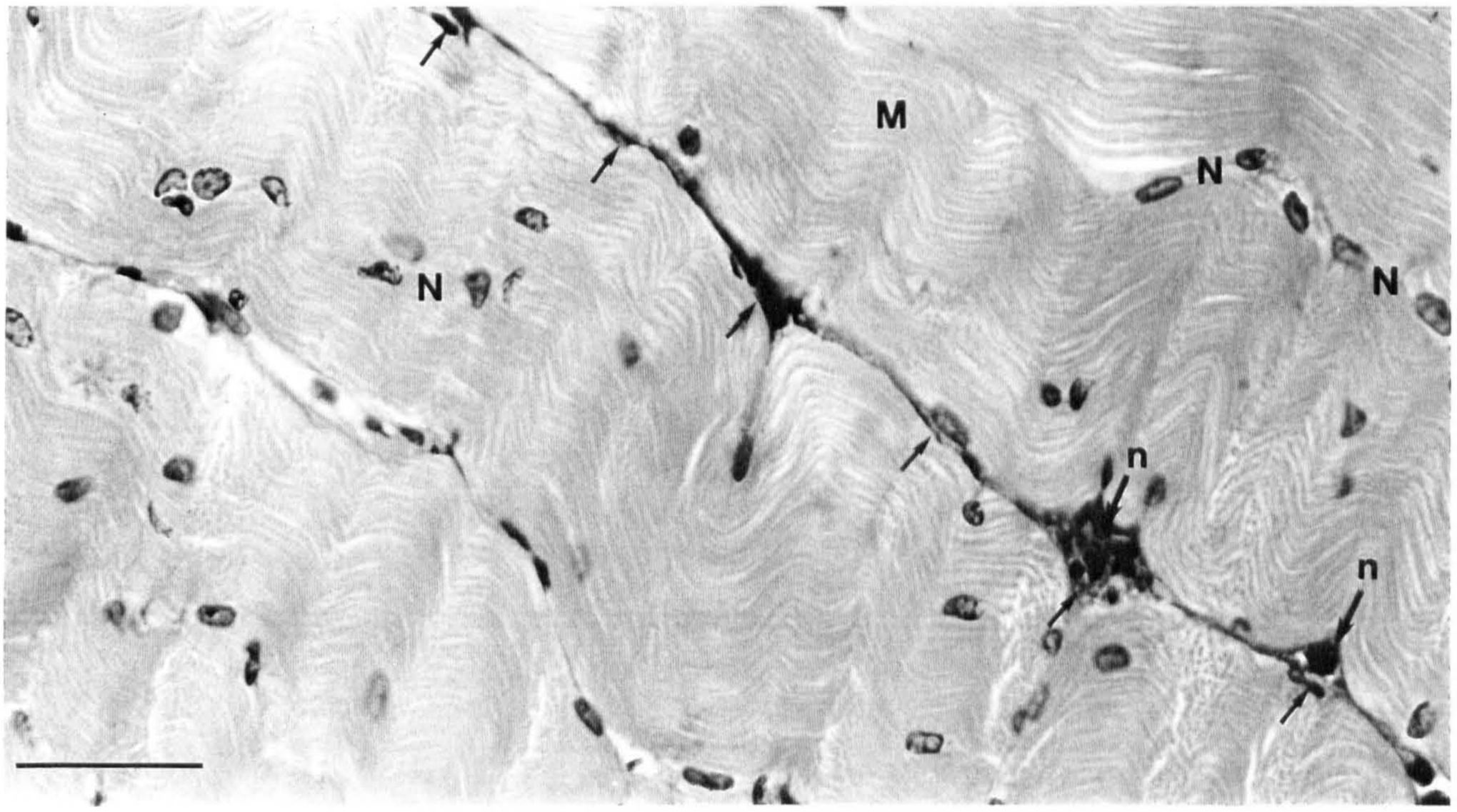
M
N
N
N
n
n

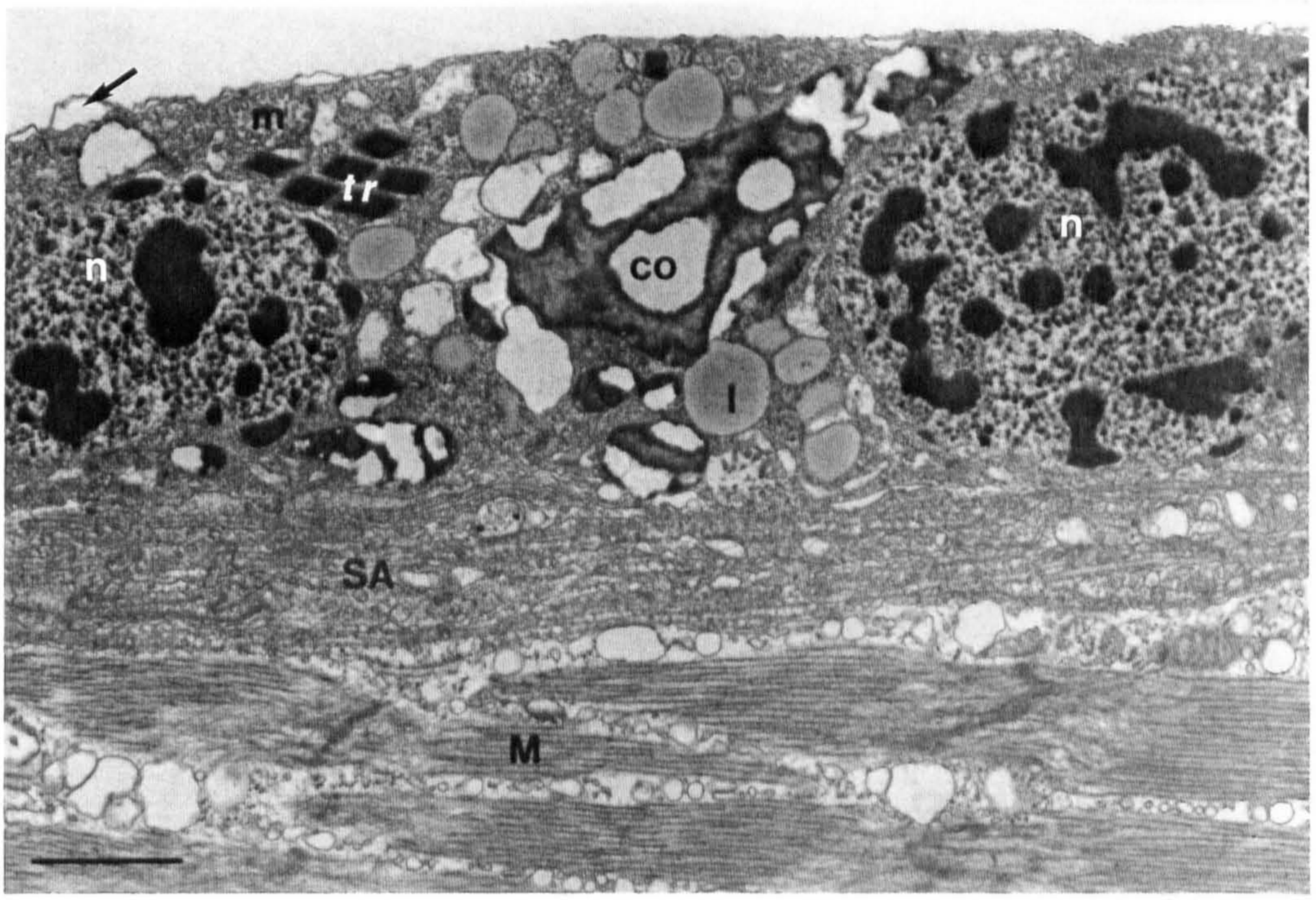
m
tr
n
co
l
n
SA
M

**Figure 5.15.** Light micrograph showing apparently active haemopoietic tissue of a stage IV infected lobster, surrounded by many uninucleate and multinucleate dinoflagellates (p). NO = haemopoietic node, ST = probable stem cell, MF = mitotic figure of host cell, D = differentiating cells, arrow = host haemocyte. A 0.5µm resin section stained with toluidine blue. Scale bar = 50µm

**Figure 5.16.** Light micrograph of the myocardium of the heart of a stage II infected individual, showing the presence of both filamentous syncytia attached to myocardial muscle within the lumen and arachnoid syncytia between the muscles. L = lumen of heart, M = myocardial muscle, p = tightly packed filamentous dinoflagellate syncytia, arrows = arachnoid-like dinoflagellate syncytia, N = myocardial nuclei, CT = connective tissue. Wax section stained with haematoxylin and eosin. Scale bar = 50µm.

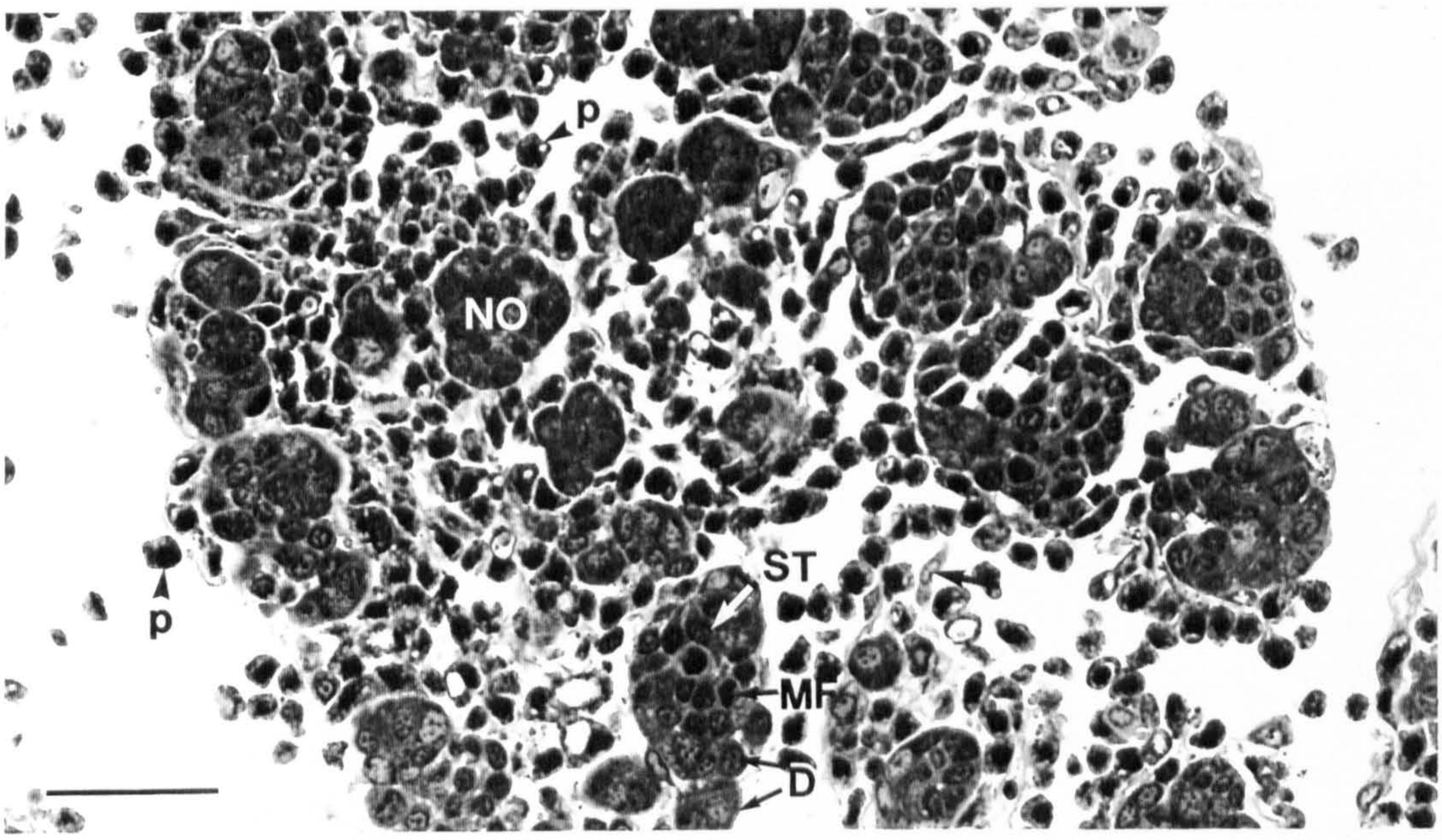
p
NO
p
ST
MF
D


N
M
L
N
CT
p

**Figure 5.17.** A transmission electron micrograph showing part of an arachnoid-like syncytium located within the myocardial muscle. The parasite (p) is stained darker than the surrounding host tissue, the dark material arrowed may represent ramifying parasite cytoplasmic threads connecting nucleated parts of the syncytium. n = nucleus of parasite, l = lipid droplet, v = large vesicles, a = amphiesmal alveolus of parasite, M = myocardial muscle. Scale bar = 5μm.

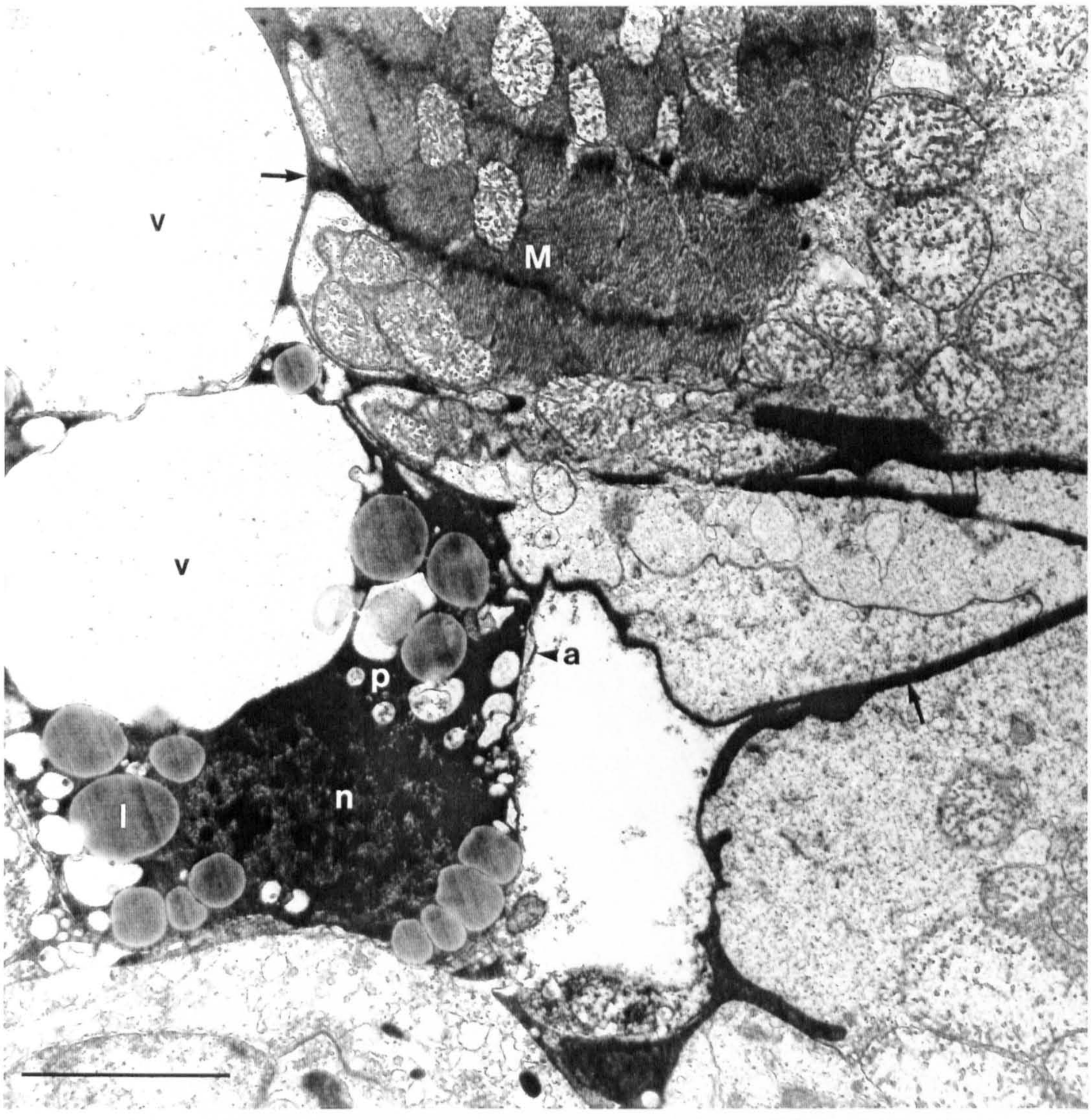
v
M
v
a
p
n
l

**Figure 5.18** Light micrograph showing detail of the labyrinthal epithelium of antennal gland from a stage IV infected lobster. The flagella (f) indicate the presence of biflagellate spores of the parasite within the haemal spaces. L = labyrinthal lumen; H = haemal spaces of labyrinth; p = biflagellate spores of the parasite; LE = epithelial cells of the labyrinth. A 0.5μm resin section stained with toluidine blue. Brightfield. Scale bar = 10μm.

**Figure 5.19** A transmission electron micrograph of an early macrospore circulating in the haemolymph of a stage IV infected lobster. f = flagellum, n = nucleus, ch = condensed chromosome, fv = flagellar hair vesicle, tr = trichocysts, m = mitochondrion, l = lipid droplet. Scale bar = 2μm.

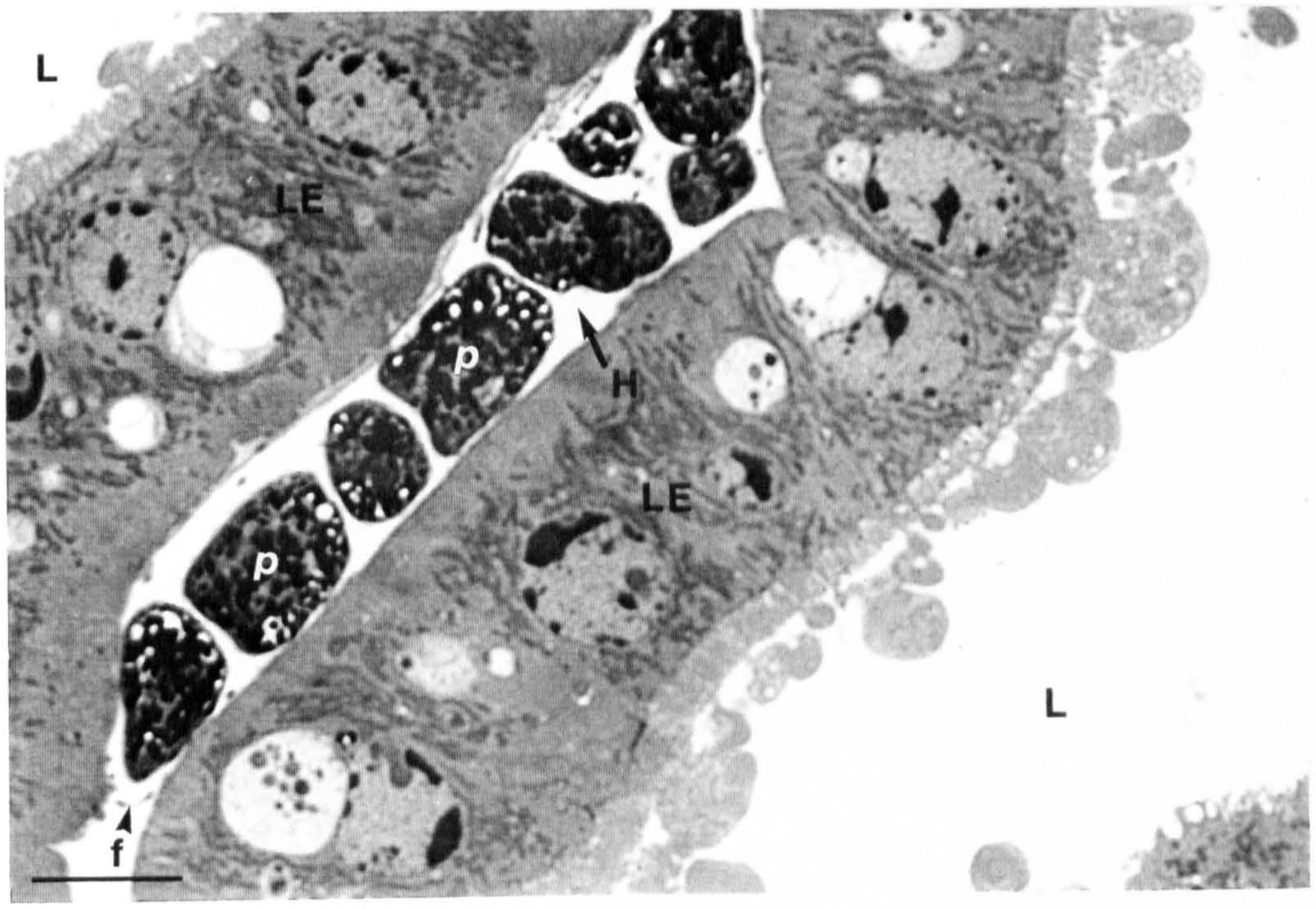
L
LE
p
H
LE
p
L
f

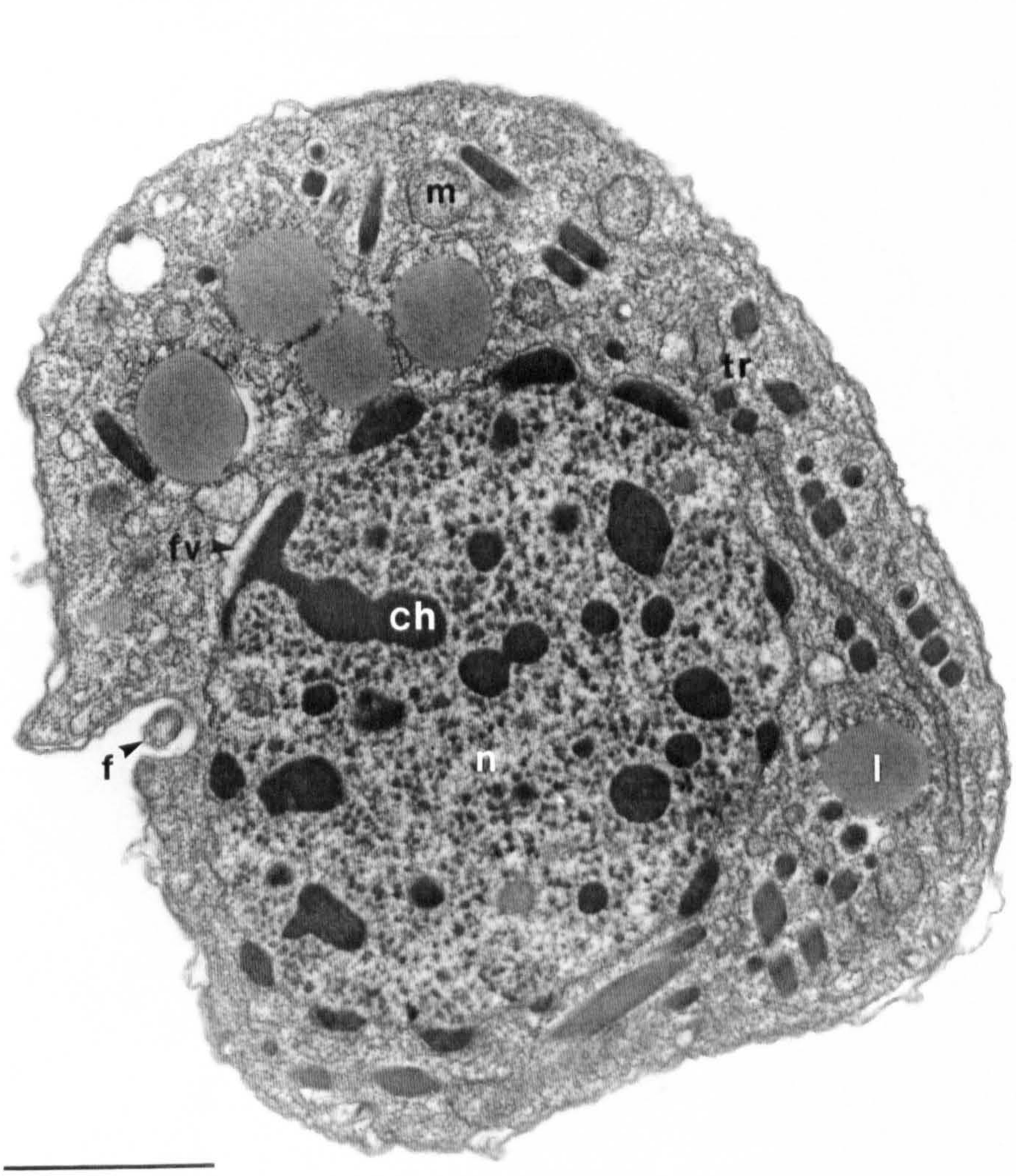
m
tr
fv
ch
f
n
l

**Figure 5.20.** Transmission electron micrographs of circulating macrospores in the haemolymph of a stage IV infected lobster.

**a)** A transverse section through a circulating macrospore showing the two flagella (f) in grooves separated by a ridge. The arrow points to the lateral 'keel' which is visible in some macrospores. v = empty vesicles, a = amphiesmal alveoli, T = tubule of hepatopancreas. Scale bar = 2μm.

**b)** A section through two circulating macrospores showing the presence of numerous caseiform organelles (co). tr = trichocysts, a = amphiesmal alveoli. Scale bar = 2μm.

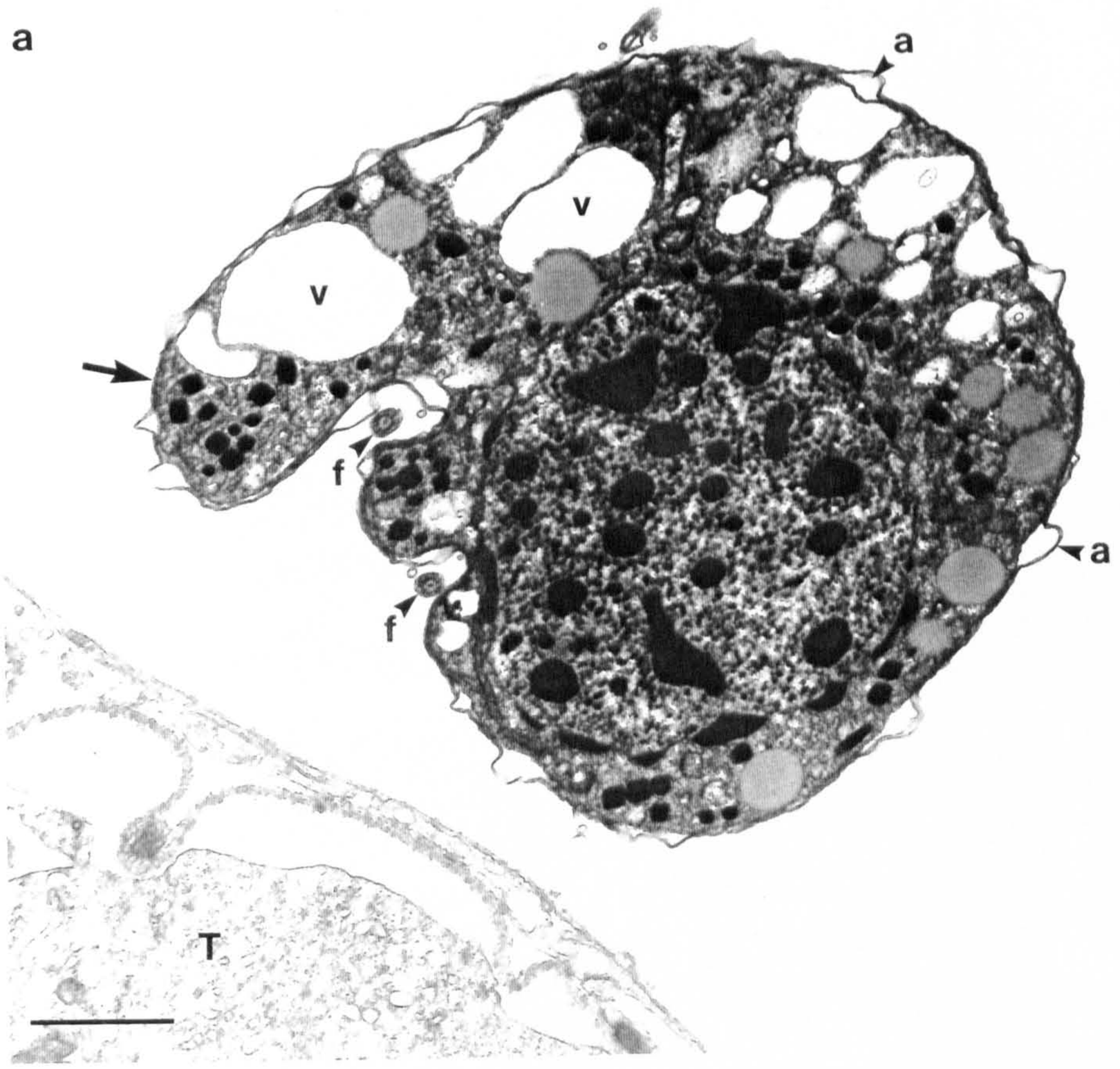
a
a
v
v
f
f
a
T
b
co
co
co
tr
a
a

**Figure 5.21.** Light micrographs showing specificity of immunolabelling of *Hematodinium* with polyclonal antiserum in a fixed *N. norvegicus* haemolymph smear.

**a)** Under phase contrast illumination.

**b)** Under UV epifluoresence, showing DAPI nuclear counter stain.

**c)** Under UV epifluorescence, showing fluorescent labelling of *Hematodinium* whilst haemocytes remain unlabelled. Arrows = *Hematodinium* parasites. Scale bars = 50μm.

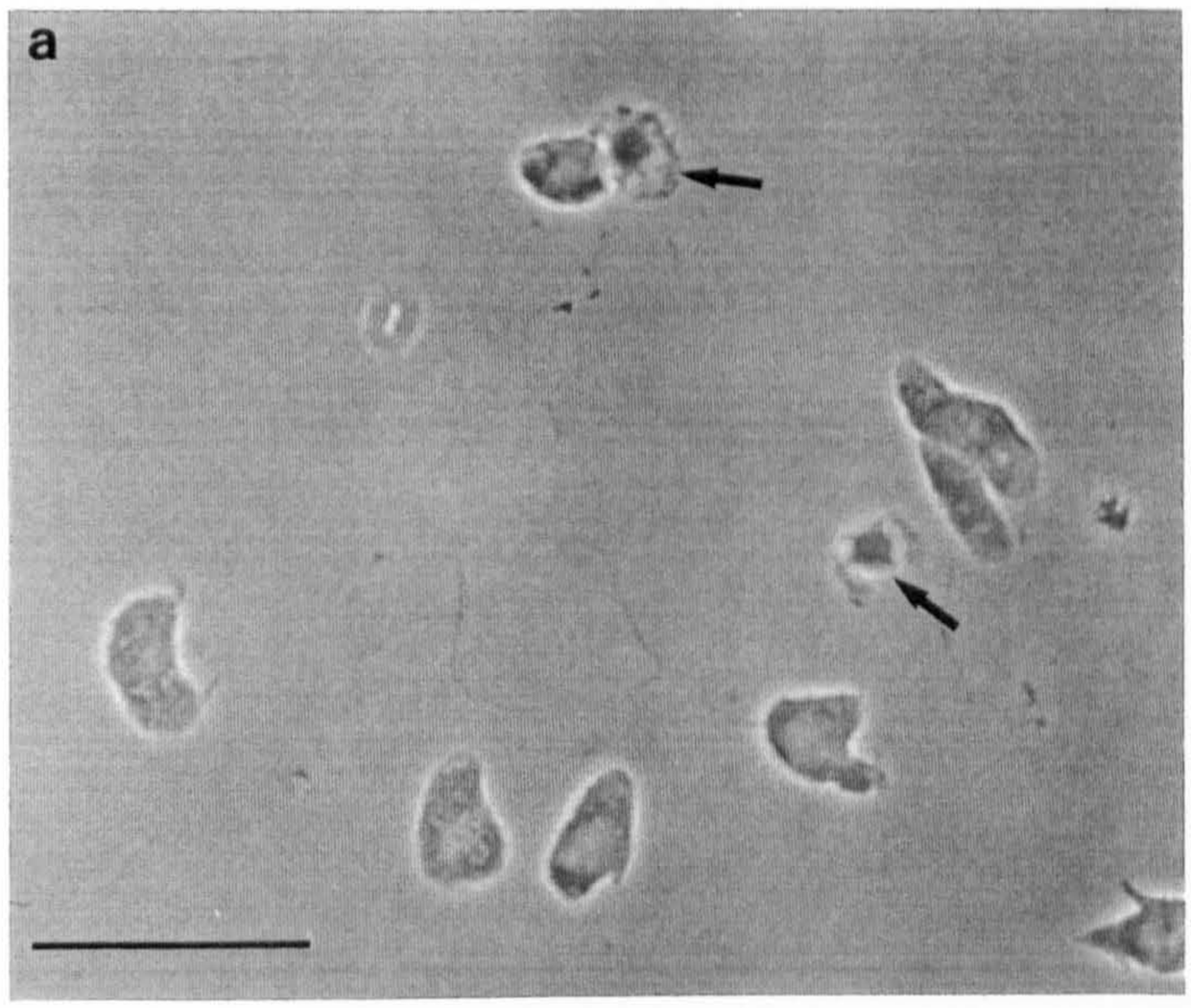
a

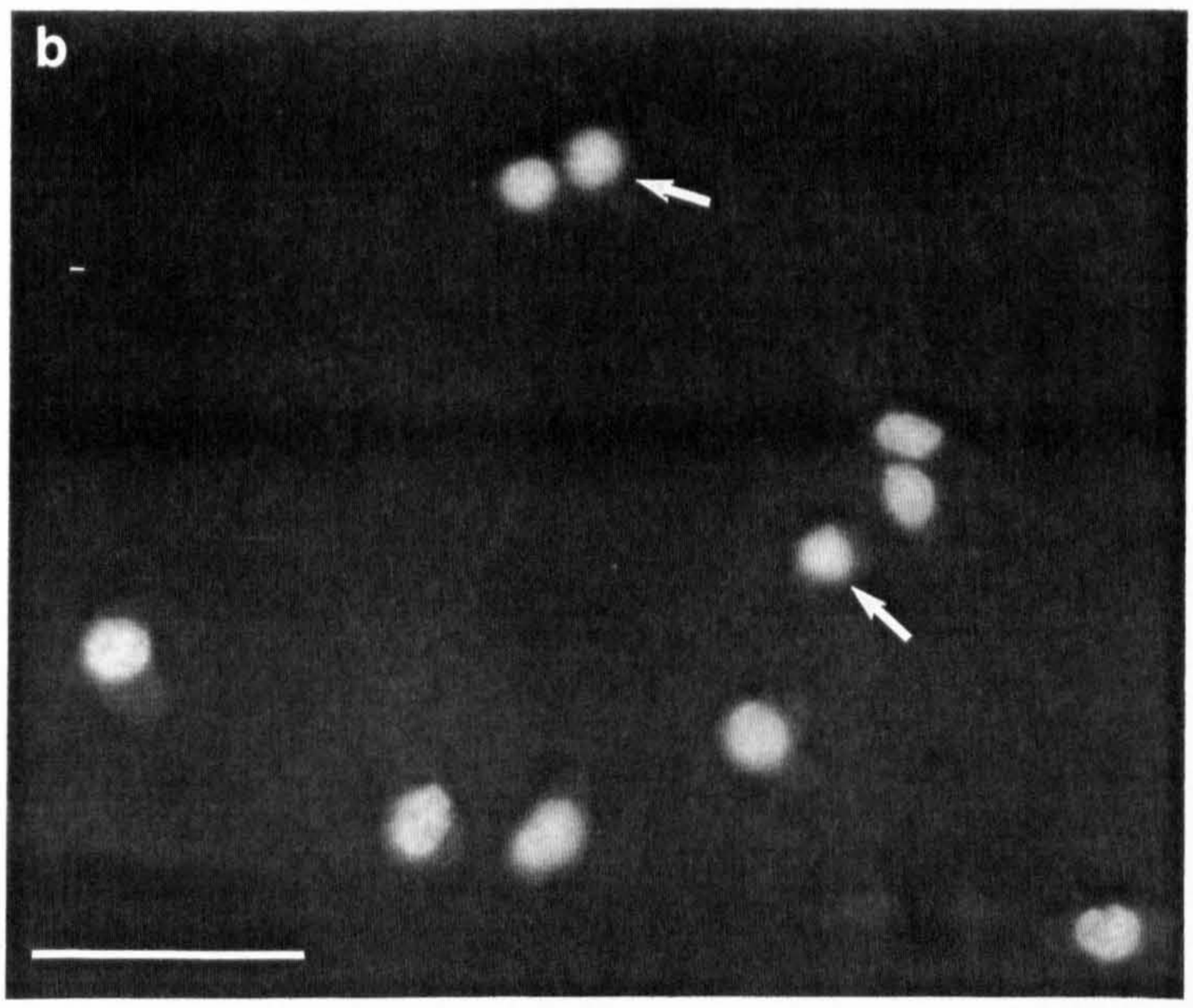
b

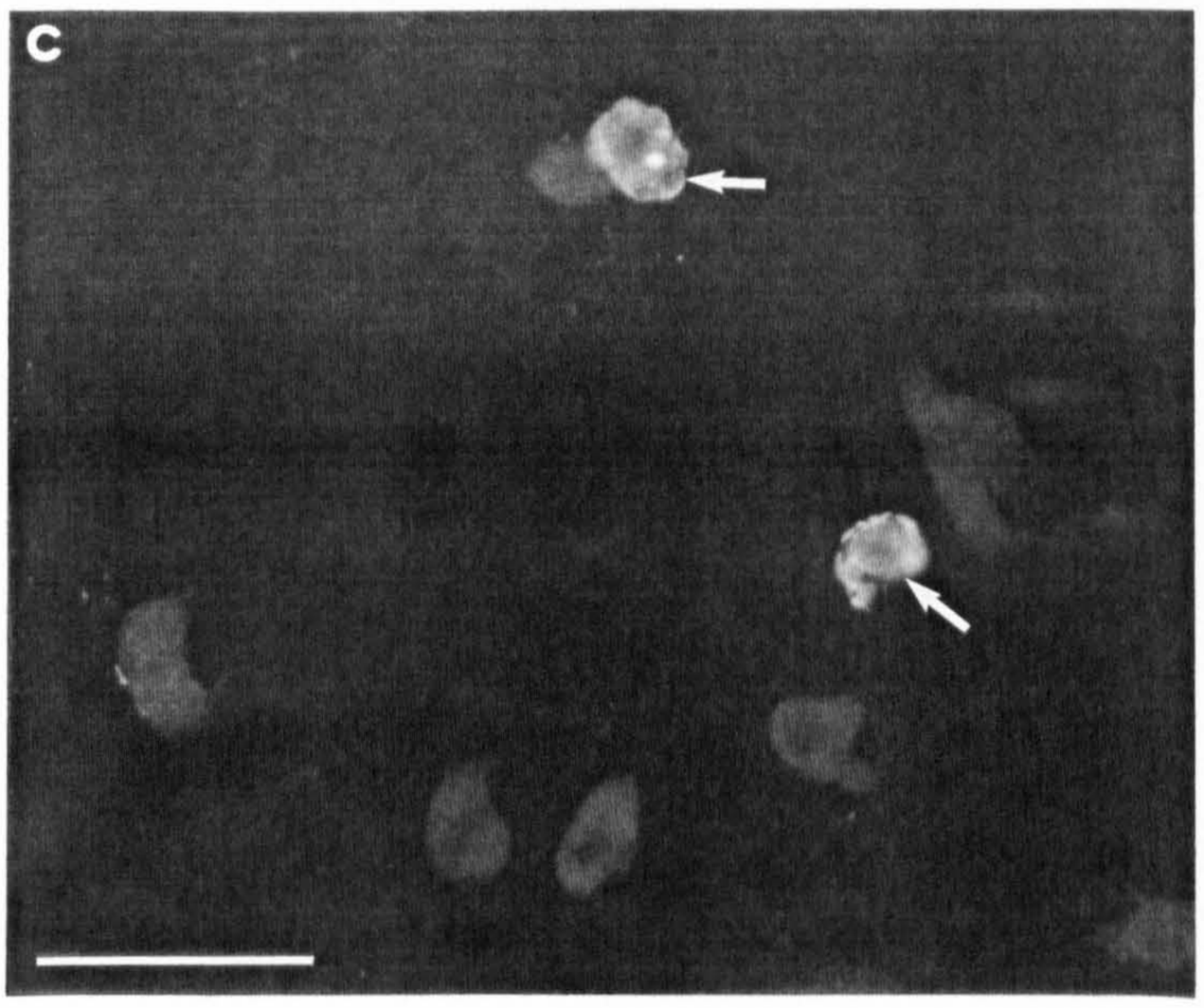
c

**Figure 5.22.** Light micrograph showing a fluorescently labelled uninucleate *Hematodinium* parasite (arrow) next to unlabelled abdominal muscle (M). Indirect fluorescent antibody technique. UV epifluorescence. Scale bar = 50µm.

**Figure 5.23.** Light micrograph showing fluorescently labelled multinucleate parasite arachnoid syncytium in a fixed hepatopancreas smear. Indirect fluorescent antibody technique. n = parasite nuclei. UV epifluorescence. Scale bar = 50µm.

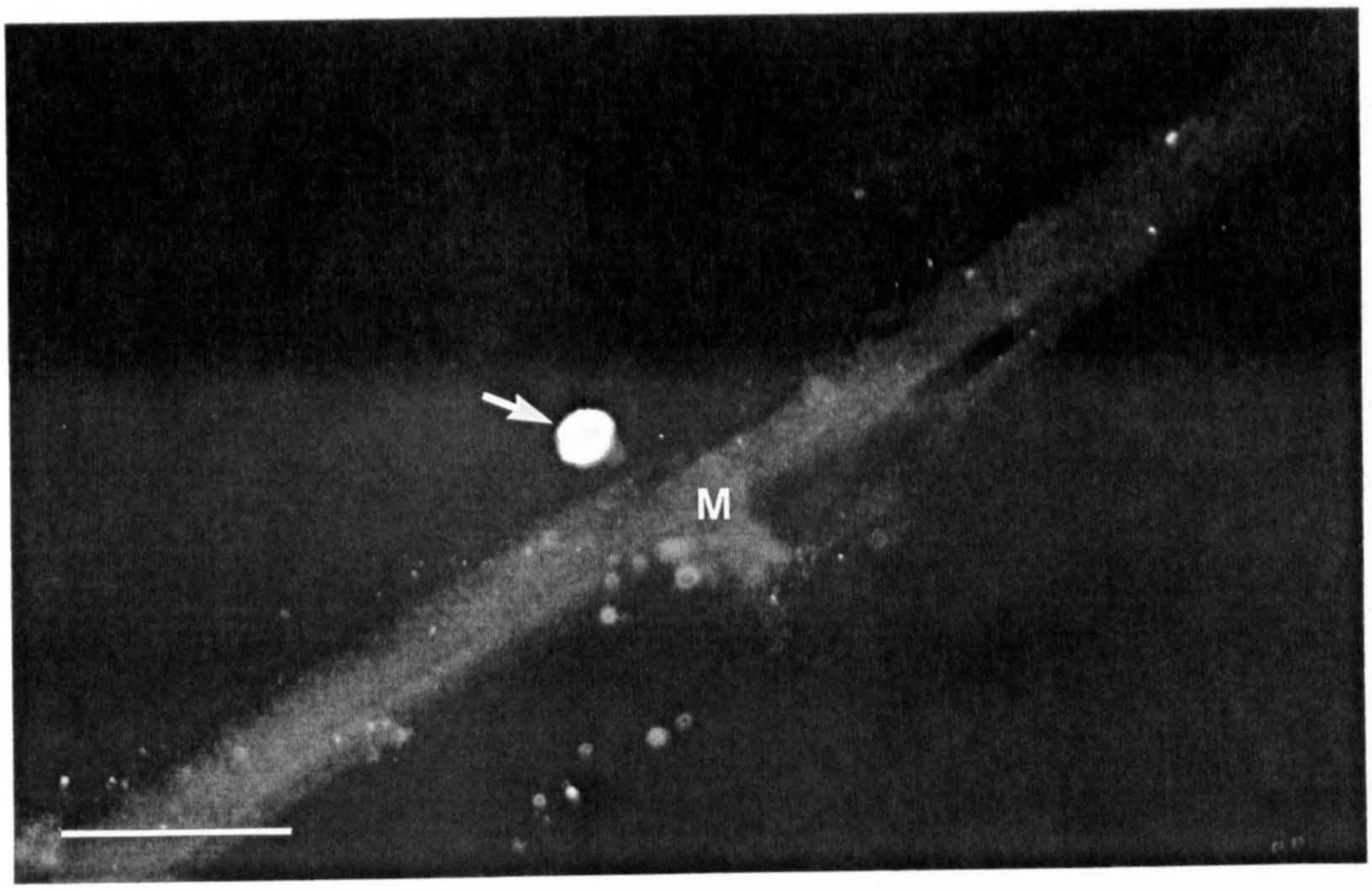
M

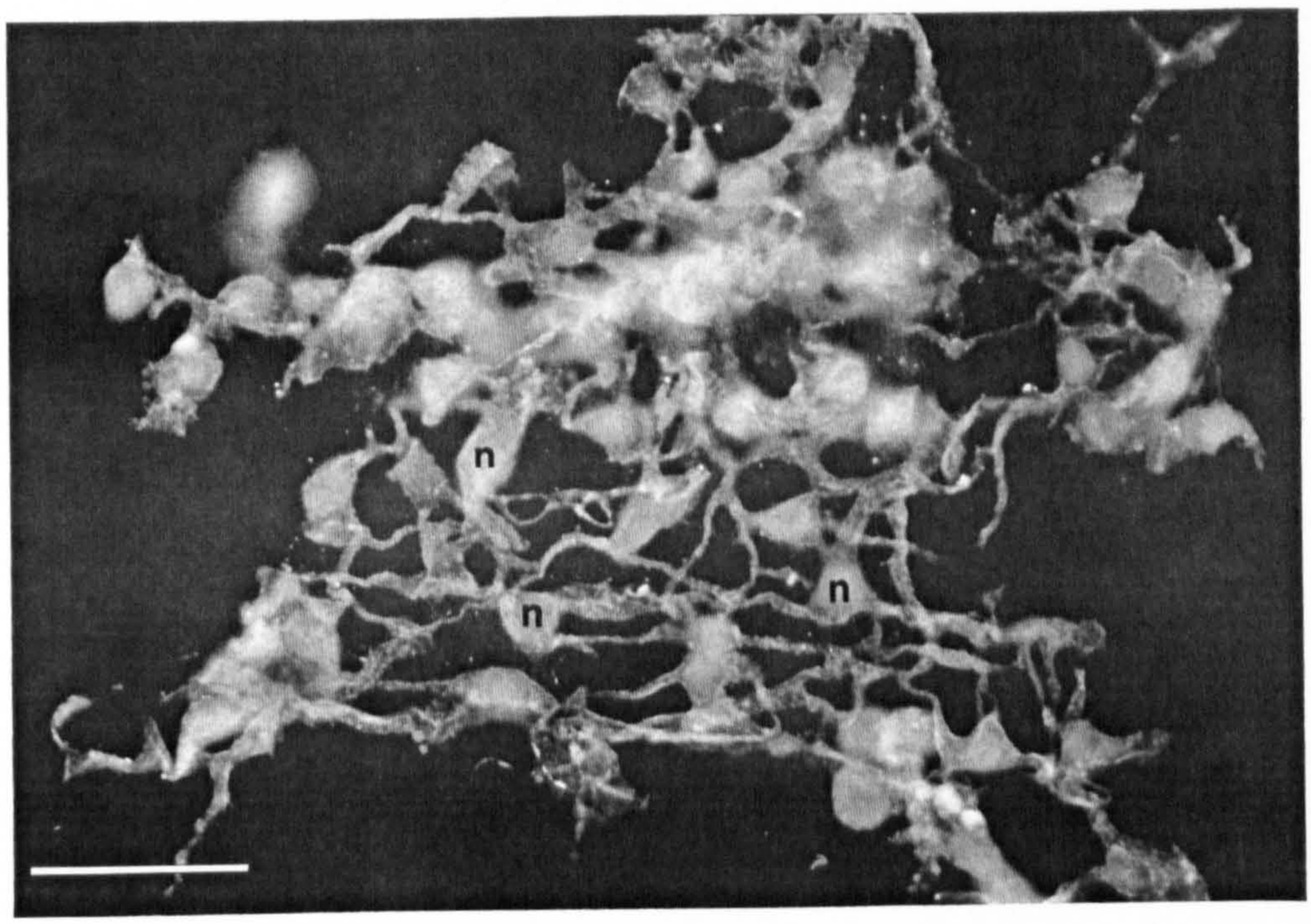
n
n
n

**Figures 5.24 - 5.26.** Haemolymph cell counts performed on infected lobsters No.4 (Figure 5.24), No.8 (Figure 5.25) and No.15 (Figure 5.26) from Tables 5.3 and 5.4. In figure 5.26 the parasites were present as dinospores only at the final count after death of the host.

Figure 5.24

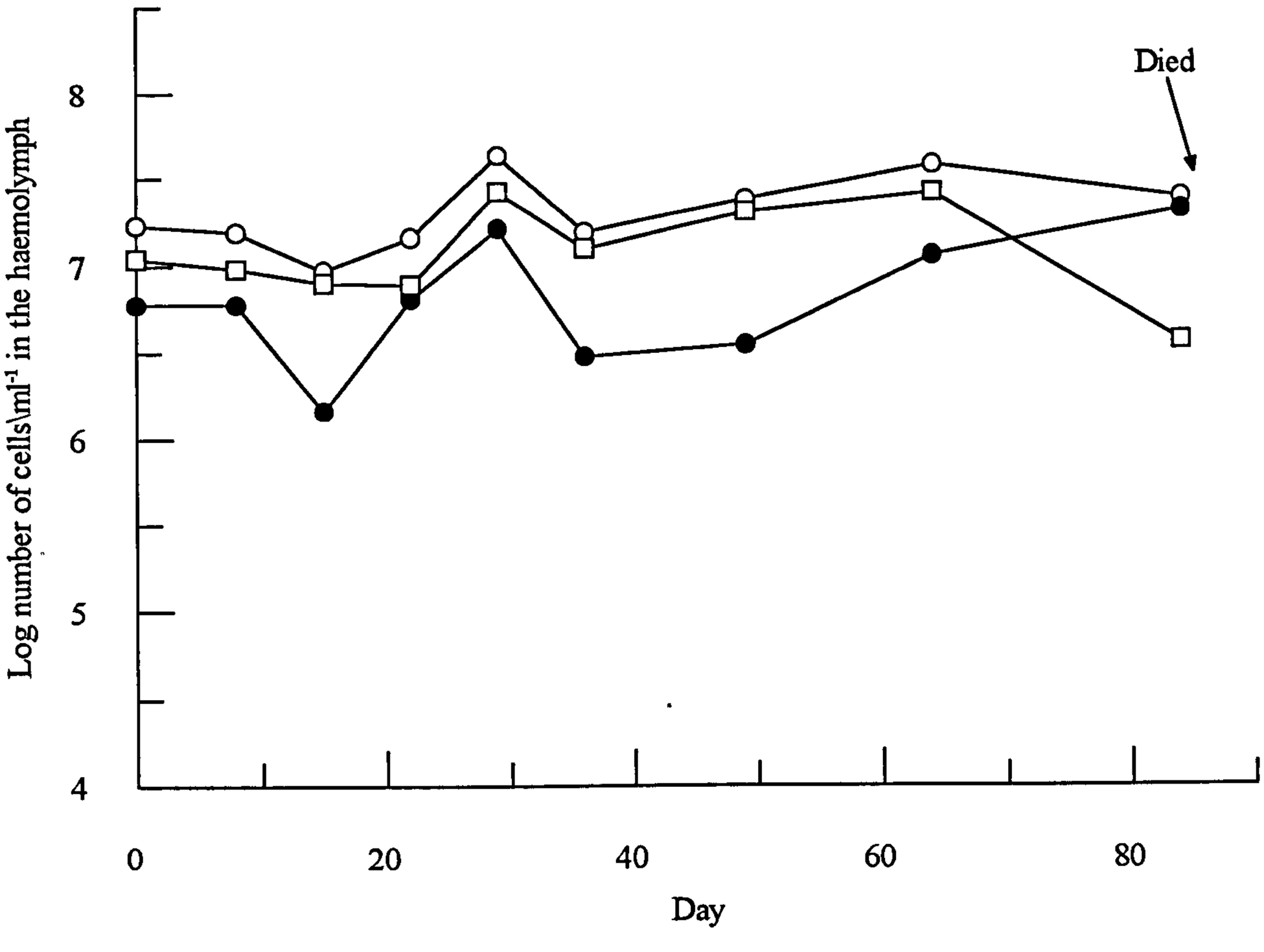


Figure 5.25

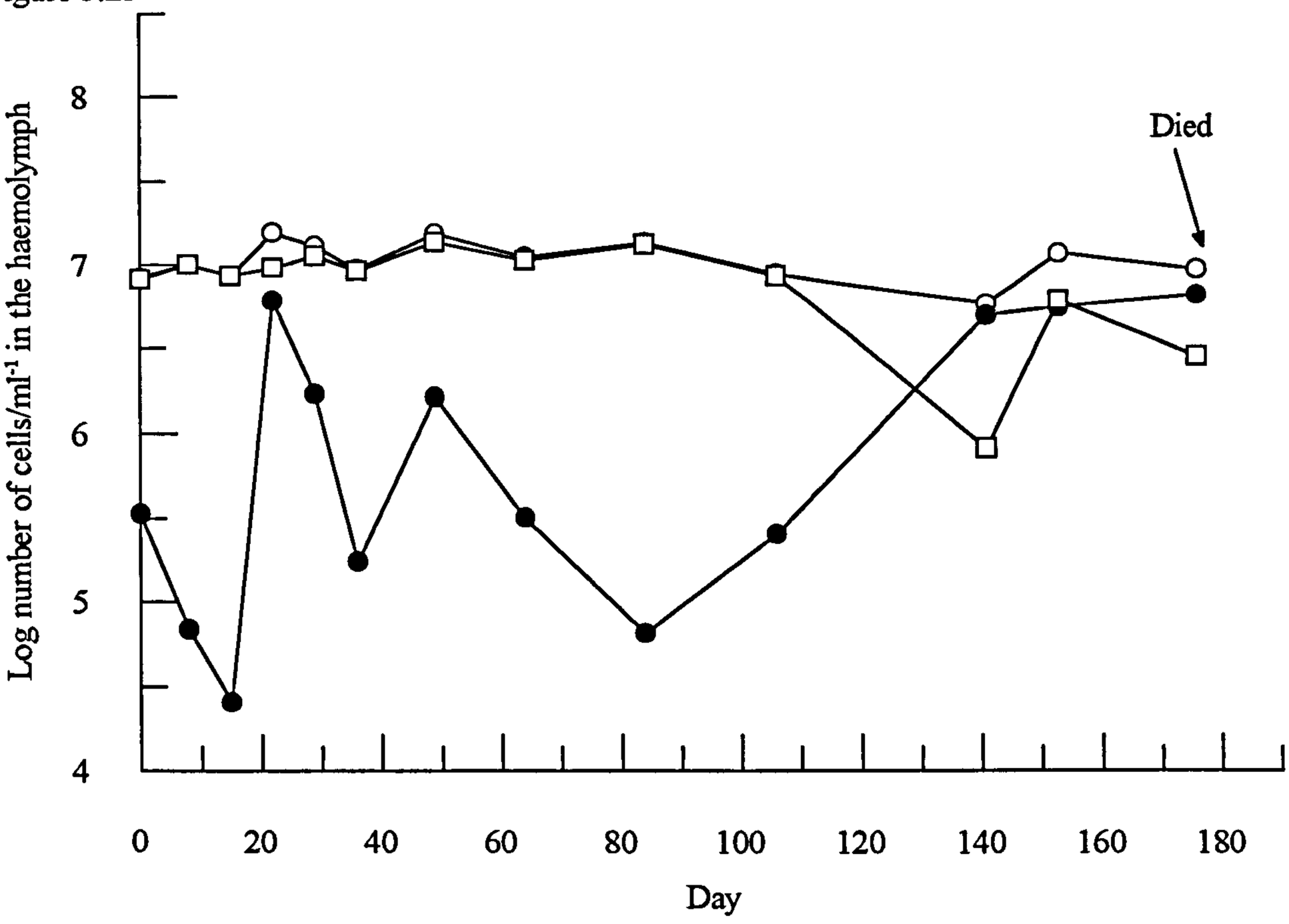

**Figure 5.27.** Haemolymph cell counts performed on an uninfected lobster. This shows that small fluctuations in the numbers of circulating haemocytes occur in healthy lobsters.

Figure 5.26

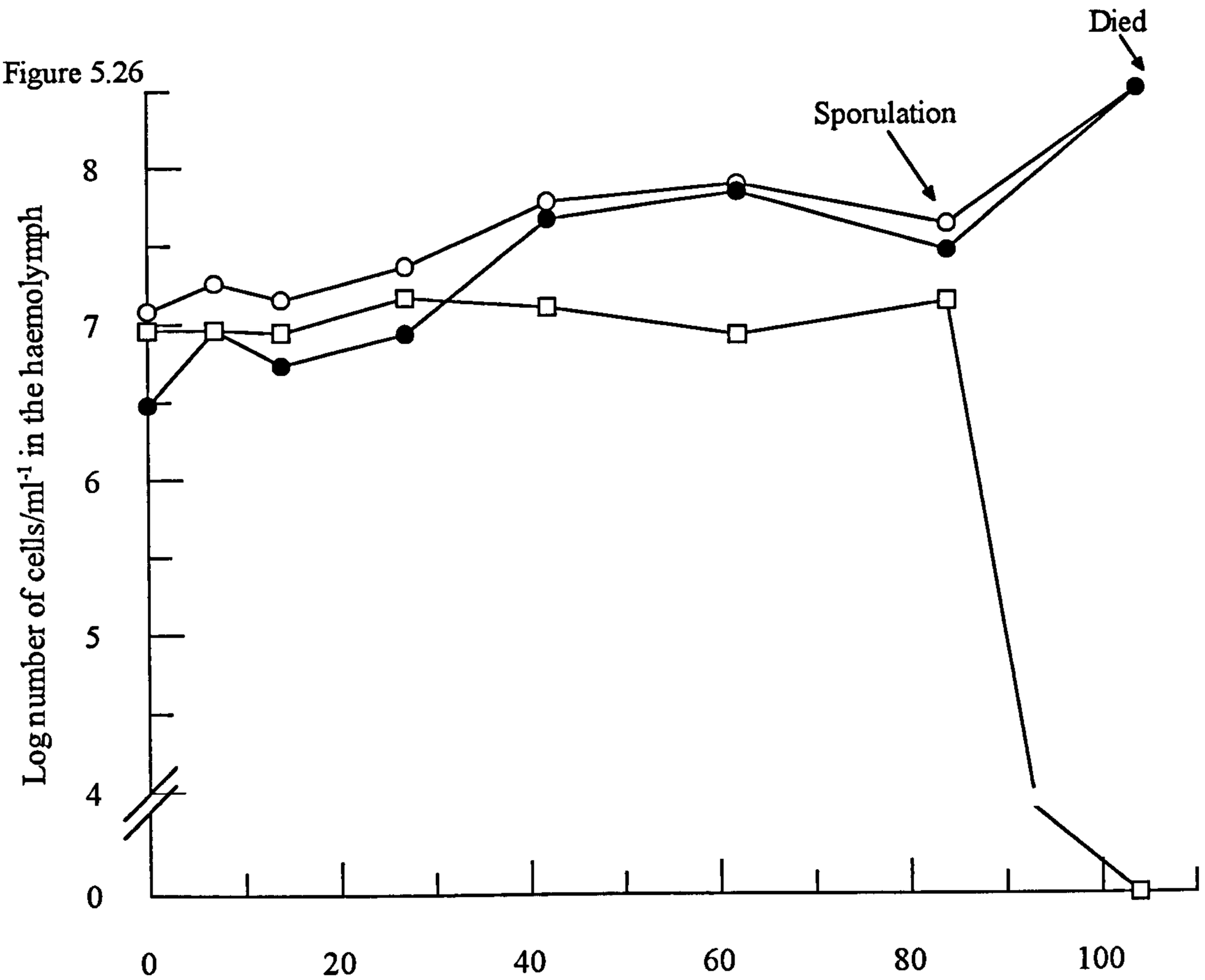


Figure 5.27

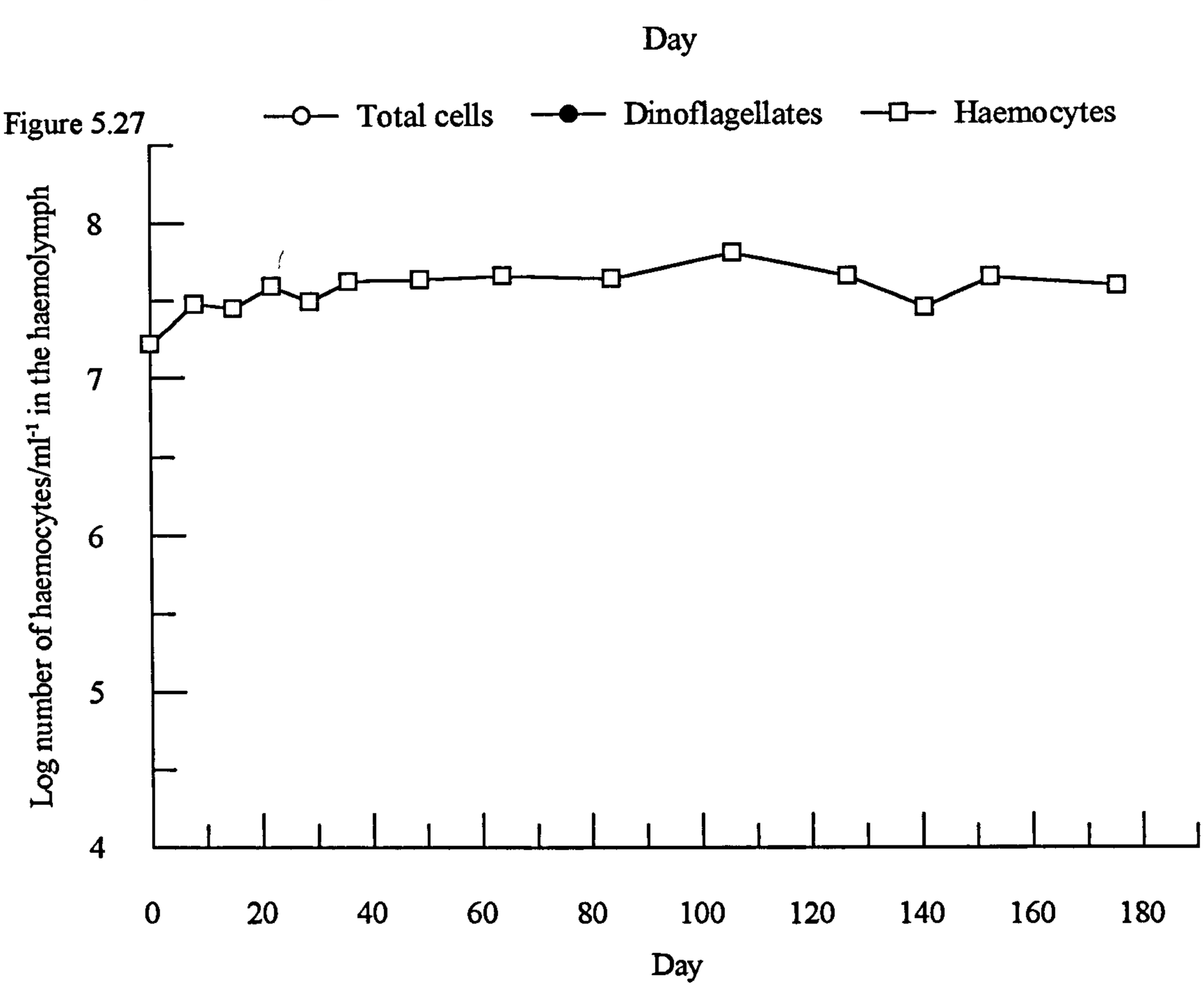

**Figure 5.28.** A still picture taken from a videotape recording of the release of dinospores from an infected lobster. The dinospores are released as white clouds in the exhalant gill currents (arrow).

**Figure 5.29.** A still picture taken from a videotape recording of the release of dinospores from an infected lobster. A stream of dinospores are being released from the ventral side of a lobster where a previously damaged pleopod had become melanized (arrow). The released dinospores have formed a sediment on the bottom of the tank.

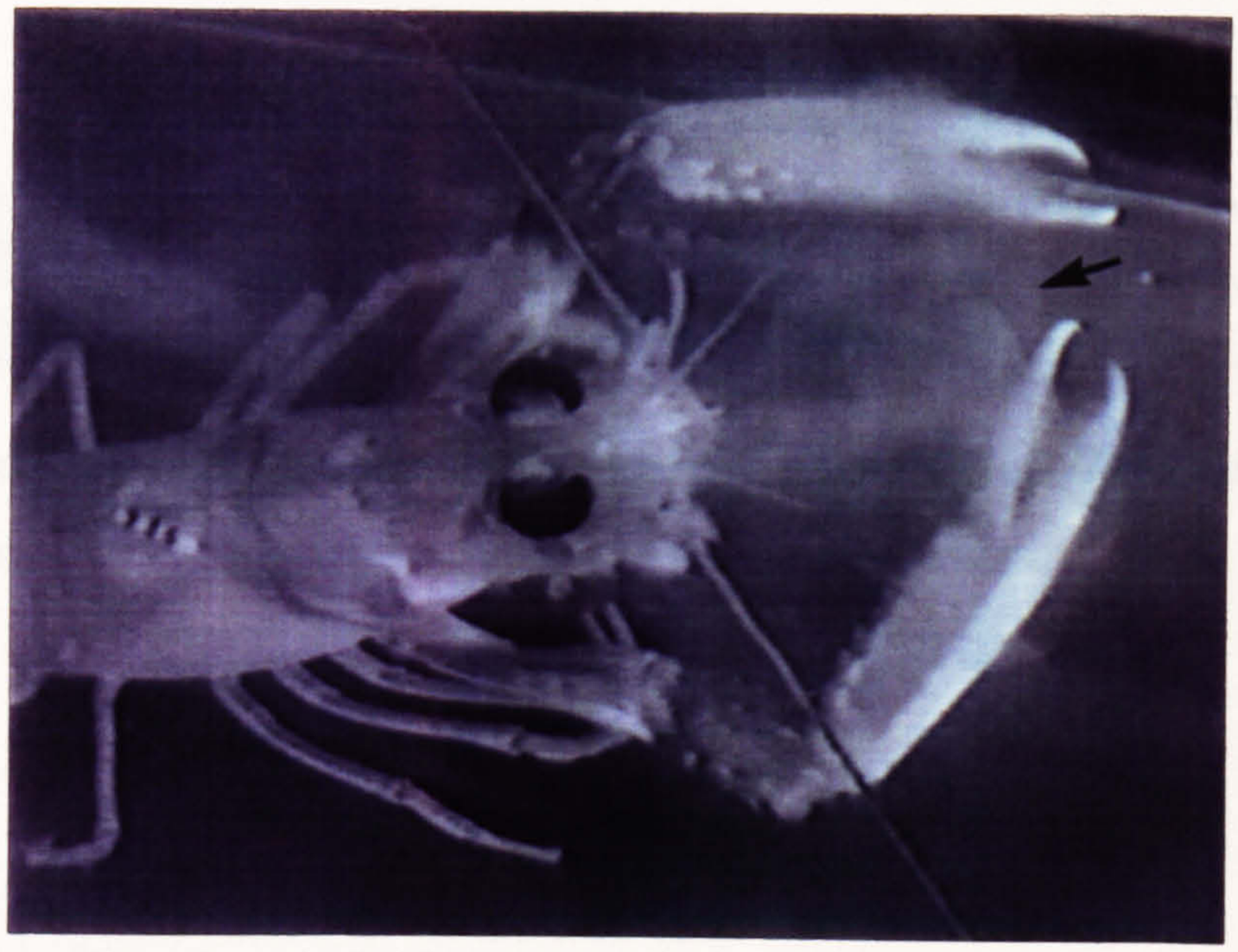

| | Diagnostic Method | | |
|---|---|---|---|
| | **Pleopod** | **Leishman's Stain** | **Immunostaining** |
| **Number of Animals/165** | 25 | 34 | 37 |
| **% Prevalence** | 15.1 | 20.6 | 22.4 |

**Table 5.1.** Comparison of the accuracy of pleopod diagnosis of *Hematodinium* infection with diagnosis made by two methods of haemolymph staining.

| Month | Number infected: Haemolymph and Tissues | Tissues | Total infected /sample size | Infected Tissues |
|---|---|---|---|---|
| January | 3 | 2 | 5/11 | Muscle,midgut,Hp |
| February | 2 | 2 | 4/30 | Heart |
| March | 0 | 1 | 1/12 | Midgut |
| August | 2 | 2 | 4/15 | Hp |
| October | 1 | 2 | 3/15 | Muscle |
| November | 2 | 2 | 4/15 | Midgut,Hp |

**Table 5.2.** Results of fluorescent antibody survey for prepatent *Hematodinium* sp. infection of *Nephrops norvegicus* between January and November 1994. (Hp = hepatopancreas).

| Lobster number | Date caught | Sex | C L (mm) | Initial % of total cells being parasite | Date of death | Number of days observed | Final infection status | Final % of total cells being parasite |
|---|---|---|---|---|---|---|---|---|
| 1 | 11/10/94 | M | 24 | 0.5[1] | 23/2/95 | 135 | N | 0 |
| 2 | 22/11/94 | F | 24 | 1.5 | 25/1/95 | 64 | II | 72 |
| 3 | 22/11/94 | F | 26 | 4.7 | 13/3/95 | 111 | I | 23 |
| 4 | 22/11/94 | F | 27 | 9.9 | 10/4/95 | 139 | II | 85 |
| 5 | 22/11/94 | F | 26 | v.low[2] | after 20/7/95 | 240 | ND | 0 |
| 6 | 22/11/94 | F | 28 | 5 | 24/1/95 | 63 | I | 66 |
| 7 | 11/10/94 | M | 24 | 0.9 | 29/3/95 | 169 | I | 14 (17/2/95) |
| 8 | 22/11/94 | F | 26 | 0.7 | 20/7/95[3] | 240 | I | 70 |
| 9 | 22/11/94 | M | 25 | 0.4 | 20/2/95[4] | 90 | I | 4 (3/2/95) |
| 10 | 22/11/94 | F | 24 | 1.4 | 24/3/95 | 122 | n.a[5] | 29 (17/2/95) |
| 11 | 22/11/94 | M | 29 | 2.7 | 1/5/95 | 160 | I | 95 |
| 12 | 22/11/94 | F | 23 | 0.7 | 10/2/95 | 80 | II | 63 |
| 13 | 22/11/94 | F | 24 | 0.7 | 24/2/95 | 94 | I | 37 (3/2/95) |
| 14 | 22/11/94 | M | 25 | 8.2 | 29/3/95[6] | 127 | I | 86 |

**Table 5.3.** Summary of infection progress data obtained from lobsters trawl caught during the autumn 1994. All lobsters were originally diagnosed by pleopod as being uninfected; immunostaining of haemolymph smears revealed a sub-patent infection. Lobsters were observed daily. Haemolymph samples were taken for immunostaining and pleopod diagnosis was carried out soon after death. If this was not possible soon after death the previous parasite count, infection status and (date) is given. ND = infection not detected. CL = carapace length.

[1] no parasite detected on 12/11/94, first detected on subsequent screening of 11/1/95

[2] only 1 parasite cell detected on whole smear, no parasites detected on 11/1/95 or thereafter. Still alive when experiment terminated on 20/7/95

[3] moulted on 19/5/95

[4] moulted on 9/2/95

[5] not available, pleopods damaged

[6] moulted on 3/3/95

| Lobster number | Date caught | Sex | C L (mm) | Initial infection status (3/2/95) | Initial % of total cells being parasite | Date of death | Number of days observed | Final infection status | Final % of total cells being parasite |
|---|---|---|---|---|---|---|---|---|---|
| 15 | 1/95 | F | 27 | I | 25 | 18/5/95 | 104 | IV | 100[1] |
| 16 | 1/95 | F | 28 | ND | 0 | -[2] | 167 | ND | 0 |
| 17 | 1/95 | M | 37 | I | 8 | 9/3/95 | 34 | I | 8.2 (3/2/95) |
| 18 | 1/95 | M | 37 | II | 43 | 6/3/95 | 31 | III | 43 (3/2/95) |
| 19 | 1/95 | F | 29 | I | 9 | 13/3/95 | 38 | I | 9 (3/2/95) |
| 20 | 1/95 | M | 31 | ND | 7 | 20/2/95 | 17 | I | 7 (3/2/95) |
| 21 | 1/95 | M | 28 | ND | 2 | 18/2/95 | 15 | I | 2 (3/2/95) |
| 22 | 1/95 | F | 29 | I | 8 | 13/2/95 | 10 | I | 8 (3/2/95) |
| 23 | 1/95 | M | 33 | I | 7 | 10/2/95 | 7 | I | 7 (3/2/95) |
| 24 | 1/95 | F | 27 | ND | 0 | -[2] | 167 | ND | 0 |
| 25 | 1/95 | F | 29 | ND | 8 | 7/3/95 | 32 | I | 8 (3/2/95) |
| 26 | 1/95 | F | 27 | ND | 13 | 7/2/95 | 4 | ND | 13 |
| 27 | 1/95 | F | 28 | ND | 0 | -[2] | 167 | ND | 0 |
| 28 | 1/95 | M | 32 | ND | 29 | 6/2/95 | 3 | ND | 29 |

**Table 5.4.** Summary of infection progress data from lobsters trawl caught during January 1995. Lobsters were initially diagnosed as infected by colour only, immunostaining revealed that three were uninfected. Lobsters were observed daily. Haemolymph samples were taken for immunostaining and pleopod diagnosis was carried out soon after death where possible. If this was not possible soon after death the previous parasite count, infection status and (date) is given. CL = carapace length. ND = infection not detected.

[1] parasites were present as dinospores, but were not escaping from the host

[2] lobster still alive when experiment terminated on 20/7/95

| Lobster number | Sex | CL (mm) | Infection status | Date of death | Survival time (days) |
|---|---|---|---|---|---|
| 1 | M | 26 | I | 5/5 | 11 |
| 2 | M | 32 | I | 16/5 | 22 |
| 3 | M | 32 | I | 16/5 | 22 |
| 4 | M | 35 | I | 3/6 | 40 |
| 5 | M | 43 | I | 15/6[1] | 52 |
| 6 | F | 24 | I | 29/4 | 5 |
| 7 | F | 28 | I | 18/5 | 24 |
| 8 | F | 29 | I | 17/5 | 23 |
| 9 | F | 29 | I | 17/5 | 23 |
| 10 | M | 27 | II | 1/5 | 7 |
| 11 | M | 28 | II | 3/5 | 9 |
| 12 | M | 30 | II | 12/5 | 18 |
| 13 | M | 31 | II | 29/4[2] | 5 |
| 14 | M | 31 | II | 29/4 | 5 |
| 15 | M | 32 | II | 29/4 | 5 |
| 16 | M | 33 | II | 31/5 | 37 |
| 17 | F | 25 | II | N.A | * |
| 18 | F | 27 | II | 15/5 | 21 |
| 19 | F | 27 | II | 29/4 | 5 |
| 20 | F | 29 | II | 18/5 | 24 |
| 21 | M | 27 | III | 13/5 | 19 |
| 22 | M | 29 | III | 2/5 | 8 |
| 23 | M | 30 | III | 5/5 | 11 |
| 24 | M | 32 | III | 9/5[3] | 15 |
| 25 | F | 30 | III | 5/5 | 11 |
| 26 | M | 29 | IV | 29/4 | 5 |
| 27 | M | 33 | IV | 6/5 | 12 |
| 28 | F | 29 | IV | 3/5 | 9 |
| 29 | F | 29 | IV | N.A | * |
| 30 | F | 31 | IV | N.A | * |

**Table 5.5.** The results of an experiment to investigate the proportion of infected lobsters that released spores naturally. Lobsters were trawl caught on 24/4/95, placed in the aquarium and checked each day for signs of spore release. Lobsters are grouped according to infection status. Survival times of infected lobsters are summarised in Table 5.6. * = cannibalised

[1] started releasing macrospores on 14/6

[2] started releasing macrospores on 28/4

[3] started releasing macrospores on 30/5

| Infection status | Number of lobsters | Mean survival time in days (standard deviation) |
|---|---|---|
| I | 9 | 25 (±14.04) |
| II | 10 | 14 (±11.01) |
| III | 5 | 13 (±4.27) |
| IV | 3 | 9 (±3.51) |

**Table 5.6.** The mean survival time in days of infected *Nephrops* trawl caught on 24/4/95. Data for individual lobsters are shown table 5.5.

| Sex | C L (mm) | Infection status | Dinospore type released | Total number of cells $ml^{-1}$ in haemolymph |
|---|---|---|---|---|
| F | 29 | III | microspore | $2.10x10^8$ |
| M | 43 | I | macrospore | $4.09x10^8$ |
| M | 31 | II | macrospore | $2.01x10^8$ |

**Table 5.7.** Data obtained from three lobsters that were naturally releasing dinospores. CL = carapace length.

# CHAPTER 6.
# HOST PHAGOCYTE RESPONSE TO INFECTION BY *HEMATODINIUM*

## 6.1. Introduction

Invertebrate immunity is not well understood, but is believed to depend on the non-specific recognition of material that represents non-self. There is no evidence that invertebrates produce antibodies against specific antigens (McCumber and Clem 1983). Foreign material may be removed from the circulation by the cell mediated processes of pinocytosis and phagocytosis. In decapod crustaceans circulating phagocytic haemocytes are important effectors of cell mediated immunity (reviewed by Bauchau 1981 and Johnson 1987). *In vitro* studies have shown that haemocytes are capable of engulfing introduced mammalian erythrocytes (Paterson and Stewart 1974, Paterson *et al.* 1976, Goldenberg *et al.* 1984) and bacteria (Paterson *et al.* 1976). *In vivo* studies have also shown the removal of foreign material by circulating haemocytes (Cornick and Stewart 1968, Hoover 1977, Johnson *et al.* 1981). Fixed cells in the gills play a role in the clearance of foreign material including proteins and small particles (McCumber and Clem 1983, Johnson 1987).

Phagocytic uptake has long been attributed to sedentary cells found in the hepatopancreas. The digestive gland of the lobster comprises several large lobes on each side of the animal; each lobe is comprised of thousands of blind-ending digestive tubules. The digestive tubules are supported by a network of connective tissue. The hepatopancreas is supplied with haemolymph by the hepatic artery. The terminal

arterioles of this artery lie in the haemal spaces among the digestive tubules. The outer layer of cells on the terminal arterioles are actively phagocytic and termed fixed phagocytes.

Cuénot in 1905 described the presence of fixed phagocytes in the hepatopancreas of 43 species of decapod crustacean including *Nephrops*. He injected Chinese ink into the haemocoel of the crustaceans to determine the phagocytic capacity of the fixed phagocytes. Several more recent studies have shown the fixed phagocytes capable of clearing foreign particles from the haemolymph. Hoover (1977) implicated fixed phagocytes in the removal of injected colloidal carbon from the haemolymph of *Carcinus maenas*; Cooper-Willis (1979) injected natural particles into the haemolymph of the grass shrimp *Palaemonetes intermedia* and found that the fixed phagocytes removed the larger particles. Johnson (1980) showed the uptake of viral and bacterial particles by the fixed phagocytes of the blue crab *Callinectes sapidus* and later that the fixed phagocytes were capable of removing the gaffkemia-bacterium, *Aerococcus viridans var. homari* from the haemolymph of infected lobsters, *Homarus americanus* (Johnson *et al.* 1981). Fixed phagocytes are efficient at sequestering large amounts of particulate matter, not only through phagocytosis, but by retaining material within a perforated envelope which surrounds the free surface of the fixed phagocytes.

There is limited evidence of protozoan pathogens being phagocytosed by the fixed phagocytes found in the hepatopancreas. Johnson (1987) showed that *Carcinus maenas* infected with *Paramoeba pernicosa* did contain parasite material within the fixed phagocytes. Johnson (1986) described *Ampelisca agassizi* (Amphipoda) infected with a Syndinian dinoflagellate and a fungus. The haemocytes and fixed phagocytes were actively destroying the fungi but there appeared to be no phagocytosis of the dinoflagellate.

It is clear from present and previous studies that the *Hematodinium* parasitaemia in *Nephrops* reaches a very high level (a maximum of $4.09x10^8ml^{-1}$ was recorded - see Chapter 5), with most of the haemal spaces becoming congested with parasite. The only previous evidence for any host response was the presence of large aggregations of degenerating host haemocytes in the gills, which may be an encapsulation reaction against the parasite (Field *et al.* 1992)

In this chapter I look into the question of whether *Nephrops* has a similar phagocyte response to that of other decapods and whether that response includes the ability to destroy *Hematodinium* parasites. The phagocyte response was investigated by following the uptake of fluorescently labelled particulate matter injected into the haemolymph. Close analysis of material previously prepared for electron microscopy was intended to investigate the ability of *Nephrops* to destroy the parasite.

## 6.2. Materials and Methods

### 6.2.1. Confirmation of the location and activity of fixed phagocytes

Four healthy *Nephrops* (as determined by pleopod examination) were injected with either 100µl of 150nm fluorescent latex beads or 200µl of fluorescein labelled *Pseudomonas citreus* (courtesy of Dr A. Rogerson, Millport Marine Station) through the base of the fifth periopod. After 1 hour the lobsters were cold anaesthetised for 30 minutes before being dissected and the hepatopancreas fixed in the aldehyde mixture as described in Chapter 3. A small sample of fixed hepatopancreas tissue was then squashed on a slide for a preliminary examination under a fluorescence microscope. The remainder of the tissue samples were dehydrated in an ethanol series as in Chapter

3, but were not subjected to postfixation or block-staining. The hepatopancreas was then embedded in either LR White (London Resin Company) or Historesin (Leica).

Semi-thin sections (1μm thick) were cut on a glass knife, mounted on slides and examined with a Zeiss microscope in epifluorescence mode with a fluorescein filter set. A sample of hepatopancreas was fixed and prepared for scanning electron microscopy according to the procedures described in Chapter 3.

### 6.2.2. Activity of fixed phagocytes of *Hematodinium*-infected *Nephrops* and other host responses.

Tissue samples from infected lobsters were fixed and observed as described in Chapter 5. Sections of hepatopancreas, heart, midgut, antennal gland, testis, ovary and abdominal muscle were examined for any signs of phagocytosis by fixed phagocytes, circulating haemocytes and haemocyte encapsulations.

## 6.3. Results

### 6.3.1. The activity of the fixed phagocytes of the hepatopancreas in uninfected *Nephrops*

Examination of the material prepared for scanning electron microscopy illustrated well the location and appearance of the fixed phagocytes which are found on the outside of the endothelium of the terminal arterioles within the hepatopancreas (Figure 6.1, 6.2). The arterioles were 60-80μm in diameter, and fixed phagocytes 15-30μm in diameter. As in other decapod crustaceans the fixed phagocytes of *Nephrops* have a close fitting envelope in the form of a sieve-like interrupted layer surrounding

their free surface (Figure 6.2). The interrupted layer was approximately 170nm thick. On both inner and outer surfaces of the interrupted layer was a layer of electron dense granules. The perforations were circular to oval in shape and ranged from 170-350nm in diameter.

An examination of squashes of the hepatopancreas from lobsters that had been injected with either fluorescent beads or bacteria showed that the fixed phagocytes attached to the arterioles were highly efficient in removing the injected material from the haemolymph (Figures 6.3a, b). The fixed phagocytes engulfed large numbers of the latex beads, but not so many of the bacteria. Low uptake of bacteria is possibly because the bacteria were injected at a lower concentration than the latex beads or that there was some unknown difference between the lobsters that determined the rate of phagocytosis. There were several problems associated with fluorescence microscopy of the embedded material. Material embedded in Historesin produced very low levels of fluorescence and the uneven section surface produced a lot of reflection. The latex beads lost most of their fluorescence in the LR White resin, although use of this technique produced good sections and better preservation of the tissues. The most obvious evidence of phagocytic activity was obtained using material which had been injected with the fluorescent bacteria and subsequently embedded in the LR White. Examination of LR White sections of hepatopancreas showed that all the fixed phagocytes surrounding every arteriole were capable of ingesting bacteria (Figure 6.4), apart from those cells situated near to the end of the terminal arteriole.

### 6.3.2. Activity of fixed phagocytes within the hepatopancreas of *Hematodinium* infected *Nephrops*

Even at the light microscopical level of examination of semi-thin sections of the hepatopancreas of infected *Nephrops*, it was possible to see that the fixed phagocytes had engulfed dinoflagellates (Figure 6.5). Dinoflagellates were also present in the haemal spaces of the hepatopancreas and in the lumen of the terminal arterioles (Figure 6.5). Activity of the fixed phagocytes surrounding the hepatic arterioles was observed in infected lobsters of all stages, as indicated by the hypertrophied state of these cells.

Electron microscopical evidence for phagocytosis and subsequent breakdown of *Hematodinium* was even better. When observed in ultra-thin sections, the fixed phagocytes of infected lobsters usually contained either a large amount of unrecognisable debris or partially-intact dinoflagellates. Fixed phagocytes that contained debris still appeared healthy; the interrupted layer was still intact and there was no obvious lysis of the fixed phagocyte (Figure 6.6).

Evidence was seen of retention of parasites in the pericellular space between the interrupted layer and the fixed phagocytes (Figure 6.7), in fact the majority of dinoflagellates associated with fixed phagocytes were retained in this manner. Stages in digestion were less commonly observed, evidence for its conduct being in the form of secondary lysosomes containing degenerating parasite material (Figure 6.7). Fixed phagocytes containing such secondary lysosomes often showed signs of damage. The parasites contained within the pericellular spaces were often degenerating and lysed. In one infected lobster that was examined, a secondary bacterial infection was discovered. Both dinoflagellates and bacteria were found in the pericellular space of the fixed phagocytes (Figure 6.8).

### 6.3.3. Host response in other tissues to infection by *Hematodinium*

Examination of the infected tissues previously fixed and sectioned for microscopy (see Chapter 5) showed that some of the remaining haemocytes of infected animals were capable of producing a host cellular defence reaction.

There was limited evidence of a host cellular defence reaction within the gut wall of stage I lobsters, where small numbers of haemocytes were seen aggregated around dinoflagellates forming encapsulations. Other haemocyte aggregations observed in the lumen of the terminal arterioles of the hepatopancreas (Figure 6.9) did not contain dinoflagellates.

Some haemocyte aggregations were seen in the lumen of the hearts of stage I to III individuals. These aggregations were tightly packed and contained nuclei of a karyolytic appearance, but whether the nuclei were parasite or host could not be determined.

Haemocyte aggregations similar to those observed in the lumen of the heart were seen in gill filaments, sometimes apparently blocking the lumen. Aggregations were more frequent in the gills than in the heart, but were only seen in the narrower regions of the gill filaments. Free haemocytes were rarely observed in sections, particularly in those lobsters with gills having large numbers of free parasites.

Examination of infected tissues showed that some of the remaining free haemocytes appeared to be capable of phagocytosing dinoflagellates. Stages in phagocytosis were rarely seen, but were encountered in the ovary (Figure 6.10) and in the midgut wall (Figure 6.11).

## 6.4. Discussion

The above results show that some important information has been obtained to answer the questions of whether *Nephrops* has a similar fixed phagocyte response to other decapods and whether it is able to destroy *Hematodinium*.

The use of fluorescent bacteria and latex beads has shown that the fixed phagocytes in the hepatopancreas are capable of removal of foreign particles from the haemolymph. The fixed phagocyte response was similar to that of other decapods (Hoover 1977, Johnson 1980).

Examination of sectioned material showed that fixed phagocytes were able to destroy *Hematodinium*. The presence of degenerating dinoflagellates within the pericellular space of the fixed phagocytes suggests that entrapment alone may result in parasite death followed by subsequent phagocytosis.

The paucity of haemocytes observed in infected lobsters may be explained by sequestration into aggregations and encapsulations. Aggregations of haemocytes (not containing parasites) were more numerous than haemocyte encapsulations of parasites. The aggregations resembled the haemocyte encapsulations observed in response to bacterial infections in *Homarus americanus* (Johnson *et al.* 1981) and *Callinectes sapidus* (Johnson 1976), and previously reported in *Nephrops norvegicus* gills (Field *et al.* 1992), however, they did not appear to contain parasites. Haemocyte aggregations may obstruct the haemolymph flow through the gills, this was postulated by Rittenburg *et al.* (1979) as contributing to tissue hypoxia in gaffkaemic lobsters. The aggregation of haemocytes, and the formation of acellular haemolymph clots in blue crabs (*Callinectes sapidus*) responding to bacterial infections, have also been implicated in impeding blood flow through the gills (Johnson 1976).

Despite the ability of fixed phagocytes even in stage IV infected lobsters to sequester dinoflagellates the lobsters appear unable to control parasite numbers. It is possible that in the early stages of infection the defensive responses are able to combat the parasites and halt infection. Evidence for this is so far lacking except for lobster no.1 (Table 5.3) which was examined during the *in vivo* growth studies described in Chapter 5.

Infections of crustaceans by other Syndinian dinoflagellates have not produced a response by the fixed phagocytes (Johnson 1986, Meyers *et al.* 1987). *Nephrops* infected with *Hematodinium* sp. do appear to recognise the dinoflagellate as foreign and produce a defensive response, largely by the fixed phagocytes in the hepatopancreas.

**Figure 6.1.** A scanning electron micrograph showing a tubule of the hepatopancreas and an arteriole. The arteriole is closely associated with the tubule (T) and runs parallel to its axis. The outer surface of the arteriole is covered with fixed phagocytes (FP). Scale bar = 50μm.

**Figure 6.2.** A scanning electron micrograph of the surface of an arteriole. The fixed phagocytes (FP) are covered with an interrupted extracellular layer that contains numerous pores (arrows). The fixed phagocytes have distinct furrows at the surface that are reflected in the overlying interrupted layer. Scale bar = 5μm.

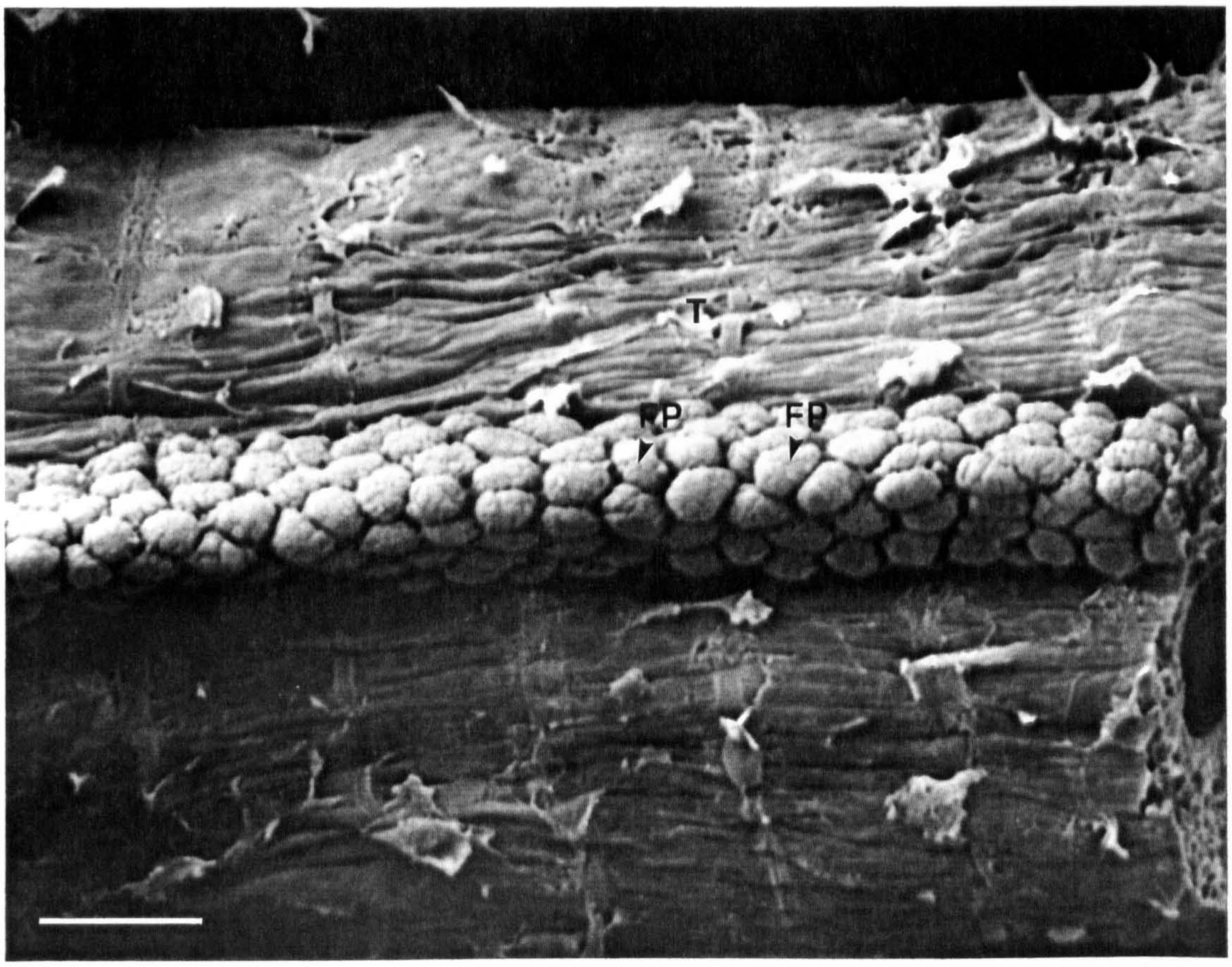
T
FP
FP

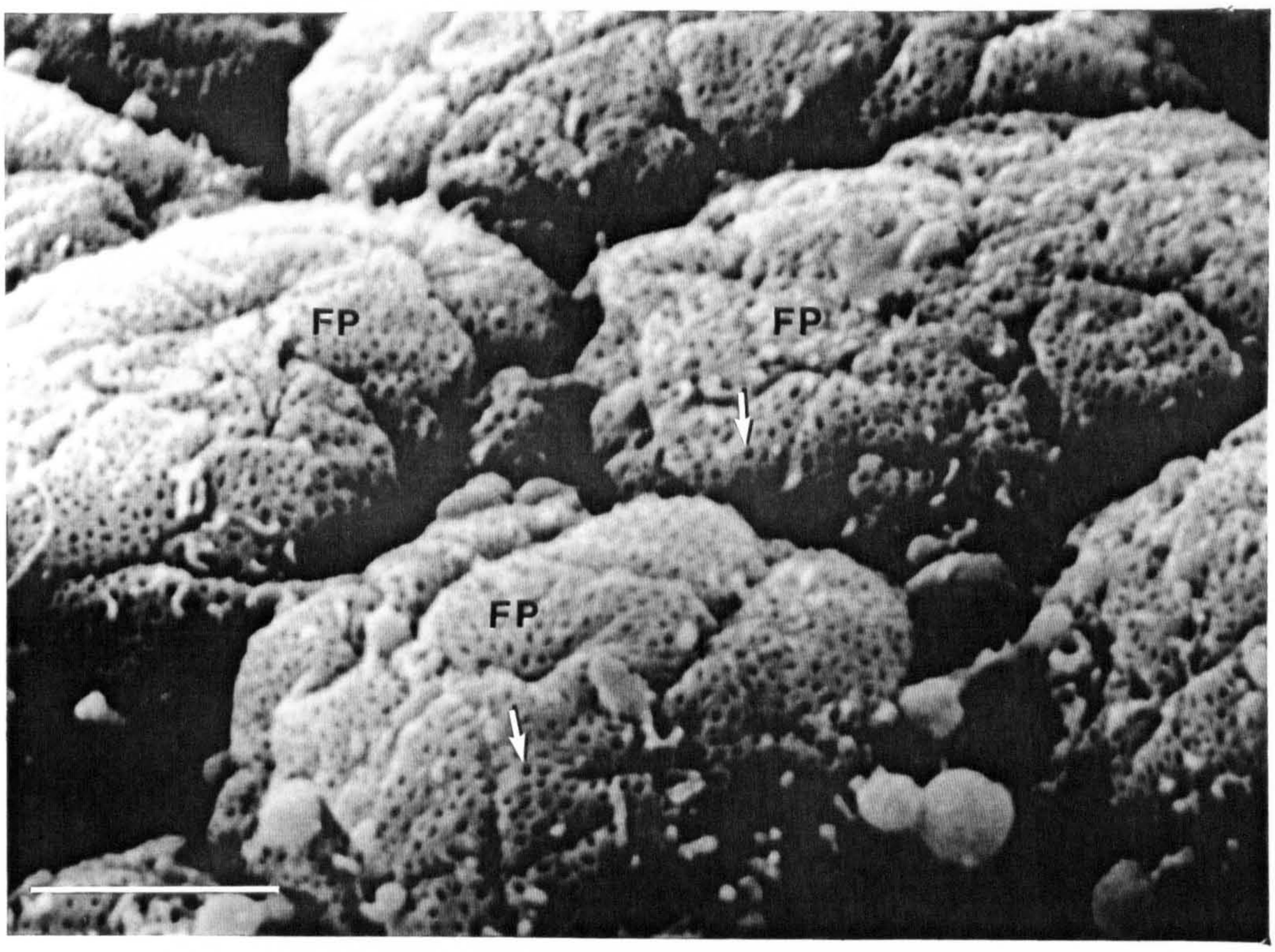
FP
FP
FP

**Figure 6.3.** Light micrographs of intact hepatopancreas arterioles after injection of lobster with fluorescent particles; viewed with epifluorescence.

**a.** An arteriole from a lobster that had been injected with fluorescein labelled latex beads. The fixed phagocytes surrounding the arterioles have phagocytosed large numbers of the beads. Phagocyte nuclei (N) are visible as darker areas that do not contain any beads.

**b.** An arteriole from a lobster that had been injected with fluorescein labelled bacteria, showing some uptake by the fixed phagocytes.

Scale bars = 50μm.

**Figure 6.4.** A light micrograph of a LR White section of hepatopancreas viewed with epifluorescence. The sample was from a lobster that had previously been injected with fluorescent bacteria. The transverse profiles of 3 arterioles can be clearly identified by the surrounding fixed phagocytes which have engulfed the bacteria. T = tubules of hepatopancreas, L = lumen of terminal arterioles. Scale bar = 50μm.

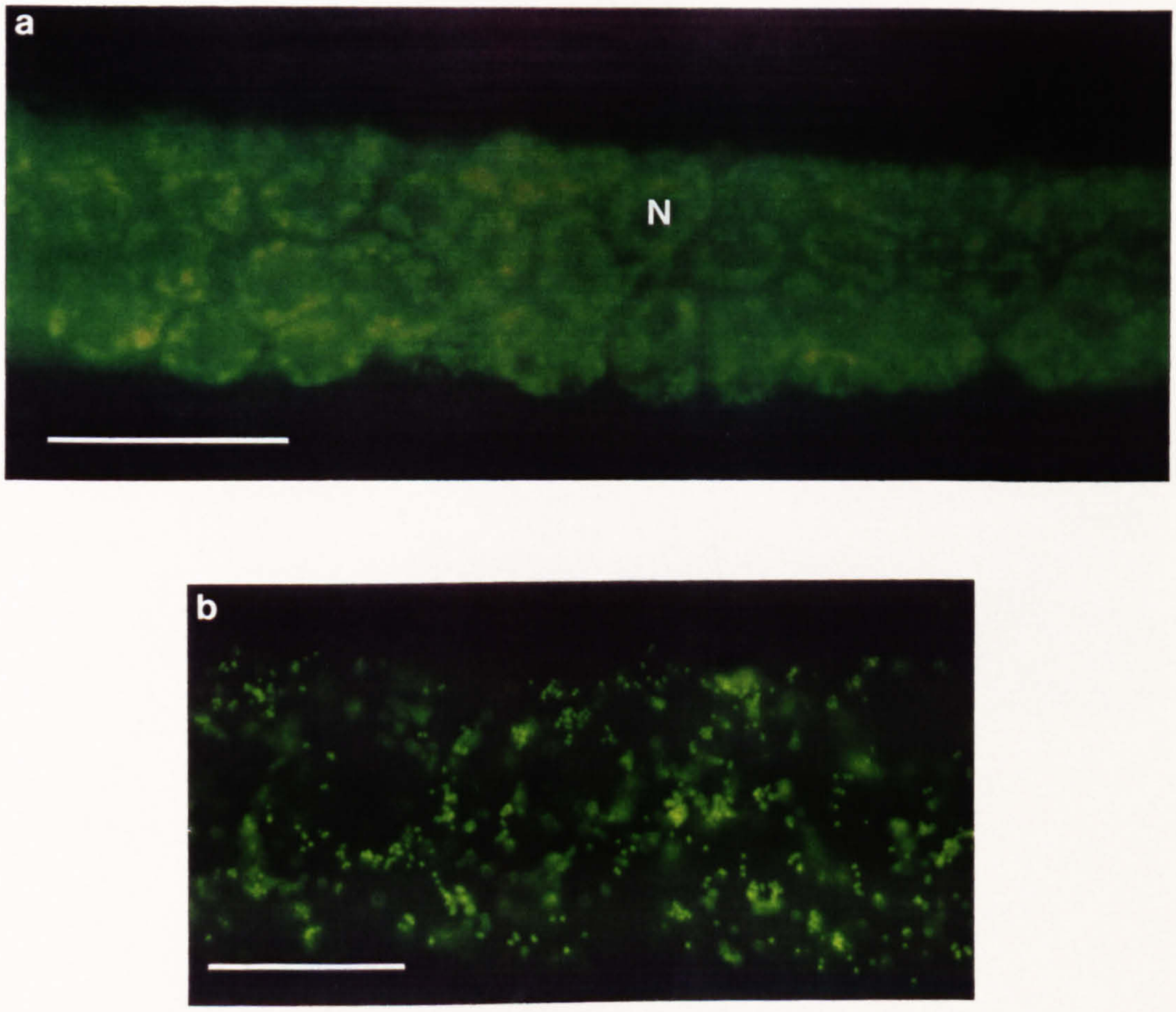
a
N
b
T
L
T
T
L
L

**Figure 6.5.** A light micrograph showing fixed phagocytes surrounding an arteriole in the hepatopancreas of a stage IV infected lobster. Parasites have been engulfed by two fixed phagocytes (arrows). Dinoflagellates (p) are present in the haemal sinus (H) and in the lumen of the arteriole (L). FP = fixed phagocytes, T = hepatopancreatic tubule. A 0.5µm resin section; toluidine blue stained. Scale bar = 10µm.

**Figure 6.6.** A transmission electron micrograph showing detail of a fixed phagocyte associated with an arteriole in the hepatopancreas of a stage IV infected lobster. The fixed phagocyte is attached to the outer surface of the endothelial cells (E) that form the wall of the arteriole. The outer surface of the fixed phagocyte is covered with a close-fitting interrupted layer (I) which contains numerous pores. The cytoplasm of the fixed phagocyte contains numerous debris filled vesicles. H = haemal sinus, N = nucleus of fixed phagocyte, L = lumen of arteriole. Scale bar = 5µm.

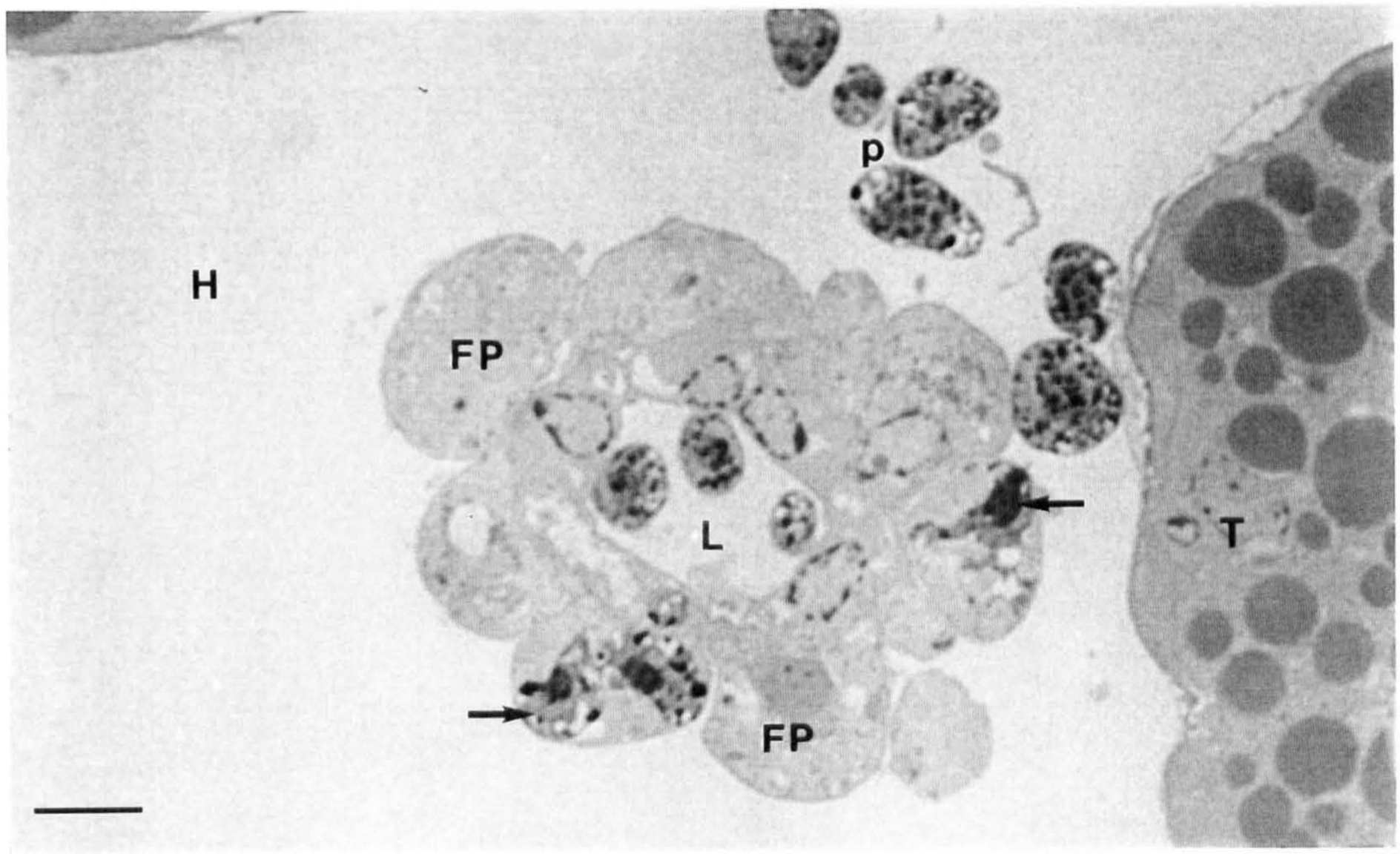
H
FP
p
L
T
FP

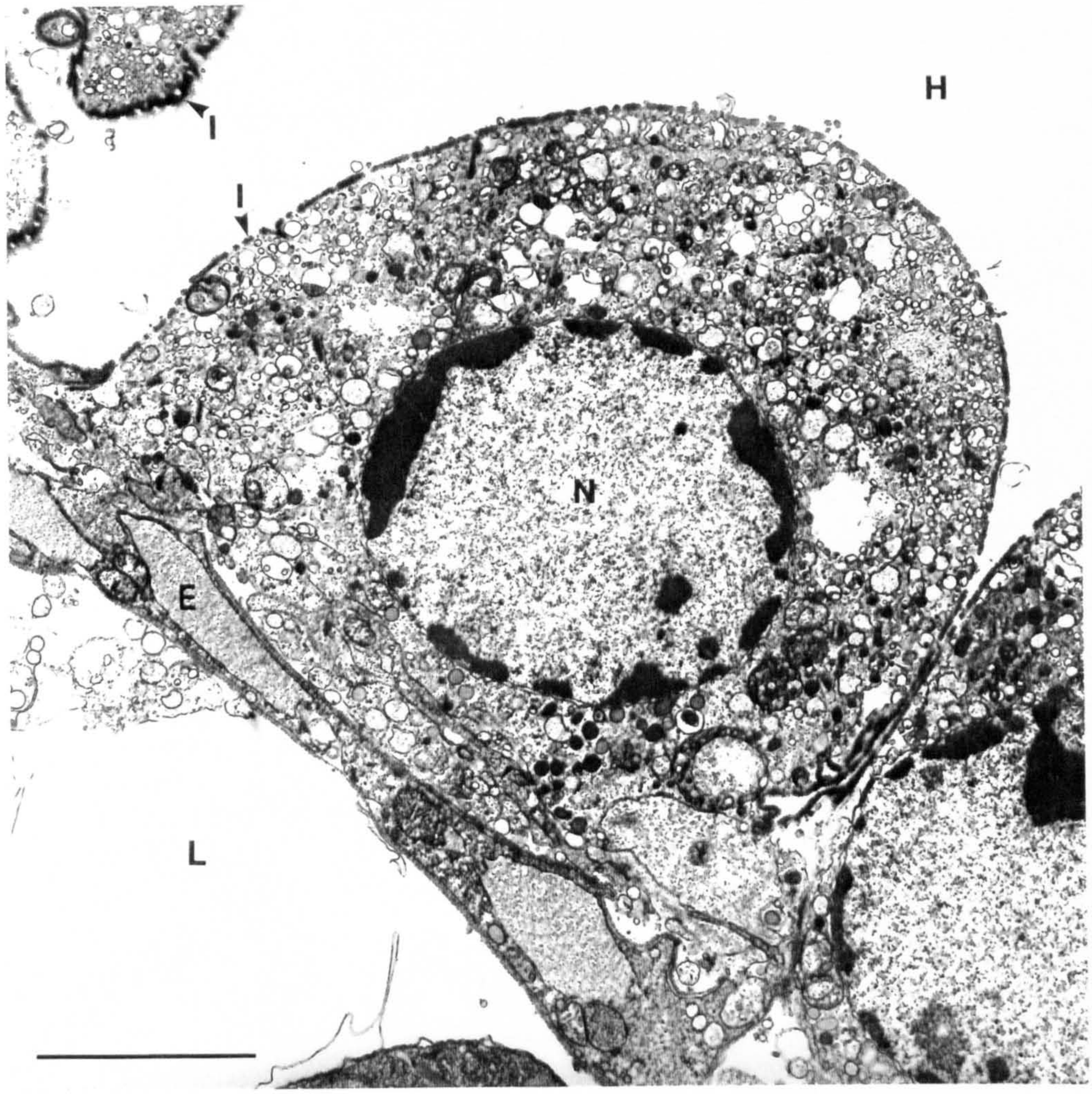
I
I
H
N
E
L

**Figure 6.7.** A transmisson electron micrograph showing detail of a fixed phagocyte associated with an arteriole in the hepatopancreas of a stage IV infected lobster. At least one sporoblast (p) is enclosed within the pericellular space. Vesicles (V) within the cytoplasm of the fixed phagocyte are probably secondary lysosomes containing cellular debris, possibly parasite derived. H = haemal sinus, N = nucleus of fixed phagocyte, n = nucleus of dinoflagellate, I = interrupted layer. Scale bar = 5µm.

**Figure 6.8.** A transmission electron micrograph of the pericellular space of a fixed phagocyte from a stage III infected lobster. Two degenerating dinoflagellates (p) are contained within the pericellular space. Numerous bacteria (arrows) from a secondary infection are also present within the pericellular space. H = haemal sinus, I = interrupted layer. Scale bar = 5µm.

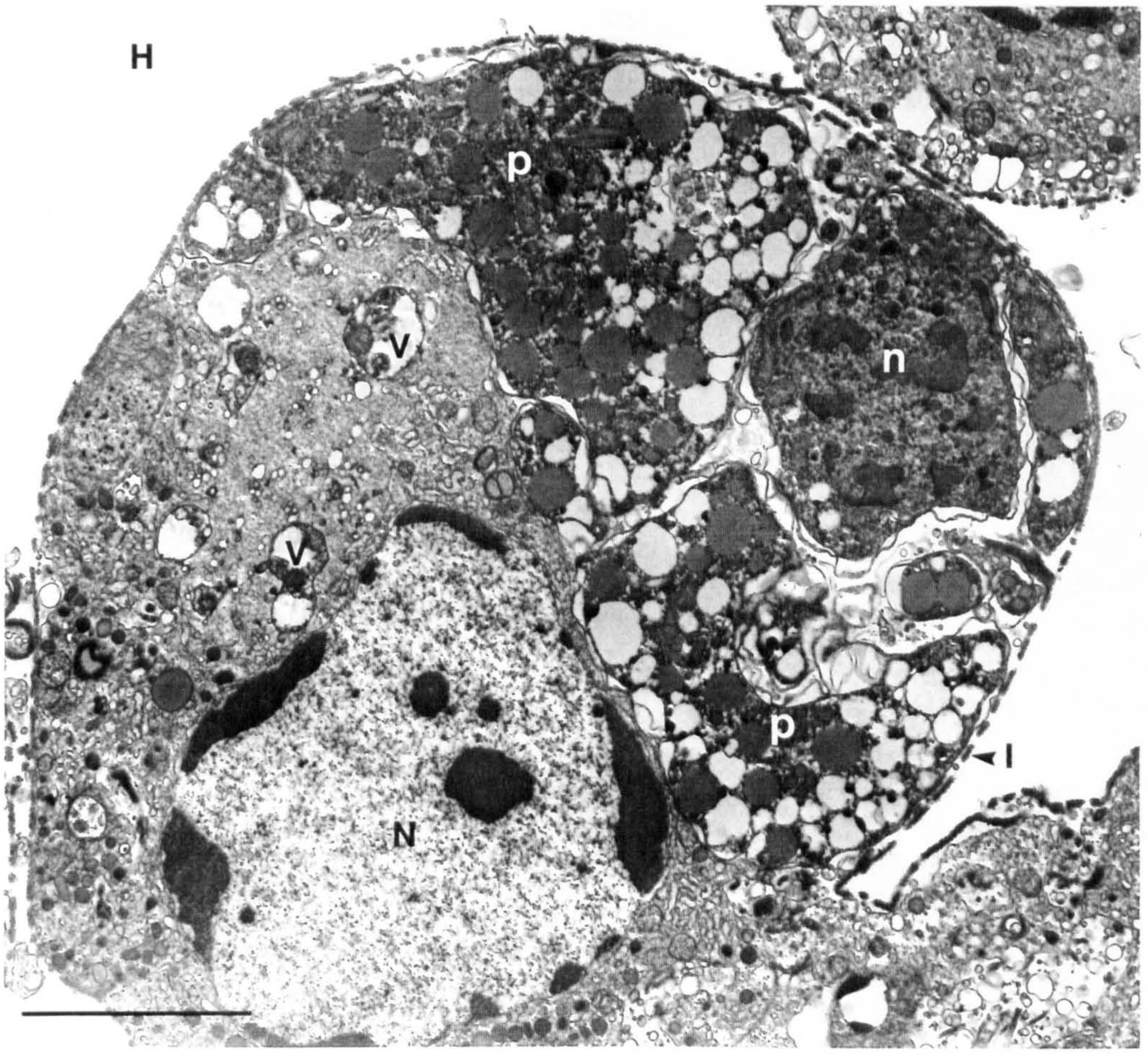
H
p
v
v
n
N
p
l

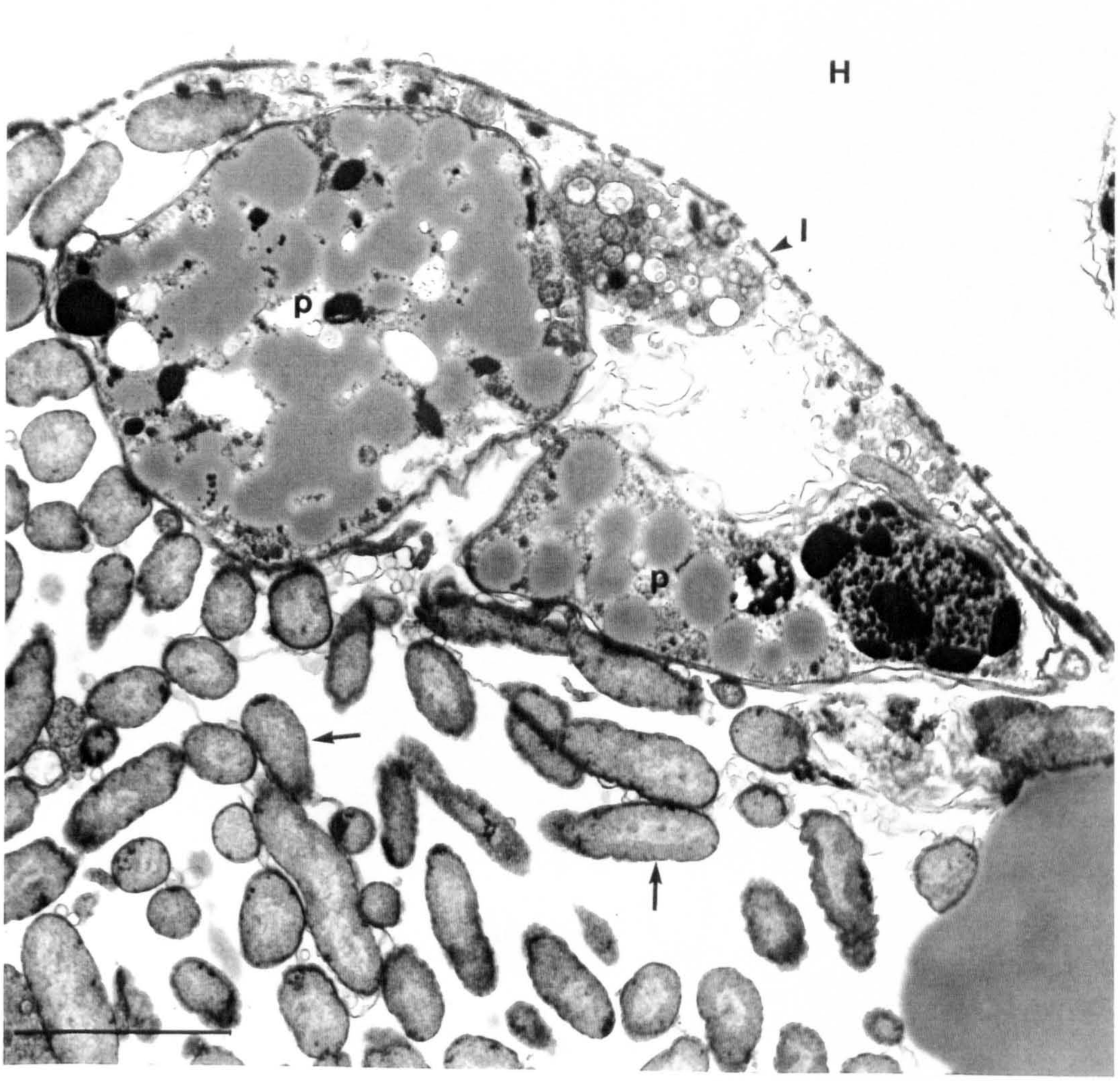
H
l
p
p

**Figure 6.9.** A light micrograph showing a section of part of the hepatopancreas from a stage II infected lobster. A haemocyte aggregation (A) has formed within the lumen of an arteriole. T = hepatopancreatic tubule. A 0.5µm resin section toluidine blue stained. Scale bar = 30µm.

**Figure 6.10.** A light micrograph of a section of part of the ovary from a stage IV infected lobster. Large numbers of sporoblasts are present within the haemal sinus (H) of the ovary. Two dinoflagellates (p) appear to be contained within haemocytes. 0.5µm resin section; toluidine blue stained. Scale bar = 10µm.

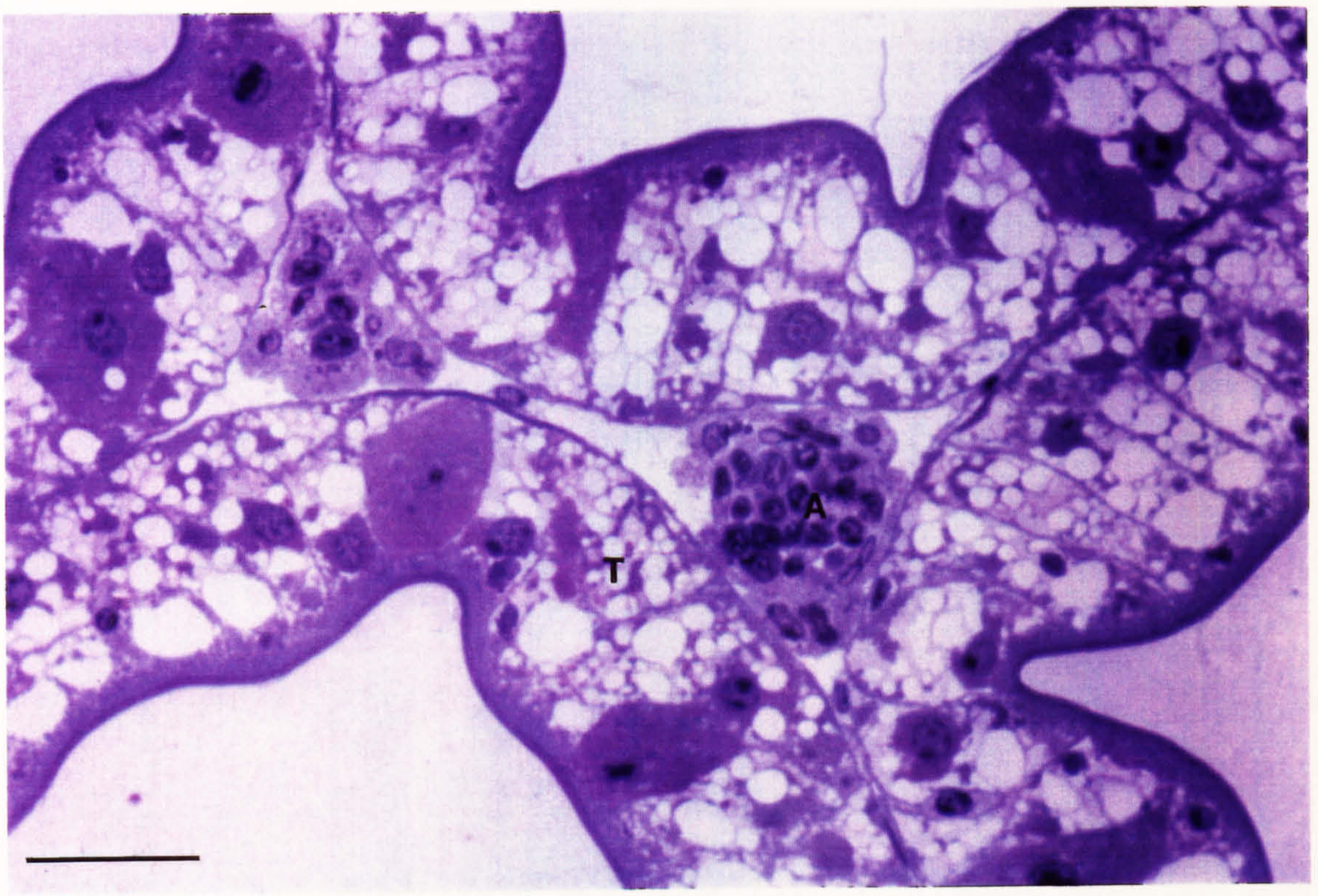
A
T

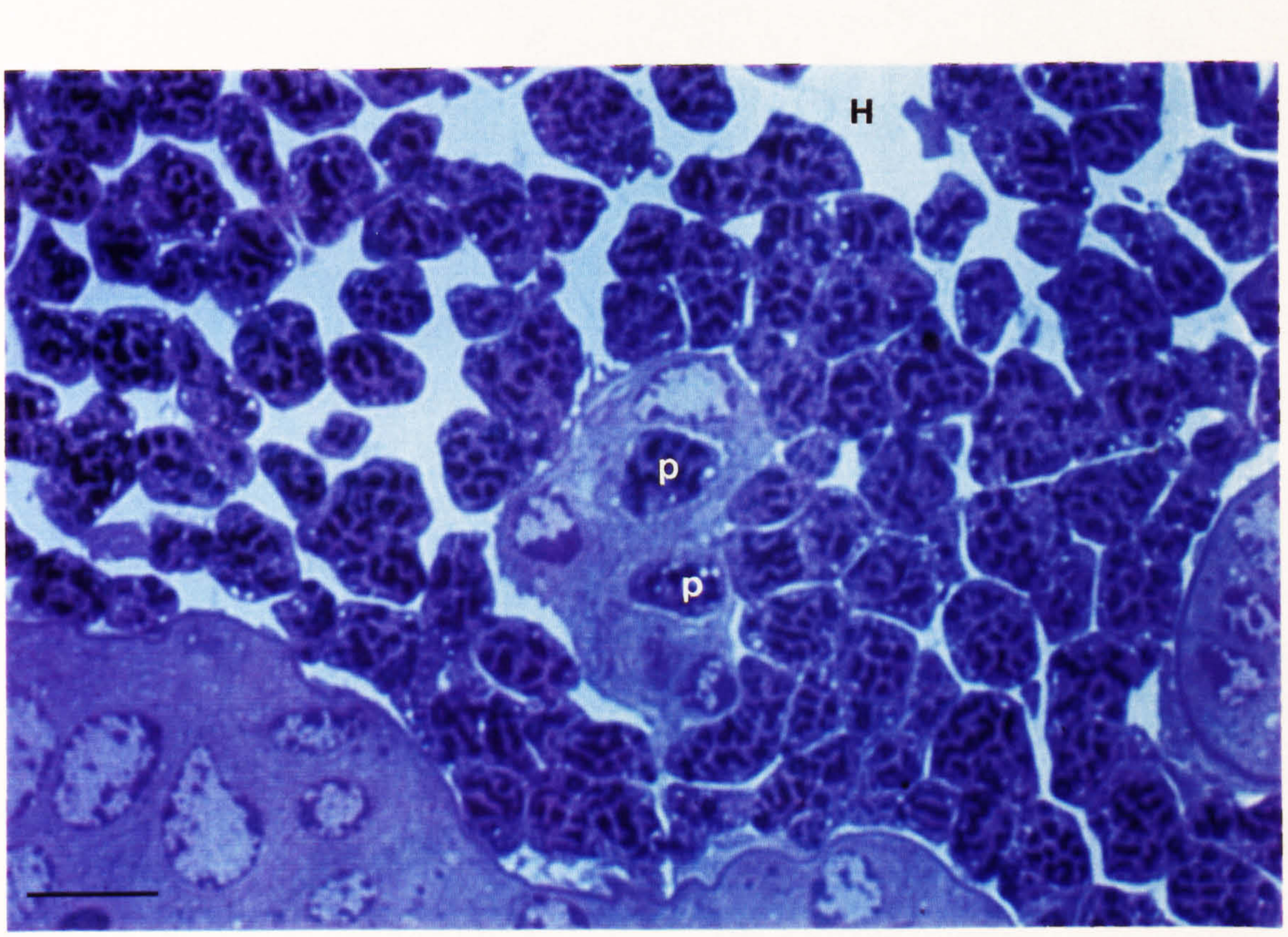
H
p
p

**Figure 6.11.** A composite transmission electron micrograph showing part of the haemal sinus of the midgut wall of a stage III infected lobster. At least one degenerating parasite sporoblast (p) appears to have been phagocytosed by a haemocyte. Note the extreme closeness of fit of the parasite amphiesma (a) to the host food vacuole membrane. Another haemocyte (HC) is attached to the phagocytosing haemocyte. N = nucleus of phagocytosing haemocyte, l = lipid, tr = trichocysts. Scale bar = 5μm.


HC
N
a
tr
l
l
p

# CHAPTER 7
# THE GROWTH OF FILAMENTOUS TROPHONTS IN AN ENRICHED CULTURE MEDIUM

## 7.1. Introduction

A major reservation about the relevance of *in vitro* life cycles to the *in vivo* situation is that the artificial culture medium may induce morphogenetic changes that are not observed in the living host and select these forms for survival. I therefore sought to change the composition of the culture medium in order to see if such changes could be observed.

I chose to supplement the medium with mixtures of free amino acids because these have been used successfully in the *in vitro* culture of other parasitic protozoa grown in media containing foetal calf serum, e.g. *Leishmania* spp. The added amino acids are used as a source of nutrients not present in the foetal calf serum. The crowded habit of growth of the filamentous trophonts is perhaps explained by their use of extracellular enzyme secretion. Secreted enzymes would be more concentrated in areas where trophonts were aggregated and would presumably break down large proteins into smaller units that could be taken up by parasite.

In this chapter I will describe the effect of an amino acid enriched medium on the morphology and pattern of growth of one particular culture isolate.

## 7.2. Materials and Methods.

The *Hematodinium* used in this experiment was isolated from a stage III/IV infected lobster. Parasite was isolated from the haemolymph, midgut wall (isolate No. 4) and ovary (isolate No. 3). The isolates from the midgut and ovary produced macrospores after 20 days. After about 40 days the macrospores were beginning to germinate and produce filamentous trophonts. At this point the germinating macrospores were transferred into the enriched medium.

The enriched culture medium consisted of the FCSG medium as described in Chapter 2 with the additions of Minimal Essential Medium essential amino acids solution without L-glutamine (GIBCO BRL) and MEM non-essential amino acids (GIBCO BRL). The sterile amino acids solutions were added to the culture medium after the addition of the foetal calf serum and antibiotics. The MEM amino acids (50x solution) and MEM non-essential amino acids (100x solution) were added at 2mls and 1ml per 97mls of complete culture medium respectively. The final concentrations of the added amino acids are shown in tables 7.1 and 7.2.

Before the short filaments were transferred into the enriched medium a small sample was taken and fixed in 2% formol saline before being stained with DAPI (10µg $ml^{-1}$). The stained filaments were viewed by fluorescence microscopy as described in Chapter 2 and the number of nuclei per filament counted. After 8 weeks in the enriched culture medium further samples of filamentous trophonts were taken, DAPI stained and also processed for transmission electron microscopy as described previously in Chapter 3.

| Amino acid | Final concentration in medium mg/L |
|---|---|
| L-Arginine | 126.4 |
| L-Cystine | 24 |
| L-Histidine HCL | 139.9 |
| L-Isoleucine | 52.5 |
| L-Leucine | 52.5 |
| L-Lysine HCL | 73.1 |
| L-Methionine | 14.9 |
| L-Phenylalanine | 33 |
| L-Threonine | 47.6 |
| L-Tryptophan | 10.2 |
| L-Tyrosine | 36.2 |
| L-Valine | 46.9 |

**Table 7.1.** The final concentration of amino acids from the MEM essential amino acids solution in the culture medium.

| Amino acid | Final concentration in medium mg/L |
|---|---|
| L-Alanine | 8.9 |
| L-Asparagine | 13.2 |
| L-Aspartic acid | 13.3 |
| L-Glutamine Acid | 14.7 |
| Glycine | 7.5 |
| L-Proline | 11.5 |
| L-Serine | 10.5 |

**Table 7.2.** The final concentration of amino acids from the MEM non-essential amino acids solution in the culture medium.

## 7.3. RESULTS

### 7.3.1. Effects of the addition of amino acids to the culture medium

It was found that the short unbranched filaments of an isolate derived from the midgut and ovary of an infected lobster changed significantly in size and form when placed in medium enriched with additional amino acids.

The short filaments that were initially maintained in FCSG medium were mostly unbranched (Figure 7.1). The short filaments up to 50 μm in length contained between 1 and 4 nuclei; the majority contained one nucleus (Figure 7.4). Upon transfer into the enriched medium the vegetative filaments grew much longer, up to 200μm in length. The filaments grew in tangled masses (Figure 7.2) congregated at the centre of the wells. The long filamentous trophonts contained from 3 to 59 nuclei, very often tightly packed within each filament (Figure 7.3). The distribution ranges for the number of nuclei per filament are shown in figure 7.5. The isolates obtained from the midgut wall and ovary both developed in a similar manner when placed in the enriched medium. The isolates were serially subcultured into fresh enriched medium every two weeks and the parasite remained mainly as filaments and gorgonlocks colonies. The gorgonlocks possessed up to 90 nuclei per colony as seen in DAPI stained preparations.

Occasionally some of the long filaments were observed to segment into long trails of uninucleate cells connected by cytoplasmic threads. Eventually the cytoplasmic threads disappeared, and, uninucleate cells appeared in the culture (Figure 7.6 a, b). Some of the long filaments were returned to the normal FCSG medium and within 2 weeks produced arachnoid syncytia and clumps of cells. None of the isolates maintained in enriched medium could be subcultured indefinitely; the filaments became vacuolated and swollen after about 6 months.

### 7.3.2. Ultrastructure of the filamentous trophonts maintained in enriched medium

The long filaments grown in the enriched medium were similar in the ultrastructure to the shorter filaments maintained in the FCSG medium. The long filaments possessed prominent mitochondria (Figures 7.7, 7.8). Micropores were present in the longer filaments (Figure 7.7) and were more frequently encountered in sections than in the shorter filaments. The long filaments contained numerous peripheral inclusion organelles 0.5-4.5μm in diameter (Figures 7.7, 7.8), these were found infrequently in the shorter filaments; granular matrix organelles were present in both the longer (Figure 7.8) and shorter filaments. The amphiesmal alveoli were often very flattened (Figure 7.7), but in some filaments were more swollen and visible (Figure 7.8).

The nuclei of the long filaments took up a large volume of the filament, as shown by figure 7.3. The chromosomes in the nucleus were condensed, and the nucleolus was always visible. Centrioles were often visible at opposite ends of a tunnel through the nucleus indicating that mitosis was taking place (Figure 7.9). When a nucleus was not actively dividing the centrioles were located in a pit of the nucleus and no tunnel was formed (Figure 7.11). The kinetochores of the chromosomes were inserted in the nuclear envelope and were attached to the base of the centrioles through a bundle of microtubules. Only rarely was the extranuclear spindle observed, possibly indicating that this was a short lived structure during mitosis.

## 7.4. Discussion

The transfer of short filamentous trophonts into the enriched culture medium produced marked changes in the gross morphology of the filaments. The most obvious changes were that individual filaments grew much longer and contained many more nuclei. The fact that the filaments grew much longer (up to 200μm maximum length compared to 50μm maximum length in normal medium) in the enriched medium suggests that this medium was more suitable nutritionally for growth of the filamentous trophonts than the FCSG medium. The growth into longer filaments also suggests that there is a failure of cytoplasmic fission into smaller filaments. The fact that the long filaments did not develop into sporogenic forms such as arachnoid syncytia indicates that the enriched medium was specific for the growth of trophonts and the stimulus for attachment was lacking.

The long filaments with large numbers of nuclei have not been observed either in other *in vitro* cultures or in any of the infected tissues that were examined. The filamentous syncytia that have been observed in sections of the midgut wall of infected lobsters have contained a maximum of 5 nuclei (Field *et al.* 1992 and Chapter five). Maclean and Ruddell (1978) observed multinucleate vermiform parasites in *Cancer irroratus*, *C. borealis* and *Ovalipes ocellatus* up to 64μm long containing up to 12 nuclei. The filamentous forms first described by Chatton and Poisson (1931) contained up to 10 nuclei.

I have shown that the gross morphology of trophonts may be changed by varying the composition of the medium - while ultrastructure remains unchanged.

**Figure 7.1. (Top)** Short filamentous trophonts from FCSG medium containing 1 or 3 nuclei (n). Glutaraldehyde fixation; DAPI stain. Phase contrast and epifluorescence. Isolate no. 2. Scale bar = 20μm.

**Figure 7.2. (Middle)** A tangled mass of long filamentous trophonts that have developed three weeks after extra amino acids were added to a culture of shorter filaments. Phase contrast. Scale bar = 100μm.

**Figure 7.3 a, b. (Bottom)** DAPI stained filaments after growth in amino acid-enriched medium. A large number of nuclei (n) are present in the filaments, although strangely not in a branch of the filament (arrow). The nuclei in b) are dividing. Glutaraldehyde fixation; DAPI stain. Phase contrast and epifluorescence. Scale bars = 30μm.

n


a
n
b
n

**Figure 7.4.** A histogram showing the distribution of numbers of nuclei in filamentous trophonts grown in FCSG medium. From the sample of filaments counted (n=104) the majority contained only 1 or two nuclei.

**Figure 7.5.** A histogram showing the distribution of numbers of nuclei in filamentous trophonts maintained in amino-acid enriched FCSG medium. From the sample of filaments counted (n=50) the minimum number of nuclei in a filaments was 3 and the maximum 59.

**7.4**

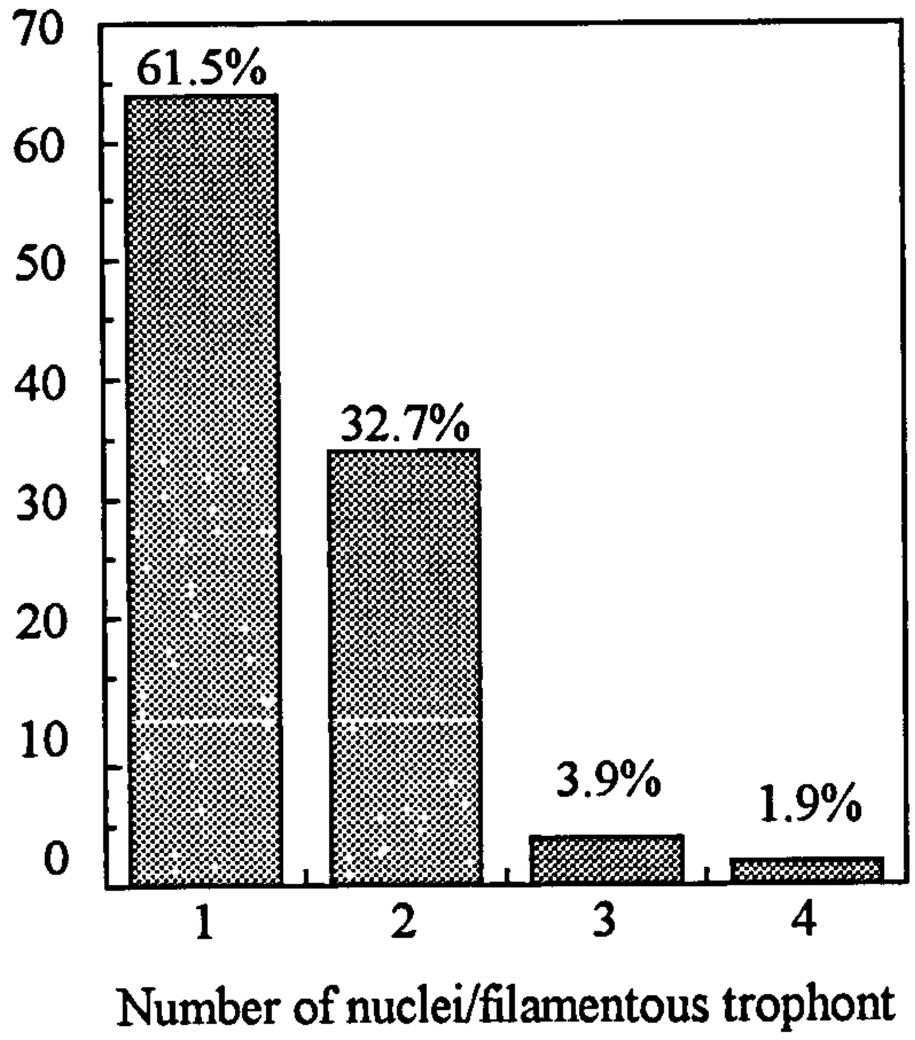
Number of filaments
70
60
50
40
30
20
10
0
61.5%
32.7%
3.9%
1.9%
1
2
3
4
Number of nuclei/filamentous trophont

**7.5**

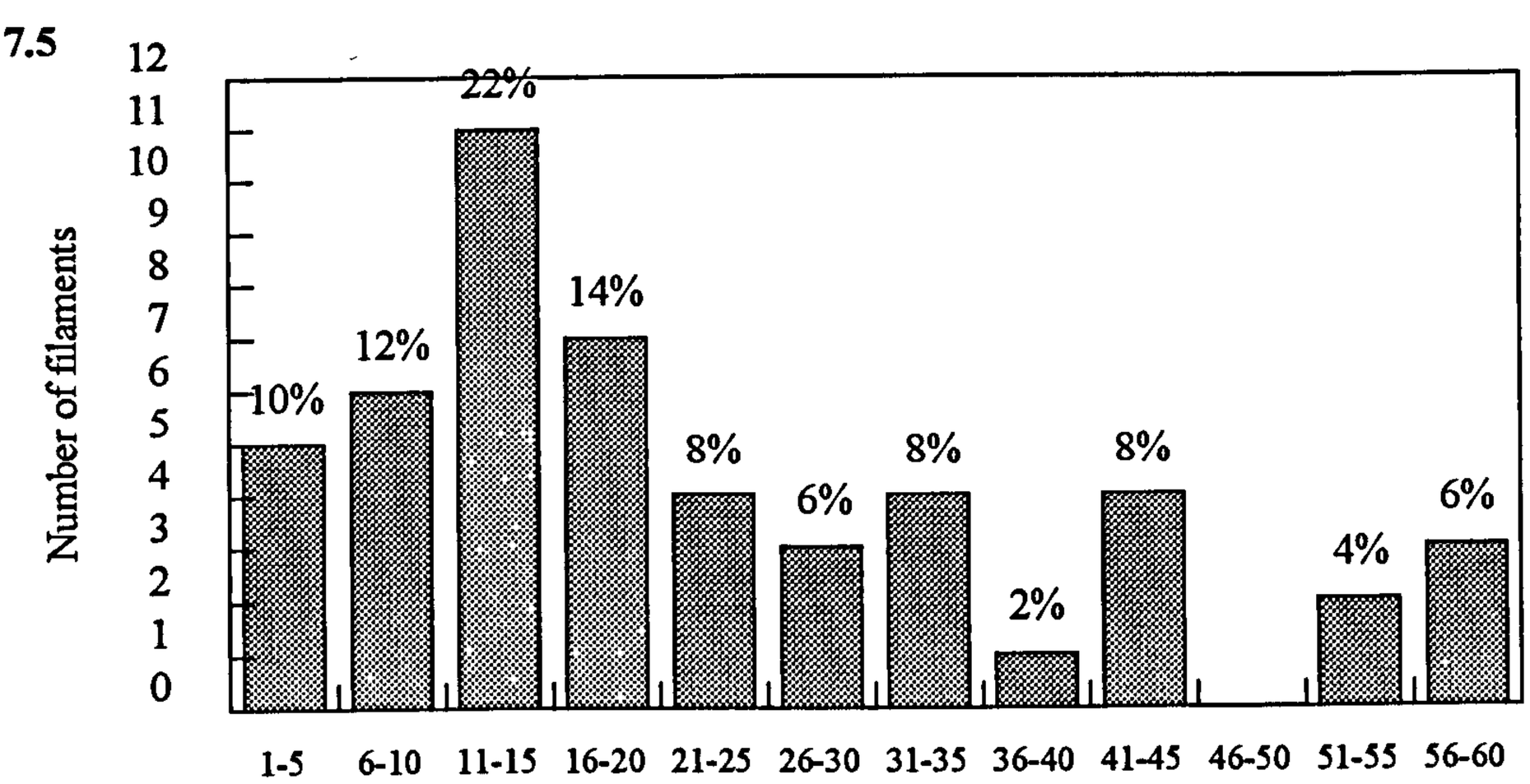
Number of filaments
12
11
10
9
8
7
6
5
4
3
2
1
0
10%
12%
22%
14%
8%
6%
8%
2%
8%
4%
6%
1-5
6-10
11-15
16-20
21-25
26-30
31-35
36-40
41-45
46-50
51-55
56-60
Number of nuclei/filamentous trophont

**Figure 7.6 a&b.** Amino acid enriched culture. Some of the long filamentous trophonts (v) which developed in the amino acid enriched culture were observed to divide into long 'chains' of cells connected by threads (arrows). It is thought that the thin threads disappeared leaving uninucleate cells (u).

Phase contrast. Scale bars = 100μm.

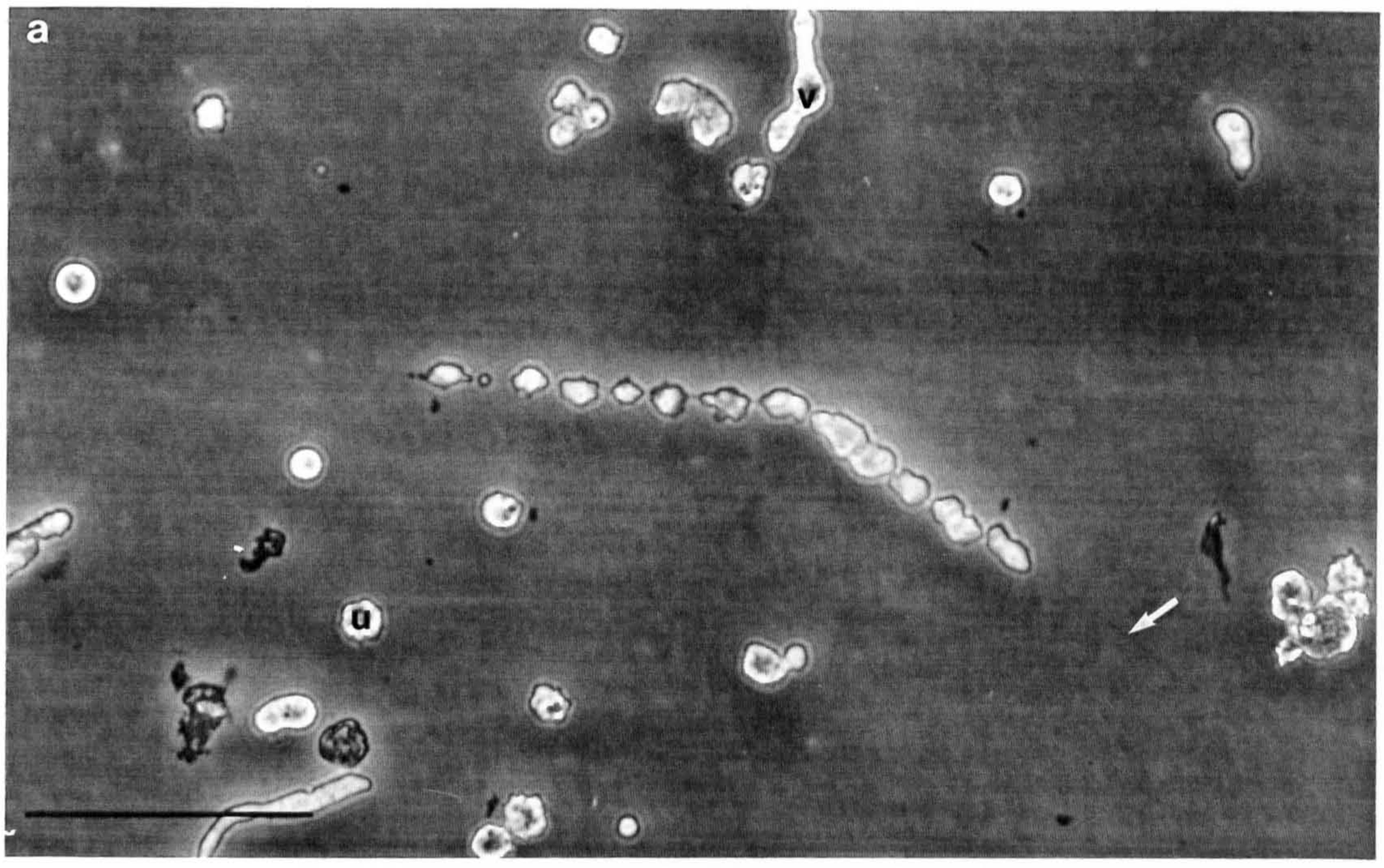
a
v
u


b
v
u
v

**Figures 7.7 - 7.11.** Transmission electron micrographs of sections of filamentous trophonts maintained in amino acid-enriched medium. The initial culture was isolated from the ovary of an infected lobster. Compare with figures 3.22a&b (trophonts grown in FCSG medium).

**Figure 7.7.** A longitudinal section through a filament. m = mitochondria, pio = peripheral inclusion organelle, arrow = micropore. Scale bar = 5μm.

**Figure 7.8.** A transverse section through a filament. g = Golgi apparatus, m = mitochondria, pio = peripheral inclusion organelle, gmo = granular matrix organelle, a = amphiesmal alveoli, nu = nucleolus. Scale bar = 5μm.

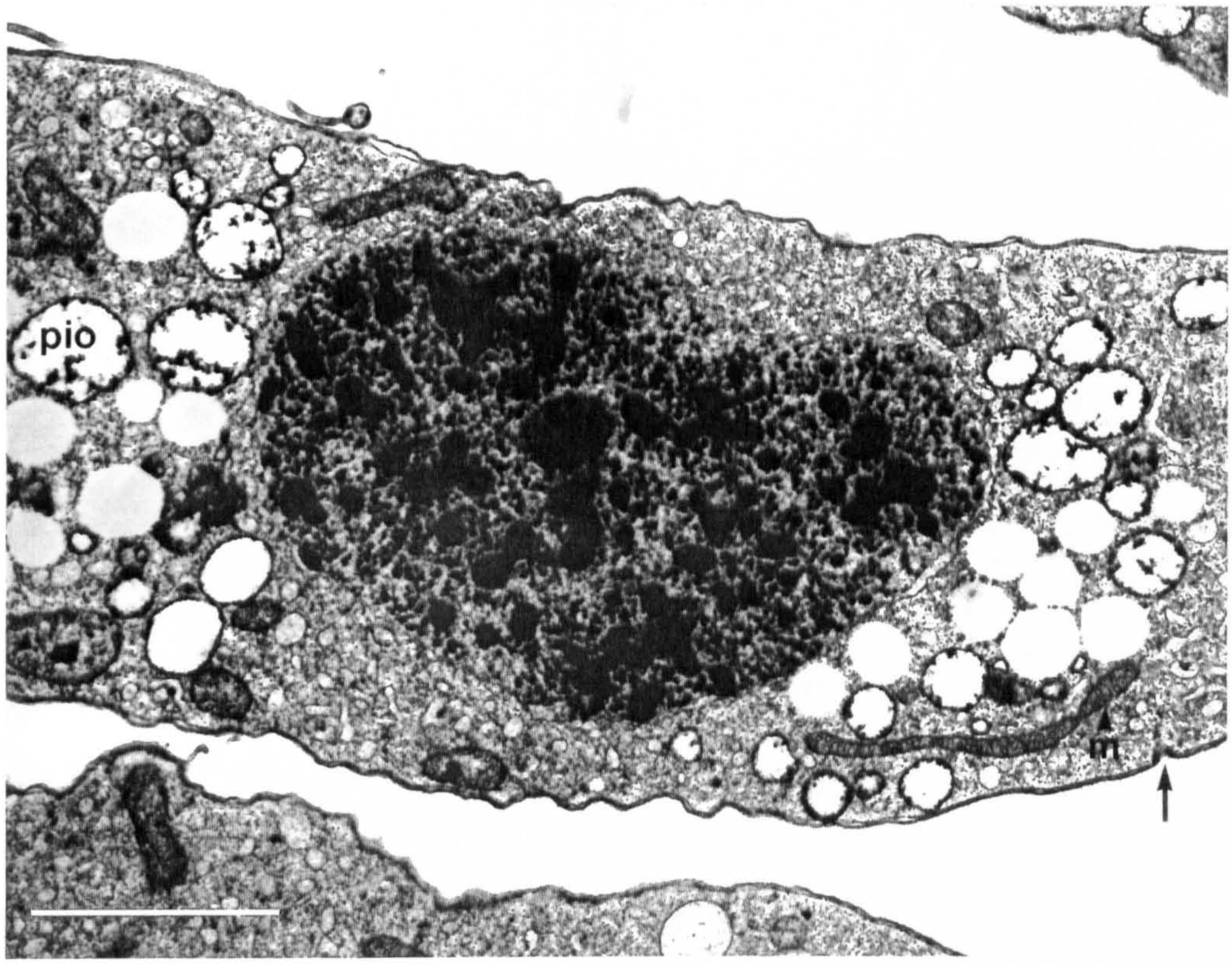
pio
m

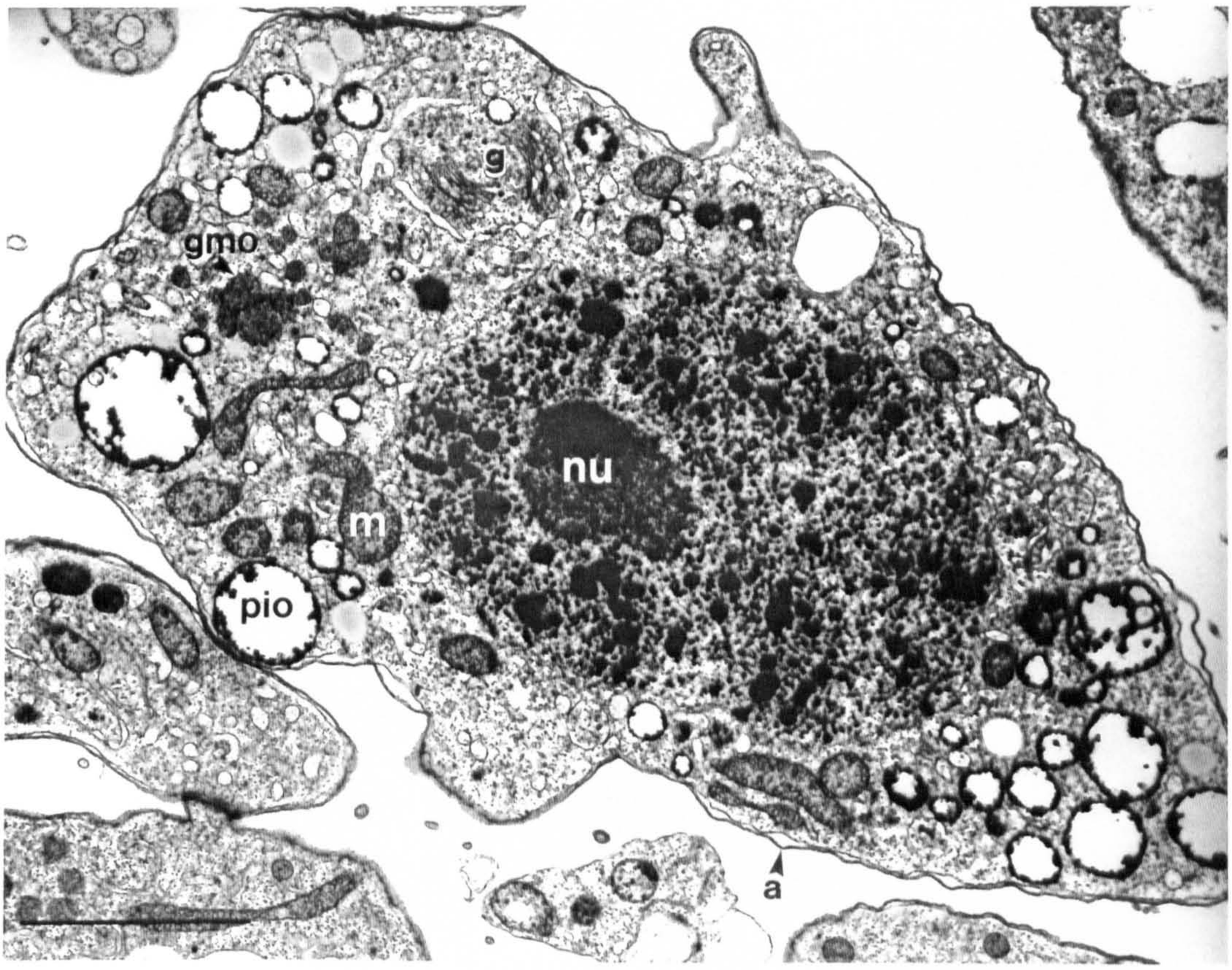
g
gmo
nu
m
pio
a

**Figure 7.9.** Section of part of a dividing nucleus in a filament. Two centrioles (arrows) are located in a deep furrow of the nucleus. ch = chromosome, nu = nucleolus, m = mitochondrion. Scale bar = 1μm.

**Figure 7.10. (Left)** A transverse section through two centrioles located in a pit of the nucleus. Chromosomal kinetochores (arrows) are located in the nuclear envelope. Scale bar = 1μm.

**Figure 7.11. (Right)** A longitudinal section through a centriole located in a pit of the nucleus. Microtubules (mt) connect the centriole to the kinetochores which are located in the nuclear envelope. cn = centriole, ch = chromosome. Scale bar = 0.5μm.

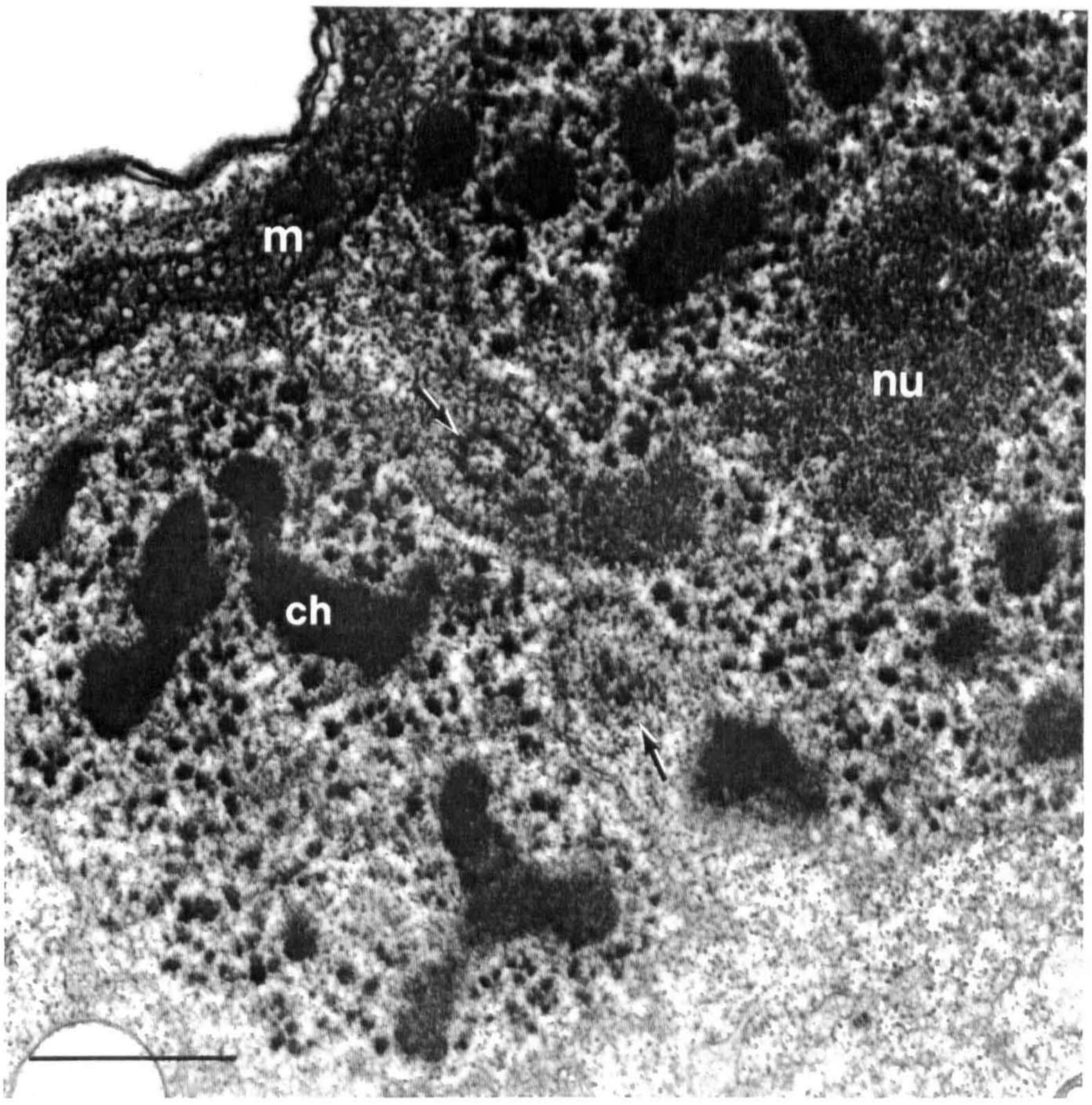
m
nu
ch

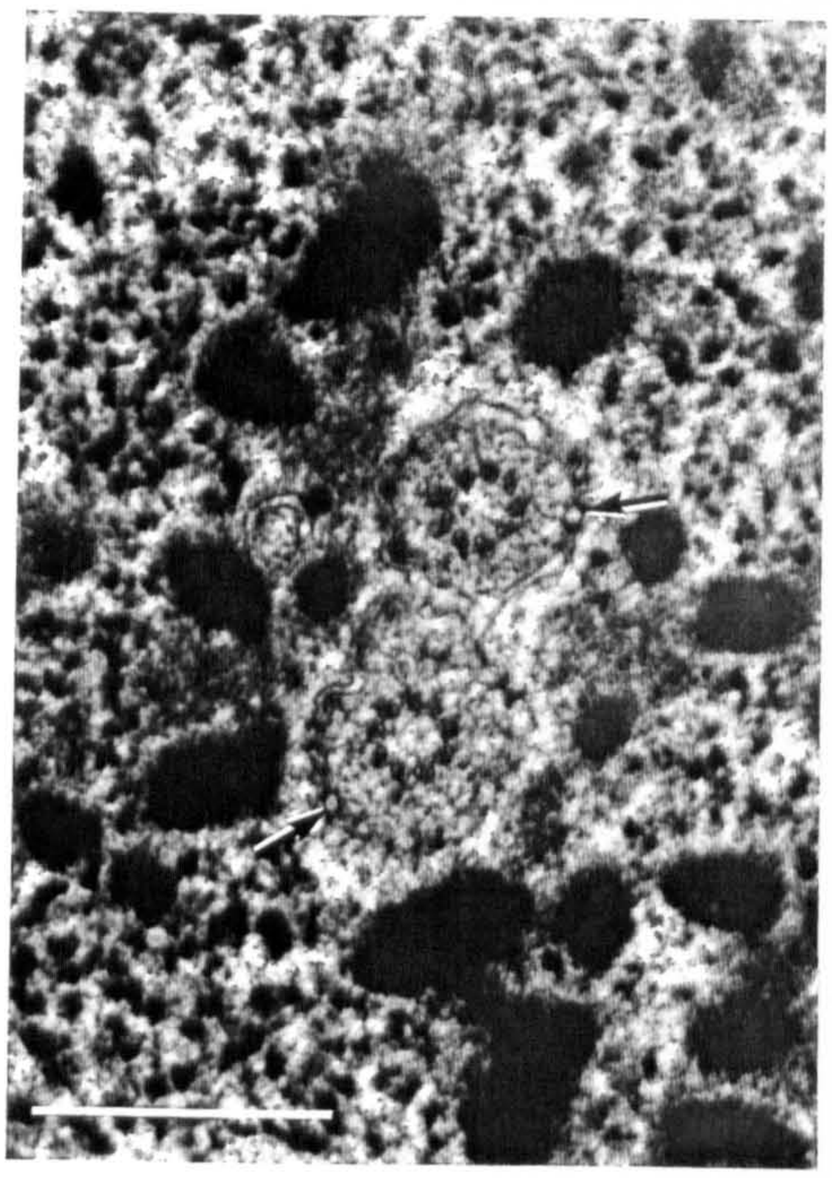

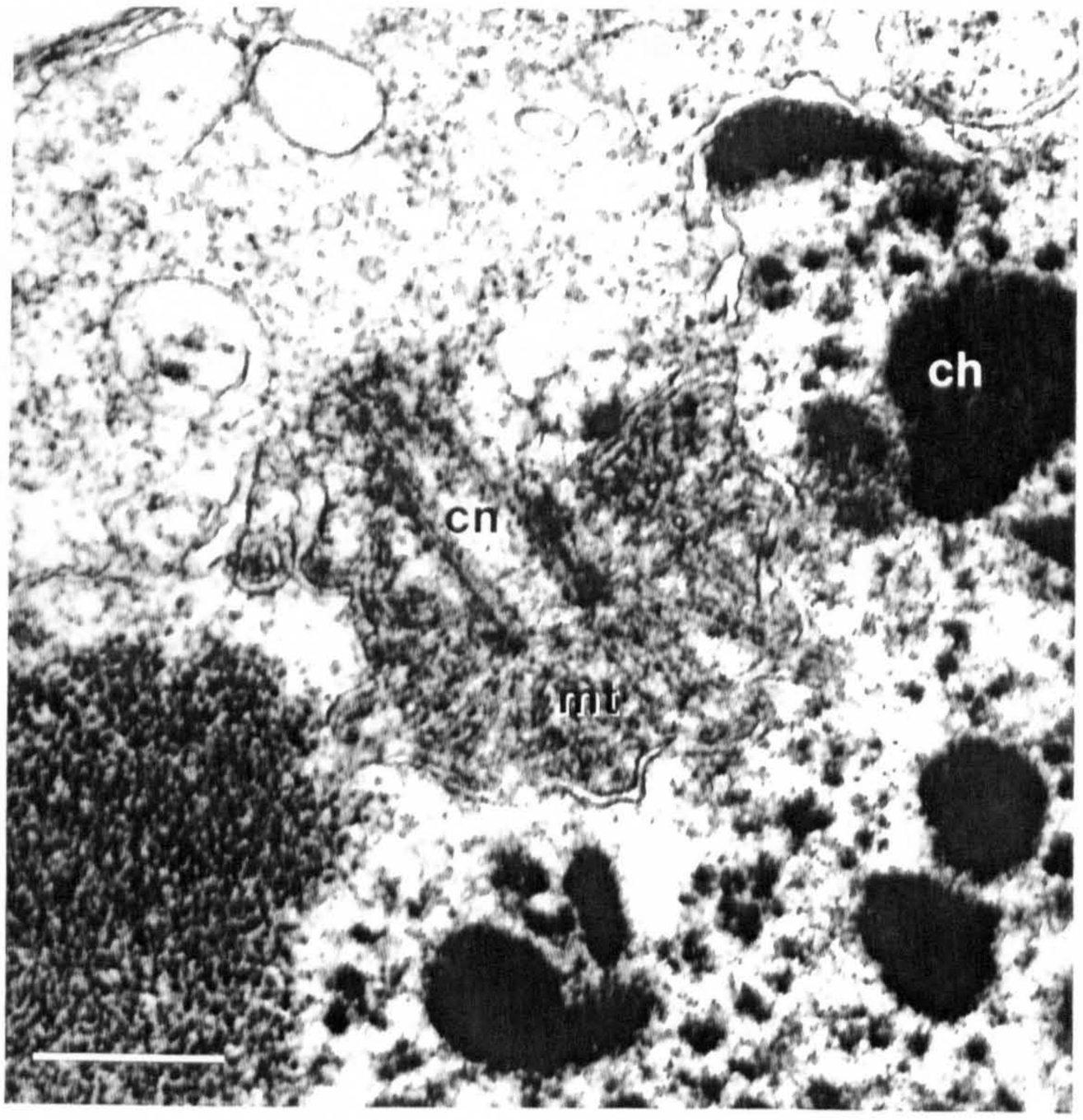
ch
cn
mt

# CHAPTER 8

# THE PRESENCE OF APICOMPLEXAN-TYPE MICROPORES IN *HEMATODINIUM* SP.

## 8.1. Introduction

One of the most surprising revelations of molecular systematics is that the apicomplexans (sporozoans), dinoflagellates and ciliates form a single clade (Gajadhar *et al.*, 1991). Although remnants of a plastid in the apicomplexans have been cited as providing a possible connection with the photosynthetic dinoflagellates (Gardner *et al.*, 1993), not all dinoflagellates possess plastids or plastid remnants. Morphological resemblance between the three groups is slight and their nuclear organisation could not be more different. All that the three groups have in common is the alveolate cortex - hence adoption of the name Alveolata (Cavalier Smith 1993) for the clade.

This chapter reports the presence of a micropore - a structure characteristic of Apicomplexa - in different developmental stages of the dinoflagellate found *in vivo* and in *in vitro* culture. The question of whether the micropore served as a cytostome, as has been demonstrated for certain Apicomplexa (reviewed by Senaud *et al.* 1976), was answered by demonstrating uptake of colloidal electron dense markers into the parasite by endocytosis.

## 8.2. Materials and Methods

Samples were taken from a culture of short filamentous trophonts grown in FCSG medium and also from a culture of long filamentous trophonts grown in amino acid-enriched medium and processed for transmission electron microscopy as described in Chapter 3. Both long and short filaments were incubated either with 35nm colloidal gold particles (courtesy of Dr L. Tetley, Biological EM Unit Glasgow University) or with 0.1mg/ml of cationized ferritin (Sigma) in the appropriate culture medium for 24 hours. These filaments were fixed in aldehyde fixative only before washing, dehydrating and embedding in LR White acrylic resin. Sections of this material were viewed unstained by transmission electron microscopy to locate the electron-dense markers (colloidal gold and ferritin).

Some of the tissue samples prepared for the investigation of *in vivo* developmental forms of the dinoflagellate in Chapter 5 were searched to look for the presence of micropores.

## 8.3. Results

Transmission electron microscopy of sections of the short filamentous trophonts grown in FCSG medium, revealed the presence among the cortical alveoli of caveolae (Figures 8.1, 8.2), ~ 110-200 nm in diameter with an electron-dense reinforcing sleeve replacing the alveolar sacs, in the underlying cortex along the wall of the pit (Figures 8.3, 8.4). These structures being structurally identical with those designated micropores in Apicomplexa will be referred to by the same name.

Abundant clear vacuoles were visible by transmission electron microscopy of sections of trophonts (Figures 8.1, 8.2). The tracer work showed uptake of electron dense markers into these clear vacuoles (Figures 8.4, 8.5). Both ferritin and colloidal gold were observed in the clear vacuoles, however, the colloidal gold particles were easier to identify due to their larger particle size.

Micropores were more frequently encountered in sections of long filaments grown in the enriched medium than in the short filaments grown in the FCSG medium. The micropores in the long filaments (Figures 8.6, 8.7) were of comparable morphology to those in the shorter filaments.

Similar micropores have been demonstrated in stages of development of *Hematodinium in vivo*, notably in sporogenic circulating stages (sporoblasts) (Figures 8.8-8.10). Micropores were found to be particularly numerous in sporoblasts in a sample of ovary. On two occasions micropores were found in the lining of the flagellar pocket of microspores (Chapter 3).

## 8.4. Discussion

Micropores may be a feature of several stages in the life cycle of *Hematodinium*, as they frequently are in coccidians, malaria parasites and other apicomplexans (Scholtyseck and Mehlhorn, 1970; Ferguson *et al.*, 1977). As yet to my knowledge, micropores have not been recorded in the alveolate cortex of the dinokaryote dinoflagellates. In ciliates the parasomal sacs, which open close to the ciliary bases, have been shown to be engaged in pinocytosis (Nilsson and Van Deuers, 1983). Interestingly, in the non-ciliated Suctoria and in sedentary ciliates with reduced

ciliation (chonotrichs, peritrichs), cortical pores, virtually identical in structure to the micropores of apicomplexans and syndinean dinoflagellates will take up ferritin from the surrounding medium (Rudzinska, 1977). The role of the micropore in nutrition of apicomplexans has been reviewed by Senaud *et al.* (1976) and for *Plasmodium* spp in particular by Olliaro and Goldberg (1995). Micropores appear to be a widespread component of the cortex in the Alveolata. The role of micropores in *Hematodinium* is not entirely clear but uptake of markers suggests they may have a cytostome function in the trophont phase of the parasite. The uptake of the markers into vacuoles suggests these vacuoles represent material endocytosed from the surrounding medium.

Despite the apicomplexan-like flexing movements, no other apicomplexan features (e.g. conoid, polar ring, cortical microtubules, rhoptries) have been observed in the trophont of *Hematodinium*.

**Figures 8.1-8.3.** Transmission electron micrographs of filamentous trophonts from a well established culture maintained in FCSG medium.

**Figure 8.1. (Top)** A short filament in transverse section showing vacuolated cytoplasm, absence of trichocysts and a single micropore (arrowed). g = Golgi apparatus, m = mitochondrion, l = lipid, v = vacuole. Scale bar = 2µm.

**Figure 8.2. (Bottom left)** Vertical section of a micropore. The alveolar sacs (as) of the cortex are replaced by an electron dense sleeve (arrowed) around the wall of the pit (pt) which is lined by the plasma membrane (pm) only. v = vacuoles. Scale bar = 200nm.

**Figure 8.3a, b.** Horizontal sections through a micropore.

**a. (Middle right)** Micropore visible as two electron dense circular bands situated close to the surface of the filament. Scale bar = 200nm.

**b. (Bottom right)** The electron dense sleeve (arrowed) is situated beneath the plasma membrane (pm). Radial fibrils connect the two structures. as = aveolar sac. Scale bar = 200nm.

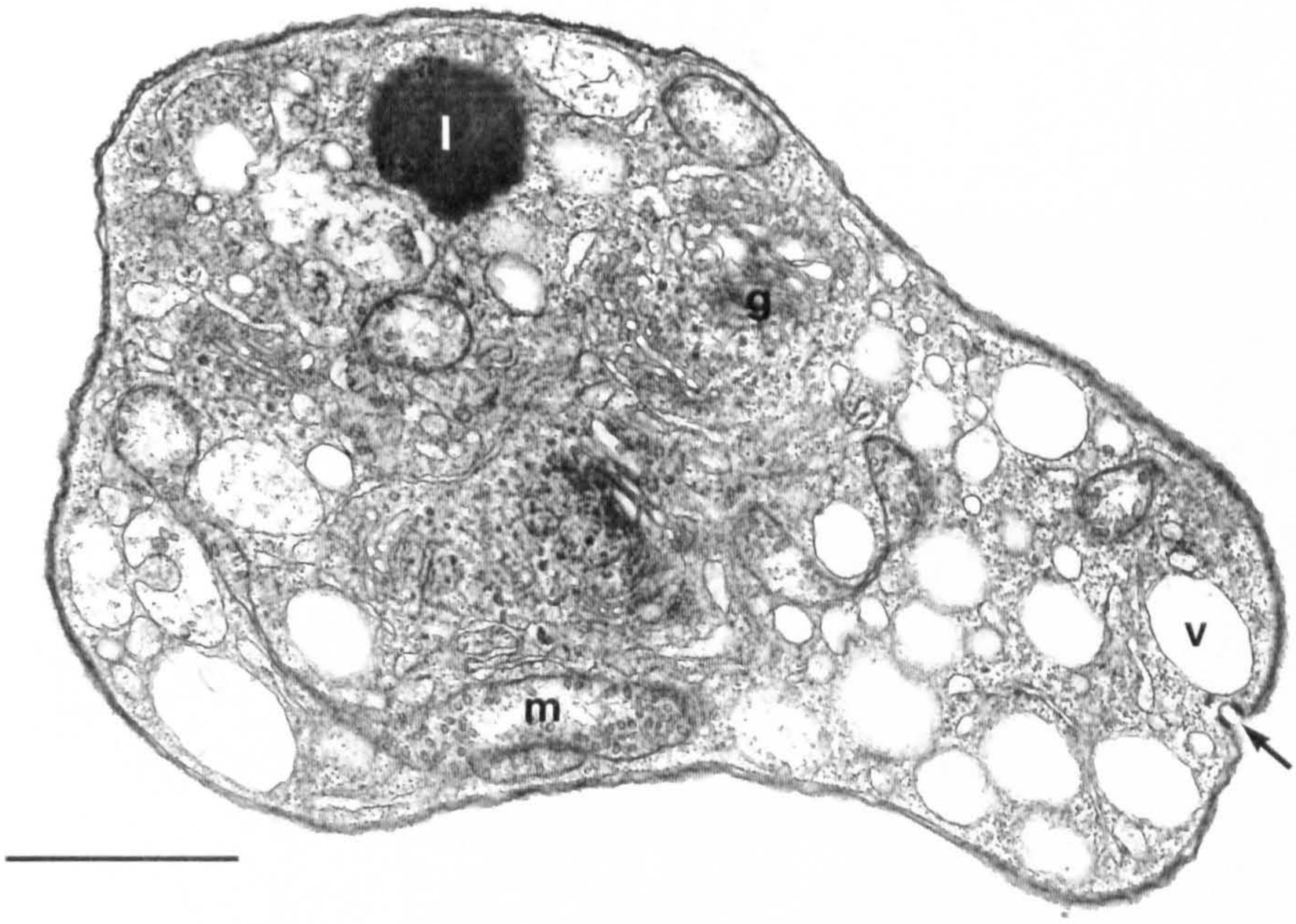
l
g
m
v

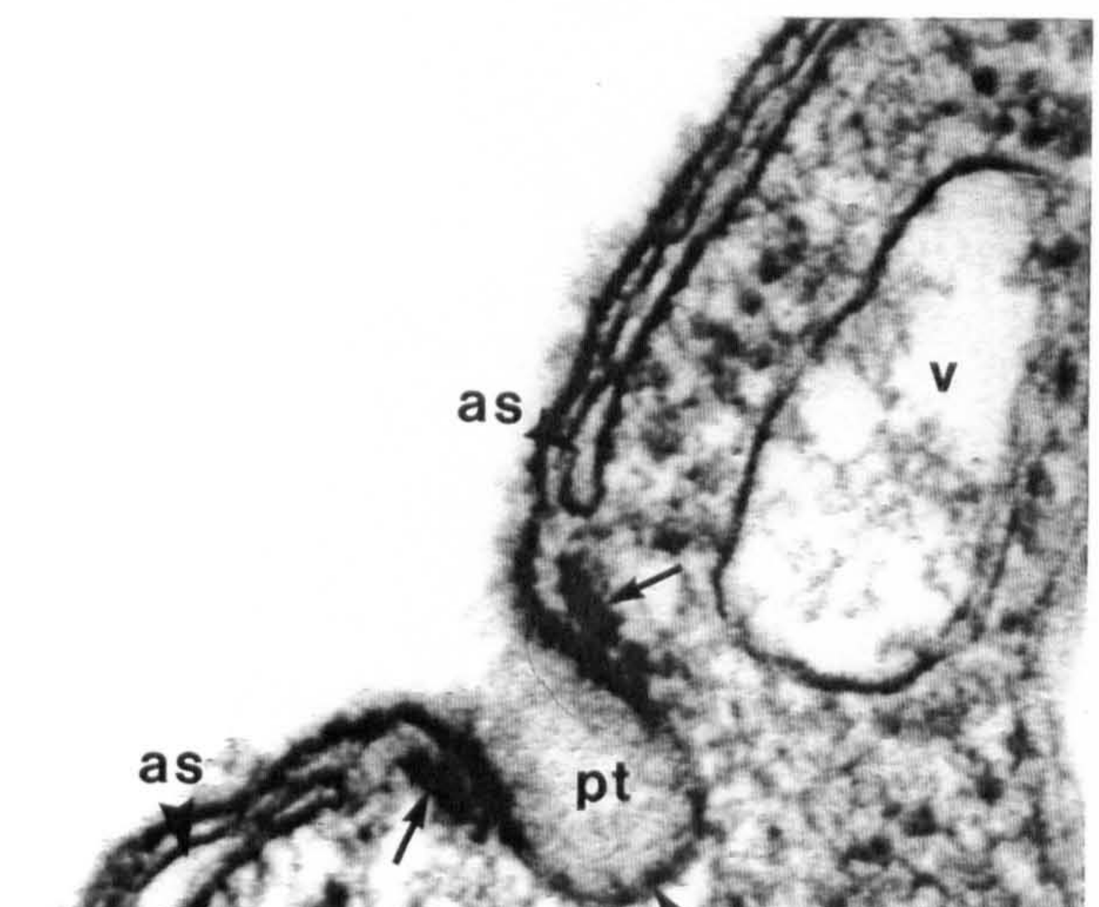
as
v
as
pt
pm
v

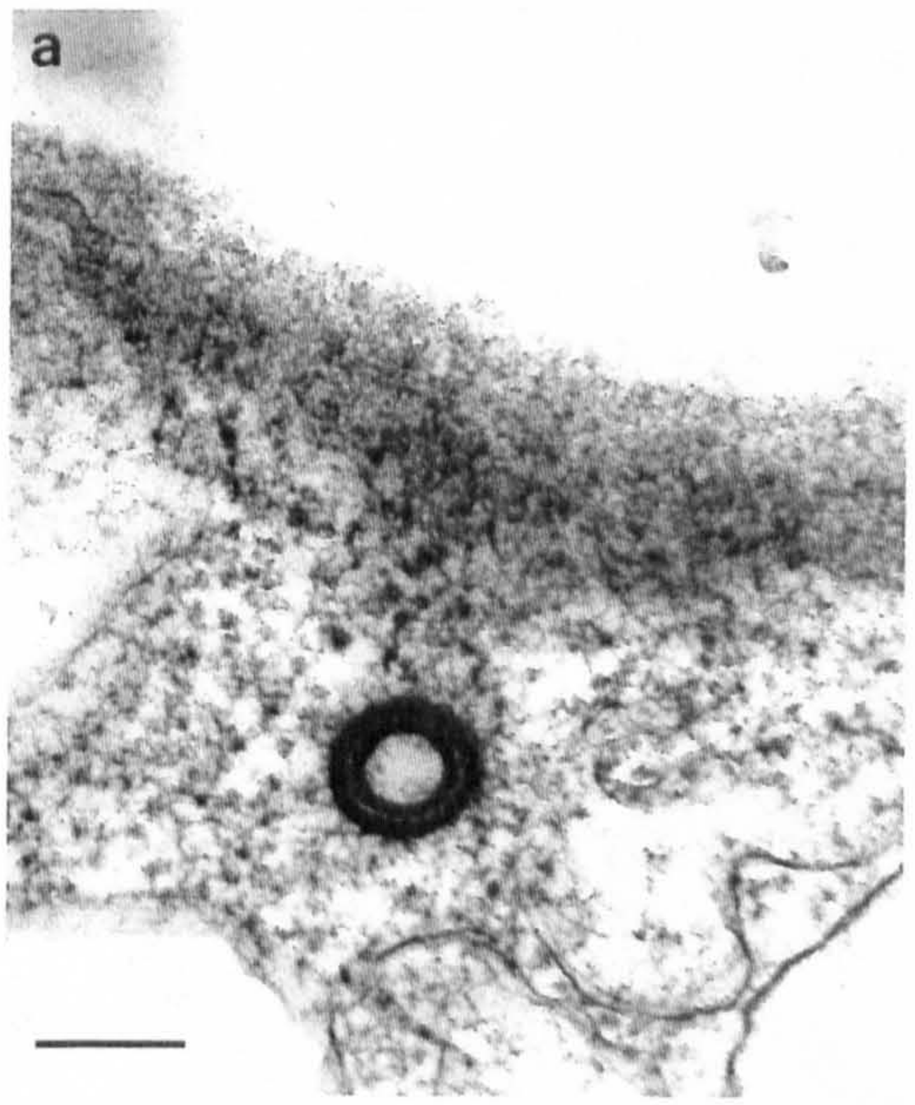
a

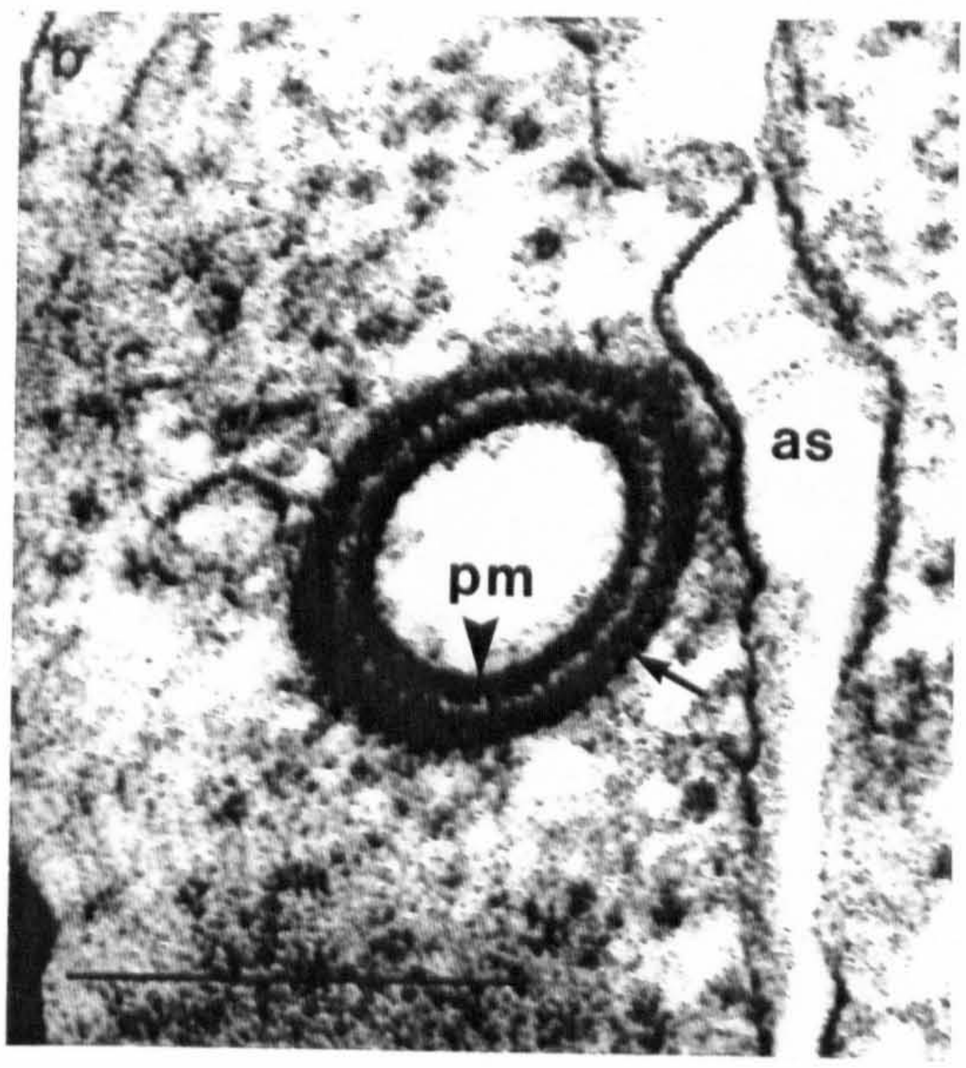
b
as
pm

**Figures 8.4-8.5.** Unstained sections of filamentous trophonts embedded in LR White resin, after incubating for 24h in colloidal gold suspension.

**Figure 8.4. (Left)** Three gold particles (arrow) are shown lodged in a micropore pit. n = nucleus. Scale bar = 0.5μm.

**Figure 8.5. (Right)** The vacuolated cytoplasm of a filamentous trophont, gold particles (arrows) are shown in two vacuoles. Scale bar = 0.5μm.

**Figures 8.6-8.7.** Transmission electron micrographs of long filamentous trophonts maintained in enriched culture medium.

**Figure 8.6. (Left)** A transverse section through a long filament, micropores are arrowed. pio = peripheral inclusion organelle. Scale bar = 5μm.

**Figure 8.7. (Right)** A vertical section through a micropore, the electron dense sleeve is arrowed. Numerous vacuoles (v) surround the micropore. Scale bar = 0.5μm.

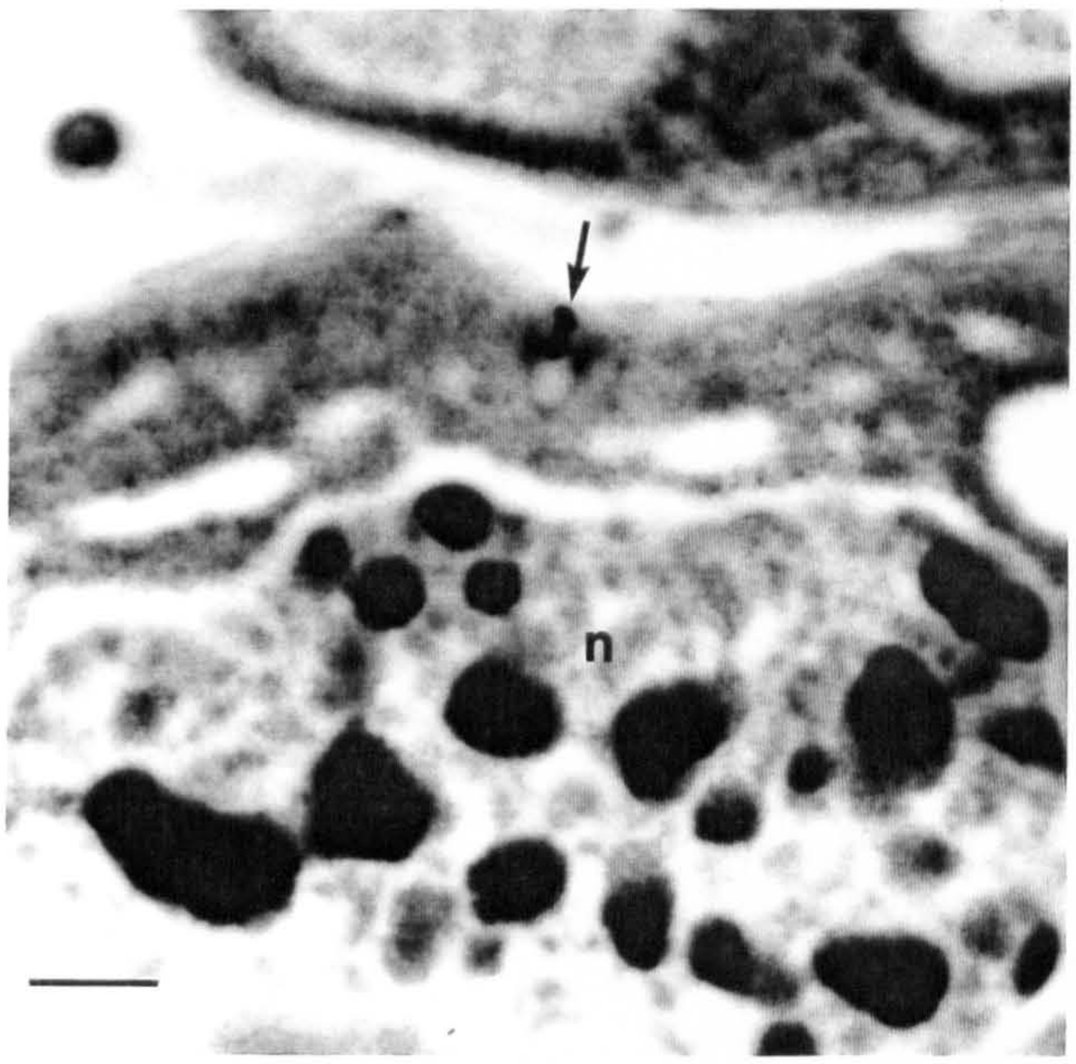
n

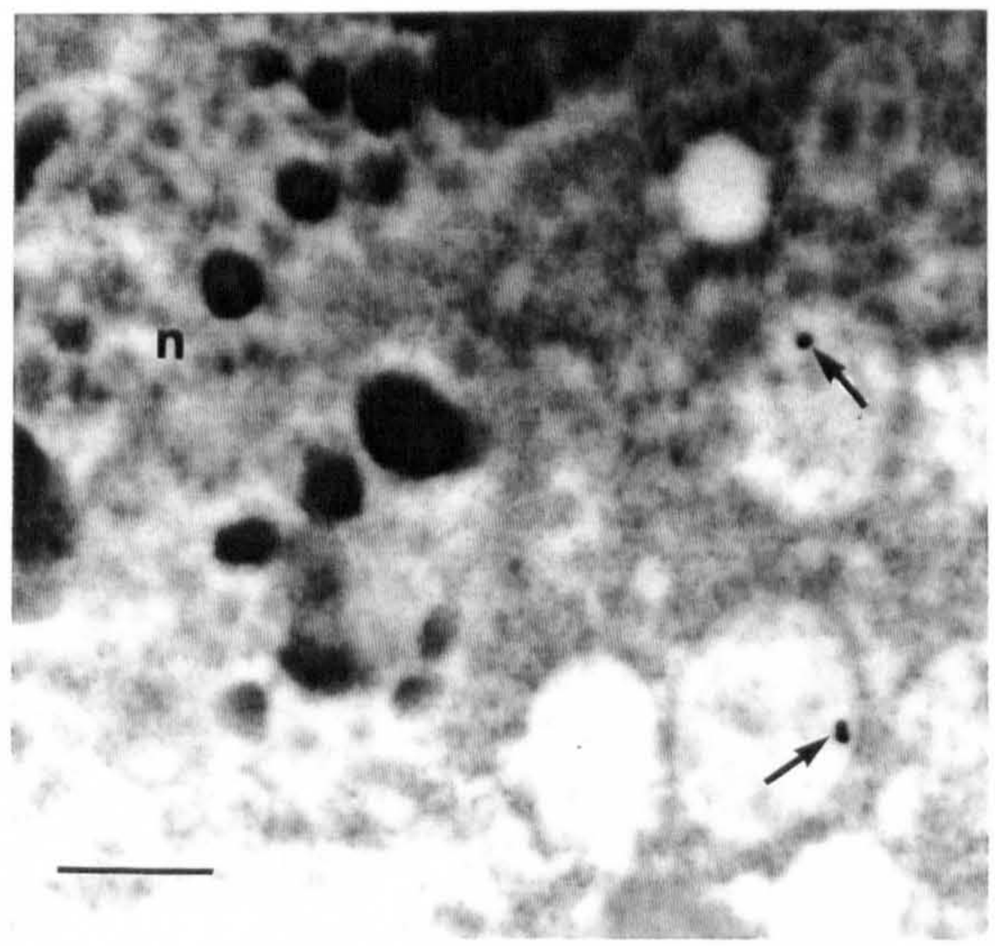
n

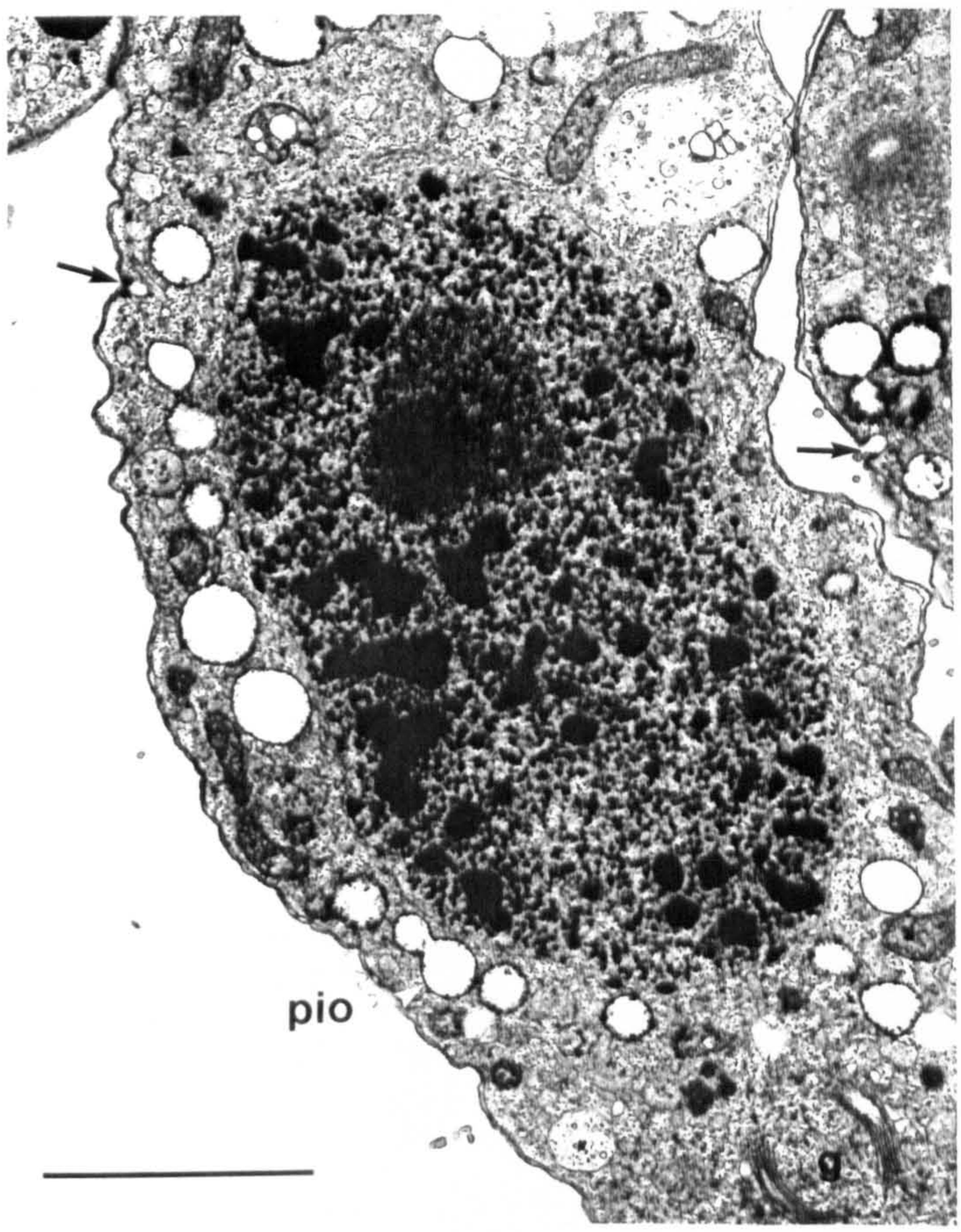
pio
g

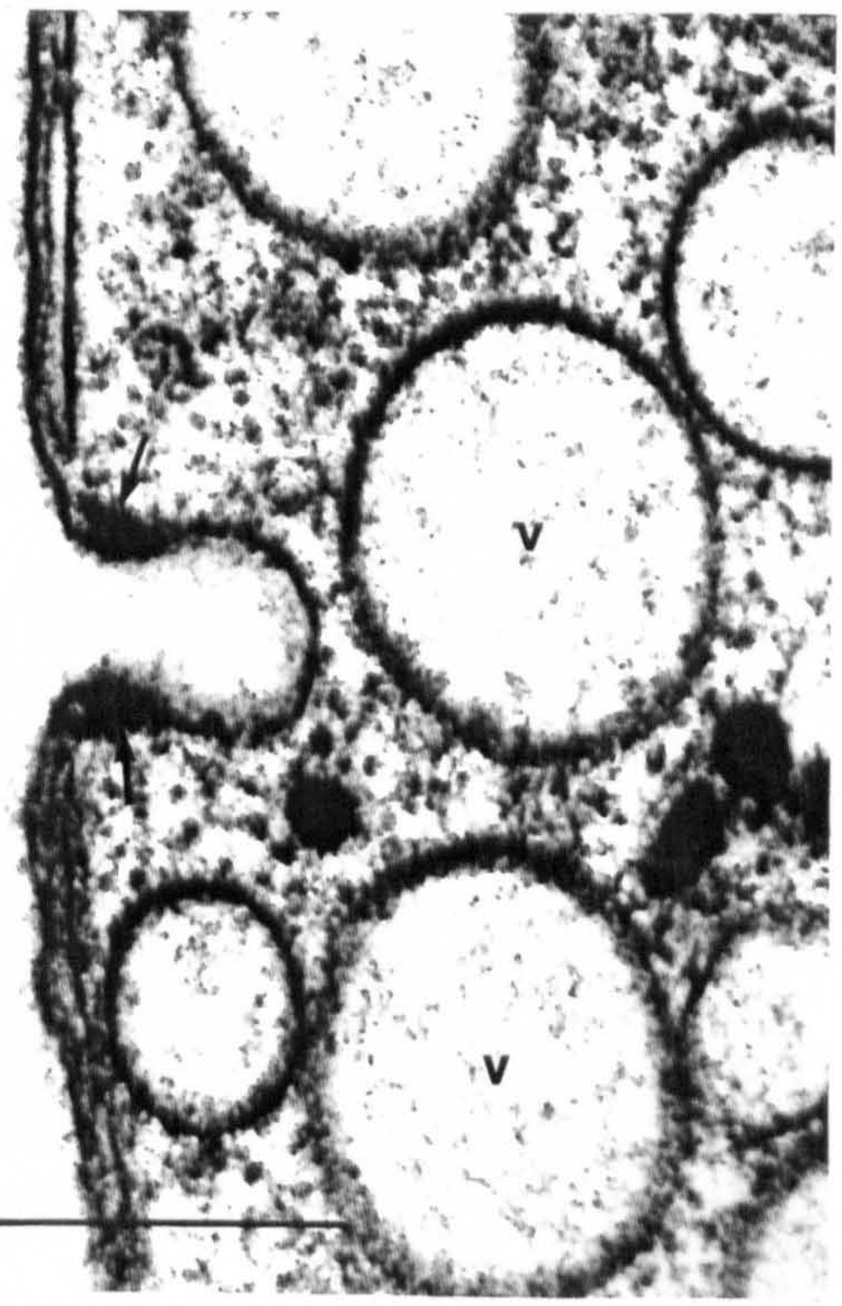
v
v

**Figures 8.8-8.10.** Transmission electron micrographs of sporoblasts found in the ovary of a stage III infected lobster.

**Figure 8.8. (Top)** The marked changes in the appearance of the chromosomes (ch) which become highly condensed (nucleus on the right) indicates that microsporogenesis is taking place. A micropore in a sporogenic cell is indicated by an arrow. tr = trichocysts, fv = flagellar hair vesicles. Scale bar = 5μm.

**Figure 8.9. (Left)** A sporoblast with a nucleus (n) containing highly condensed chromosomes. A micropore (arrow) is facing some host tissue (HT). tr = trichocyst. Scale bar = 0.5μm.

**Figure 8.10. (Right)** A vertical section through a micropore (arrow). The electron dense sleeve is just visible. Scale bar = 0.5μm.

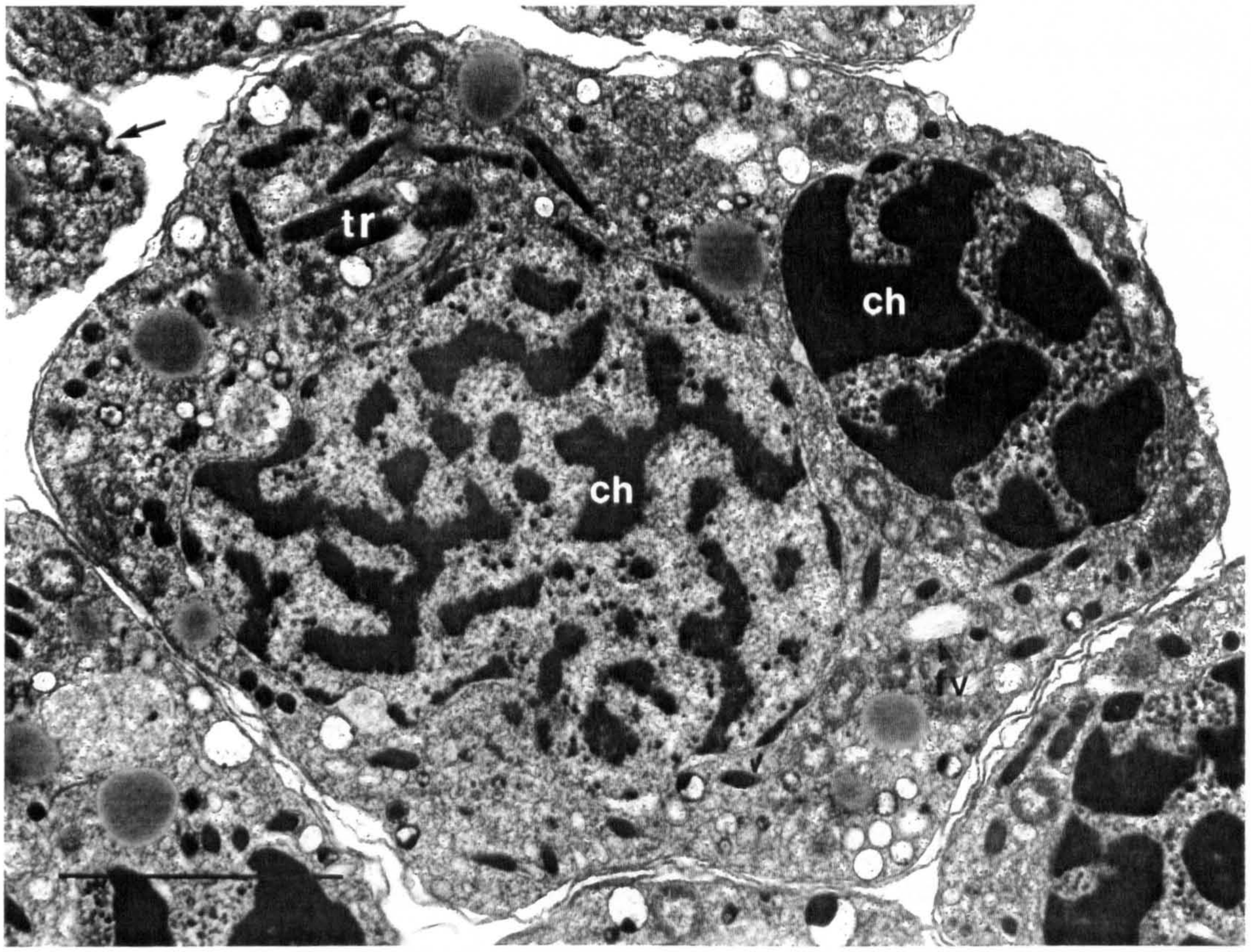
tr
ch
ch
IV
V


HT
tr
n

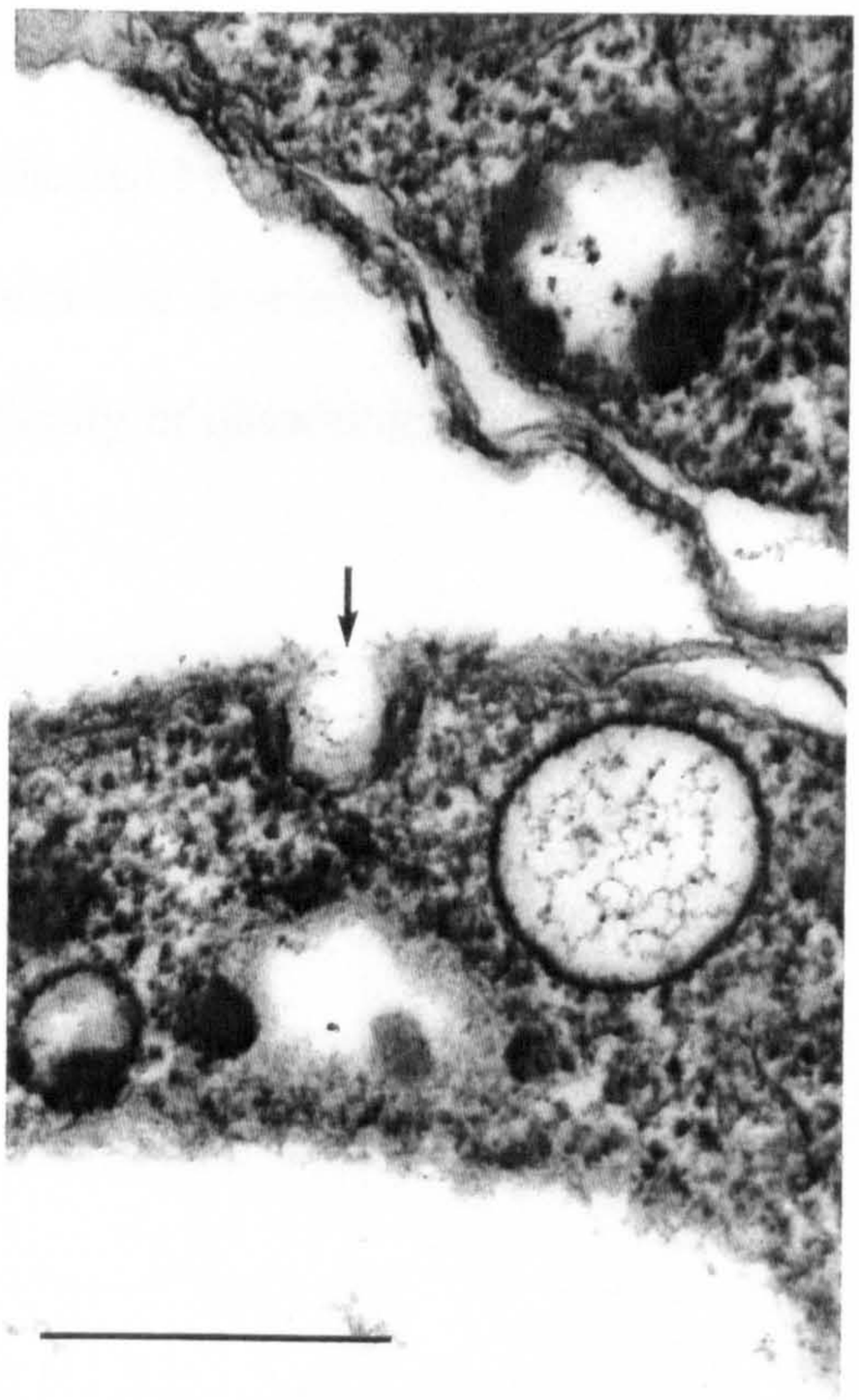

# CHAPTER 9
# GENERAL DISCUSSION

## 9.1. *In vitro* development

The *in vitro* culture of *Hematodinium* sp. from *Nephrops norvegicus* described in this thesis has made possible the elucidation of the life cycle of a syndinean dinoflagellate for the first time (Figure 9.1). The life cycle of protists consist of a series of developmental stages. Transition from one to the next may depend on induction by environmental stimuli or may be genetically programmed. In the case of environmentally induced change a commitment step may render the transition irreversible. For example the dinospore to trophont and sporoblast to dinospore transition changes appear to be irreversible. The trophont to sporont (arachnoid) transition appears to be reversible, until a stage of commitment to sporoblast production is reached. It is proposed that this commitment is indicated by production of flagellar hairs and trichocysts. Some of the transitions between one developmental form and another have not been fully confirmed due to the difficulty of observing these changes in asynchronous cultures.

I have shown that both types of dinospore are capable of germinating *in vitro* and give rise to similar developmental cycles. The functional significance of two spore types is not clear but it seems unlikely that they represent two species. It is possible that the two spore types develop at different rates within hosts, and may even have different means of entry into the host.

The long period between sporogenic events suggests that vital components may be in short supply or absent from the FCSG medium or the appropriate stimulus for differentiation into a sporogenic form is missing. Although the FCSG medium appears capable of supporting all developmental forms of *Hematodinium*, further changes to the culture conditions or medium constituents may encourage the production of sporogenic forms over a shorter time scale. Meyers *et al.* (1987) also suggested that prolonged *in vitro* maintenance of 'vegetative' stages slowed or altered their normal development towards sporulation.

The presence of micropores in both trophonts and sporogenic stages of *Hematodinium* is an important new morphological character to be found within the dinoflagellates. Although I have shown that the micropores are capable of taking up material from the surrounding medium it is not clear how important a role they play in the nutrition of the parasite. Filamentous trophonts grow in shoals towards the centre of the well plates with the gorgonlocks colonies usually at the periphery. If enzymes are secreted into the medium then the socialising habit of the trophonts will increase the effectiveness of the digestion per unit volume. Enrichment of the medium with amino acids changed the size and number of nuclei in the filamentous trophonts but did not accelerate the production of sporogenic forms of the parasite. This experiment illustrates, however, that parasite morphology can be manipulated by changing the medium.

## 9.2. *In vivo* development

Assuming that the dinospore is the infective stage of the parasite as has been demonstrated by Eaton *et al.* (1991) I have constructed a tentative life-cycle for

*Hematodinium* in *N. norvegicus* (Figure 9.2). Dinospores of both types give rise filamentous trophonts i*n vitro* and it seems reasonable to assume that they do so *in vivo* after infecting a lobster either through the gut or the cuticle. I suggest that the dinospore becomes lodged in a tissue, therefore escaping the attention of circulating haemocytes and fixed phagocytes associated with the hepatopancreas. The spore then germinates into a trophont while lodged in a tissue. The evidence collected so far supports this hypothesis; circulating filaments have only occasionally been observed in infected animals (Chatton and Poisson 1931). The evidence from the immunostaining described in Chapter 5 indicates that the earliest detectable infections are present in the tissues and not in the haemolymph. Filamentous trophonts multiply *in vitro* but the site of multiplication *in vivo* is unclear. It is possible that multiplication of the filamentous trophont is a short lived phase. It seems more likely that the trophonts lodged in tissues give rise to the circulating trophonts that are found in early haemolymph infections. The motility of filamentous trophonts that was observed *in vitro* may be of use in their migration through tissues *in vivo*. The existence of either the gorgonlocks or clump colonies *in vivo* is unknown, although branched filaments which may represent gorgonlocks colonies have been observed attached to tubules of the hepatopancreas (Chapter 5). The arachnoid syncytia develop flagellar hairs and trichocysts, transforming into sporonts. The accumulation of flagellar hairs and trichocysts in the arachnoid syncytium suggests that this is the stage responsible for the accumulation of host derived products into the organelles necessary for sporogenesis.

I propose that the sporonts release sporoblasts into the haemolymph, these are capable of attaching to tissue and forming secondary sporonts; sporoblasts can develop into secondary sporonts *in vitro*. The attached sporogenic columnar syncytia (Figure 5.9) observed in all patent infections could be attached secondary sporonts constrained

in their growth by the effects of crowding. Another possibility is that the columnar syncytia arise from an arachnoid base in the tissues, however no underlying parasite material has been found associated with them. When suitable sites for tissue invasion/attachment are no longer available the number of circulating sporoblasts increases and a patent infection results. Histological evidence (Chapter 5) shows that tissues can be heavily infiltrated with parasites in lobsters with a subpatent infection i.e. where there is a low density of parasites in the haemolymph.

The method by which *Hematodinium* gains nutrition from the host is not known. Circulating sporoblasts possess micropores which have been shown to participate in endocytosis. The possibility exists that *Hematodinium* secretes enzymes into the host which digest host tissues and the products are taken in by the parasite through the micropores. Phagocytosis of host tissues has not been observed in sections.

When large numbers of circulating sporoblasts fill the haemolymph and haemal spaces, sporogenesis occurs. The trigger for sporogenesis is not known, it may be a physiological trigger produced by *Nephrops* as a result of infection (anoxia, pH change) or may be parasite dependent (accumulation of sufficient energy reserves). Field *et al.* (1992, 1995) have shown that *Nephrops* with advanced stages of infection have significantly lower haemocyanin concentrations than healthy lobsters and hence the oxygen carrying capacity of infected haemolymph is significantly lower than that of healthy lobsters. Further experiments have shown that there was an increase in the total oxygen consumption of *Nephrops* after infection, but also an increase in the oxygen consumption of the haemolymph itself. The physiological studies show that infection must be a significant strain on the lobster because oxygen demand increases but the ability to supply it decreases. The physiological stress caused by oxygen and nutrient consumption by the parasite may explain why many infected lobsters cannot sustain the

parasite burden until sporogenesis is reached. It is not clear whether spore formation causes host death or impending host death triggers spore formation, but there is a clear link between the two.

## 9.3. Transmission of *Hematodinium*

The mode of transmission of the parasite from one host to another is one of the least known parts of the parasite life-cycle. Although dinospores are released from the dying host their destiny after that is unknown. Dinospores are capable of survival in seawater for several weeks (Chapter 4, Meyers *et al.* 1987); it is not known if dinospores encyst or directly infect another host. It has been shown by previous workers that 'vegetative' cells (trophonts) (Meyers *et al.* 1987), (sporoblasts) (Hudson and Shields 1994) and dinospores (Eaton *et al.* 1991) are infectious only when injected directly into a new host; infections have not been transmitted by cannibalism or exposure to free-swimming dinospores.

There are conflicting opinions as to the part played by the moult in the transmission of *Hematodinium* sp. Eaton *et al.* (1991) state that dinospores are not present during the ecdysial season of the Tanner crab (April-June); they are present later in summer, after ecdysis. Eaton and colleagues therefore suggest that because moulting and dinoflagellate sporulation do not overlap much, transmission of the parasite must be possible by a different route.

The peak occurrence of *Hematodinium* infection of *Nephrops* coincides with the main annual moult period. There are differences in the prevalence of infection between males and females with higher prevalence in females and smaller lobsters (Field *et al.* 1992). Female *Nephrops* moult before males in the early spring; small males moult in

the late spring to early summer and larger males in the autumn. Therefore most females will be exposed to dinospores during the peak season of prevalence when dinospore release has been observed. Males are exposed to dinospores to a lesser extent because they moult later. The larger males which moult in the autumn, when sporulation does not occur, are not exposed to dinospores and subsequently have very low infection prevalence. Smaller lobsters moult more frequently than larger lobsters and this may explain why smaller lobsters have a higher prevalence of infection. The pattern of moulting and infection distribution within the *Nephrops* population and the seasonality of *Hematodinium* infection suggests a link between moult and infection of *Nephrops*, although this has yet to be proven.

Another possible route for transmission of the parasite to a new host other than through the cuticle is by ingestion of parasite. Ingestion of parasite could be through the cannibalism of infected *Nephrops* or through consuming another host species (not yet found). If infection occurred through ingestion of infective parasite then all lobster size ranges and sexes would be equally exposed and would express similar infection prevalences - and this has been shown not to be the case (Field *et al.* 1992, 1995).

## 9.4. Seasonality

Lack of firm data on the transmission of the infection limits explanations for the seasonality of the disease to hypotheses. I suggest that the dinospores are the infective stage of the parasite which infect healthy lobsters in postmoult. For a few days after lobsters have moulted their new cuticle remains very soft, providing less of a barrier against invading organisms. If dinospores are the infective developmental form then all

infections are initiated during the patent disease season from about January until June when dinospores are present.

I have shown that all lobsters which harbour a prepatent infection in the autumn develop a patent infection the following winter/spring. What is not yet clear is how long the latent period lasts. The latent period will be the time from initial infection when parasite is present only in the tissues until the time when parasite disseminates into the haemolymph (patency). The latent period may be only weeks/months long or could possibly be a year or longer. It is only the ability to infect healthy hosts in the laboratory that would provide this information.

The evidence I have presented in this thesis suggests that an annual cycle of *Hematodinium* exists. It is not clear if some lobsters become infected and develop the disease within a single season. In Chapter 4 I suggested that macrospore could carry the infection from year to year and the microspore is capable of transmitting the parasite to new hosts within a single season. The evidence from a study on *Hematodinium* in the Tanner crab would not fit in with this hypothesis because it suggests an annual cycle for infections produced by both dinospore types (Eaton *et al.* 1991). If it is the case that both dinospore types produce an annual cycle of infection then the question of why the two dinospore types remains unanswered.

This work represents a contribution to our knowledge of the largely unexplored realm of parasitic dinoflagellates. There are still many questions that remain to be answered of the genus *Hematodinium*, which are increasingly recognised as both scientifically and commercially important parasites.

**9.1.** Schematic developmental cycle of *Hematodinium in vitro*.

**1.** Sporoblasts circulating in *Nephrops* haemolymph are used to initiate the culture.

**2.** Sporoblasts either attach to substratum and form secondary sporonts or they form an aggregation without attachment.

**3.** Secondary sporont and aggregation of sporoblasts disintegrate into individual sporoblasts.

**4.** Sporoblasts develop flagella and through a series of uneven divisions give rise to either macro- or microspores.

**5.** After several weeks dinospores of both types lose their flagella and germinate into trophonts. Trophonts multiply as a result of branching and fission of branches and can be maintained indefinitely *in vitro*.

**6.** Gorgonlock colonies develop when the branches of the filamentous trophont fail to undergo fission.

**7.** Clump colonies appear to be formed by condensation and imbrication of gorgonlocks so that spherical masses are generated.

**8.** Clump colonies can resolve into trophonts upon transfer into fresh medium.

**9.** Alternatively clump colonies can attach to the substratum by their filopodia-like extensions and develop into sporonts.

**10.** Trophonts are able to attach to the substratum and develop into sporonts.

**11.** The quick appearance of sporonts soon after germination, especially in microspore derived cultures suggests that the spherical trophont precursors which occur at germination may be able to develop directly into sporonts.

**12.** It is not yet clear if sporonts are able to revert back into trophonts but this remains a possibility.

**13.** Sporonts become recognisably sporogenic when they develop a crater-like nucleated mass of cytoplasm at their centre.

**14.** Sporoblasts are released from the central mass of nucleated cytoplasm and either form aggregates or remain separated. Sporoblasts give rise to dinospores as described above.

Dashed arrow represents an unproven developmental route.

Illustrations are not to a comparable scale.

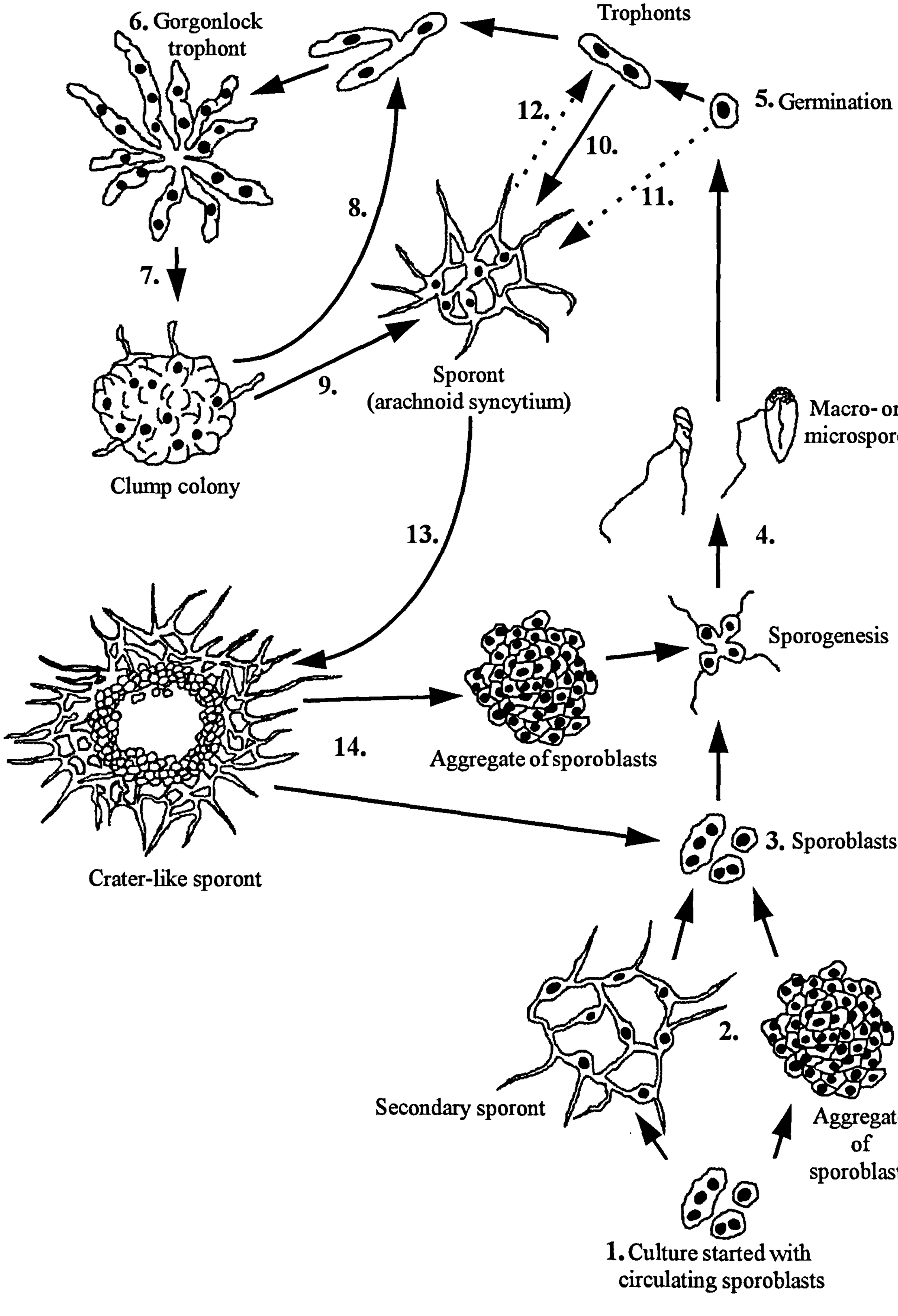
Trophonts
6. Gorgonlock trophont
5. Germination
12.
10.
11.
8.
7.
9.
Sporont (arachnoid syncytium)
Clump colony
Macro- or microspore
4.
13.
Sporogenesis
14.
Aggregate of sporoblasts
Crater-like sporont
3. Sporoblasts
Secondary sporont
2.
Aggregate of sporoblasts
1. Culture started with circulating sporoblasts

**9.2.** Hypothetical developmental cycle of *Hematodinium* in *Nephrops*.

**1.** Dinospores of both types can enter the host and germinate into trophonts.

**2.** *In vitro* observations show that arachnoids (primary sporonts) can develop soon after germination. It seems likely that primary sporonts can develop from both the spherical precursors to filamentous trophonts and the short filaments themselves. The fact that the earliest infections I have so far detected have been found only in the tissues - not in the haemolymph suggests that germination occurs in the tissues. *In vitro* cultures give rise quickly to both trophonts and primary sporonts upon germination, suggesting the formation of a trophont and sporont population early in the infection.

**4.** Primary sporonts give rise to circulating sporoblasts.

**5.** I suggest that the trophonts embedded in tissues branch and divide, releasing trophonts into the circulating haemolymph.

**6.** Trophonts are able to infiltrate tissues and develop into attached primary sporonts.

**7.** In *in vitro* culture sporoblasts are capable of producing attached secondary sporonts (arachnoid syncytia). I propose that the sporogenic columnar syncytia found *in vivo* (chapter 5) are also secondary sporonts which have this appearance because of the confined spaces in which they grow. When all suitable sites for attachment to tissues are taken sporoblasts remain in circulation and the haemolymph infection increases producing a patent infection.

**8.** When the parasitaemia reaches a peak the attached primary and secondary sporonts disperse entirely into sporoblasts which develop flagella.

9. The flagellated prespores divide and give rise to either macro- or microspores.

**10.** Dinspores escape from the lobster into the gill chambers and are dispersed by the exhalent seawater currents. After 18-24 hours all the dinospores have been released from the host and the host dies. Dinospores do not encyst and there is no known intermediate host. It is thought that dinospores remain free-living until able to infect another *Nephrops*.

I have not included clump colonies in this scheme because this developmental form has not yet been found *in vivo*. This form could be an artifact of *in vitro* culture methods.

Dashed arrow represents an unproven developmental route.

Illustrations are not to a comparable scale.

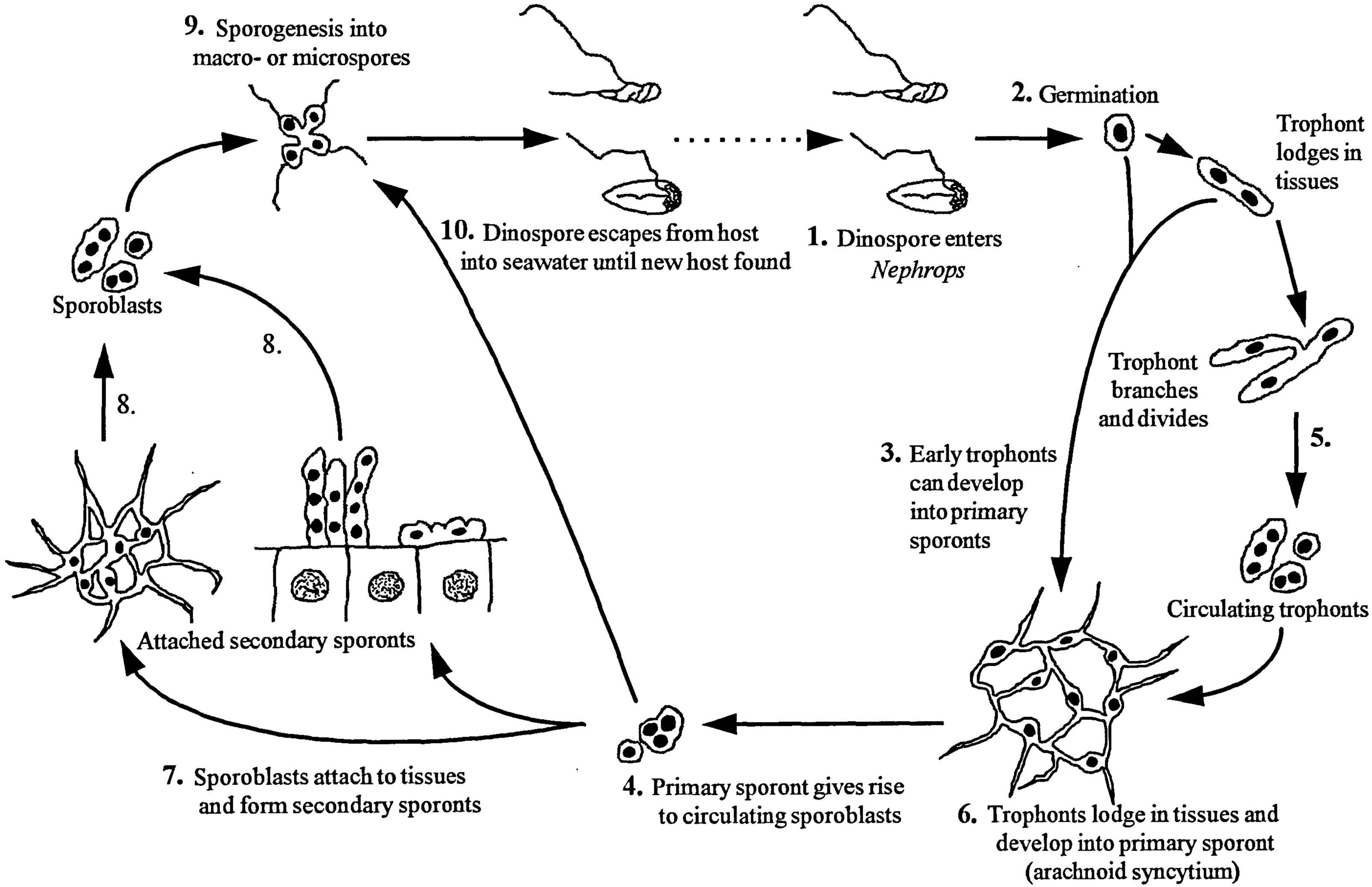
9. Sporogenesis into macro- or microspores
10. Dinospore escapes from host into seawater until new host found
1. Dinospore enters *Nephrops*
2. Germination
Trophont lodges in tissues
Trophont branches and divides
5.
3. Early trophonts can develop into primary sporonts
Circulating trophonts
Sporoblasts
8.
8.
Attached secondary sporonts
7. Sporoblasts attach to tissues and form secondary sporonts
4. Primary sporont gives rise to circulating sporoblasts
6. Trophonts lodge in tissues and develop into primary sporont (arachnoid syncytium)

# REFERENCES

**Adoutte, A.** (1988) Exocytosis: biogenesis, transport and secretion of trichocysts. In, Görtz, H.-D. (ed.) Paramecium. Springer-Verlag, Berlin-Heidelberg. pp. 325-362

**Aiken, D. E.** (1980) Moulting and Growth. In: Cobb, J. S. and Phillips, B. F. (eds.) The Biology and Management of Lobsters. Vol. 1. Academic Press, New York. p. 91-163

**Bauchau, A.G.** (1981) Crustaceans, In N.A. Ratcliffe and A.F. Rowley (eds): Invertebrate Blood Cells. London and New York: Academic Press, Vol.2, pp. 385-420.

**Bower, S.M., Meyer, G.R. and Boutillier, J.A.** (1993) Diseases of spot prawns *Pandalus platyceros* caused by an intracellular bacterium and a *Hematodinium*-like Protozoa. J. Shellfish Res. 12: 135

**Cachon, J., Cachon, M.** (1968) Cytologie et cycle évolutif des *Chytriodinium* (Chatton). Protistologica 4: 249-262

**Cachon, J., Cachon, M.** (1987) Parasitic Dinoflagellates. In: Taylor, F.J.R. (ed.) The Biology of Dinoflagellates, Blackwell Scientific, Oxford, UK, pp. 571-610.

**Cavalier-Smith, T.** (1981) Eukaryote kingdoms: seven or nine? Biosystems. 14: 461-481

**Cavalier-Smith, T.** (1993) Kingdom Protozoa and its 18 phyla. Microbiol Rev 57: 953-994

**Chatton, É.** (1906) Les Blastodinides, ordre nouveau de Dinoflagellés parasites. C. R. Hebd. Séanc. Acad. Sci., Paris 143: 981-983

**Chatton, É.** (1920) Les Péridiniens parasites: morphologie, reproduction, ethology. Arch. Zool. Exp.Gen. 59: 1-475

**Chatton, É.** (1923) Les Péridiniens parasites des Radiolaires. C. R. Hebd. Séanc. Acad. Sci., Paris. 177: 1246

**Chatton, É.** (1938) Titres et travaux scientifiques (1906-1937), 1-406. Sottano, Séte.

**Chatton, É.** (1952) Classe des Dinoflagelles ou Péridiniens. In: Grassé, P.-P. (ed.) Traité de Zoologie, Vol. 1. Masson et Cie, Paris, pp. 309-390

**Chatton, É., Hovasse, H.** (1938) *Actinodinium apsteini* n. g., n. sp. Péridinien parasite entérocoelomique des *Acartia* (Copépodes). Arch. Zool. Exp. Gen. 79: 24-29

**Chatton, É., Poisson, R.** (1931) Sur l'existence, dans le sand des Crabes, de Péridiniens parasites: *Hematodinium perezi* n. g., n. sp. (Syndinidae). C. R. Seances Soc. Biol., Paris 105: 553-557.

**Cooper-Willis, C.A.** (1979) *In vivo* clearance by fixed cells in the grass shrimp, *Palaemonetes intermedia*. Am. Zool. 19: 877

**Cornick, J.W. and Stewart, J.** (1968) Interaction of the pathogen *Gaffkya homari* with natural defense mechanisms of *Homarus americanus*. J. Fish. Res. Bd. Canada. 25: 695-709

**Cuénot, L.** (1905) L'organe phagocytaire des Crustacés Décapodes. Arch. Zool. Exp. Gén., Sér. 4,3: 1-16

**Dodge, J.D.** (1967) Fine structure of the dinoflagellate *Aureodinium pigmentosum* gen. et sp. nov. Br. phycol. Bull. 3: 327-336

**Dodge, J.D. and Crawford, R.M.** (1968) Fine structure of the dinoflagellate *Amphidinium carteri* Hulbert. Protistologica. 4: 231-242

**Drebes, G.** (1978) *Dissodinium pseudolunula* (Dinophyta), a parasite on copepod eggs. Br. Phycol. J. 13: 319-327

**Drebes, G.** (1981) Possible resting spores of *Dissodinium pseudolunula* (Dinophyta) and their relation to other taxa. Br. Phycol. J. 16: 207-215

**Drebes, G.** (1984) Life cycle and host specificity of marine parasitic dinophytes. Helgoländer Meeresunters. 37: 603-622

**Eaton, W.D., Love, D.C., Botelho, C., Meyers, T.R., Imamura, K. and Koeneman, T.** (1991) Preliminary results on the seasonality and life cycle of the parasitic dinoflagellate causing bitter crab disease in Alaskan tanner crabs (*Chionoecetes bairdi*). J. Invertebr. Pathol. 57: 426-434

**Fensome, R.A., Taylor, F.J.R., Norris, G., Sergeant, W.A.S., Wharton, D.I. and Williams, G.L.** (1993) A classification of living and fossil dinoflagellates. Micropaleontology, Special Publ. No.7

**Ferguson, D.J.P., Birch-Anderson, A., Hutchison W.M. and Siim J.C.** (1977) The ultrastructure and distribution of micropores in the various developmental forms of *Eimeria brunetti.* Acta path microbiol scand.Sect B 85: 363-373

**Field, R.H.** (1992) The control of escape behaviour in, and the histopathology of, the Norway lobster, Nephrops norvegicus (L.). PhD Thesis, University of Glasgow.

**Field, R.H., Chapman, C.J., Taylor, A.C., Neil, D.M. and Vickerman, K.** (1992) Infection of the Norway lobster *Nephrops norvegicus* by a *Hermatodinuim*-like species of dinoflagellate on the west coast of Scotland. Dis. aquat. Org. 13: 1-15

**Field, R.H., Appleton, P.L., Vickerman, K., Atkinson, R.J.A., Taylor, A.C., Rogerson, A., Neil, D.M., Shanks, A.** (1995) Mortality of *Nephrops norvegicus* on the West Coast of Scotland. Project Ref: CSA 2139. Report to the Ministry of Agriculture Fisheries and Food. 76 pp.

**Field, R.H. and Appleton, P.L.** (1995) A *Hematodinium*-like dinoflagellate infection of the Norway lobster *Nephrops norvegicus*: observations on pathology and progression of infection. Dis. aquat. Org. 22: 115-128

**Gajadhar, A.A., Marquardt, W.C., Hall, R., Gunderson, J., Ariztia-Carmona, E.V. and Sogin, M.L.** (1991) Ribosomal RNA sequences of *Sarcocystis muris, Theileria annulata* and *Crypthecodinium cohnii* reveal evolutionary relationships among apicomplexans, dinoflagellates and ciliates. Mol biochem Parasitol. 45: 147-154

**Gardner, M.J., Feagin, J.E., Moore, D.J., Rangachari, K., Williamson, D.H. and Wilson, R.J.M.** (1993) Sequence and organisation of large subunit rRNA genes from the extra-chromosomal 35kb circular DNA of the malaria parasite *Plasmodium falciparum*. Nucl Acid Res. 21: 1067-1071

**Goldenberg, P.Z., Huebner, E., and Greenberg, A.H.** (1984) Activation of lobster hemocytes for phagocytosis. J. Invert. Pathol. 43: 77-88

**Haacke-Bell, B., Hohenberger-Bregger, R., Plattner, H.** (1990) Trichocysts of *Paramecium*: secretory organelles in search of their function. Europ. J. Protistol., 25, 289-305

**Harlow, E. and Lane, D.P.** (1988) Antibodies: a Laboratory Manual. Cold Spring Harbor Laboratory. Cold Spring Harbor.

**Hausmann, K.** (1978) Extrusive organelles in protists. Int. Rev. Cytol., 52: 197-276

**Hollande, A.** (1974) Étude comparée de la mitose syndinienne et de celle des péridiniens libres et des Hypermastigines infrastructure et cycle évolutif des Syndinides parasites de Radiolaires. Protistologica. 10: 413-451

**Hollande, A. and Enjumet,** (1953) Contribution à l'étude des Sphaerocollides et de leurs parasites. Ann. Sci. Nat. Zool. Biol. Anim. 15: 405

**Hollande, A. and Enjumet,** (1955) Parasites et cycle évolutif des Radiolaires et des Acanthaires. Bull. Stat. Aquic. et Pêche Castiglione. 7: 153

**Hoover, K.L.** (1977) The Effect of a Virus Infection on the Hemocyte Population in *Carcinus maenas*. Sc.D. Thesis, Johns Hopkins University.

**Hudson, D.A., Hudson, N.B. and Shields, J.D.** (1993) Infection of *Trapezia* spp. (Decapoda: Xanthidae) by *Hematodinium* sp. (Duboscquodinida: Syndinidae): a new family record of infection. J. Fish. Dis. 16: 273-276

**Hudson, D.A., Lester, R.J.G.** (1994) Parasites and symbionts of wild mud crabs *Scylla serrata* (Forskal) of potential significance in aquaculture. Aquaculture. 120: 183-199

**Hudson, D.A., Shields, J.D.** (1994) *Hematodinium australis*, n. sp., a parasitic dinoflagellate of the sand crab, *Portunus pelagicus*, and the mud crab, *Scylla serrata*, from Moreton Bay, Australia. Dis. aquat. Orgs. 19: 109-119

**Ianora, A., Mazzocchi, M.G., Scotto di Carlo, B.** (1987) Impact of parasitism and intersexuality on Mediterranean populations of *Paracalanus parvus* (Copepoda: Calanoida). Dis. Aquat. Orgs. 3: 29-36

**Ianora, A., Scotto di Carlo, B., Mazzocchi, M.G., Mascellaro, P.** (1990) Histomorphological changes in the reproductive condition of parasitized marine planktonic copepods. J. Plankt. Res. 12: 249-258

**Jepps, M.W.** (1937) On the protozoan parasites of *Calanus finmarchicus* in the Clyde Sea area. Quart. J. Microsc. Sci. 79: 589-658

**John, A.W.G., Reid, P.C.** (1983) Possible resting cysts of *Dissodinium pseudolunula* Swift ex Elbrächter et Drebes in the Northeast Atlantic and the North Sea. Br. Phycol. J. 18: 61-67

**Johnson, P.T.** (1976). Bacterial infection in the blue crab, *Callinectes sapidus*: course of infection and histopathology. *J. Invertebr. Pathol.* **28:** 25 - 36

**Johnson, P.T.** (1980) Histology of the blue crab, *Callinectes sapidus*. A model for the Decapoda. Praeger, New York.

**Johnson, P.T.** (1986) Parasites of benthic amphipods: dinoflagellates (Duboscquodinida: Syndinidae). Fish. Bull. 84: 605-614

**Johnson, P.T.** (1987) A review of fixed phagocytic and pinocytotic cells of decapod crustaceans, with remarks on hemocytes. Dev. Comp. Immunol. 11: 679-704

**Johnson, P.T., Stewart, J.E. and Arie, B.** (1981) Histopathology of *Aerococcus viridans* var. *homari infection* (Gaffkemia) in the lobster, *Homarus americanus*, and a comparison with histological reactions to a Gram-negative species *Pseudomonas perolens*. J. Invertebr. Pathol. 38: 127-148

**Kimmerer, W.J., McKinnon, A.D.** (1990) High mortality in a copepod population caused by a parasitic dinoflagellate. Mar. Biol. 107: 449-452

**Knoll, G., Haacke-Bell, B., Plattner, H.** (1991) Local trichocyst exocytosis provides an efficient escape mechanism for *Paramecium* cells. Europ. J. Protistol. 27: 381-385

**Koch, R.** (1891) eber bakteriologische Forschung. Verhandlungen X International Medizinisch Kongress 1890, 1. Hirschwald, Berlin.

**Kubai, D.F., Ris, H.** (1969) Division in the Dinoflagellate, Gyrodinium cohnii (Schiller). A new type of nuclear reproduction. J. Cell. Biol. 40: 508-528

**Latrouite, D., Morizur, Y., Noel, P., Chagot, D. and Wilhelm, G.** (1988) Mortalité du torteau *Cancer pagurus* provoquée par le dinoflagelle parasite: *Hematodinium* sp. I. C. E. S. C. M. 1988/K:32 (mimeo)

**Leadbeater, B.S.C.** (1971) The intracellular origin of flagellar hairs in the dinoflagellate *Woloszynskia micra* Leadbeater and Dodge. J. Cell Sci. 9: 443-451

**Livolant, F.** (1982) Dinoflagellate trichocyst ultrastructure. I. The Shaft. Biol. Cell. 43: 201-210

**Love, D.C., Rice, S.D., Moles, D.A. and Eaton, W.D.** (1993) Seasonal prevalence and intensity of Bitter Crab dinoflagellate infection and host mortality in Alaskan tanner crabs *Chionoecetes bairdi* from Auke Bay, Alaska, USA. Dis. aquat. Org. 15: 1-7

**Maclean, S.A. and Ruddell, C.L.** (1978) Three new crustacean hosts for the parasitic dinoflagellate *Hematodinium perezi* (Dinoflagellata: Syndinidae). J. Parasitol. 64: 158-160

**Manier, J-F., Fize, A. and Grizel, H.** (1971) *Syndinium gammari* n. sp. pèridinien Duboscquodinida syndinidae, parasite de *Gammarus locusta* (Lin.) Crustacè Amphipode. Protistologica. VII (2) : 213-219

**Marks, L.J., Stewart, J.E. and Håstein, T.** (1992) Evaluation of and indirect fluorescent antibody technique for detection of *Aerococcus viridans* (var.) *homari*, pathogen of homarid lobsters. Dis. aquat. Org. 13: 133-138

**Marshall, S.M., Nicholls, A.G., Orr, A.P.** (1934) On the biology of *Calanus finmarchicus*. V. Seasonal distribution, size, weight and chemical compositionin Loch Striven in 1933 and their relation to the phytoplankton. J. Mar. Biol. Assoc. UK. 19: 793-819

**Maupas, E.** (1883) Contribution à l'étude morphologique et anatomique des infussoires ciliés. Arch. Zool. Exp. Gen. 1: 427-664.

**McCumber, L.J. and Clem, L.W.** (1983) Recognition of non-self in crustaceans. Am. Zool. 23: 173-183

**Messick, G.A.** (1994) *Hematodinium perezi* infections in adult and juvenile blue crabs *Callinectes sapidus* from coastal bays of Maryland and Virginia, USA. Dis. aquat. Org. 19: 77-82

**Meyers, T.R.** (1990) Disease of Crustacea - Diseases caused by protistans and metazoans. In: Kinne, O. (ed.) Diseases of Marine Animals. Vol. 3. Biologische Anstalt Helgoland, Hamburg. p. 350-389

**Meyers, T.R., Koeneman, T.M., Botelho, C. and Short, S.** (1987) Bitter Crab Disease: A fatal dinoflagellate infection and marketing problem for Alaskan tanner crabs *Chionoecetes bairdi.* Dis. aquat. Org. 3: 195-216

**Meyers, T.R., Botelho, C., Koeneman, T.M., Short, S. and Imamura, K.** (1990) Distribution of bitter crab dinoflagellate syndrome in southeast Alaskan tanner crabs *Chionoecetes bairdi.* Dis. aquat. Org. 9: 37-43

**Meyers, T., Lightner, D.V. and Redman, R.M.** (1994) A dinoflagellate-like parasite in Alaskan spot shrimp *Pandalus platyceros* and pink shrimp *P.borealis*. Dis. aquat. Orgs. 18:71-76

**Newman, M.W. and Johnson, C.A.** (1975) A disease of blue crabs (*Callinectes sapidus*) caused by a parasitic dinoflagellate, *Hematodinium* sp. J. Parasitol. 61: 554-557

**Nilsson, J.R. and Van Deuers, B.** (1983) Coated pits and pinocytosis in *Tetrahymena*.J Cell Sci. 63: 209-222

**Oakley, B., Dodge, J.D.** (1974) Kinetochores associated with the nuclear envelope in the mitosis of a dinoflagellate. J. Cell. Biol. 63: 322-325

**Olliaro, P.L. and Goldberg, D.E.** (1995) The *Plasmodium* digestive vacuole: metabolic headquarters and choice drug target. Parasitology Today 11: 294-297

**Pasternak, A.F., Arashkevich, Y.G., Sorokin, Y.S.** (1984) The role of parasitic algal genus *Blastodinium* in the ecology of planktic copepods. Oceanology. 24: 748-751

**Patterson, W.D. and Stewart, J.E.** (1974) In vitro phagocytosis by hemocytes of the American lobster (*Homarus americanus*). J. Fish.Res. Bd. Canada. 31: 1051-1056

**Patterson, W.D., Stewart, J.E. and Zwicker, B.M.** (1976) Phagocytosis as a cellular immune response mechanism in the American lobster, *Homarus americanus*. J. Invert. Pathol. 27: 95-104

**Pouchet, G.** (1884) Sur en Péridinien parasite. C. R. Acad. sci. Paris, 98, 1345-1346

**Pringsheim, E.G.** (1956) Micro-organisms from decaying seaweed. Nature. 178: 480-481

**Provasoli, L., Gold, K.** (1962) Nutrition of the American strain of *Gyrodinium cohnii*. Arch. Mikrobiol. 42: 196-203

**Ris, H., Kubai, D.F.** (1974) An unusual mitotic mechanism in the parasitic protozoan *Syndinium* sp. J. Cell. Biol. 60: 701-720

**Rittenberg, J.H., Gallagher, M.L., Bayer, R.C., Leavitt, D.F.** (1979) The effect of *Aerococcus viridans* var. *homari* on the oxygen binding capacity of hemocyanin in the American lobster (*Homarus americanus*). Trans. Am. Fish. Soc. 108: 172-177

**Rudzinska, M.A.** (1977) Uptake of ferritin from the medium in Suctoria. Experientia 33: 1595-1598

**Scholtyseck, E. and Mehlhorn, H.** (1970) Ultrastructural study of characteristic organelles (paired organelles, micronemes, micropores) of Sporozoa and related organisms. Z Parasitenk. 34: 97-127

**Senaud, J., Chabotar, B. and Scholtyseck, E.** (1976) Role of the micropore in nutrition of the Sporozoa. Ultrastructural study of *Plasmodium cathemerium, Eimeria ferrisi, E. steidae, Besnoitia jellisoni* and *Frankelia* sp. Tropenmed Parasit. 27: 145-159

**Shields, J.D.** (1992) Parasites and symbionts of the crab *Portunus pelagicus*, from Moreton Bay, Australia. J. Crust. Biol. 12: 94-100

**Soyer, M-O.** (1969) Rapports existant entre chromosomes et membrane nucléaire chez un Dinoflagellé parasite du genre *Blastodinium* Chatton. C.R. Hebd. Séanc. Acad. Sci., Paris, Ser. D. 268: 2082-2084

**Soyer, M-O.** (1974) Ètude ultrastructurale de Syndinium sp. Chatton parasite coelomique de copèpodes pèlagiques. Vie Millieu. 24 (2A) : 191-212

**Spurr, A.R.** (1969) A low viscosity epoxy embedding resin for electron microscopy. J. Ultrastruct. Res. 26: 31-43

**Stosch, H.A., von.** (1973) Observations on vegetative reproduction and sexual life of two freshwater dinoflagellates, *Gymnodinium pseudopalustre* Schiller and *Woloszynskia apiculata* sp. nov. Br. Phycol. J. 8: 105-134

**Wichterman R.** (1986) The biology of Paramecium. '2. ed. Plenum Press, New York.

**Wickham, D.E.** (1986) Epizootic infestations by nemertean brood parasites on commercially important crustaceans. Can. J. Fish. Aquat. Sci. 43: 2295-2302

**Wilhelm, G. and Boulo, V.** (1988) Infection de l'étrille *Liocarcinus puber* (L.) par un dinoflagelle parasite de type *Hematodinium* sp. I. C. E. S. C. M. 1988/K:41 (mimeo)

# APPENDIX 1.

Vol. 22: 115–128, 1995 | DISEASES OF AQUATIC ORGANISMS
Dis aquat Org | Published June 15

# A *Hematodinium*-like dinoflagellate infection of the Norway lobster *Nephrops norvegicus*: observations on pathology and progression of infection

**R. H. Field, P. L. Appleton**

**Division of Environmental and Evolutionary Biology, Graham Kerr Building, University of Glasgow, Glasgow G12 8QQ, Scotland, UK**

ABSTRACT: The discovery of a *Hematodinium*-like dinoflagellate infecting *Nephrops norvegicus* has led to a pathological investigation into the effects on the host and the apparent progression of the disease syndrome. The parasite is systemic, invading the haemocoel and the connective tissues of most organs via the haemal spaces. An increase in the combined number of parasites and haemocytes in the haemolymph was due to an increase in the relative proportion of dinoflagellates and suggested a reduction in numbers of haemocytes. These parameters did not correlate directly with severity. Comparison of the level to which tissues were invaded and the relationship between haemocyte and parasite numbers in the haemolymph suggests that at least some organs may be invaded very early in infection, if not before parasites enter the 0haemolymph. There was evidence of host cellular defence reactions, in the form of haemocyte encapsulations in the gills and heart, and phagocytosis of dinoflagellates by the fixed phagocytes of the hepatopancreas.

KEY WORDS: *Nephrops norvegicus* · *Hematodinium* spp. · Parasitic dinoflagellate · Crustacea · Pathology

## INTRODUCTION

In recent years, individuals of the commercially important species *Nephrops norvegicus* (L.), caught on grounds around the west coast of Scotland have been observed to be infected by a parasitic dinoflagellate of the botanical order Syndiniales (Field et al. 1992). In particular, this organism resembles *Hematodinium* spp., first reported in *Carcinus maenas* and *Liocarcinus depurator* by Chatton & Poisson (1931), and other similar types of parasitic dinoflagellate reported recently in an increasing number of crustaceans over a wide geographic range [*Callinectes sapidus* in the eastern Atlantic (Newman & Johnson 1975), several species of benthic amphipod (Johnson 1986), *Cancer irroratus*, *C. borealis* and *Ovalipes ocellatus* (Maclean & Ruddell 1978) in the western Atlantic, *Necora puber* and *Cancer pagurus* on the northern coast of France and the west coast of Scotland (Latrouite et al. 1988, Wilhelm & Boulo 1988), *Chionoecetes bairdi* and *C. opilio* in Alaska, USA (Meyers et al. 1987, 1990, Meyers 1990, 1990, Eaton et al. 1991, Love et al. 1993), and *Portunus pelagicus* (Shields 1992) and *Trapezia* sp. (Hudson et al. 1992) in Australia].

Field (1992) and Field et al. (1992) have described preliminary investigations into the pathology and epizootiology of *Hematodinium*-like infection of *Nephrops norvegicus*. Following several years of high infection prevalences, catches of *N. norvegicus*, and in particular infected individuals, have been poor. In view of the commercial importance of *N. norvegicus*, and the implication from previous work that infection may be leading to significant mortalities, further research was instigated. Despite the paucity of infected material, reported here are further investigations into the pathology of infection and the course of the disease, undertaken in conjunction with investigations into the *in vitro* culture of the organism and its life cycle (Vickerman et al. 1993).

Diagnosis of infection and determination of severity were made by pleopod examination as described by Field et al. (1992) (see Fig. 1). This technique estimates the relative degree of parasite aggregation beneath the cuticle of the pleopods (and presumably throughout the haemocoel), and makes the premise that as infection progresses the number of parasitic cells, and hence the thickness of the aggregation layer in the

pleopod, increases. Field et al. (1992) conducted some counts of haemocytes and parasites together to investigate this hypothesis and to assess its potential as a field diagnostic method for infection and severity. We have now conducted combined parasite and haemocyte counts in fresh haemolymph and determined the relative proportions of haemocytes and parasites in stained haemolymph smears, from both apparently uninfected and infected lobsters, to assess the accuracy of this technique in disease and severity diagnosis. Since individuals examined in the pathological investigation were assigned an infection status by this method, it is now possible to relate haemolymph parasite numbers and tissue changes. In this way it has been possible to determine whether increasing parasite numbers in the haemolymph actually reflect the progression of infection, or are merely the result of variation between individual infections.

## MATERIALS AND METHODS

**Experimental lobsters.** *Nephrops norvegicus* were caught by trawling on grounds around the Isle of Cumbrae, Clyde Sea area, Scotland, and transported to the Zoology Department, University of Glasgow, where they were maintained in well-aerated sea water for up to 5 d. The aquarium water temperature ranged between 10 and 13°C and the salinity between 33 and 34‰. Lobsters were fed ad libitum on squid and mussel flesh. All lobsters were in intermoult as defined by the moult staging technique of Aiken (1980). Diagnosis of infection was made by the pleopod assessment method of Field et al. (1992) (Fig. 1).

**Counts of haemocytes and dinoflagellate parasites.** After assessment of infection severity by pleopod examination, counts were performed of numbers, in fresh haemolymph, of haemocytes and parasites together in 28 infected and uninfected *Nephrops norvegicus*, by the method given in Field et al. (1992), based on that of Stewart et al. (1967). For statistical analysis, these counts were combined with those reported in Field et al. (1992), since the protocols employed were identical.

Since it was not possible to reliably distinguish between parasites and haemocytes in fresh haemolymph, haemolymph smears were made from an additional 89 infected and uninfected lobsters (again after pleopod examination) as follows. Haemolymph was withdrawn directly from the haemocoel into a disposable syringe containing chilled 5% formalin in sea water (33‰), in a ratio of approximately 1:1, from the base of a fifth pereiopod. After 5 to 10 min fixation, samples were gently agitated to re-suspend cells and a small drop of each was smeared on a clean glass slide. Smears were allowed to dry thoroughly, post-fixed in methanol and stained with a 0.2% w/v solution of Leishman's stain (BDH Chemicals Ltd, Poole, England). Each smear was examined at ×400 magnification, and the relative numbers of host haemocytes and dinoflagellates from a total of 200 cells were counted. From these counts the number of parasites was expressed as a percentage of the total of both haemocytes and dinoflagellates together in the haemolymph of each lobster.

**Light and electron microscopy.** Major tissues and organs were dissected from a total of 29 *Nephrops norvegicus*, previously staged by pleopod examination. Of these, 9 were apparently uninfected, 5 showed stage I infection, 5 stage II, 5 stage III and 5 stage IV. The organs and tissues removed were hepatopancreas, antennal gland, midgut, abdominal muscle, haemopoietic tissue, heart, gills, and, in some cases, brain and eye/eyestalk. Prior to dissection, lobsters were narcotised in ice for about 1 h. Immediately upon removal, tissue samples for histopathology were fixed in Helly's mercuric chloride fixative (Johnson 1980) and embedded in paraffin wax. Thick sections (6 µm) were treated with Lugol's iodine solution to remove mercury, and stained with haematoxylin and eosin (H&E).

Tissues removed for electron microscopy were fixed in 1% glutaraldehyde, 2% paraformaldehyde in 0.1M phosphate buffer, pH 7.4 with 2% sucrose and 1.5% sodium chloride for 2 h at room temperature. Specimens were then rinsed in 0.1M phosphate buffer with 4% sucrose, then post-fixed in 1% osmium tetroxide in phosphate buffer for 1 h. Specimens were washed in several changes of distilled water and block stained in 0.5% aqueous uranyl acetate for 1 h. After dehydrating

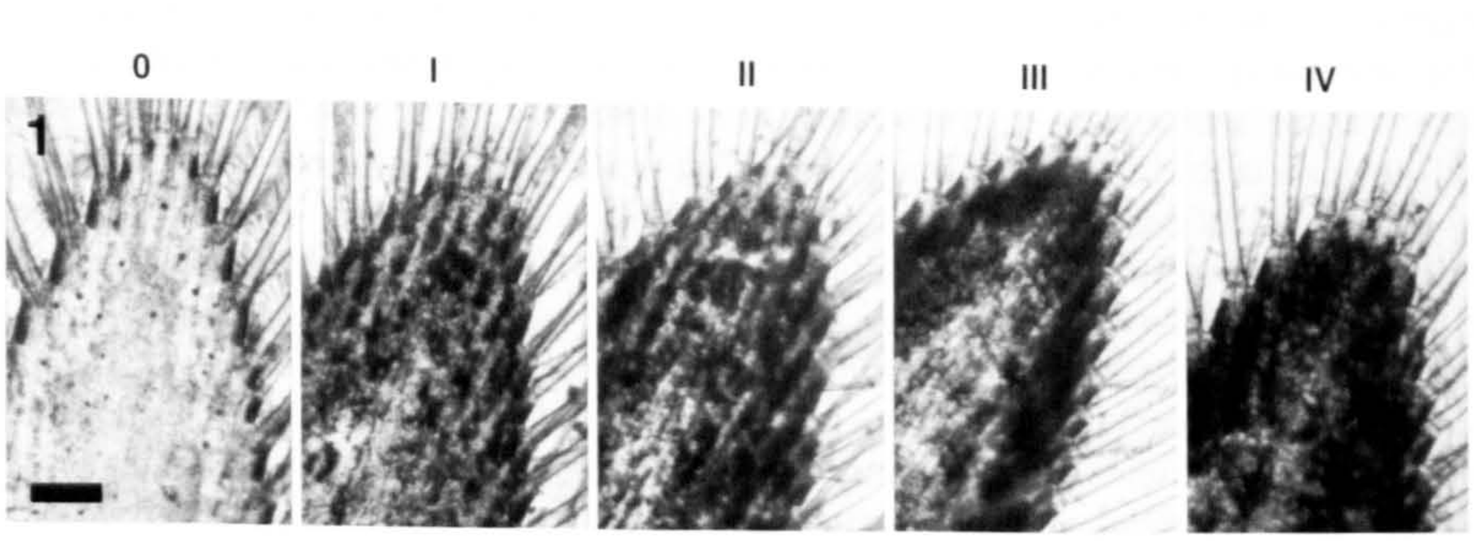


Fig. 1. *Nephrops norvegicus*. Light micrographs showing the appearance of pleopods of healthy and dinoflagellate-infected lobsters. The density of the layer of aggregated haemocytes and parasites beneath the cuticle indicates the severity of infection on an arbitrary scale from I to IV. 0: uninfected; I: slight infection; IV: heavy infection. Scale bar = 0.5 mm

through an ethanol series specimens were embedded in Spurr resin (Spurr 1969), using propylene oxide as a transitional solvent.

Thick sections (1 µm) for light microscopy were stained with 1% toluidine blue. Suitable areas of tissue were selected and thin sections were cut and mounted on uncoated 300 mesh copper/palladium grids and stained with uranyl acetate (methanolic) and lead citrate.

Thin sections were examined in a Zeiss 902 transmission electron microscope operating at 80 kV.

## RESULTS

### Numbers of haemocytes and dinoflagellate parasites in the haemolymph

Table 1 shows the results of the counts of haemocytes and parasites together performed on haemolymph from staged *Nephrops norvegicus*. These results indicate that there was an increase in the total number of haemocytes and dinoflagellates in the haemolymph of infected *N. norvegicus*. This increase was significant only in individuals staged at III and IV. The increase was due to the higher proportion of dinoflagellates within the haemolymph (Table 2). Stage I individuals showed a slight increase above stage 0 lobsters, but stage II, III and IV individuals showed a further significant rise above this. Although all those lobsters placed in stage 0 were diagnosed as uninfected by pleopod examination a small number were misdiagnosed. Three apparently uninfected lobsters were found to have dinoflagellate parasites in their haemolymph when smears were examined. This discrepancy accounts for the above zero percentage of dinoflagellate parasites in group 0. Three uninfected lobsters were also misdiagnosed as infected stage I, since their smears contained no detectable parasites.

Table 1. *Nephrops norvegicus*. Variation of the combined count of haemocytes and parasites in the haemolymph (combined count) in relation to severity of infection as determined by pleopod examination. *Significantly higher than the previous stage, $p < 0.005$ (1-way ANOVA). (This table incorporates data from Field et al. 1992)

| Pleopod infection stage | No. of lobsters | Combined count ($\times 10^4$ mm$^{-3}$) Mean | SD |
|---|---|---|---|
| 0 | 20 | 1.117 | 0.626 |
| I | 20 | 1.247 | 0.815 |
| II | 17 | 1.926 | 1.248 |
| III | 10 | 6.937 | 5.304* |
| IV | 7 | 8.305 | 7.332* |

Table 2. *Nephrops norvegicus*. Variation in percentage dinoflagellates in the haemolymph in relation to severity of infection as determined by pleopod examination. *Significantly higher than the previous stage, $p < 0.005$ (1-way ANOVA)

| Pleopod infection stage | No. of lobsters | % Dinoflagellates Mean | SD |
|---|---|---|---|
| 0 | 45 | 0.10 | 1.8 |
| I | 17 | 19.65 | 11.22* |
| II | 14 | 70.69 | 11.34 } |
| III | 8 | 75.74 | 18.90 }* |
| IV | 5 | 97.07 | 0.09 } |

### Pathology and electron microscopy

The initial report of this disease syndrome (Field et al. 1992) recognised 2 dinoflagellate cell forms in *Nephrops norvegicus*, uninucleate and multinucleate/plasmodial cells in the haemolymph and vermiform cells attached in the tissues. Since publication of this work, we have made much progress in the *in vitro* culture and study of the life cycle of this organism, revealing a more complex range of developmental forms (Vickerman et al. 1993) comprising both filamentous and network syncytia, uninucleate and multinucleate/plasmodial cells, and 2 types of biflagellate motile dinospores.

During the current study we identified 4 separate parasite morphologies within *Nephrops norvegicus*. Filamentous syncytia (see Fig. 3), sometimes radiating from a central mass, were attached to host tissue bounding haemal spaces and lumina in several organs. These were multinucleate, individual filaments containing up to 5 nuclei. Filament nuclei contained the prominent condensed chromosomes typical of the dinoflagellate dinokaryon (see Figs. 3 & 13). This parasite form corresponds to the vermiform type described by Field et al. (1992), and resembles the filamentous syncytia observed *in vitro* by Vickerman et al. (1993). A separate network syncytial form was observed, ramifying between muscle fibres in abdominal muscle (see Fig. 12) and heart, which may correspond to the network form described by Vickerman et al. (1993).

#### Hepatopancreas

In infected individuals, the spacing between hepatopancreatic tubules was much enlarged compared with that of uninfected lobsters (Fig. 2). This was sometimes seen as an artefact of dissection and fixation, even in uninfected lobsters, but tubule separation increased with infection severity. The hepatopancreas of infected individuals was difficult to

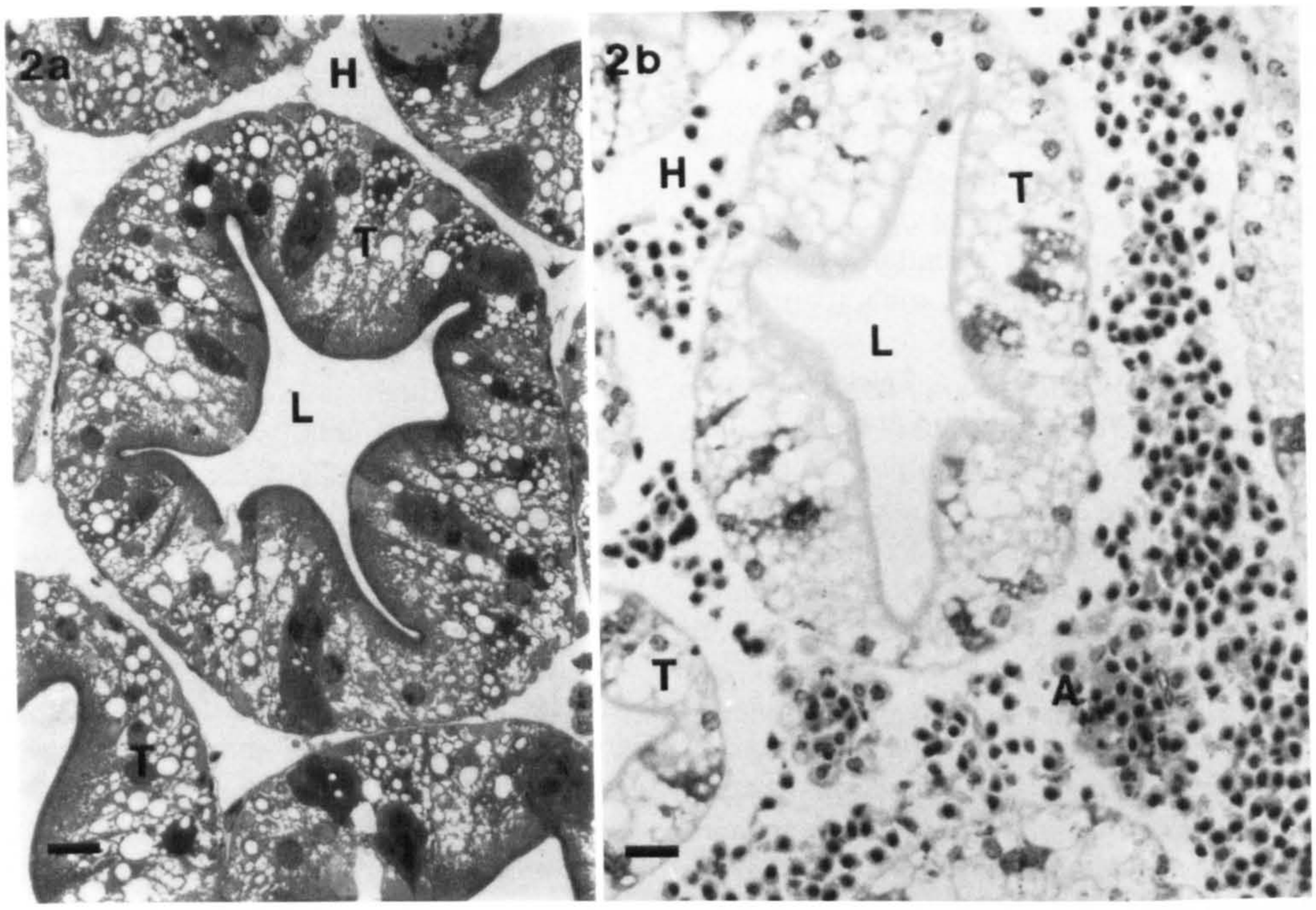


Fig. 2. *Nephrops norvegicus*. Light micrographs showing the enlargement of spacing between hepatopancreatic tubules in dinoflagellate-infected lobsters. (a) Hepatopancreas of uninfected individual. Toluidine blue. (b) Hepatopancreas of stage IV infected individual, showing increased spacing between the tubules, and the concurrent presence of many uninucleate parasites. H: haemal sinus; L: lumen of tubule; T: tubule epithelium; A: hepatopancreatic arteriole. H&E. Scale bars = 20 µm

remove because of its almost liquid state. Enlarged spaces within the hepatopancreatic haemal sinus were found to contain large numbers of uninucleate (and occasionally binucleate) parasites, but haemocytes were rarely seen. Occasionally, filamentous syncytia were seen in heavily infected lobsters, attached to the outside of tubules (Fig. 3). Tubule damage in the heavier infections was more profound, involving not only vacuolation of epithelial cells (Figs. 2 & 3) but the breach of tubule walls, as indicated by the presence of uninucleate parasites within the lumina of tubules in both stage III and stage IV lobsters (Fig. 4).

Activity of the fixed phagocytes surrounding the hepatic arterioles was observed in infected lobsters of all stages, as indicated by the hypertrophied state of these cells (Fig. 5) and the presence of an interrupted layer (Johnson 1987) (Fig. 6). Evidence was seen of retention of parasites in the extracellular space between the interrupted layer and the fixed phagocytes. The majority of dinoflagellates associated with fixed phagocytes were retained in this manner. Phagocytosis was also observed, but less often, evidenced by the form of phagosomes containing degenerative parasite material (Fig. 6). Fixed phagocytes containing such phagosomes were often necrotic. Extracellular spaces contained normal dinoflagellates and parasite debris (Fig. 6).

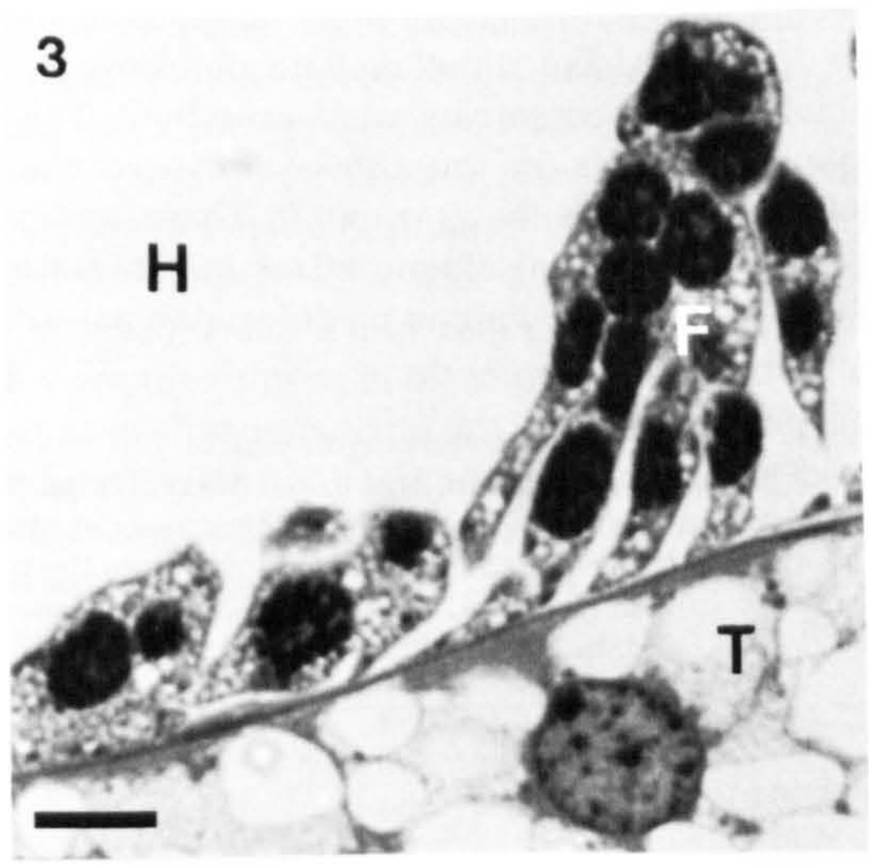


Fig. 3. *Nephrops norvegicus*. Light micrograph showing filamentous dinoflagellate syncytium attached to the outer wall of a hepatopancreatic tubule of a stage III infected lobster. H: haemal sinus of hepatopancreas; F: parasite syncytium; T: epithelial cell of hepatopancreatic tubule. Toluidine blue. Scale bar = 15 µm

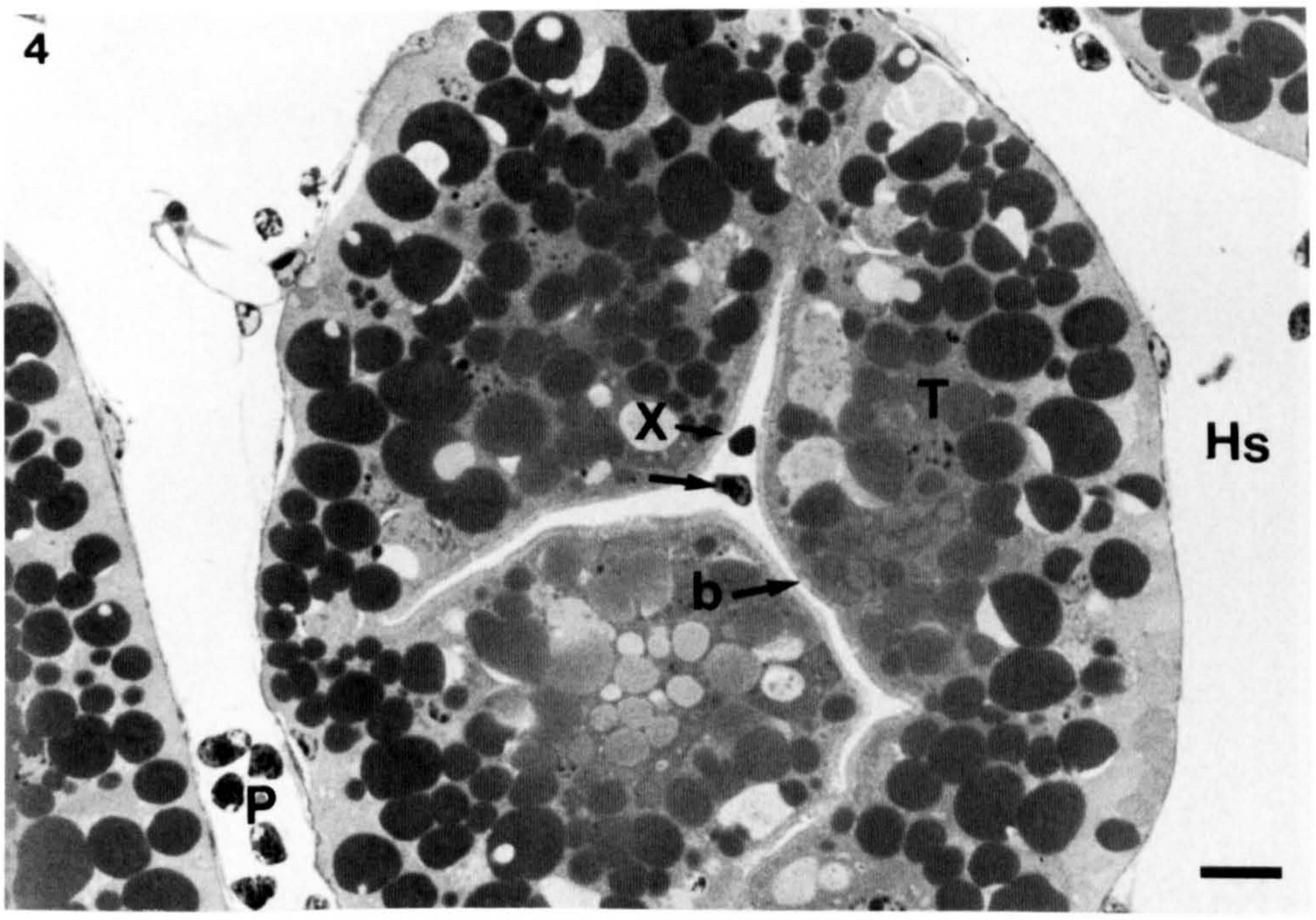


Fig. 4. *Nephrops norvegicus*. Light micrograph showing the presence of a dinoflagellate within the lumen of a hepatopancreatic tubule of a stage IV infected individual. Note also the presence of flagellate spores in the haemal spaces surrounding the tubules, and a 'secretory packet' (Johnson 1980) in the tubule lumen, possibly a shed 'B'-cell. T: tubule epithelium; b: brush border of epithelial cells; Hs: haemal sinus of hepatopancreas; X: 'secretory packet'; P: biflagellate spores of the parasite; arrow: dinoflagellate within tubule lumen. Toluidine blue. Scale bar = 20 µm

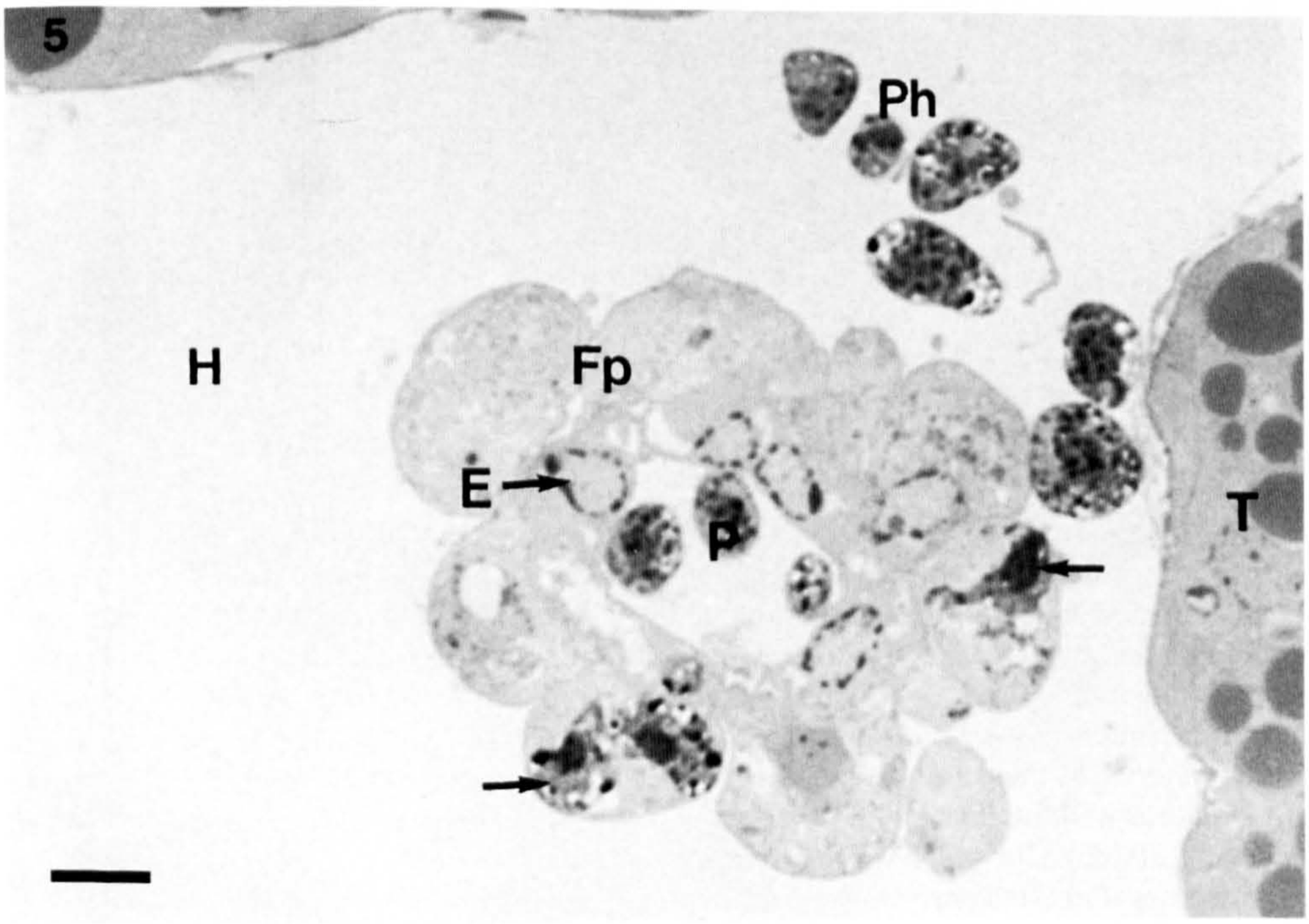


Fig. 5. *Nephrops norvegicus*. Light micrograph showing fixed phagocytes surrounding an hepatic arteriole in a stage IV infected lobster. Note the dinoflagellates associated with 2 fixed phagocytes (arrows). Ph: parasites in hepatopancreatic haemal sinus; T: hepatopancreatic tubule; Fp: fixed phagocytes; E: endothelium of arteriole; P: parasites within lumen of arteriole. Toluidine blue. Scale bar = 10 µm

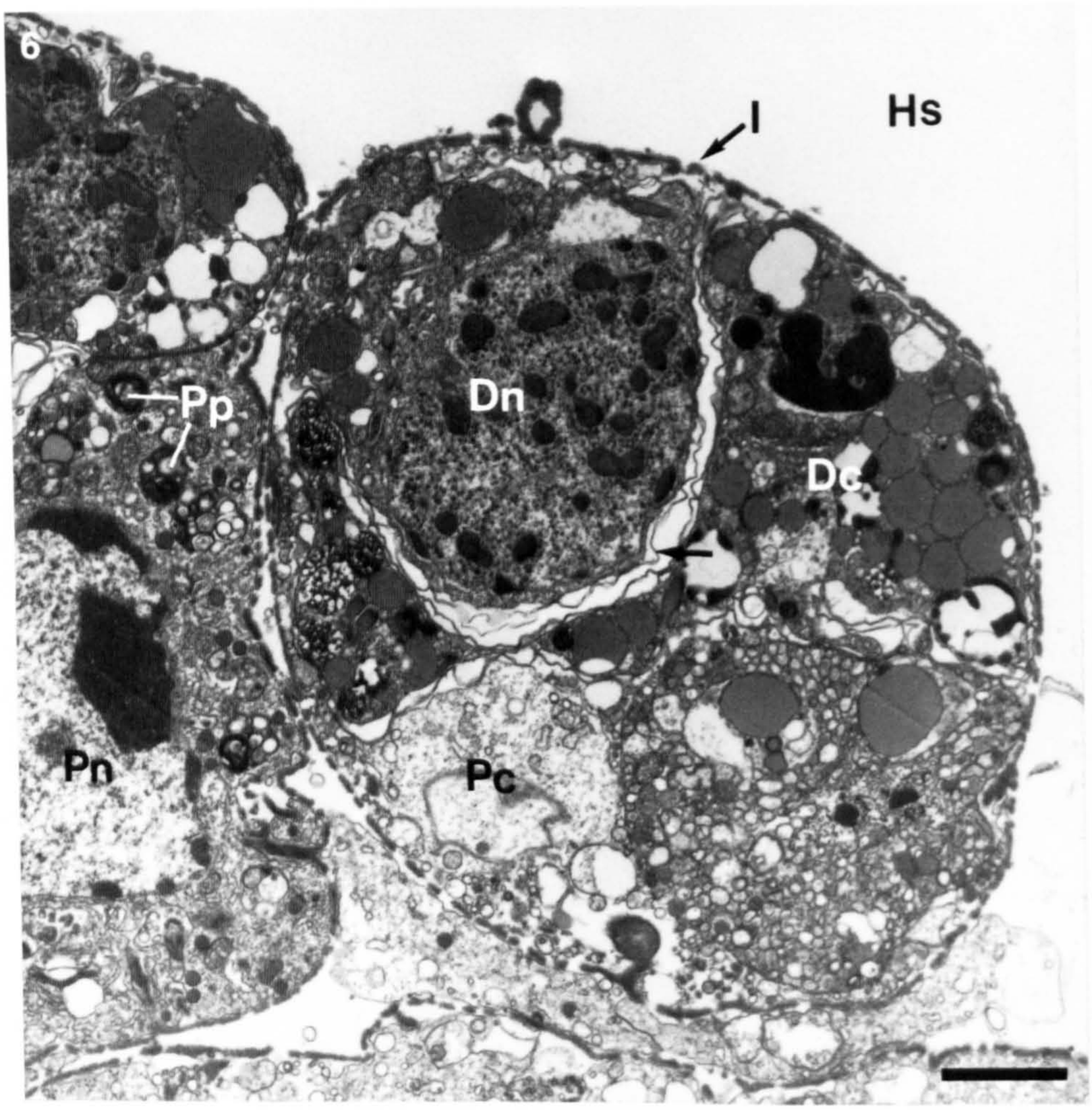


Fig. 6. *Nephrops norvegicus*. Transmission electron micrograph showing detail of a dinoflagellate associated with an hepatopancreatic fixed phagocyte of a stage IV infected lobster. Note the vesicular cytoplasm and the interrupted layer surrounding the fixed phagocyte, and the granular nature of the cytoplasm of the parasite. I: interrupted layer; Hs: haemal sinus of hepatopancreas; Dn: nucleus of dinoflagellate; Dc: cytoplasm of dinoflagellate; Pn: nucleus of adjacent phagocyte; Pc: cytoplasm of fixed phagocyte; Pp: phagosomes. Scale bar = 2.5 µm

## Antennal gland

The structure of the antennal glands of infected *Nephrops norvegicus* was largely unaffected in all but the most heavily infected individuals, despite the presence of many dinoflagellates within the haemal spaces and connective tissue of the labyrinth and coelomosac, and branches of the antennary artery. As in the hepatopancreas, the majority of the parasites were uninucleate, but filamentous multinucleate stages were also present, especially attached to the basal side of the labyrinthal epithelium (Fig. 7). There was an increase in numbers of attached parasites with increasing infection stage, though even light infections of stage I showed well-established groups of attached parasite syncytia in the labyrinth. The coelomosac epithelium was unchanged, except for the presence of dinoflagellates in the narrow haemal spaces surrounding it. The labyrinthal epithelium showed some vacuolation, and parasites were present in the lumen of the labyrinth itself (Fig. 7), indicating breach of the epithelium. The labyrinthal epithelium of infected and uninfected lobsters showed a high degree of secretory activity when compared to that of the grass shrimp *Palaemonetes pugio*, which only showed such activity levels after exposure to biocides (Doughtie & Rao 1983). This activity was evident even in the antennal gland of heavily infected stage IV *Nephrops norvegicus*, with the apical brush border of cells often showing extruded granular bodies (Fig. 8), similar to those seen in the antennal gland of *Astacus* sp. (Parry 1960) and *P. pugio* (Doughtie & Rao 1983).

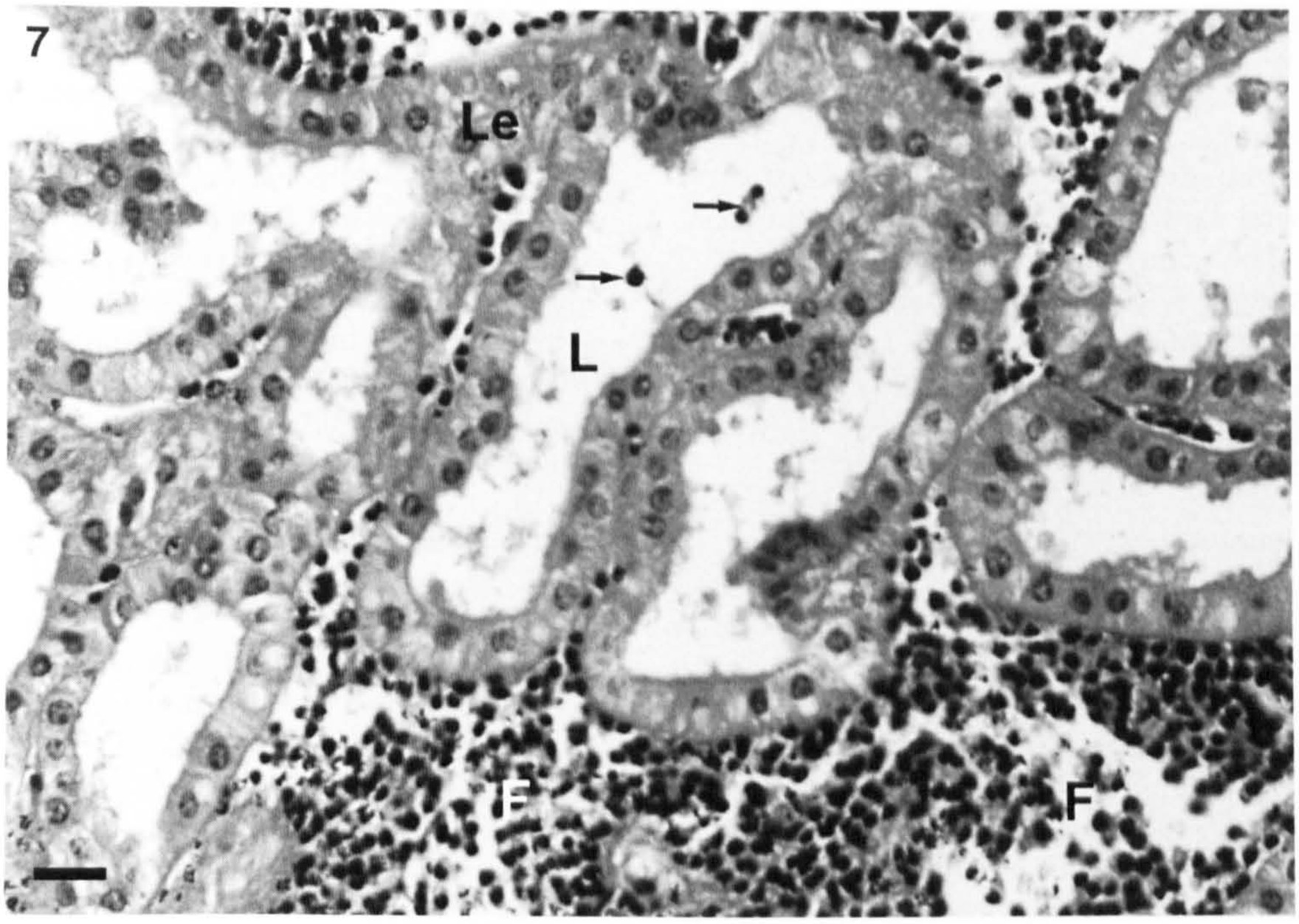


Fig. 7. *Nephrops norvegicus*. Light micrograph of the labyrinthal epithelium of the antennal gland of a stage III infected individual, showing attachment of filamentous parasite syncytia within the haemal spaces and the presence of dinoflagellates within the lumen of the labyrinth (arrows). Le: labyrinthal epithelium; L: labyrinthal lumen; F: filamentous parasite syncytia. H&E. Scale bar = 20 µm

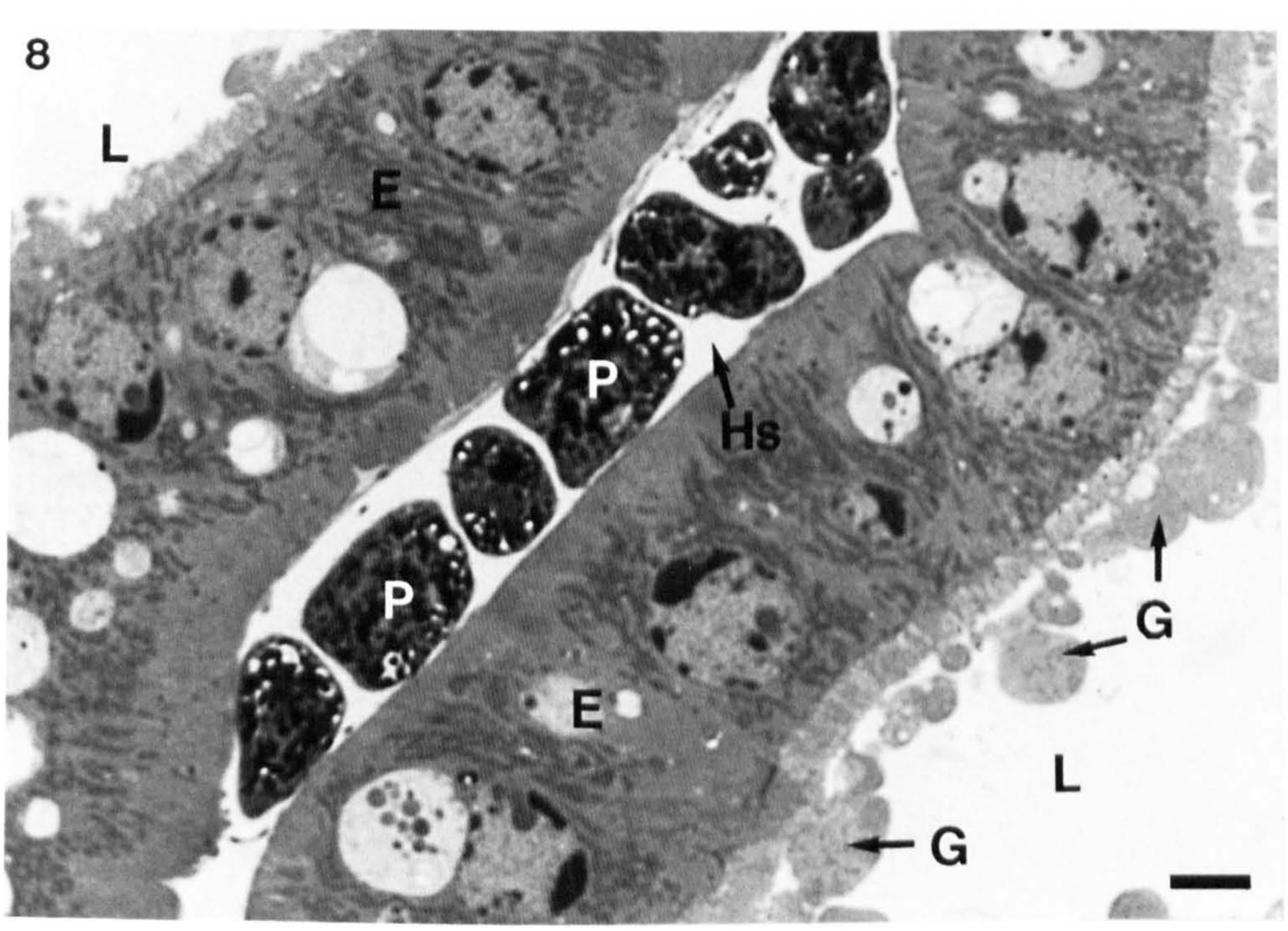


Fig. 8. *Nephrops norvegicus*. Light micrograph showing detail of the labyrinthal epithelium of a stage IV infected lobster, and the presence of biflagellate spores of the parasite within the haemal spaces. L: labyrinthal lumen; Hs: haemal spaces of labyrinth; P: biflagellate spores of the parasite; E: epithelial cells; G: granular bodies. Toluidine blue. Scale bar = 5 µm

### Midgut

Tissue of the midgut exhibited some of the most marked changes as a result of infection by the parasite. The midgut wall of lobsters from all pleopod infection stages showed large-scale infiltration by the dinoflagellates. The connective tissue and muscles of the outer midgut wall had been almost completely replaced by parasites, even in stage I lobsters. The muscle tissue still present in stage I and II individuals (Fig. 9) appeared fragmentary and reduced when compared with that of uninfected lobsters (Fig. 10). The haemal spaces were enlarged and partially occluded by large numbers of attached filamentous parasite syncytia. Few haemocytes were observed in these haemal spaces in infected lobsters, especially in stage III and IV individuals. There was limited evidence of a host cellular defence reaction within the gut wall of stage I lobsters, where small numbers of haemocytes were aggregated around dinoflagellates.

Parasites in the midgut wall were predominantly filamentous syncytia, especially in light infections, where uninucleate forms were less apparent. Histologically, the basement membrane and the layers of granular cells underlying it were unaffected by infection. The frequency of occurrence of these granular cells did not seem to correlate with infection. The identity of these granular cells is as yet uncertain, though they resemble granulocytes.

Evidence of any alteration of the midgut epithelium was scant, with both villi and epithelial corrugations still present in stage IV infected lobsters. Lysis and vacuolation of epithelial cells by infection was not readily distinguished from that caused by prefixation artefact. There was also no evidence of parasite invasion of the epithelium or any tissues on the lumen side of the basement membrane. A concurrent gregarine infection, tentatively identified as an eugregarine was found in the midgut lumen of one of the stage IV lobsters (Fig. 11).

### Abdominal muscle

The abdominal muscle of healthy *Nephrops norvegicus* displayed histologic features typical of crustacean homogeneous fast phasic skeletal muscle. The fibres had a short sarcomere length (2 to 4 µm) and lightly staining nuclei, with peripherally dense chromatin. In general, these features remained unchanged in the abdominal deep muscles of dinoflagellate-infected individuals. In wax-embedded sections parasite invasion of muscle fibres was not apparent, even though free uninucleate parasites were frequently encountered in interstices between muscle fibres in stage I

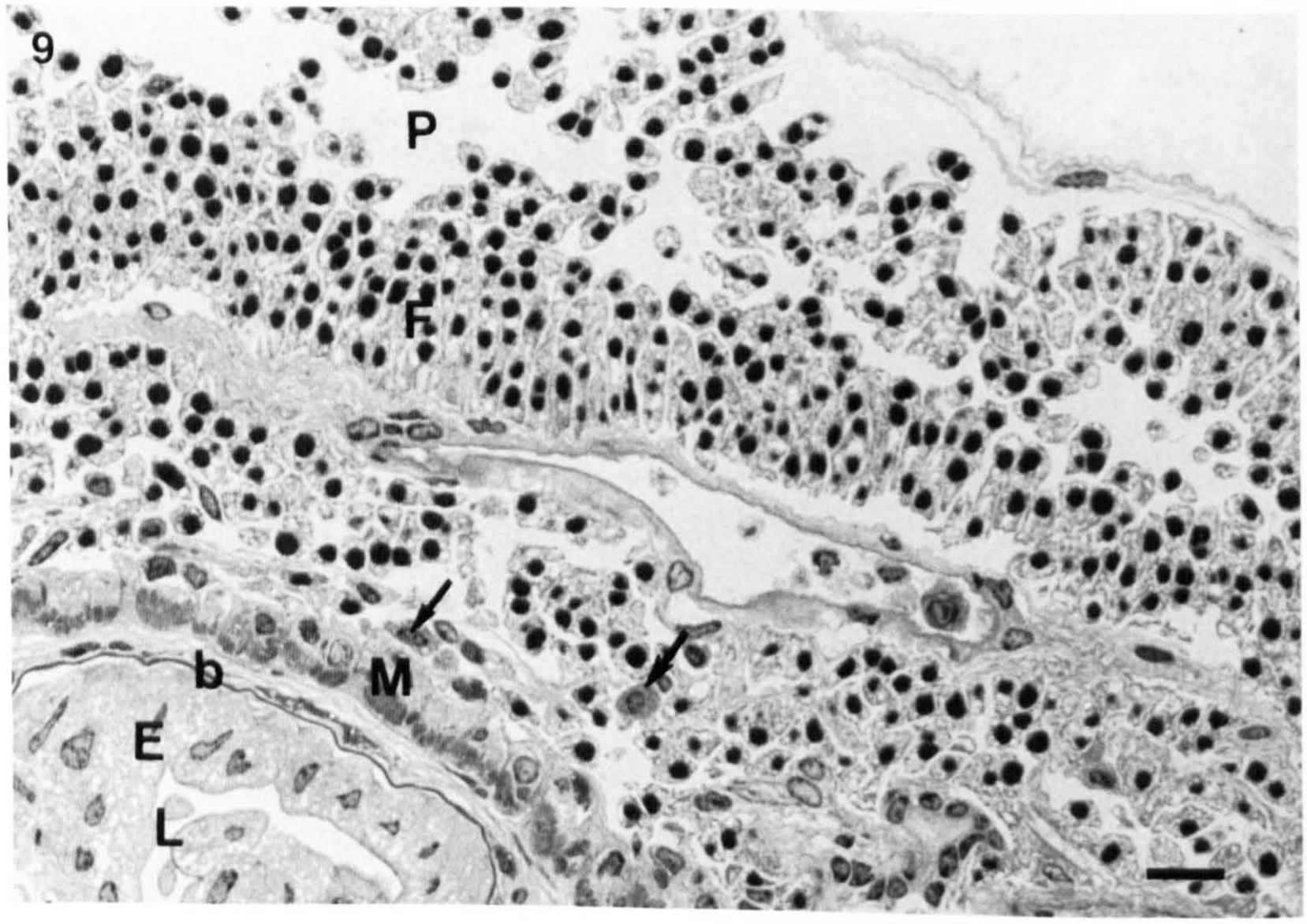


Fig. 9. *Nephrops norvegicus*. Light micrograph of the midgut wall of a stage II infected individual showing both attached filamentous syncytia and possibly uninucleate parasites. P: possibly uninucleate parasites; F: filamentous syncytia; M: circular muscle layer of midgut wall; b: basement membrane; E: epithelium; L: lumen. Toluidine blue. Scale bar = 20 µm

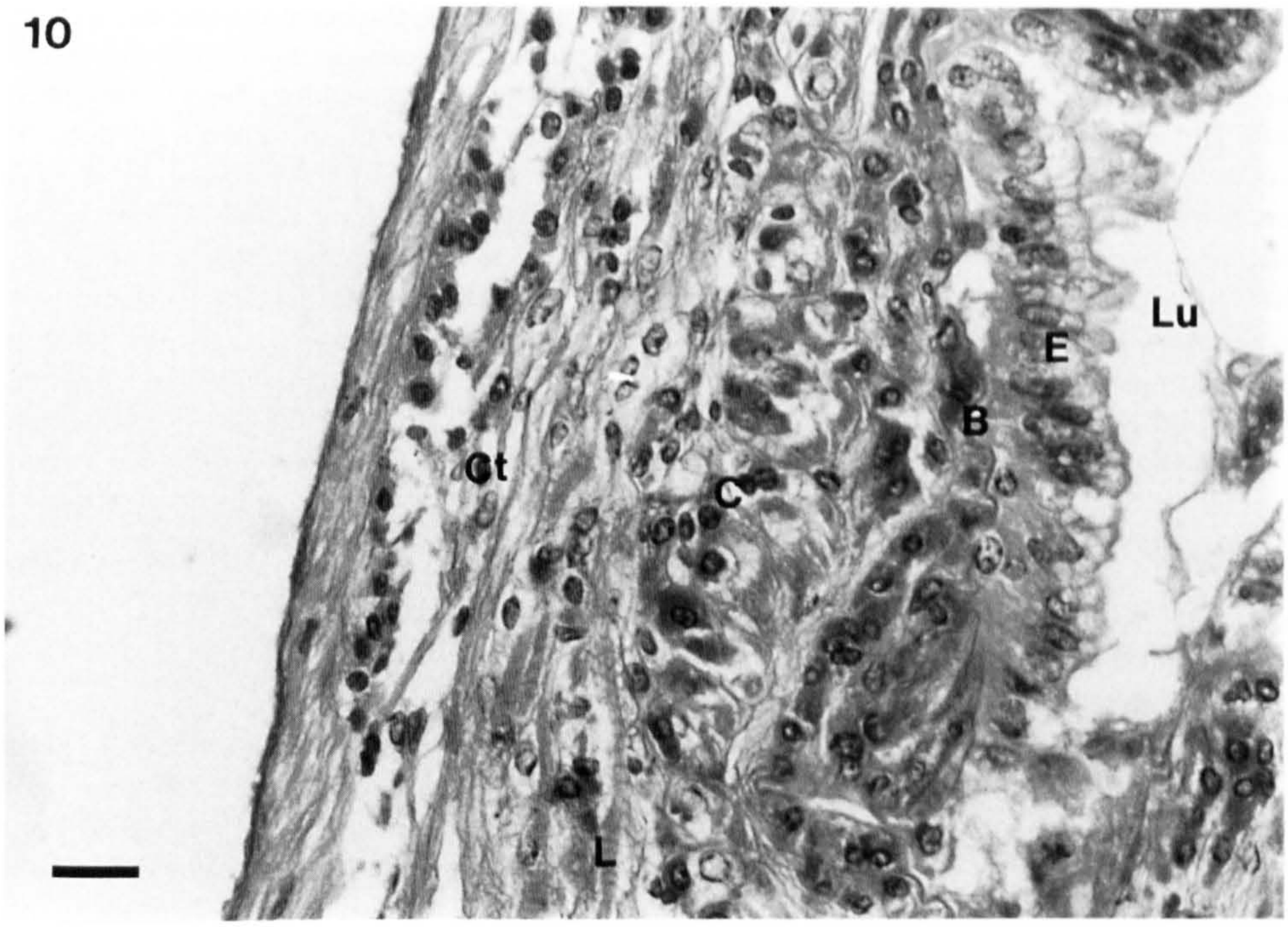


Fig. 10. *Nephrops norvegicus*. Light micrograph of the midgut wall of an uninfected lobster showing the connective tissue and muscles of the outer wall. Ct: connective tissue; L: longitudinal muscle; C: circular muscle; B: basement membrane; E: epithelium; Lu: lumen. H&E. Scale bar = 20 µm

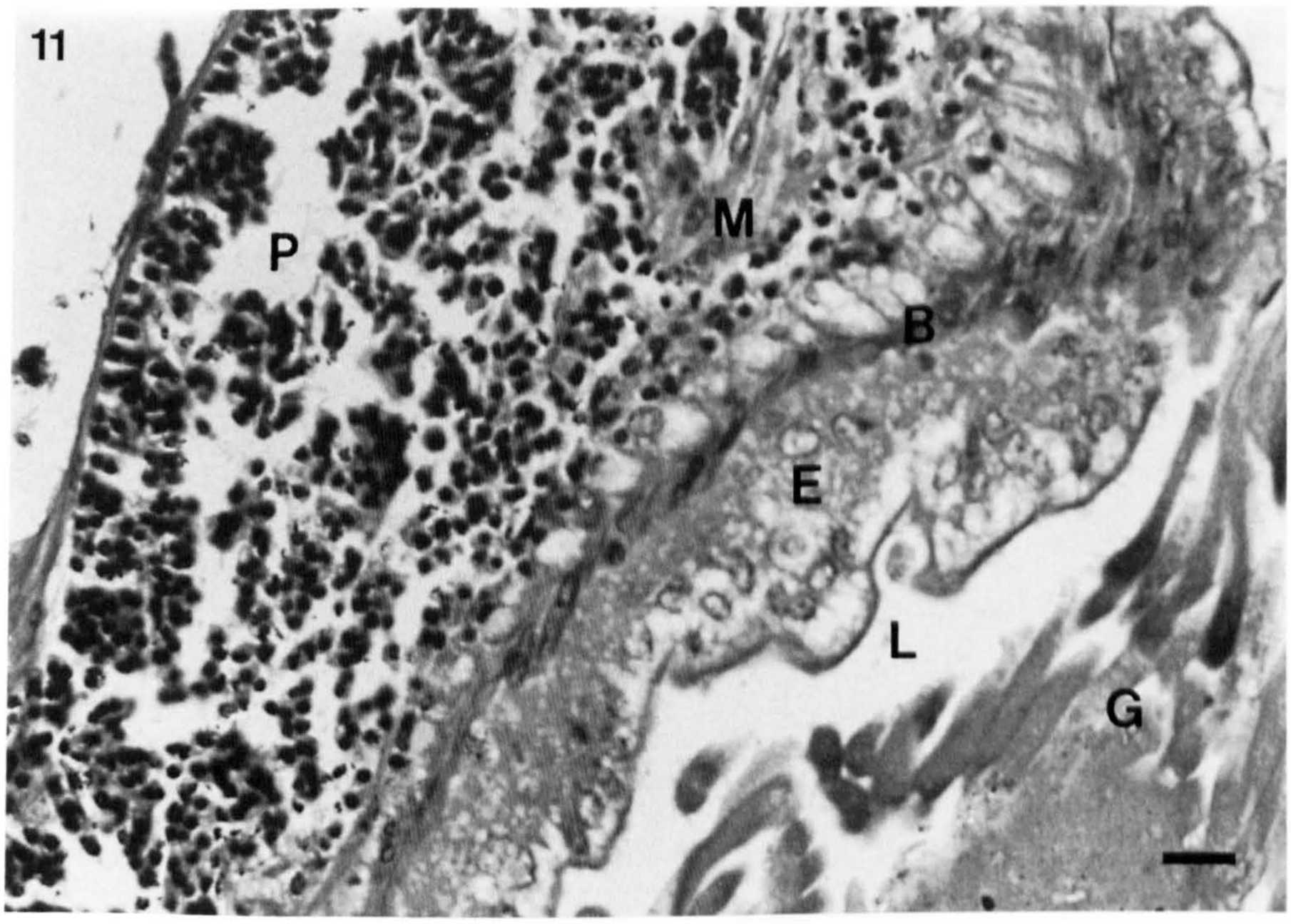


Fig. 11. *Nephrops norvegicus*. Light micrograph of the midgut wall of a stage III infected lobster showing a simultaneous infection by dinoflagellates and an unidentified gregarine. P: dinoflagellates within the midgut wall; M: muscle layer; B: basement membrane; E: midgut epithelium; L: midgut lumen; G: gregarines within midgut lumen. H&E. Scale bar = 20 µm

lobsters. The interstitial connective tissues of skeletal muscle remained intact. In stage III and IV lobsters, however, network-like parasite syncytia were present within skeletal muscle interstices (Fig. 12), and connective tissue was reduced. Furthermore, peripheral areas of some fibres were lysed, and uninucleate parasites were also present in the haemal spaces surrounding the fibres. Uninucleate and multinucleate forms of the parasite, like those found in the haemolymph, were often closely associated with the sarcolemma of fibres (Fig. 13).

## Haemopoietic tissue

The haemopoietic tissue of *Nephrops norvegicus* is a thin sheet of tissue on the dorsal and lateral surfaces of the cardiac stomach (gastric mill) and probably on the ventral floor of the cephalic cavity, adjoining the antennal glands. The haemopoietic tissue of healthy lobsters was difficult to locate, despite the removal and examination of the entire roof of the cardiac stomach with its attendant epithelium and connective tissues. A few nodes were located, but these generally showed little activity, possibly because specimens were dissected in winter, when Johnson (1980) reported haemocyte production to be low in *Callinectes sapidus*.

In contrast, the haemopoietic tissue of dinoflagellate-infected *Nephrops norvegicus* showed a dramatic increase in size, evident even to the naked eye during dissection of stage III and IV lobsters. This was due, in part, to a much increased level of haemopoietic activity, with many nodes containing differentiating cells, mitotic figures and what appeared to be stem cells. However, despite this vast increase in both the number and activity of stem cells, very few newly differentiated haemocytes were visible in the haemal spaces surrounding the haemopoietic nodes (Fig. 14). Instead these spaces were filled with many uninucleate and multinucleate dinoflagellates, even in lower level stage I and II infections.

## Heart

The general microscopic structure of the heart of infected individuals remained unchanged in all except the most moribund of stage IV lobsters. There was again invasion of all haemal spaces by the parasite. The lumen, haemal spaces and connective tissue of the myocardium were massively infiltrated mainly by attached filamentous dinoflagellate syncytia, already well established in stage I individuals. Network-like parasite syncytia were also seen to ramify through the interstices of the myo-


Fig. 12. *Nephrops norvegicus*. Light micrograph of abdominal muscle of a stage II infected individual showing network-like parasite syncytia within the muscle interstices. M: abdominal muscle fibres; N: parasite nuclei; S: muscle nuclei; arrows: parasite syncytia within muscle interstices. H&E. Scale bar = 20 µm

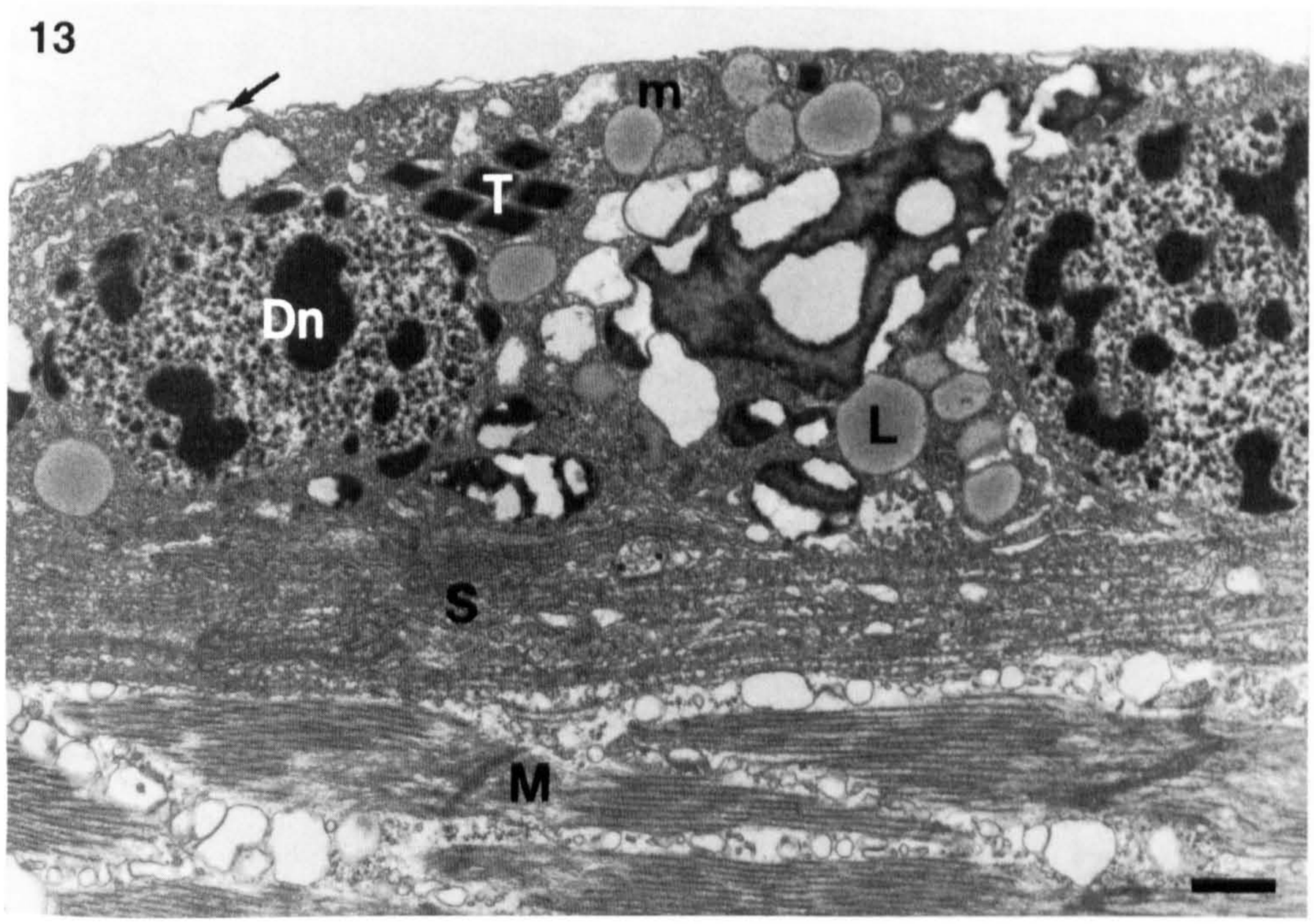


Fig. 13. *Nephrops norvegicus*. Transmission electron micrograph showing a dinoflagellate associated with the sarcolemmal membrane of an abdominal muscle fibre from a stage IV infected lobster. m: mitochondrion of parasite; T: trichocysts; Dn: dinoflagellate nucleus; L: lipid-like droplet; S: sarcolemma of abdominal muscle fibre; M: muscle fibre; arrow: amphiesmal alveolus of dinoflagellate plasma membrane. Scale bar = 1 µm

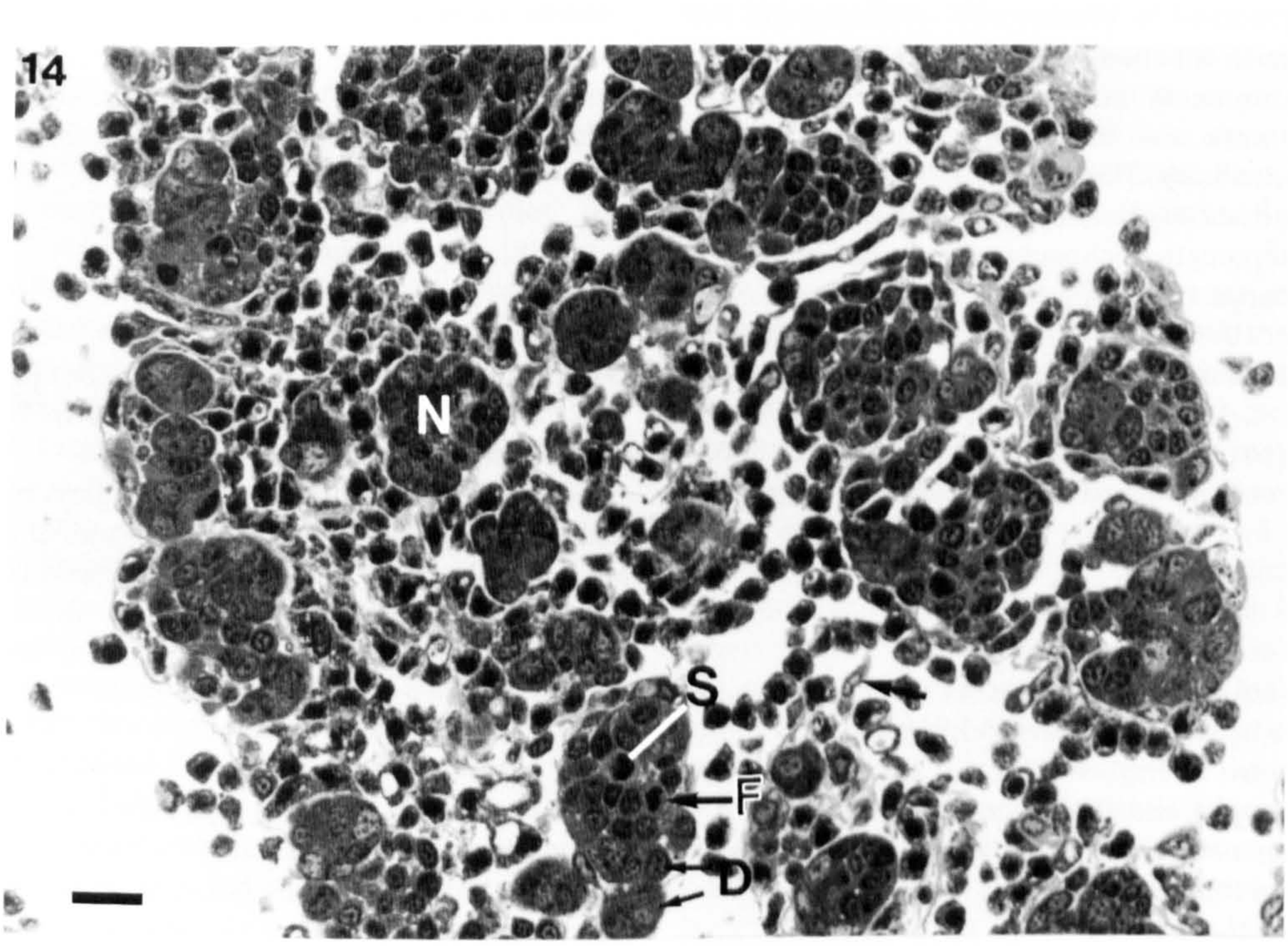


Fig. 14. *Nephrops norvegicus*. Light micrograph showing apparently active haemopoietic tissue of a stage IV infected lobster, surrounded by many uninucleate and multinucleate dinoflagellates. N: haemopoietic node; S: probable stem cell; F: mitotic figure; D: differentiating cells; arrow: host haemocyte. Toluidine blue. Scale bar = 20 µm

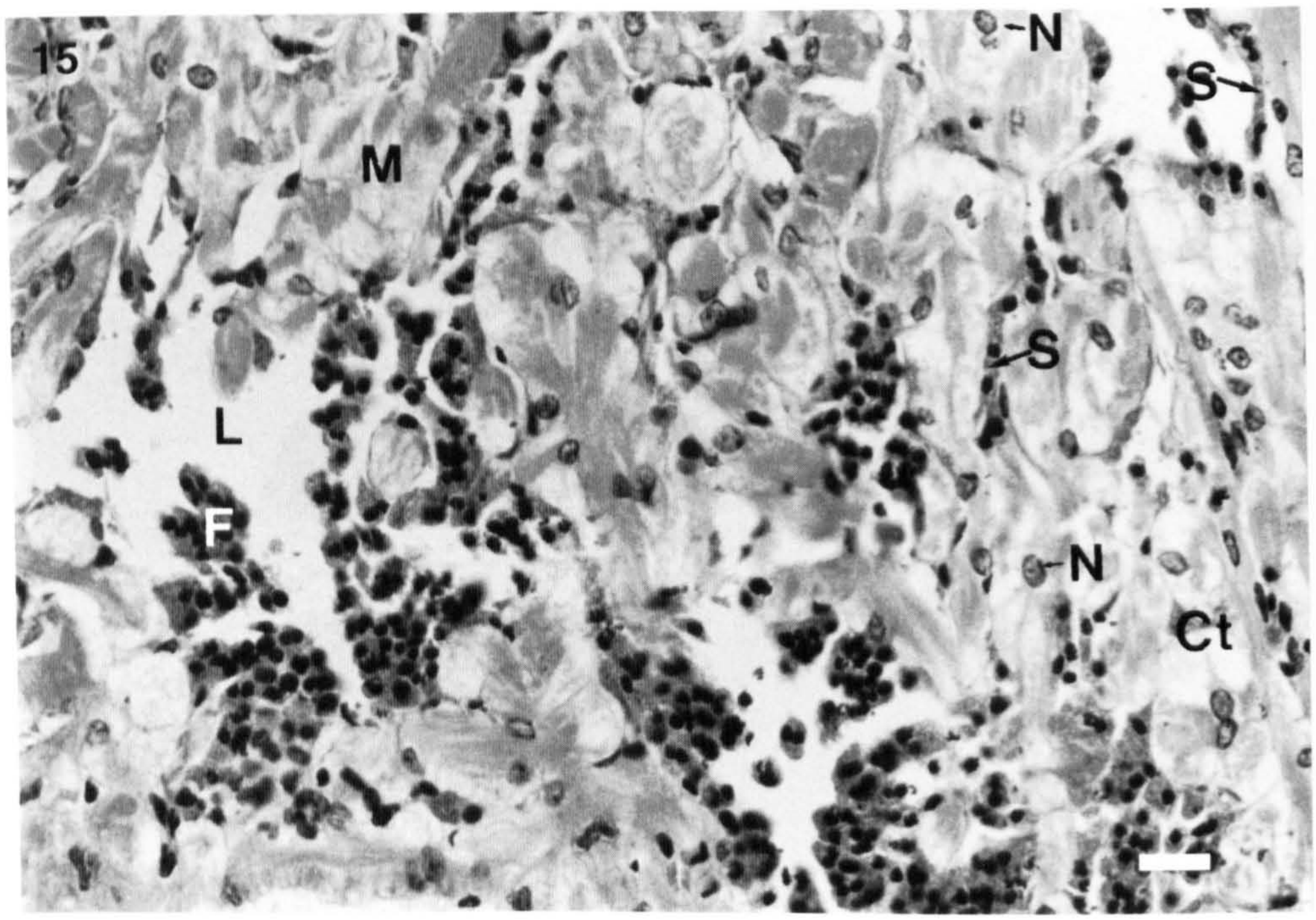


Fig. 15. *Nephrops norvegicus*. Light micrograph of the myocardium of the heart of a stage II infected individual, showing the presence of both filamentous and network syncytia of parasites attached to myocardial muscle within the lumen. L: lumen of heart; M: myocardial muscle; F: filamentous dinoflagellate syncytia; S: network-like dinoflagellate syncytia; N: myocardial nuclei; Ct: connective tissue. H&E. Scale bar = 20 µm

cardial muscle in all stages (Fig. 15), similar to those in abdominal muscle interstices. Some haemocyte aggregations were seen in the lumen of the hearts of stage I to III individuals. These aggregations were tightly packed and had nuclei of a karyolytic appearance. These resembled haemocyte encapsulations observed in response to bacterial infections in *Homarus americanus* (Johnson et al. 1981) and *Callinectes sapidus* (Johnson 1976), and previously reported in *Nephrops norvegicus* gills (Field et al. 1992), and may represent a degree of host response to parasites, although aggregations have not yet been confirmed as containing dinoflagellates.

### Gills

The major effect on the gills was the occlusion of haemal spaces by large numbers of dinoflagellates. This was more severe in higher infection stages, but still apparent in stage I and II lobsters. Attached parasite syncytia were not observed in this tissue, but evidence of host reaction to infection was seen. Haemocyte aggregations similar to those observed in the lumen of the heart were seen in gill filaments (Field et al. 1992), sometimes apparently blocking them. Aggregations were more frequent in the gills than the heart, but were only seen in the narrower regions of the filaments. Free haemocytes were rare, particularly in those lobsters with gills having large numbers of free parasites.

### Other organs

In brain and eyestalk tissues there were no overt signs of parasite infiltration or tissue change. Parasites were restricted to uninucleate forms in the haemal sinuses and vessels of these tissues.

It should be noted that in some organs (particularly heart and hepatopancreas) the numbers of unattached parasites observed in haemal spaces and lumina may be an under-representation of actual numbers, due to losses during processing for both light and electron microscopy.

## DISCUSSION

The effects of dinoflagellate infection of *Nephrops norvegicus* are typical of those reported for haemocoelic infections of decapods by both protistans and bacteria of several groups. The general histologic features of tissue change of the digestive and excretory

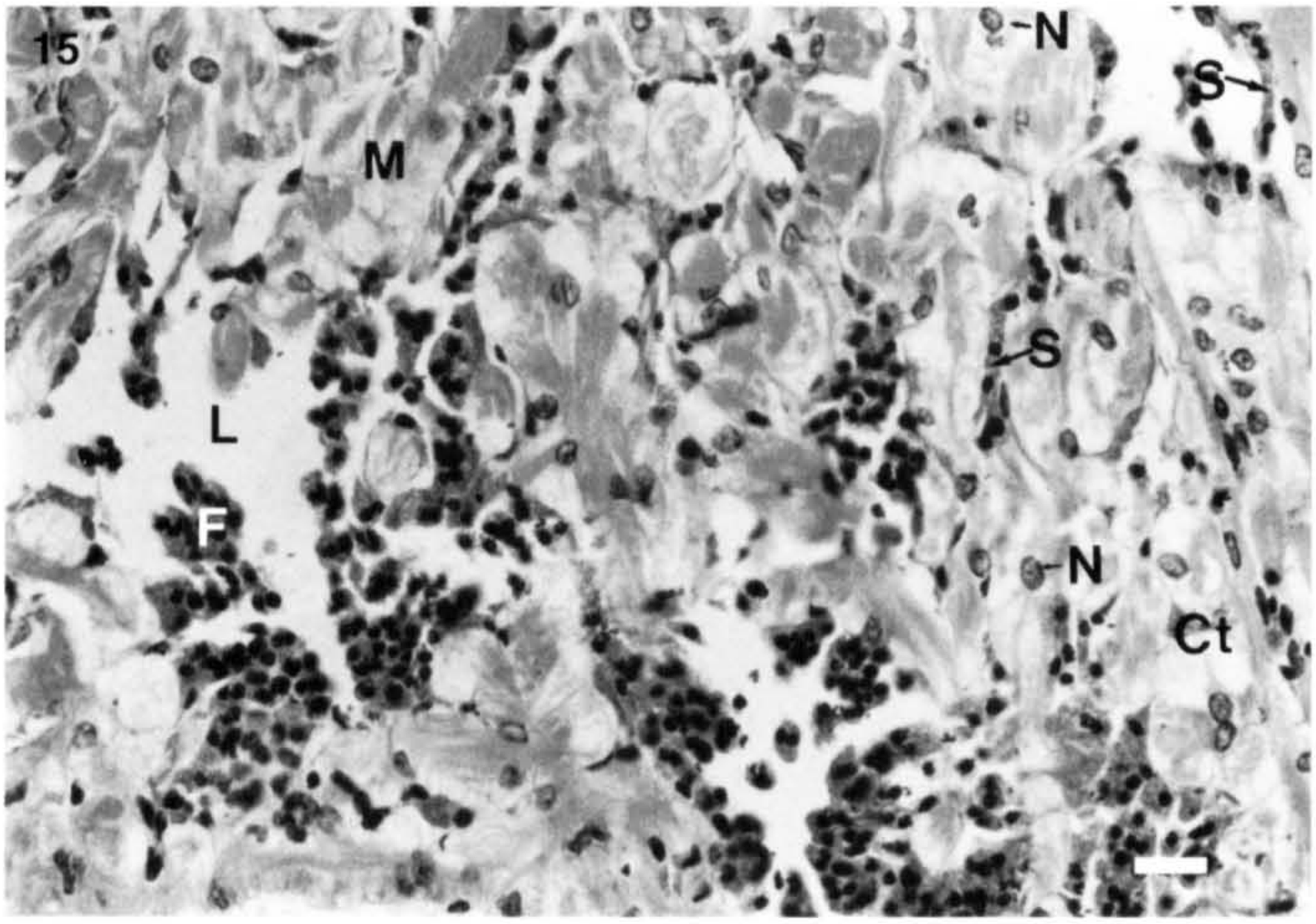


Fig. 15. *Nephrops norvegicus*. Light micrograph of the myocardium of the heart of a stage II infected individual, showing the presence of both filamentous and network syncytia of parasites attached to myocardial muscle within the lumen. L: lumen of heart; M: myocardial muscle; F: filamentous dinoflagellate syncytia; S: network-like dinoflagellate syncytia; N: myocardial nuclei; Ct: connective tissue. H&E. Scale bar = 20 µm

cardial muscle in all stages (Fig. 15), similar to those in abdominal muscle interstices. Some haemocyte aggregations were seen in the lumen of the hearts of stage I to III individuals. These aggregations were tightly packed and had nuclei of a karyolytic appearance. These resembled haemocyte encapsulations observed in response to bacterial infections in *Homarus americanus* (Johnson et al. 1981) and *Callinectes sapidus* (Johnson 1976), and previously reported in *Nephrops norvegicus* gills (Field et al. 1992), and may represent a degree of host response to parasites, although aggregations have not yet been confirmed as containing dinoflagellates.

### Gills

The major effect on the gills was the occlusion of haemal spaces by large numbers of dinoflagellates. This was more severe in higher infection stages, but still apparent in stage I and II lobsters. Attached parasite syncytia were not observed in this tissue, but evidence of host reaction to infection was seen. Haemocyte aggregations similar to those observed in the lumen of the heart were seen in gill filaments (Field et al. 1992), sometimes apparently blocking them. Aggregations were more frequent in the gills than the heart, but were only seen in the narrower regions of the filaments. Free haemocytes were rare, particularly in those lobsters with gills having large numbers of free parasites.

### Other organs

In brain and eyestalk tissues there were no overt signs of parasite infiltration or tissue change. Parasites were restricted to uninucleate forms in the haemal sinuses and vessels of these tissues.

It should be noted that in some organs (particularly heart and hepatopancreas) the numbers of unattached parasites observed in haemal spaces and lumina may be an under-representation of actual numbers, due to losses during processing for both light and electron microscopy.

## DISCUSSION

The effects of dinoflagellate infection of *Nephrops norvegicus* are typical of those reported for haemocoelic infections of decapods by both protistans and bacteria of several groups. The general histologic features of tissue change of the digestive and excretory

organs and of interference with respiratory exchange, haemopoiesis or metabolism (Field 1992) are characteristic of such haemocoelic infections caused by bacteria (Johnson 1976), dinoflagellates (Maclean & Ruddell 1978, Meyers et al. 1987, Meyers 1990), Chlamydia-like organisms (Sparks et al. 1985) and ciliates (Sparks et al. 1982). However, many protistan and bacterial diseases, such as gaffkemia and the presently reported dinoflagellate infection, may have notable effects on the serum of the haemolymph, as well as on the physiology and metabolism of their hosts. These aspects remain largely un-investigated. More information is available upon the histopathology of infected hosts, on haemocyte changes and responses and on their progenitor, the haemopoietic tissue.

The results presented here confirm that there is an increase in the combined number of haemocytes and parasites in the haemolymph with infection, due to increases in the proportion of dinoflagellates, and that this increases with severity as determined by the pleopod staging method. These increases did not correlate directly with the pleopod staging series; combined haemocyte/parasite counts were not raised significantly above the range of apparently uninfected levels until the pleopod assessment indicated stage III or stage IV infection. At this stage, dinoflagellate parasites comprised over 70% of the combined haemocyte/dinoflagellate numbers. This also suggests a reduction in the number of haemocytes in the circulation, coincident with parasite proliferation. The staging technique detects an increase in the severity of haemolymph/haemocoel infection even in stage I lobsters. However, histopathological evidence suggests that dinoflagellate infection is much more severe than indicated by haemolymph infection alone, and that the pleopod staging method is less sensitive than previously believed. Most major organs and tissues were heavily infiltrated with parasite stages in the stage I lobsters examined, raising the possibility that parasites in the haemolymph originate from earlier tissue forms. These results indicate that the pleopod staging method is relatively reliable as a field method for detecting the presence of dinoflagellates in the haemolymph, but may be less so as an indicator of absolute infection and the involvement of the tissues.

Haemocytopoenia has been noted as a sign of many haemocoelic infections of crustaceans caused by both bacteria and protists. Disappearance of haemocytes from circulation has been noted in gaffkemia of *Homarus americanus* (Stewart et al. 1969, Johnson et al. 1981), *Paranophrys* sp. infection of dungeness crabs *Cancer magister* (Sparks et al. 1982), and *Paramoeba perniciosa* infections (Johnson 1977) and bacterial infections (Johnson 1976) of blue crabs *Callinectes sapidus*. Sparks et al. (1982) attribute the haemocytopoenia in dungeness crabs infected with ciliates to consumption of haemocytes by the invading cells. However, reduction in haemocyte numbers in *P. perniciosa* infections was reported to be the result of host cellular defence reactions, the possible lysis of host cells after phagocytosing parasite cells, and possible disruption of haemopoietic tissue function (Johnson 1977). Similarly, in gaffkaemic lobsters, haemocyte aggregations are widely reported in response to the invading bacteria (Rittenburg et al. 1979, Johnson et al. 1981). It is, therefore, possible that in *Nephrops norvegicus* infected with dinoflagellates, increased activity in the haemopoietic tissue and the presence of haemocyte aggregations are indications of the initiation of a host reaction to infection. The haemocytes may be removed from circulation by encapsulating dinoflagellates, forming the aggregations observed. The increase in haemopoietic activity may be explained, in part at least, by the time of year at which infected individuals were available. The occurence of lobsters infected with the dinoflagellate is seasonal (Field 1992, Field et al. 1992), occurring in the spring and early summer, a time when large-scale haemocyte production is known to occur in some decapods, e.g. *C. sapidus* (Johnson 1980). Even stage IV dinoflagellate-infected *N. norvegicus* retain apparently functional fixed phagocytes, but despite this and the increased haemopoietic activity, appear unable to control the parasites. The paucity of haemocytes may be explained by their sequestration into haemocyte capsules and other defence reactions at an early stage of infection. These reactions are apparently overwhelmed by the increasing parasite load. An alternative view is that the host fails to respond due to some action of the parasite.

Another salient feature of the presence of so many invading parasites within the haemocoel is the mechanical disruption they cause to blood circulation. Apart from the hydrostatic effects of this overburden of circulating cells, clogging of blood vessels and sinuses may also occur. This will be particularly so in areas of restricted diameter, such as the smaller capillaries and sinuses, and the haemal spaces within organs. Restriction of blood flow is likely to be further exacerbated within areas where large numbers of filamentous parasite syncytia are attached to host tissues. Clogging may also result from the formation of haemocyte aggregations as part of a host response to infection, as seen in the gill filaments of *Nephrops norvegicus*, and postulated by Rittenburg et al. (1979) to contribute to tissue hypoxia in gaffkaemic lobsters. The aggregation of haemocytes, and the formation of acellular haemolymph clots in blue crabs *Callinectes sapidus* in response to bacterial infections, have also been implicated in impeding blood flow through the gills (Johnson 1976).

As yet there is no irrefutable evidence that this condition is always fatal to infected lobsters (Field et al. 1992), although the systemic nature of the infection and its wide variety of effects upon the host suggest that severe debility and death probably result in many, if not all, cases.

*Acknowledgements:* This work was conducted with support partly from the Science and Engineering and Research Council (CASE award to R.H.F.) and partly from the Ministry of Agriculture, Fisheries and Food.

## LITERATURE CITED

Aiken DE (1980) Moulting and growth. In: Cobb JS, Phillips BF (eds) The biology and management of lobsters, Vol 1. Academic Press, New York, p 91–163

Chatton E, Poisson R (1931) Sur l' existence, dans le sang des crabs, de peridiniens parasites *Hematodinium* perezi n.g., n.sp. (Syndinidae). C r séanc Soc biol 105:553–557

Doughtie DG, Rao KR (1983) Ultrastructural and histological study of degenerative changes in the antennal glands, hepatopancreas, and midgut of grass shrimp exposed to two dithiocarbamate biocides. J Invertebr Pathol 41: 281–300

Eaton WD, Love DC, Botelho C, Meyers TR, Imamura K, Koeneman T (1991) Preliminary results on the seasonality and life cycle of the parasitic dinoflagellate causing bitter crab disease in Alaskan tanner crabs (*Chionoecetes bairdi*). J Invertebr Pathol 57:426–434

Field RH (1992) The control of escape behaviour in, and the histopathology of, the Norway lobster, *Nephrops norvegicus* (L.). PhD thesis, University of Glasgow

Field RH, Chapman CJ, Taylor AC, Neil DM, Vickerman K (1992) Infection of the Norway lobster *Nephrops norvegicus* by a *Hematodinium*-like species of dinoflagellate on the west coast of Scotland. Dis aquat Org 13:1–15

Hudson DA, Hudson NB, Shields JD (1992) Infection of *Trapezia* spp. (Decapoda: Xanthidae) by *Hematodinium* sp. (Duboscquodinida: Syndinidae): a new family record of infection. J Fish Dis 16:273–276

Johnson PT (1976) Bacterial infection in the blue crab, *Callinectes sapidus*: course of infection and histopathology. J Invertebr Pathol 28:25–36

Johnson PT (1977) Paramoebiasis in the blue crab *Callinectes sapidus*. J Invertebr Pathol 29:308–320

Johnson PT (1980) Histology of the blue crab, *Callinectes sapidus*. A model for the Decapoda. Praeger, New York

Johnson PT (1986) Parasites of benthic amphipods: dinoflagellates (Duboscquodinida: Syndinidae). Fish Bull 84: 605–614

Johnson PT (1987) A review of fixed phagocytes and pinocytotic cells of decapod crustaceans, with remarks on hemocytes. Dev Comp Immunol 11:679–704

Johnson PT, Stewart JE, Arie B (1981) Histopathology of *Aerococcus viridans* var. *homari infection* (Gaffkemia) in the lobster, *Homarus americanus*, and a comparison with histological reactions to a Gram-negative species *Pseudomonas perolens*. J Invertebr Pathol 38:127–148

Latrouite D, Morizur Y, Noël P, Chagot D, Wilhelm G (1988) Mortalité du torteau *Cancer pagurus* provoquée par le dinoflagelle parasite: *Hematodinium* sp. Comm Meet int Coun Explor Sea CM-ICES 1988/K:32

Love DC, Rice SD, Moles DA, Eaton WD (1993) Seasonal prevalence and intensity of Bitter Crab dinoflagellate infection and host mortality in Alaskan Tanner crabs *Chionoecetes bairdi* from Auke Bay, Alaska, USA. Dis aquat Org 15:1–7

Maclean SA, Ruddell CL (1978) Three new crustacean hosts for the parasitic dinoflagellate *Hematodinium* perezi (Dinoflagellata: Syndinidae). J Parasitol 64:158–160

Meyers TR (1990) Disease of Crustacea. Diseases caused by protistans and metazoans. In: Kinne O (ed) Diseases of marine animals, Vol 3. Biologische Anstalt Helgoland, Hamburg, p 350–389

Meyers TR, Botelho C, Koeneman TM, Short S, Imamura K (1990) Distribution of bitter crab dinoflagellate syndrome in southeast Alaskan tanner crabs *Chionoecetes bairdi*. Dis aquat Org 9:37–43

Meyers TR, Koeneman TM, Botelho C, Short S (1987) Bitter Crab Disease: a fatal dinoflagellate infection and marketing problem for Alaskan tanner crabs *Chionoecetes bairdi*. Dis. aquat. Org. 3:195–216

Newman MW, Johnson CA (1975) A disease of blue crabs (*Callinectes sapidus*) caused by a parasitic dinoflagellate, *Hematodinium* sp. J Parasitol 61:554–557

Parry G (1960) Excretion. In: Waterman TH (ed) The physiology of Crustacea, Vol 1. Metabolism and growth. Academic Press, New York, p 341–366

Rittenberg JH, Gallagher ML, Bayer RC, Leavitt DF (1979) The effect of *Aerococcus viridans* var. *homari* on the oxygen binding capacity of hemocyanin in the American lobster (*Homarus americanus*). Trans Am Fish Soc 108:172–177

Shields JD (1992) Parasites and symbionts of the crab *Portunus pelagicus*, from Moreton Bay, Australia. J Crust Biol 12:94–100

Sparks AK, Hibbits J, Fegley JC (1982) Observations on the histopathology of a systemic ciliate (*Paranophrys* sp.?) disease in the dungeness crab *Cancer magister*. J Invertebr Pathol 39:219–228

Sparks AK, Morado JF, Hawkes JW (1985) A systemic microbial disease in the dungeness crab *Cancer magister*, caused by a *Chlamydia*-like organism. J Invertebr Pathol 45:204–217

Spurr AR (1969) A low viscosity epoxy embedding resin for electron microscopy. J Ultrastruct Res 26:31–43

Stewart JE, Arie B, Zwicker BM, Dingle JR (1969) Gaffkemia, a bacterial disease of the lobster, *Homarus americanus*: effects of the pathogen, *Gaffkya homari*, on the physiology of the host. Can J Microbiol 15:925–932

Stewart JE, Cornick JW, Dingle JR (1967) An electronic method for counting lobster (*Homarus americanus* Milne Edwards) hemocytes and the influence of diet on hemocyte numbers and hemolymph proteins. Can J Zool 45: 291–304

Vickerman K, Appleton PL, Field RH (1993) Cultivation and development *in vitro* of a parasitic dinoflagellate (*Hematodinium* sp) from the Norway lobster (*Nephrops norvegicus*). In: Abstracts of the IX International Congress of Protozoology. German Society of Protozoology and German Society of Parasitology, Berlin, p 131

Wilhelm, G. & Boulo, V. (1988). Infection de l'étrille *Liocarcinus puber* (L.) par un dinoflagelle parasite de type *Hematodinium* sp. Comm Meet int Coun Explor Sea CM-ICES 1988/K:41

*Responsible Subject Editor: J. E. Stewart, Dartmouth, Nova Scotia, Canada*

*Manuscript first received: August 24, 1994*
*Revised version accepted: February 23, 1995*

Vol. 24: 199–204, 1996 | DISEASES OF AQUATIC ORGANISMS
Dis aquat Org | Published March 7

# An indirect fluorescent antibody technique for the diagnosis of *Hematodinium* sp. infection of the Norway lobster *Nephrops norvegicus*

**R. H. Field, P. L. Appleton***

**Division of Environmental and Evolutionary Biology, Institute of Biomedical and Life Sciences, Graham Kerr Building, University of Glasgow, Glasgow G12 8QQ, Scotland, UK**

ABSTRACT: An indirect fluorescent antibody technique (IFAT) has been developed to detect *Hematodinium* sp. in the haemolymph and tissues of the Norway lobster *Nephrops norvegicus*. The IFAT, being more sensitive and reliable than previously used field and laboratory diagnostic techniques, detects both lower-level haemolymph infections as well as previously undiagnosable tissue infections. Low-level haemolymph and organ *Hematodinium* sp. infections have been found in apparently uninfected lobsters at all times of year, including late summer and autumn, when the parasite was previously thought to be absent from host lobsters. Currently, IFAT is routinely used for laboratory studies and the calibration of field diagnostic techniques.

KEY WORDS: IFAT diagnosis · *Hematodinium* · *Nephrops norvegicus* · Parasitic dinoflagellate · Crustacean disease

## INTRODUCTION

*Nephrops norvegicus*, a common and commercially important decapod crustacean in Scotland, hosts pathogenic parasitic dinoflagellates of the genus *Hematodinium* (Field et al. 1992). *Hematodinium* spp. and *Hematodinium*-like organisms are becoming increasingly well known from a variety of crustacean hosts and geographical locations, often associated with mortality (Shields 1994). Such infections in *N. norvegicus* are widespread at certain times of year and the majority are thought to be fatal (Field et al. 1992).

Infection by *Hematodinium* sp. in *Nephrops norvegicus* has previously been diagnosed in the field by observation of the parasite in the haemolymph via the transparent cuticle of the pleopods (Field et al. 1992, Field & Appleton 1995). The reliability and sensitivity of this method has been evaluated by direct observation of *Hematodinium* parasites in haemolymph smears stained with Leishman's stain (Field & Appleton 1995). The pleopod examination technique has also been used successfully for the diagnosis of *Hematodinium* in blue crabs *Callinectes sapidus* (Messick 1994).

Although pleopod examination provides a simple field diagnosis requiring little technical support, and the Leishman's stained smear has provided a more direct observational confirmation of diagnoses, use of these methods requires a degree of training. Moreover, although parasites are easily recognisable in the majority of haemolymph smears stained with Leishman's stain, experience is required for reliable diagnosis and, in cases of very light infection or poorly made smears, parasites can be hard to recognise or can be confused with certain classes of host haemocyte. Low numbers of *Hematodinium* sp. in haemolymph are often hard to detect in Leishman's stained smears, and therefore remain 'sub-patent' by current diagnostic methods. Although both these methods are valid, there is a need for a better, yet easily conducted, diagnostic test. Hence, an indirect fluorescent antibody technique (IFAT) has been developed. The IFAT can be used on a routine basis for the detection of *Hematodinium* sp. not

*Addressee for reprint requests.
E-mail: 922725ap@udcf.gla.ac.uk

only in haemolymph, but also in tissue samples. Since we have previously suggested that 'latent' tissue infection (*Hematodinium* sp. being present only in organs) may precede that of the haemolymph, the ability to diagnose infections in these tissues would improve the interpretation of field prevalence data obtained by haemolymph infection-based diagnostic methods.

## MATERIALS AND METHODS

**Antibody.** A polyclonal antibody was derived from rabbits immunized with a mixture of vegetative forms of the infecting organism from *in vitro* culture (Vickerman et al. 1993). Parasite forms commonly observed in both haemolymph and tissues (Field & Appleton 1995) from axenic cultures were used. Briefly, the methods (Harlow & Lane 1988) included the following: washed pelleted cells from axenic culture were resuspended in *Nephrops norvegicus* saline and lysed by 3 cycles of freeze-thawing. Insoluble material was removed by mild centrifugation. Between 30 and 300 µg of soluble protein (dependant upon the cultured parasite form) in buffered *N. norvegicus* saline was inoculated with an equal volume of Freund's complete adjuvant into 6 rabbits at 6 subcutaneous sites. Preimmunization control serum was collected from the test rabbits beforehand. After test bleeds, the 2 rabbits showing the highest titre responses were selected for further inoculation. Secondary, tertiary and quaternary inocula were injected with Freund's incomplete adjuvant every 4 wk, with further test bleeds taken 2 wk after each inoculation. Rabbits were exsanguinated 4 wk after the final inoculation, and serum separated from clotted blood was frozen at –70°C until required.

**Indirect fluorescent antibody technique.** The IFAT employed was similar to that described by Marks et al. (1992) for the diagnosis of *Aerococcus viridans* in lobster *Homarus americanus* haemolymph. The technique was applied initially to fixed smears of cultured *Hematodinium* sp. originally isolated from infected *Nephrops norvegicus*, and later to fixed smears of haemolymph from infected and control lobsters.

Haemolymph samples were withdrawn from the ventral haemal sinus of lobsters into a syringe containing 2% formol saline (33‰) at a ratio of 2:1, allowed to fix for approximately 15 min and smeared onto clean glass slides. Culture material was smeared directly onto slides and fixed in ice cold 70% ethanol for 1 h. Tissue smears were made by removal of organs from killed lobsters directly into fixative containing 2% paraformaldehyde and 0.1% glutaraldehyde, 4% sucrose and 3% NaCl in 0.1 M phosphate buffer, pH 7.4. Tissue samples were rinsed in 0.1 M phosphate buffer containing 6.5% sucrose and stored in the same buffer, containing azide, at 4°C until required. Small pieces of tissue (~1 $mm^3$) were macerated and smeared onto clean glass slides. Tissue and haemolymph smears were then air dried at room temperature and incubated in phosphate buffered saline (PBS) (pH 7.2) with 0.2% Tween 20 and either 3% bovine serum albumen (BSA) or 10% foetal calf serum for 15 min. Slides were incubated for 1 h at room temperature with primary anti-*Hematodinium* sp. rabbit antibody diluted to 1:100 with PBS/BSA. Slides were washed with 5 changes of PBS/0.1% BSA for 10 min each and incubated with secondary donkey antirabbit fluorescein labelled antibody (Scottish Antibody Production Unit) at a dilution of 1:100 with PBS/BSA plus 10 µg $ml^{-1}$ 4',-6-diamidino-2-phenylindole (DAPI) (Sigma) as counter stain for 1 h. Finally, smears were washed thoroughly with PBS/0.1% BSA for 10 min. Control slides were exposed to PBS/BSA containing no rabbit immune serum during the first incubation, or were incubated in preimmune rabbit serum. Control staining was also performed on smears of haemolymph containing another protist commonly found in moribund *Nephrops norvegicus* in captivity, a *Paranophrys*-like ciliate. Slides were mounted in 10% PBS in glycerol with 25 mg $ml^{-1}$ 1,4-diazabicyclo-[2.2.2]-octane (DABCO) antifadant and examined using phase contrast and ultraviolet (UV) epifluorescence. Entire treated slides were examined for the presence of immunoreactive dinoflagellates under a low power objective (×10). Upon detection of parasite material, the relative proportions of haemocytes and parasites were calculated after a total of approximately 400 cells were counted and identified. A characteristic of *Hematodinium* spp. is that many individual parasites are multinucleate, therefore counts were based on the number of nuclei of parasites or haemocytes stained by the DAPI nuclear counter stain. Quantitative counts of parasites from tissue smears were not possible, so presence or absence of parasite material alone was recorded.

**Collection and maintenance of lobsters.** Lobsters *Nephrops norvegicus* (25 to 35 mm carapace length) were caught by bottom trawling around the Isle of Cumbrae, Clyde Sea Area, Scotland, and maintained in a closed seawater system at 10°C and 33‰ salinity prior to use in experimental work.

**Experimental comparison of diagnostic methods.** Haemolymph samples were obtained from a total of 165 lobsters in spring and summer 1994, and both the status of *Hematodinium* sp. infection (Field et al. 1992, Field & Appleton 1995) and moult stage (Aiken 1980) were determined by pleopod examination. One haemolymph smear from each lobster was immunostained as described, and one was stained with Leishman's stain (Field & Appleton 1995). Haemolymph smears were

examined microscopically to record the presence or absence of dinoflagellate parasites observed with each staining method.

**Detection of latent *Hematodinium* infection using IFAT.** Staining by IFAT was used to determine whether latent (not detectable in haemolymph by current diagnostic methods) *Hematodinium* sp. infections were present in adult *Nephrops norvegicus* at different times of year. Previous work showed that detectable infections were present in *N. norvegicus* populations only during spring (Field 1992, Field et al. 1992). However, evidence from pathology and *in vivo* studies suggested that latent and/or subpatent infections may be present at other times of year (Field & Appleton 1995, unpubl. obs.). Between 11 and 30 individuals were collected in January, February, March, August, October and November 1994. Lobsters were selected at random from trawl samples, but were all diagnosed as uninfected by pleopod examination. Thereafter, haemolymph smears were made from each individual. Tissue smears were prepared from samples of hepatopancreas, midgut, heart and abdominal muscle removed from lobsters killed by decapitation. Both haemolymph and tissue smears were immunostained and examined for the presence of fluorescing parasites.

Despite the range of different fixation methods used for parasites in culture, haemolymph and tissue samples, there was no difference in the reliability or sensitivity of immunostaining (results not shown).

## RESULTS

### Evaluation of *Hematodinium* antibody and the IFAT

Staining of *Hematodinium* sp. in haemolymph smears by IFAT showed good antibody specificity for the parasite (Fig. 1). Host haemocytes were unreactive whilst background staining and autofluorescence were low in haemolymph smears. Although there was no binding of the antibody to host cells in tissue smears (Fig. 2), there was a degree of autofluorescence, especially in the hepatopancreas. This autofluorescence was minimised by ensuring thorough maceration of samples. All controls tested gave negative results, the rabbit antibody showed no affinity for host haemocytes or ciliates and there was no non-specific binding of the secondary donkey antirabbit antibody.

### Comparison of diagnostic methods

The accuracy of pleopod diagnosis of *Hematodinium* sp. infection compared with 2 methods of haemolymph examination is shown in Table 1. This assessment is

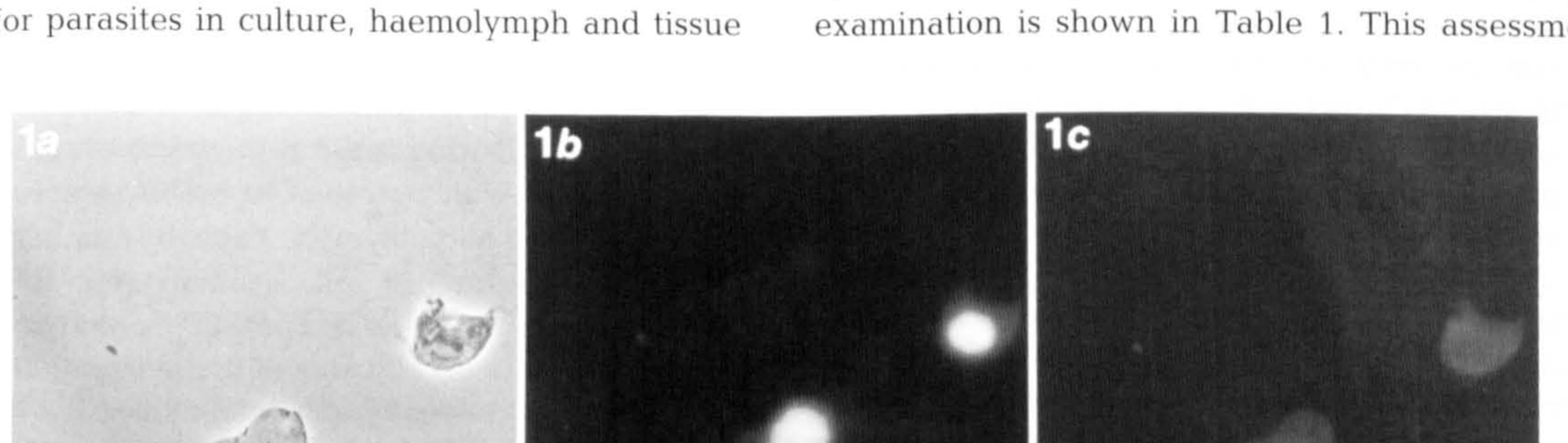


Fig. 1. Light micrographs showing specific labelling of *Hematodinium* sp. parasites by IFAT in a fixed *Nephrops norvegicus* haemolymph smear: (a) under phase contrast illumination; (b) under UV epifluorescence, showing DAPI nuclear counter stain; (c) under UV epifluorescence, showing labelling of *Hematodinium* sp. with fluorescent antibody while haemocytes remain unlabelled. Arrows: *Hematodinium* sp. parasites. Scale bars = 20 µm

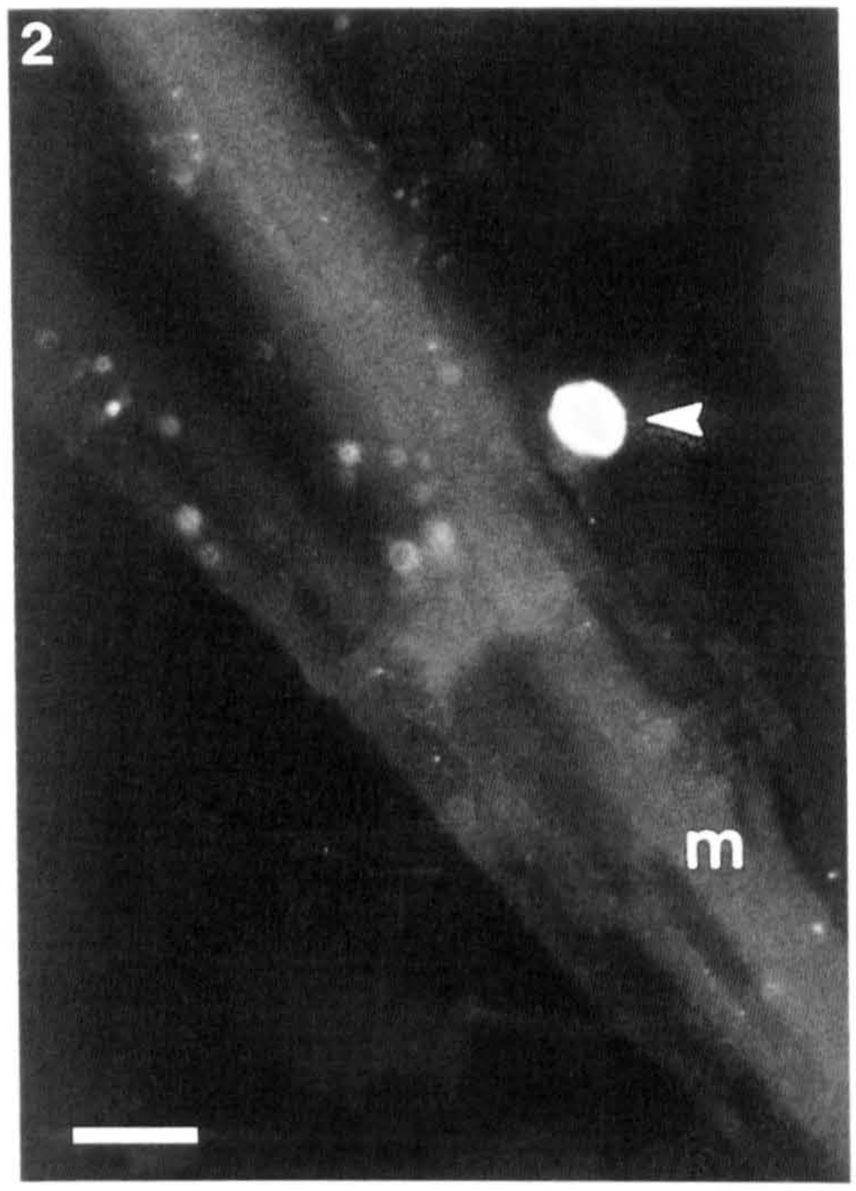


Fig. 2. Light micrograph showing a fluorescently labelled *Hematodinium* sp. parasite next to unlabelled abdominal muscle in a fixed *Nephrops norvegicus* tissue smear. m: abdominal muscle; arrow: parasite. Scale bar = 20 µm

based on the parallel examination of both sexes of lobsters by all 3 methods. Of those lobsters examined, 25 (15.1%) were diagnosed as infected by pleopod examination. Examination of Leishman's stained haemolymph smears revealed 34 individuals were harbouring *Hematodinium* sp. in their haemolymph (20.6%). Immunostaining detected 37 (22.4%) individuals within the sample that were infected, 12 more than by pleopod and 3 more than by Leishman's stain. Three individuals were diagnosed as infected by immunostaining alone. No infected lobsters diagnosed by pleopod examination were classified as being uninfected by other methods. All misdiagnoses by pleopod examination and Leishman's staining were made in lobsters initially staged as uninfected by pleopod examination but subsequently found to be infected by immunostaining or both smear examination methods. Those subpatent infections detected by immunostaining but undetected by Leishman's stain showed the lowest proportions of parasites to haemocytes, ranging from 0.3 to 1.7% (1 parasite:383 haemocytes, and 6:346 respectively). The lowest proportion detected by Leishman's stain was 2.4% (9:366).

Table 1. Comparison of the accuracy of pleopod diagnosis of *Hematodinium* sp. infection with 2 methods of haemolymph staining

| | Diagnostic method | | |
|---|---|---|---|
| | Pleopod | Leishman's stain | Immunostaining |
| Number of lobsters/165 | 25 | 34 | 37 |
| % prevalence | 15.1 | 20.6 | 22.4 |

### Detection of latent *Hematodinium* sp. infection by immunostaining

Throughout the year, lobsters diagnosed as uninfected by pleopod examination were, in fact, harbouring subpatent or latent *Hematodinium* sp. infection detectable by IFAT (Table 2). Lobsters that contained parasites only in the tissues (latent infection), with no detectable haemolymph infections, were found at all times of year. During most of the year, some lobsters were infected with parasites in both the tissues and haemolymph. Parasite numbers were low in all haemolymph infections found in this part of the study.

In all cases of tissue infection where haemolymph infection also occurred, parasites in the tissues were abundant and represented all tissue forms so far described (Field et al. 1992, Field & Appleton 1995). Well-established network syncytia were often observed in

Table 2. Results of fluorescent antibody survey for prepatent *Hematodinium* sp. infection of *Nephrops norvegicus* between January and November 1994. Hp: hepatopancreas

| Month | Number infected | | Total infected/sample size | Infected tissues |
|---|---|---|---|---|
| | Haemolymph and tissues | Tissues | | |
| January | 3 | 2 | 5/11 | Muscle, midgut, Hp |
| February | 2 | 2 | 4/30 | Heart |
| March | 0 | 1 | 1/12 | Midgut |
| August | 2 | 2 | 4/15 | Hp |
| October | 1 | 2 | 3/15 | Muscle |
| November | 2 | 2 | 4/15 | Midgut, Hp |

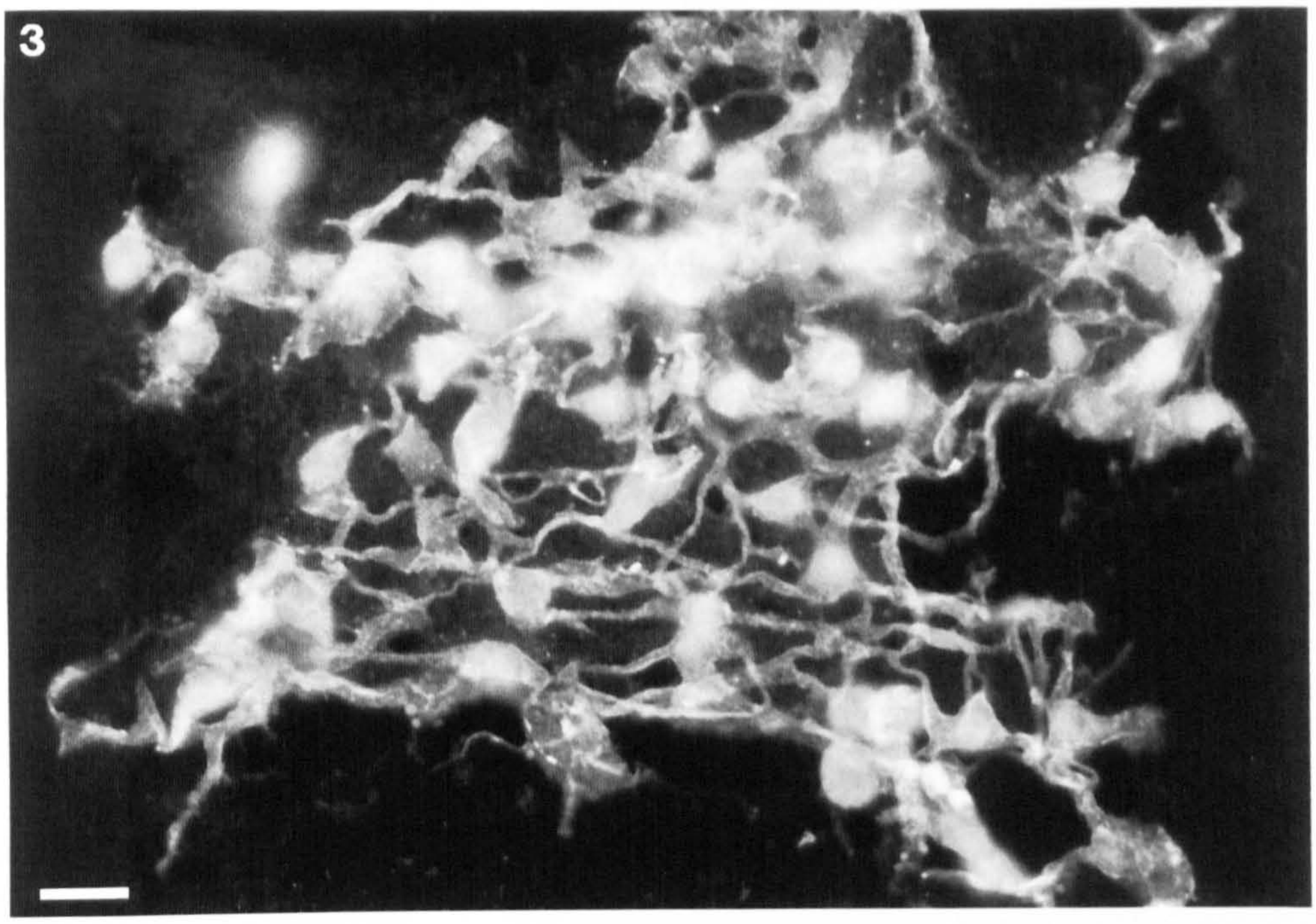


Fig. 3. Light micrograph showing fluorescently labelled multinucleate network-like parasite syncytium in a fixed hepatopancreas smear from *Nephrops norvegicus*. Scale bar = 20 µm

abdominal muscle and hepatopancreas smears (Fig. 3). The observation of this form in the hepatopancreas increased the known range of tissue sites harbouring network parasites, previously known only within abdominal skeletal muscle and myocardial muscle (Field & Appleton 1995). In all cases of tissue infection where no haemolymph infection occurred (latent) parasite abundance was lower.

## DISCUSSION

The IFAT method described shows good specificity for *Hematodinium* sp. infecting the haemolymph and tissues of *Nephrops norvegicus*. The lack of cross-reactivity of the antibody with host tissues or other commonly observed protistans makes this method suitable and effective for the identification of *Hematodinium* sp. infection in both the haemolymph and tissues of infected lobsters. It is possible to identify dinoflagellate parasites while scanning slides at relatively low magnifications, unlike the detailed examination required of Leishman's stained smears. Although IFAT is only slightly more sensitive for detecting low-level infections than Leishman's staining (0.3% as opposed to 2.4%), its unequivocal diagnosis and its relatively simple methodology make it the most reliable diagnostic method available. Pleopod examination remains the most suitable field method for disease diagnosis, but IFAT may be used to calibrate infection prevalence estimates made in the field. This calibration may be particularly useful in the identification of *Hematodinium* sp. infections in previously unexamined or uninfected stocks. Furthermore, IFAT could be used to identify *Hematodinium*-like infections in new host species as well as from new geographical locations, though the affinity of this antibody for related or similar *Hematodinium* spp. from other crustaceans must be assessed first.

Use of IFAT for *Hematodinium* spp. from other host species represents a practical and potentially more sensitive detection and diagnostic method than those in current use. The benefits over pleopod examination and Leishman's stained smear examination will probably apply to the routine modified pleopod examination method used by Messick (1994) in blue crabs *Callinectes sapidus* and haemolymph examination methods of Meyers et al. (1987) in *Chionoecetes bairdi*.

The discovery of subpatent *Hematodinium* sp. infections in the haemolymph and latent infections in the tissues of apparently uninfected *Nephrops norvegicus* has other implications for surveys of infection prevalence which are made using the pleopod examination method. This initial, small-scale study has shown the number of subpatent and latent infections to be relatively constant throughout the year, irrespective of the number of patent infections observed. However, a larger-scale investigation would elucidate any possible seasonality of subpatent and/or latent infections. The presence of *Hematodinium* sp. parasites in the tissues of lobsters which showed no haemolymph infection appears to support the original hypothesis of Field &

Appleton (1995) that invasion of various organs occurs soon after acquisition of infection, before patent haemolymph infections are detectable. The presence of subpatent and latent dinoflagellate infections at times of year when the parasite was previously thought to be absent from host lobsters suggests a long latency and development period for infection, and that infection acquisition in one year leads to disease patency in the next or even later. Slow rates of parasite growth *in vivo* support this assertion (Field & Appleton unpubl. obs.).

We now employ IFAT on a routine basis for both laboratory diagnosis and confirmation of field prevalence surveys made by pleopod examination.

*Acknowledgements.* This work was carried out with financial support from the Ministry of Agriculture, Fisheries and Food. The authors also express gratitude to Dr C. M. R. Turner for assistance with primary antibody production and testing and critical review of the manuscript, to Mr J. Laurie for technical support and to 2 anonymous reviewers.

## LITERATURE CITED

Aiken DE (1980) Moulting and growth. In: Cobb JS, Phillips BF (eds) The biology and management of lobsters, Vol 1. Academic Press, New York, p 91–163

Field RH (1992) The control of escape behaviour in, and the histopathology of, the Norway lobster, *Nephrops norvegicus* (L.). PhD thesis, University of Glasgow

Field RH, Appleton PL (1995) A *Hematodinium*-like dinoflagellate infection of the Norway lobster *Nephrops norvegicus*: observations on pathology and progression of infection. Dis aquat Org 22:115–128

Field RH, Chapman CJ, Taylor AC, Neil DM, Vickerman K (1992) Infection of the Norway lobster *Nephrops norvegicus* by a *Hematodinium*-like species of dinoflagellate on the west coast of Scotland. Dis aquat Org 13:1–15

Harlow E, Lane DP (1988) Antibodies: a laboratory manual. Cold Spring Harbor Laboratory, Cold Spring Harbor

Marks LJ, Stewart JE, Håstein T (1992) Evaluation of an indirect fluorescent antibody technique for detection of *Aerococcus viridans* (var.) *homari*, pathogen of homarid lobsters. Dis aquat Org 13:133–138

Messick GA (1994) *Hematodinium perezi* infections in adult and juvenile blue crabs *Callinectes sapidus* from coastal bays of Maryland and Virginia, USA. Dis aquat Org 19: 77–82

Meyers TR, Koeneman TM, Botelho C, Short S (1987) Bitter crab disease: a fatal dinoflagellate infection and marketing problem for Alaskan Tanner crabs *Chionoecetes bairdi*. Dis aquat Org 3:195–216

Shields JD (1994) The parasitic dinoflagellates of marine crustaceans. A Rev Fish Dis 4:241–271

Vickerman K, Appleton PL, Field RH (1993) Cultivation and development *in vitro* of a parasitic dinoflagellate (*Hematodinium* sp.) from the Norway lobster (*Nephrops norvegicus*). In: Abstracts of the IX International Congress of Protozoology. German Society of Protozoology and German Society of Parasitology, Berlin, p 131

*Responsible Subject Editor: J. E. Stewart, Dartmouth, Nova Scotia, Canada*

*Manuscript first received: July 5, 1995*
*Revised version accepted: September 19, 1995*

Parasitol Res (1996) 82:279–282



SHORT COMMUNICATION

Paul L. Appleton · Keith Vickerman

# Presence of apicomplexan-type micropores in a parasitic dinoflagellate, *Hematodinium* sp.

Received: 20 July 1995 / Accepted: 19 September 1995

**Abstract** Structures resembling apicomplexan micropores were found by transmission electron microscopy in in vitro-cultured and in in vivo forms of the parasitic dinoflagellate *Hematodinium* sp. from crustacean hosts. Uptake of colloidal gold indicated a cytostomal function for the micropores.

One of the most surprising revelations of molecular systematics is that the apicomplexans (sporozoans), dinoflagellates and ciliates form a single clade (Gajadhar et al. 1991). Although remnants of a plastid in the apicomplexans have been cited as providing a possible connection with the photyosynthetic dinoflagellates (Gardner et al. 1993), not all dinoflagellates possess plastids or plastid remnants. The morphological resemblance between the three groups is slight and their nuclear organisation could not be more different. All that the three groups have in common is the alveolate cortex – hence the adoption of the name Alveolata (Cavalier-Smith 1993) for the clade.

Contemporary classifications recognise the early divergence of the wholly parasitic but poorly known syndinean dinoflagellates (phylum Syndinea, Corliss 1984; also recognised as a subdivision of the division Dinoflagellata by Fensome et al. 1993) from the better-known dinokaryotes (phylum Peridinea, Corliss 1984; subdivision Dinokaryota; Fensome et al. 1993). The latter have chromosomes with characteristic fibrillar banding and no histone protein, whereas the former have more conventional chromosomes with histone proteins. This communication reports the presence of a micropore – a structure characteristic of Apicomplexa – in different stages of the life cycle of a parasitic dinoflagellate belonging to the phylum Syndinea and to the genus *Hematodinium* Chatton & Poisson 1931.

P.L. Appleton (✉) · K. Vickerman
Biochemical Parasitology Laboratory, Joseph Black Building, University of Glasgow, Glasgow G12 8QQ, Scotland UK
Fax: + 0141 330 8016, E-Mail: 922725ap@udcf.gla.ac.uk

A species of *Hematodinium* associated with mortality of the Norway lobster, *Nephrops norvegicus*, in the seas around Scotland (Field et al. 1992) has been serially cultivated in vitro at 6–8°C for 3 years using a 10% fetal calf serum in balanced *Nephrops* saline medium (Vickerman et al. 1993). The principal multiplicative stage in culture is the trophont, an aflagellate multinucleate filament, 28–190 µm long (Fig. 1). These filaments show the typical alveolate surface structure and characteristic flexing and longitudinal contraction movements. They multiply by branching and fission, and lack the trichocysts found in the uninucleate flagellate dinospore stage from which they were initially derived.

Transmission electron microscopy of sections of the trophont filaments (processed as described by Field et al. 1992), reveals the presence of micropore-like structures (Fig. 2) scattered among the cortical alveoli. They are seen as caveolae (Fig. 3), ~ 110–200 nm in diameter, with an electron-dense reinforcing sleeve replacing the alveolar sacs in the underlying cortex along the wall of the pit (Fig. 4). Use of colloidal gold and ferritin markers has indicated ingestion of material from the surrounding medium via the micropore (Figs. 5, 6), i.e. that the micropore has a cytostome function in the trophont phase. The role of the micropore in the nutrition of apicomplexans has been reviewed by Senaud et al. (1976) and for *Plasmodium* spp. in particular by Olliaro and Goldberg (1995).

Similar micropores have been demonstrated in stages of development of *Hematodinium* in vivo, notably in circulating stages in generation of the trichocyst-bearing biflagellate dinospore (Fig. 7). Micropores may therefore be a feature of several stages in the life cycle of the syndinean, as they frequently are in coccidians, malaria parasites and other apicomplexans (Scholtyseck and Mehlhorn 1970; Ferguson et al. 1977). To date, micropores have not been observed in mature dinospores, however.

To our knowledge, micropores have not yet been recorded in the alveolate cortex of the dinokaryote dinoflagellates. In ciliates the parasomal sacs, which open close to the ciliary bases, have been shown to be engaged in pinocytosis (Nilsson and Van Deuers 1983). Interesting-

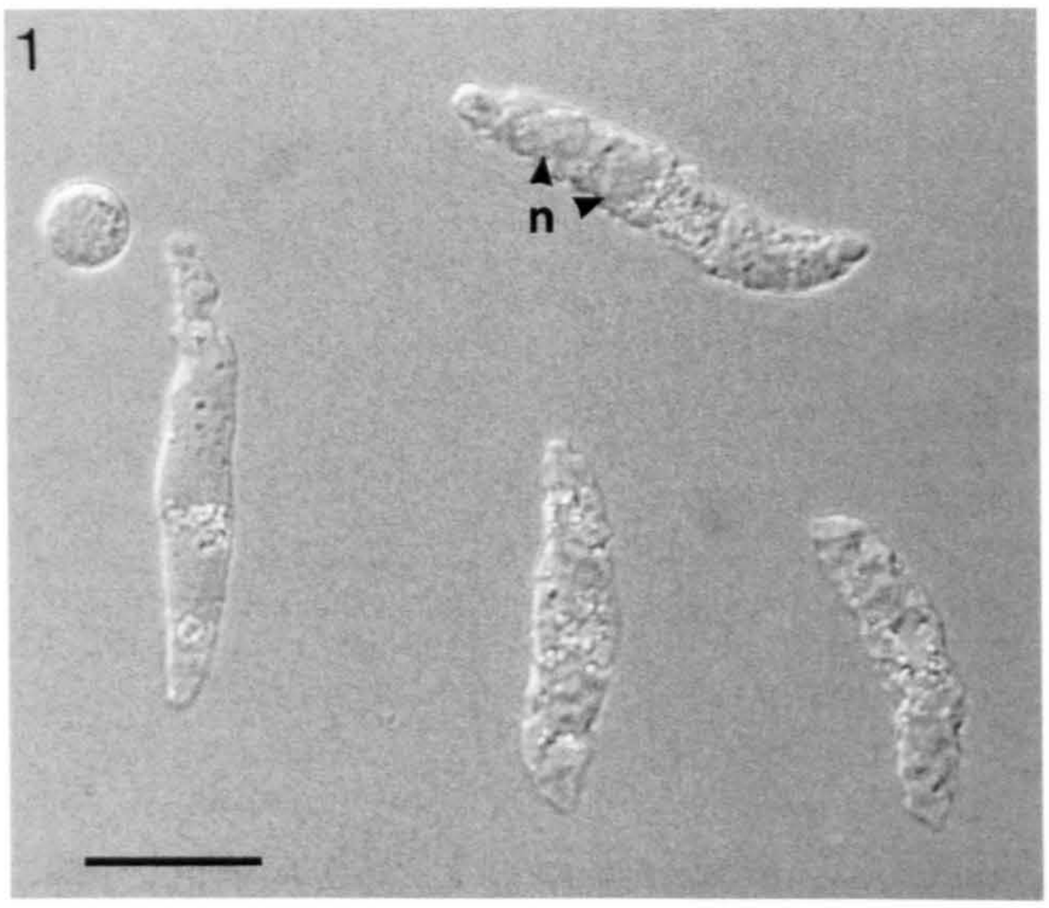


**Fig. 1** Filamentous multinucleate trophonts of *Hematodinium* sp. in culture showing a wrinkled surface and nuclei (*n*). Differential interference contrast. Bar = 20 µm

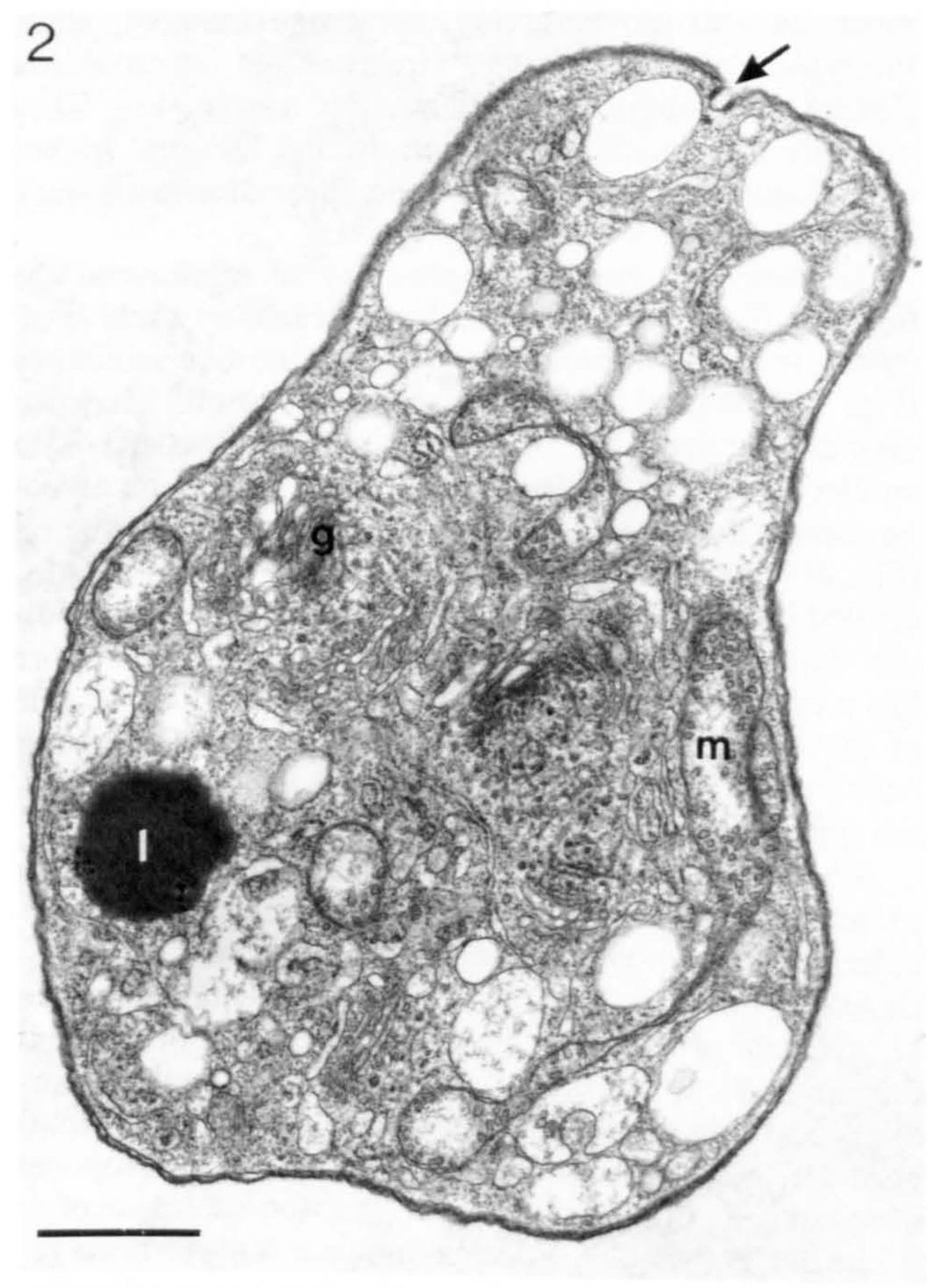


**Fig. 2** Culture trophont in transverse section, showing the vacuolated cytoplasm, the absence of trichocysts and a single (*arrow*) micropore. (*g* Golgi apparatus, *l* lipid, *m* mito-chondrion) Bar = 1.5 µm

ly, in the non-ciliated Suctoria and in sedentary ciliates with reduced ciliation (chonotrichs, peritrichs), cortical pores virtually identical in structure to the micropores of apicomplexans and syndinean dinoflagellates will take up ferritin from the surrounding medium (Rudzinska 1977). Micropores therefore appear to be a widespread component of the cortex in the Alveolata. Despite the apicomplexan-like flexing movements, no other apicomplexan feature (e.g. conoid, polar ring, cortical microtubules, rhoptries) has been observed in the trophont of *Hematodinium*.

**Acknowledgements** This work was supported by the UK Ministry of Agriculture, Fisheries and Food and the Scottish Office Agriculture and Fisheries Department.

## References

Cavalier-Smith T (1993) Kingdom Protozoa and its 18 phyla. Microbiol Rev 57: 953–994

Corliss JO (1984) The Kingdom Protista and its 45 Phyla. Biosystems 17: 87–126

Fensome RA, Taylor FJR, Norris G, Sarjeant WAS, Wharton DI, Williams GL (1993) A classification of fossil and living dinoflagellates. Micropalaeontology [Suppl] 7

Ferguson DJP, Birch-Anderson A, Hutchison WM, Siim JC (1977) The ultrastructure and distribution of micropores in the various developmental forms of *Eimeria brunetti*. Acta Pathol Microbiol Immunol Scand [B] 85: 363–373

Field RH, Chapman CJ, Taylor AC, Neil DM, Vickerman K (1992) Infection of the Norway lobster *Nephrops norvegicus* by a *Hematodinium*-like species of dinoflagellate on the west coast of Scotland. Dis Aquat Org 13: 1–15

**Figs. 2–7** Transmission electron micrographs of thin sections of *Hematodinium* sp.

**Fig. 3** Vertical section of a micropore. The alveolar sacs (*as*) of the cortex are replaced by an electron-dense sleeve (*arrow*) around the wall of the pit (*p*), which is lined by the plasma membrane (*pm*) only; radial fibrils connect the two structures. Bar = 150 nm

**Fig. 4** Horizontal section of a micropore pit, showing an electron-dense sleeve (*arrow*) beneath the plasma membrane (*pm*). (*as* Alveolar sac) Bar = 150 nm

**Fig. 5** Unstained section of a culture trophont embedded in LR White resin after incubation for 24 h in a colloidal gold suspension. Three gold particles (*arrows*) are lodged in a micropore pit. (*n* Nucleus) Bar = 1 µm

**Fig. 6** Vacuolated cytoplasm of a trophont treated similarly to that shown in Fig. 5. Gold particles (*arrows*) are present in two vacuoles. (*n* Nucleus) Bar = 1 µm

**Fig. 7** Section of parasites during microsporogenesis, from the ovary of a naturally infected *Nephrops*. The marked changes in appearance of the chromosomes (*ch*) in nuclei (*n*), characteristic of this stage in the life cycle, and the production of trichocysts (*t*) are evident. A micropore (*arrow*) is also present in a sporogenic cell. Bar = 2.5 µm

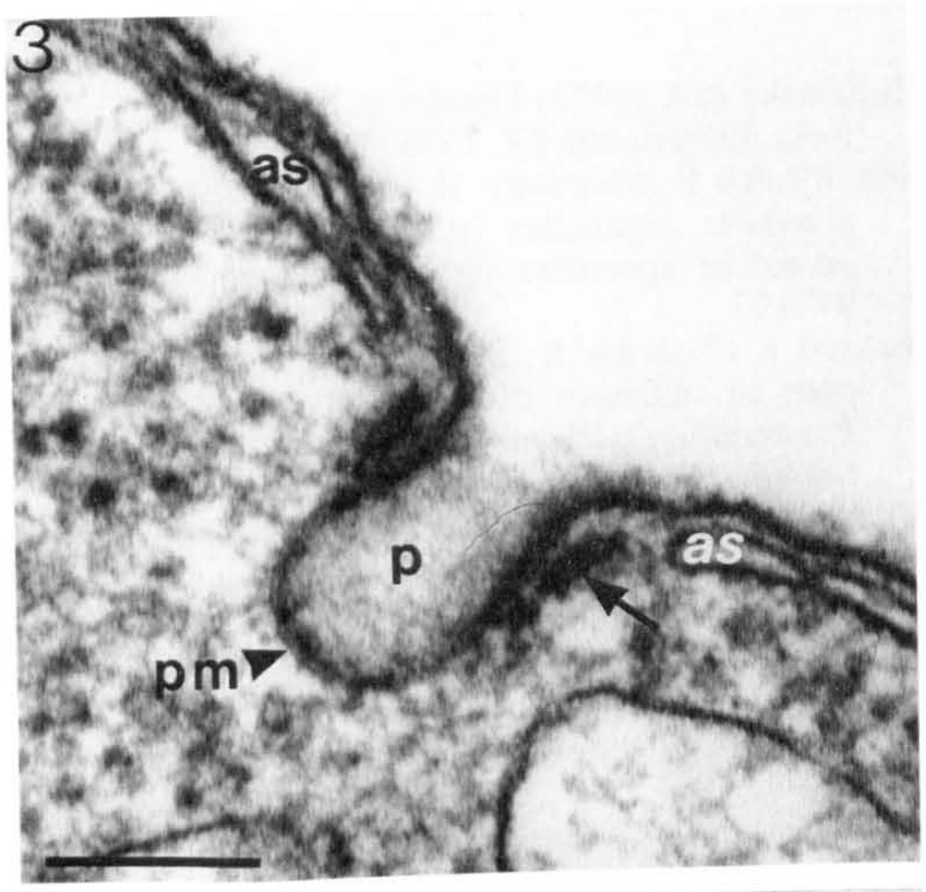
3
as
p
as
pm

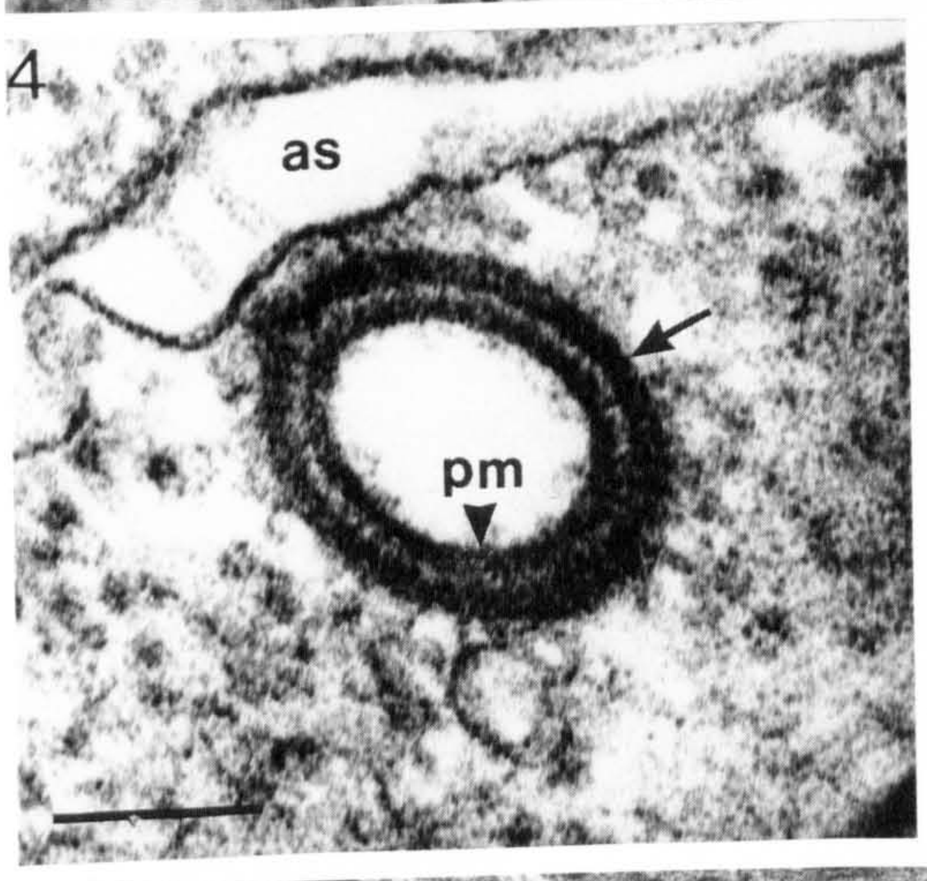
4
as
pm

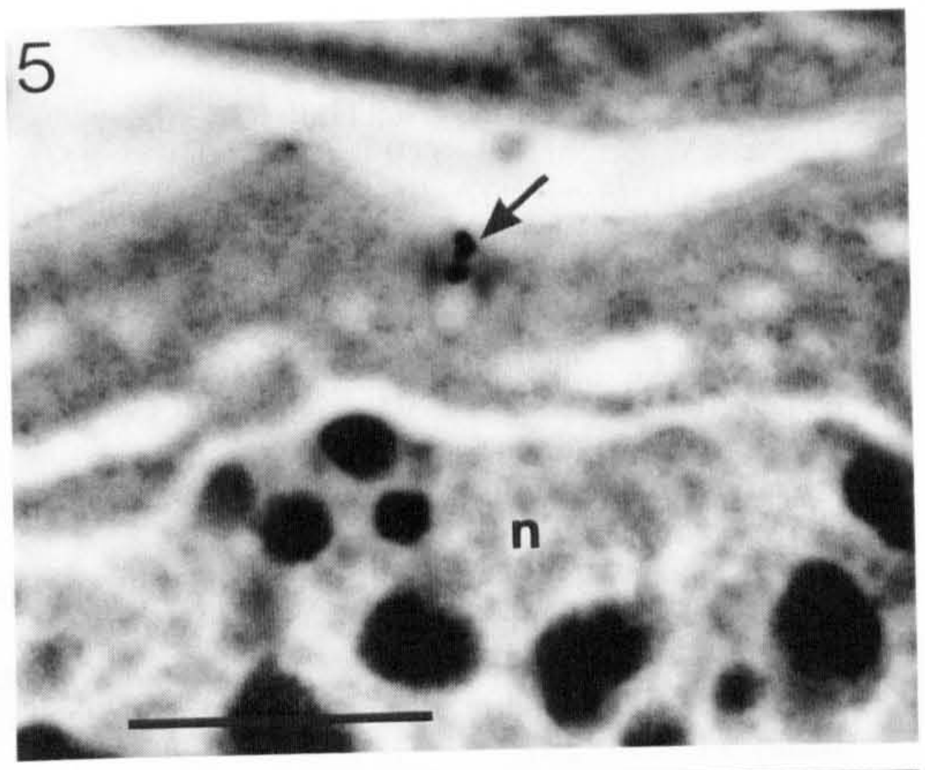
5
n

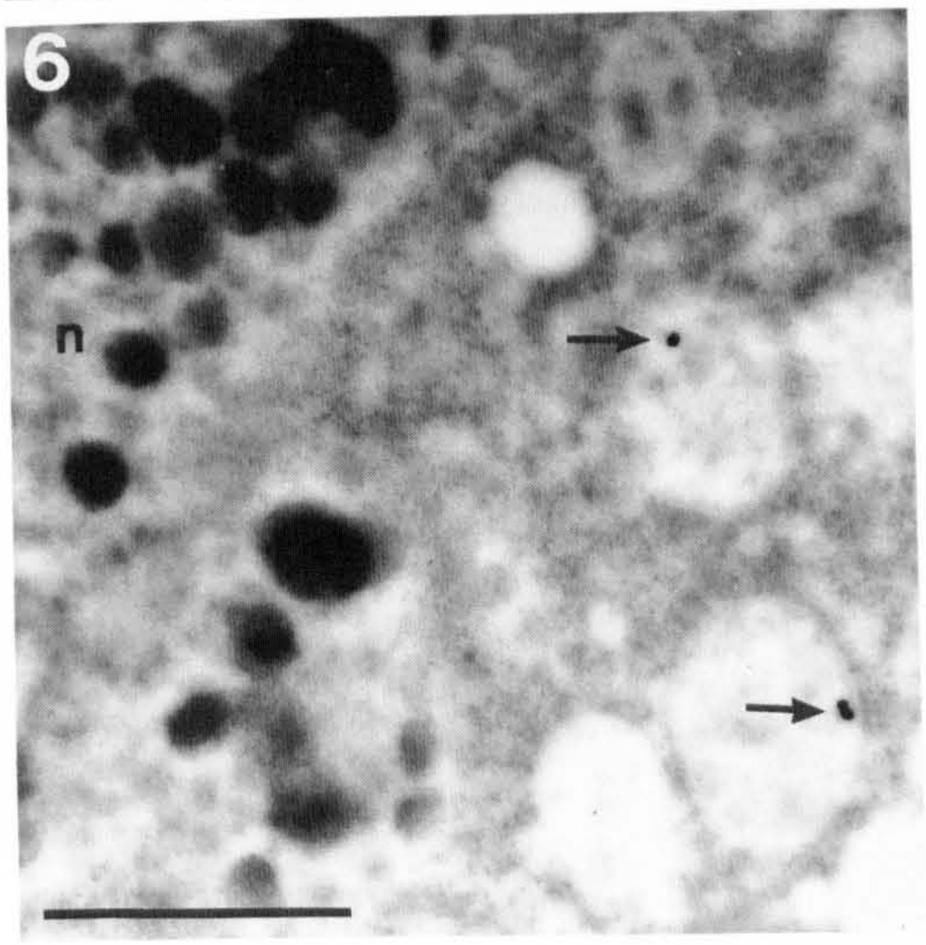
6
n

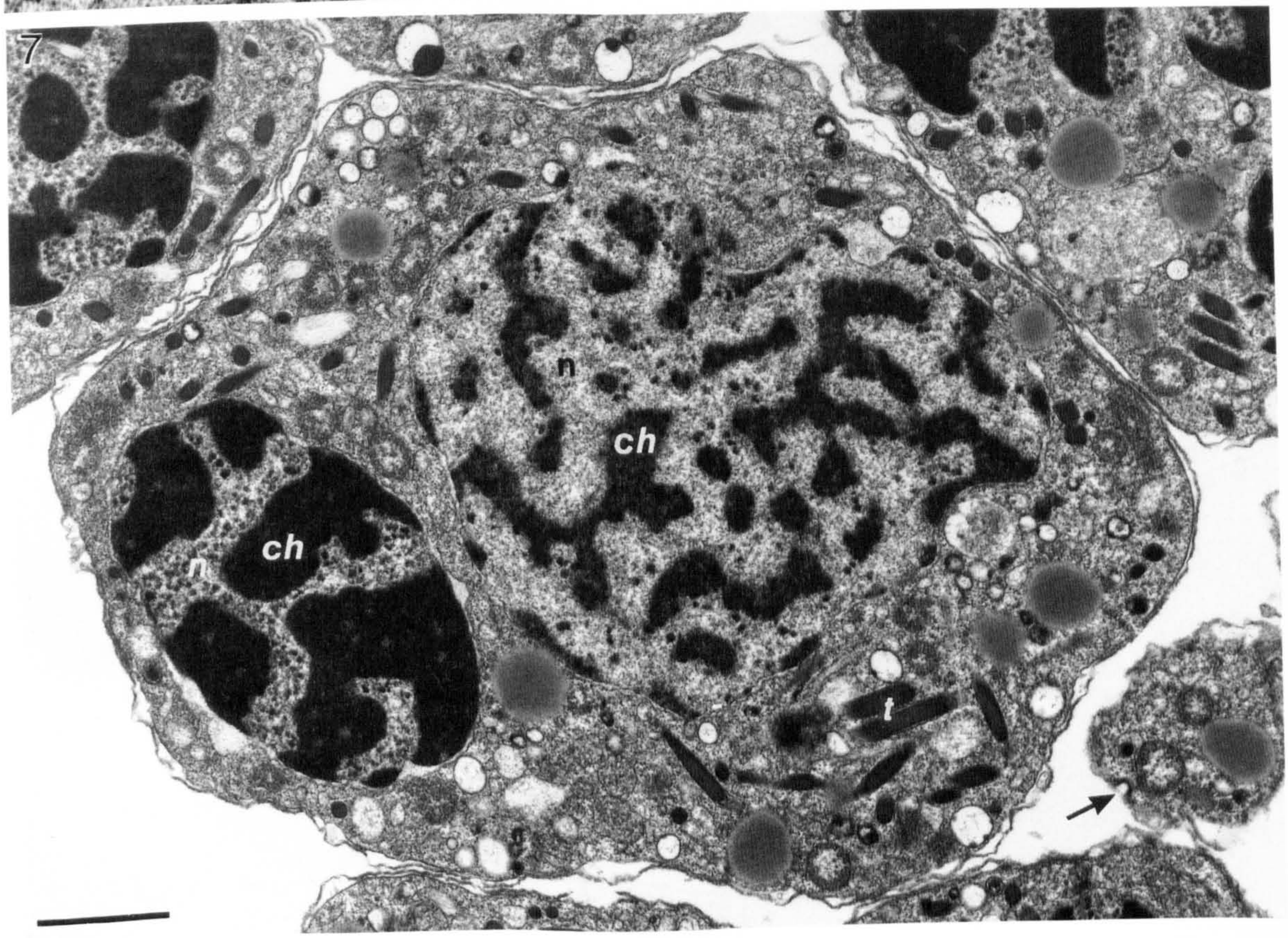
7
n
ch
ch
n
t

Gajadhar AA, Marquardt WC, Hall R, Gunderson J, Ariztia-Carmona EV, Sogin ML (1991) Ribosomal RNA sequences of *Sarcocystis muris, Theileria annulata* and *Crypthecodinium cohnii* reveal evolutionary relationships among apicomplexans, dinoflagellates and ciliates. Mol Biochem Parasitol 45: 147–154

Gardner MJ, Feagin JE, Moore DJ, Rangachari K, Williamson DH, Wilson RJM (1993) Sequence and organisation of large subunit rRNA genes from the extra-chromosomal 35 kb circular DNA of the malaria parasite *Plasmodium falciparum.* Nucleic Acids Res 21: 1067–1071

Nilsson JR, Van Deuers B (1983) Coated pits and pinocytosis in *Tetrahymena.* J Cell Sci 63: 209–222

Olliaro PL, Goldberg DE (1995) The *Plasmodium* digestive vacuole: metabolic headquarters and choice drug target. Parasitol Today 11: 294–297

Rudzinska MA (1977) Uptake of ferritin from the medium in Suctoria. Experientia 33: 1595–1598

Scholtyseck E, Mehlhorn H (1970) Ultrastructural study of characteristic organelles (paired organelles, micronemes, micropores) of Sporozoa and related organisms. Z Parasitenkd 34: 97–127

Senaud J, Chabotar B, Scholtyseck E (1976) Role of the micropore in nutrition of the Sporozoa. Ultrastructural study of *Plasmodium cathemerium, Eimeria ferrisi, E. steidae, Besnoitia jellisoni* and *Frankelia* sp. Trop Med Parasitol 27: 145–159

Vickerman K, Appleton PL, Field RH (1993) Cultivation and development in vitro of a syndinean dinoflagellate (*Hematodinium* sp.) from the Norway lobster (*Nephrops norvegicus*). Abstract, IX international congress of protozoology, Berlin, 25–31 July, p 131